Dynamic Mechanical Stimulation for Bone Tissue Engineering

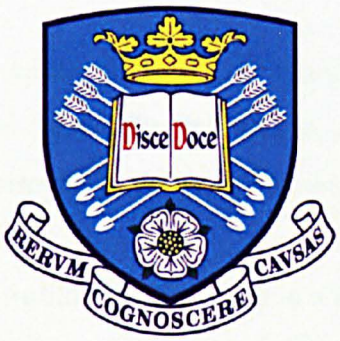

The University Of Sheffield.

Thesis submitted to the University of Sheffield for the degree of Doctor of Philosophy

Anuphan Sittichokechaiwut

Department of Engineering Materials, University of Sheffield

August 2009

ACKNOWLEDGEMENTS

I would like to thank my supervisors Dr. Gwendolen Reilly and Dr. Andy Scutt for taking me under their care, teaching, continued guidance, patience, support and encouragement.

I would like to thank the Royal Thai Government and Naresuan University, Thailand for their financial support and thank to the University of Sheffield for a travel grant from the Excellence Exchange Scheme.

I would also like to give a special thanks to many people in our lab who have done all they can for me, especially Nanette Scutt, Keith Blackwood, San Tao, Irene Canton, Claire Johnson, Hayley Morris, Jennie Robertson and Robin Rumney for their technical knowledge and expertise and for their patience in teaching me a number of valuable techniques.

I would like to thank Bose Corporation for lending the ELF 3200 to the Reilly laboratory for the first six months of my PhD under an evaluation scheme and Darren Burke form Bose for technical help with the ELF and the Biodynamic chamber.

At the Cell and Molecular Biomechanics Laboratory, Stanford University, USA. I would like to thank Professor Christopher Jacobs, Padmaja Tummala, Alesha Castillo, Ronald Kwon, Joyce Tang and Sara Temiyasathit for their help with the parallel plate flow chamber, primary cilia staining, siRNA transfection and real time PCR techniques.

A special thank you goes to my family and friends who have provided support and motivation. A personal mention goes to my mother, who has stood by me all the time, for her understanding and love.

ABBREVIATIONS

%	percentage
α	alpha
°C	degrees centigrade
µg	microgram
µl	microlitre
µM	micromolar
2-D	two dimensional
3-D	three dimensional
AA	ascorbic acid
ALP	alkaline phosphatase
ANOVA	analysis of variance
ASC	adult stem cell
BCS	bovine calf serum
BMP	bone morphogenetic protein
BMSC	bone marrow stromal cells
BSP	bone sialoprotein
Ca^{2+}	calcium
cDNA	complementary deoxyribonucleic acid
CFU-f	colony forming unit-fibroblastic
cm	centimetre
cm^2	square centimetre
cm^3	cubed centimetre
CO_2	carbon dioxide
COL1	type 1 collagen
COX2	cyclooxygenase 2
DAPI	4',6-diamidino-2-phenylindole
ddH_2O	double distilled water
DEX	dexamethasone
DMEM	Dulbecco's Modified Eagle's Medium
DMP1	dentin matrix protein 1
DMSO	dimethyl sulphoxide
DNA	deoxyribonucleic acid

DNAse	deoxyribonuclease
ECM	extracellular matrix
EDTA	ethylenediaminotetraacetic
ERK	extracellular signal-regulated kinase
ESC	embryonic stem cell
F	fungizone
FBS	fetal bovine serum
FCS	fetal calf serum
FITC	fluorescein isothiocyanate
g	gram
GAPDH	glyceraldehyde 3-phosphate dehydrogenase
HA	hyaluronic acid
HCl	hydrochloric acid
Hz	hertz
ICT	intraciliary transport
KDa	kilodaltons
KPa	kilo pascal
L	litre
M	molar
MAPK	mitogen-activated protein kinase
MEM	minimum essential medium
mg	milligram
min	minute
ml	millilitre
mm	millimetre
mM	millimolar
MPa	megapascal
mRNA	messenger ribonucleic acid
MSC	mesenchymal stem cells
MTS	3-(4,5-dimethylthiazol-2-yl)-5-(3-carboxymethoxyphenyl)-2-(4-sulfophenyl)-2H-tetrazolium
MTT	A3-(4,5-dimethylthiazol-2-yl)-2,5-diphenyltetrazolium bromide
N	number
NaOH	sodium hydroxide

nm	nanometre
nM	nanomolar
nmol	nanomole
O_2	oxygen
OCN	osteocalcin
OD	optical density
OFF	oscillatory fluid flow
OPN	osteopontin
P/S	penicillin/streptomycin
Pa	pascal
PBS	phosphate-buffered saline
PGE_2	prostaglandin E2
pH	potential of hydrogen
PI	propidium iodide
RNase	ribonuclease
RT-PCR	reverse transcriptase polymerase chain reaction
RUNX2	runt-related transcription factor 2
SD	standard deviation
SEM	scanning Electron microscopy
siRNA	small interfering ribonucleic acid
βGP	β-glycerophosphate

ABSTRACT

Mechanical loading is an important regulatory factor in bone homeostasis, and plays an essential role in maintaining the structure and mass of bone throughout a lifetime. Although the exact mechanism is unknown the data presented in this thesis supports the concept that substrate signals influence MSC growth and differentiation. A better understanding of the cellular and molecular responses of bone cells to mechanical stimuli is the key to further improvements to therapeutic approaches in orthopaedics, orthodontics, periodontics, bone repair, bone regeneration, implantology and tissue engineering. However, the mechanisms by which cells transduce mechanical signals are poorly understood. There has also been an increased awareness of the need for improvement and development of 3-D *in vitro* models of mechanotransduction to mimic the 3-D environment, as found in intact bone tissue and to validate 2-D *in vitro* results.

The aims of the project were (i) to optimize a model system by which bone cells can survive in 3-D static culture and their responses to mechanical stimuli can be examined *in vitro,* (ii) to test the effects of intermittent mechanical compressive loading on cell growth, matrix maturation and mineralization by osteoblastic cells, (iii) to examine the role of the primary cilia, (iv) to assess the effect of dynamic compressive loading on human mesenchymal stem cells in the 3-D environment.

The optimized model system has the potential to be used in *in vitro* studies of bone in 3-D environments including a better understanding of the mechanically controlled tissue differentiation process and matrix maturation in the engineered bone constructs. It has less complicated equipment and techniques compared to dynamic seeding and culture systems making it easy to use in the laboratory. In addition, cells are not pre stimulated by any mechanical stimuli during seeding and culture which enables the researcher to study selected mechanical stimuli and mechanotransduction in bone tissue constructs. The model can mimic the bone environment providing a better physiological model than cells cultured in 2-D monolayer.

Using our 3-D system, several loading regimens were compared and it was shown that intermittent short periods of compressive loading can improve cell growth and/or matrix production by MLO-A5 osteoblastic cells during 3-D static culture. This

suggests that the cells are responding to the mechanical compression stimulus either by directly sensing the substrate strain or the fluid shear stress induced by flow through the porous scaffold. We also demonstrated that our mechanical loading system has the potential to induce osteogenic differentiation and bone matrix production by human MSCs in the same way as treatment with dexamethasone. Although the exact mechanism is unknown the data presented supports the concept that the dynamic compressive loading influence MSC growth, differentiation and production.

In further experiments, we used the optimized 3-D model system to study the effects of mechanical loading on primary cilia, which have recently been shown to be potential mechanosensors in bone. We demonstrated that mature cells lacking a cilium were less responsive, less able to upregulate matrix protein gene expression and did not increase matrix production in response to mechanical stimulation suggesting that the primary cilia are sensors for mechanical forces such as fluid flow and/or strain induced shear stress.

CONTENTS

LIST OF FIGURES

LIST OF TABLES

CHAPTER ONE: Literature review

This thesis concerns bone tissue engineering and the way in which mechanical loading can modulate bone matrix production, to provide a background to these topics. The current literature on basic principle of bone, extracellular matrix and biomineralization of bone, mechanical responses in bone, bone mechanosensors such as primary cilia, bone tissue engineering strategies and clinical applications will be summarised.

1.1 Structure of bone

1.1.1 Anatomy and functions of bones

Bone is a dynamic, highly vascularised tissue that provides an essential function in the body [1]. Its main function is to provide structural support for the body. Moreover bone also serves as a mineral reservoir and rich source of growth factors and cytokines, supports muscular contraction resulting in motion, bears loads and protects internal organs [2-6]. The adult human skeleton is comprised of 206 bones, each bone supports one or more specific functions. Bone tissue in the adult skeleton is comprised of two architectural forms: cancellous, also called trabecular or spongy bone (around 20% of the total skeleton), and cortical or compact bone (around 80% of the total skeleton) [7]. Cortical bone appears dense and solid, whereas cancellous bone is a honeycomb-like network of interconnected trabecular plates and bars surrounding bone marrow [3, 5, 6]. The proportions of these two architectural forms differ at various locations in the skeleton. Cortical bone is only 10% porous. While, cancellous bone has a higher porosity, 50–90%, making its compressive strength around 20 times less than that of cortical bone [7]. Bone can withstand extremely high loads, and will remain strong even following several million cycles of loading such as alveolar bone which supports teeth during mastication and is presumed to adapt to occlusal forces.

Alveolar bone is a specialized extension of the basal bone of mandibular and maxillary jaw bones that associates with tooth eruption and forms the primary support structure of teeth [8]. While the growth and development of jaw bones determines the

position of the teeth, a certain degree of re-positioning of teeth can be accomplished through occlusal force from mastication and in response to orthodontic procedures that rely on the adaptability of the alveolar bone and associated periodontal tissues [9]. Alveolar bone remodels rapidly, which is important for positional adaptation of the teeth, but this may lead to the progression of periodontal disease [10].

The main part of alveolar bone is made up of spongy, cancellous bone, whereas the outer layer is made up of cortical plate which is dense and forms the surface of alveolar bones *(Fig. 1.1)*. Alveolar bone structure is strongly related to mechanical stimulation and completely dependent on masticatory function, since, in the absence of teeth and denture-transmittied mechanical stimulation, it undergoes disuse atrophy [11]. The sensitivitiy of the periosteal and endosteal alveolar bone surfaces to mechanical stress is the reason for the relatively high levels of remodeling activity that are seen, even under physiological conditions. An understanding of the biological response of alveolar bone to mechanical loading could further advance the clinical mangement of periodontal bone loss.

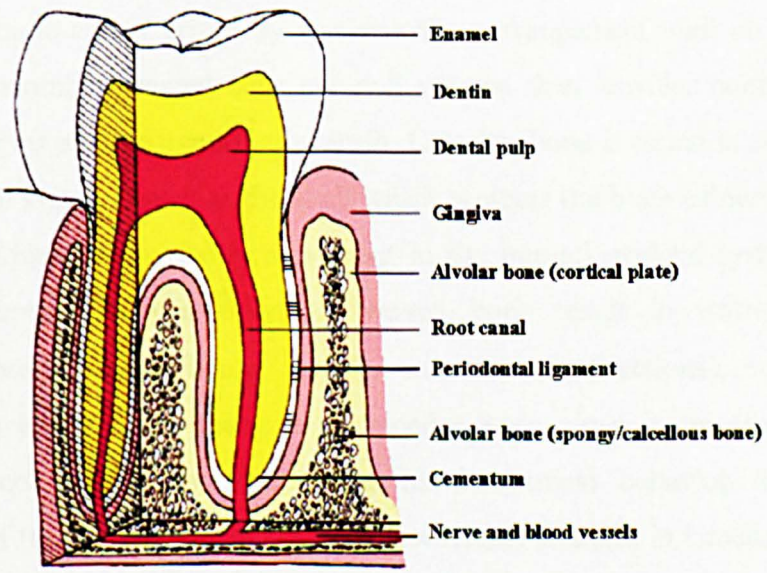

***Fig. 1.1**: The anatomy of a tooth and periodontium. The periodontium consists of gingiva (gum), periodontal ligament and supporting structures alveolar bone, surrounding a tooth. The periodontal ligament attaching the cementum of the tooth root to the alveolar bone of the socket; the collagen fibers of the ligament are grouped into bundles.*
(Picture is modified from http://www.uabhealth.org/14134/; March 2008).

1.1.2 Macroscopic anatomy

Bones can be distinguished into two main types; Flat bones, such as skull, mandible, and scapula, and long bones, such as femur, tibia and radius. Long bones consist of a hollow tube (shaft or diaphysis), which flairs at the ends to form cone-shaped metaphyses and epiphyses. The shaft is comprised primarily of cortical bone, whereas the metaphyses and epiphyses contain cancellous bone surrounded by a shell of cortical bone [7]. Bones have an outer fibrous sheath called the periosteum, and an inner surface called endosteum, which contacts the marrow. The periosteum is formed by fibrous connective tissue and covers all bone surfaces except at the joint where the bone is lined by articular cartilage. The periosteum is anchored to the bone by strong collagenous fibers called Sharpey's fibers that penetrate into the bone tissue [7]. The endosteum is a membranous sheath lining the marrow cavity.

1.1.3 Microscopic anatomy

At the microscopic level, bone has two forms, woven and lamellar. Woven bone is immature bone characterized by a coarse fiber arrangement with no orientation and has more randomly arranged cells per unit volume than lamellar bone. Lamella bone formation begins about 1 month after birth. Lamellar bone is found in several structural and functional systems, such as the skull which protects the brain of nervous system and long bones which involve body movement in the musculoskeletal system [7, 10, 12]. The non-oriented collagen fibers of woven bone result in isotropic mechanical properties (properties of bones are the same in all directions), while the highly organized, stress oriented collagen of lamellar bone gives it anisotropic properties. Lamellar bone's anisotropy means that its mechanical behavior depends on the orientation of the applied forces. The greatest tensile strength in lamellar bone is found parallel to the long axis of the collagen fibers, while compression or shear strength may be found in a different direction [4, 12]. The arrangement of lamellar bone around vascular channels forms an osteon which is usually oriented in the long axis of the bone and is the major structural unit of mature cortical bone. Cortical bone becomes a complex of many adjacent osteons and their interstitial and circumferential lamellae [13] *(Fig. 1.2)*. When an osteon results from remodelling of bone it is called a Haversian system.

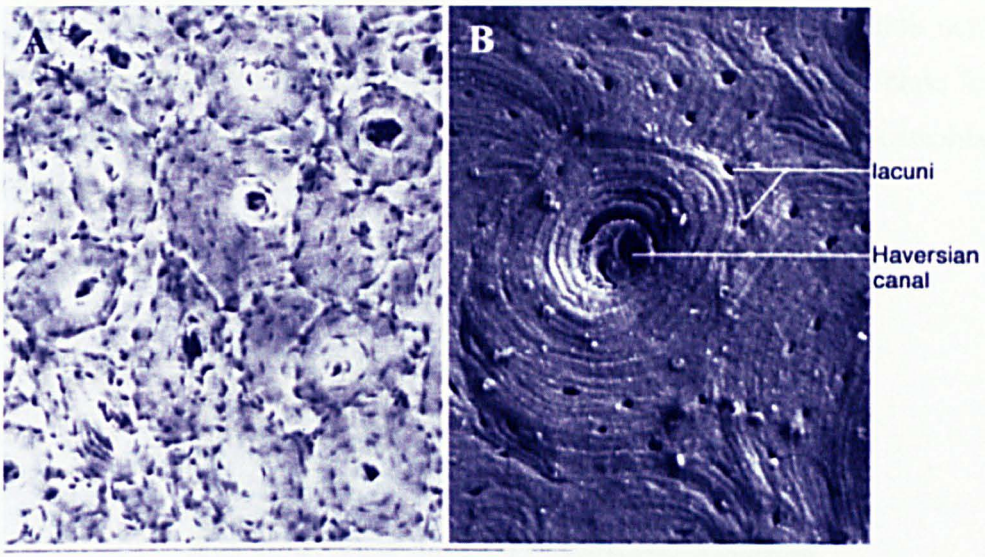

***Fig. 1.2**: Ultrastructure of bone. A, light microscope image of a ground section of compact bone. Osteon or Harversian systems can be seen. The central dark circle is the Haversian canal which contains a nutrient vessel and is surrounded by concentric lamellae of calcified bone matrix. The dark spots visible within the system are the lacunae in which osteocytes become entrapped. B, Scanning electron micrograph (SEM) of Haversian system (Hollinger et al. 2005).*

1.2 Cell biology of bone

Bone contains four cell types: osteoblasts (matrix-producing cells), osteocytes (fully differentiated osteoblasts), osteoclasts and osteoprogenitor cells. All of them have defined functions and are essential for healthy bone tissue maintenance *(Table 1.1)*. Osteoblasts and osteocytes derive from pluripotent mesenchymal stem cells or osteoprogenitor cells [10], whereas osteoclasts differentiate from hematopoietic precursors which are located in the bone marrow [14, 15].

1.2.1 Osteoblasts

Osteoblasts are mononucleate cells that produce and deposit the matrix that is needed for the development of new bone and consists primarily of collagen fibers. They lay down 0.5-1.5 μm osteoid (the organic portion of the bone matrix that has not been

calcified) per day *in vivo* [8]. They are primarily responsible for the production of the organic matrix of bone which consists predominantly of type I collagen and various other non collagenous bone proteins and plasma proteins [8]. Inactive osteoblasts at the bone surface called bone lining cells create the intercellular communication network. It is hypothesised that bone lining cells sense the need for and direct new bone formation [10]. Osteoblasts can be immortalised and cultured *in vitro* such as pre-osteoblastic cell line MC3T3-E1 *(Fig. 1.3)*.

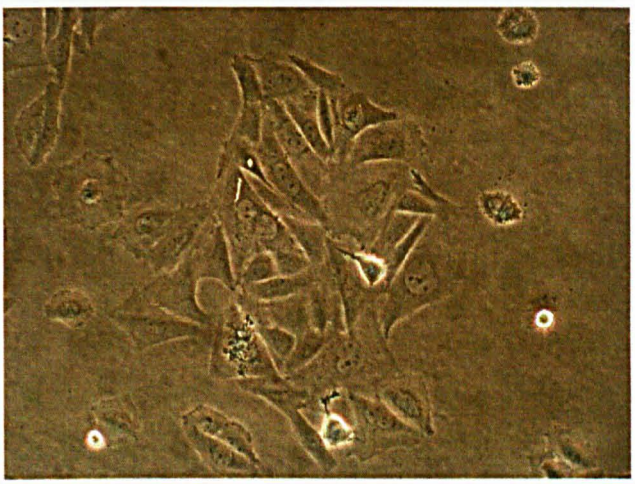

***Fig. 1.3**: Light micrograph of MC3T3-E1 osteoblast-like cells cultured on tissue culture plate. The cells were immortalised from mouse bone cells (x10).*

1.2.2 Osteocytes

Osteocytes are the most abundant cells in bone, they are stellate shaped with a higher number of cytoplasmic extensions or processes [16]. They are smaller in size than osteoblasts and have a decreased quantity of synthetic and secretory organelles but have an increased nucleus/cytoplasm ratio [8, 17]. Although they are diminished in size, these cells still have the full complement of organelles capable of effecting protein secretion [8, 10]. The major feature of osteocytes is the presence of numerous and extensive cell processes that penetrate throughout the bone canaliculi and make contact via gap junctions with the processes of other osteocytes or with processes extending from osteoblasts or bone lining cells at the surface of bone [17]. An osteocyte-like cell line (MLO-Y4) was developed by Ahuja et al. (2003) [18] *(Fig. 1.4)*.

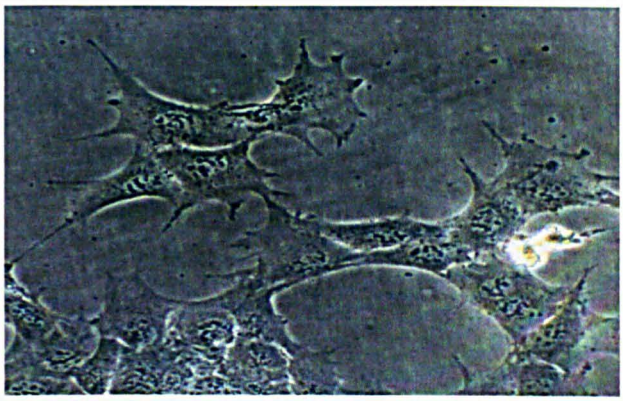

***Fig. 1.4**: Light micrograph of MLO-Y4 osteocytic cells. Cellular processes reach out towards the tissue culture plate (x20).*

1.2.3 Osteoclast

Osteoclasts are multinucleated cells derived from hematopoietic stem cells and play important role in the the bone remodeling process. Their average lifespan is about 15-20 days. They secrete lysosomal enzymes which have the ability to break down mineralized bone. An activated osteoclast is able to resorb 200,000 μm^3/day of bone matrix, an amount of bone formed by 7 to 10 generations of osteoblasts [19] *(Fig. 1.5)*.

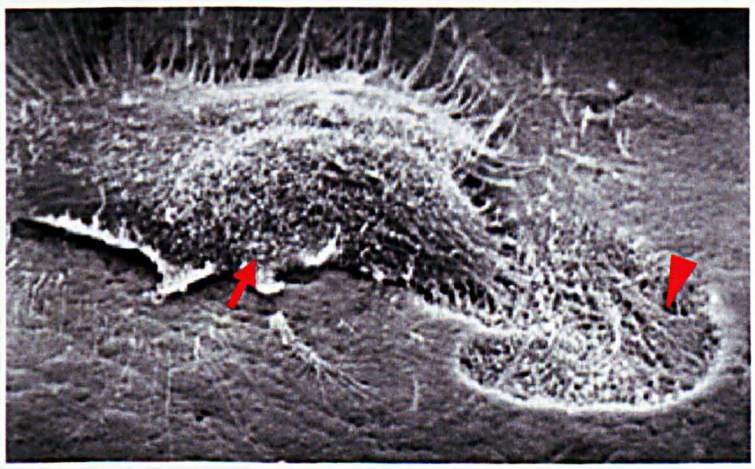

***Fig. 1.5**: Scanning electron micrograph of an osteoclast. Arrow points an osteoclast cell. Arrow head indicates bone resorption area (Picture from: http://theyorf.blogspot.com/2007/05/osteoclasts-are-cool.html; March 2009).*

***Table 1.1**: Types of bone cells and respective functions.*

Cell type	Morphological characteristics	Function
Osteoblasts	Cuboidal shaped [8]. Located at the bone surface, where they form a tight layer of cells [8, 10].	Synthesis and regulation of bone ECM deposition and mineralization [8]. Respond to mechanical stimuli [8, 20].
Osteocytes	Stellate shaped [20-22]. Possess fewer organelles than the osteoblasts such as ribosomes and endoplasmic reticula [8, 17]. Nucleus/cytoplasm ratio higher than that of osteoblasts [8, 10]. Smaller size than that of osteoblasts [8, 10].	Calcification of the osteoid matrix [10] . Blood-calcium homeostasis [5, 8, 20] . Mechanosensor cells of the bone [5].
Osteoclasts	Multinucleated cells [21, 22]. Finger-like processes called ruffled border [8, 10].	Bone resorption [10]. Bone remodeling [8, 10].
Osteoprogenitor cells e.g. Mesenchymal stem cell (MSC).	Fibroblast-like shaped . Pluripotent undifferentiated cells[8, 10].	Osteogenic precursor [5, 20-23]. May respond to mechanical stimuli [5, 20-23].

1.3 Morphogenesis of Bone

Bone is the product of cells from three embryonic lineages which migrate to the locations where the skeleton will develop and form characteristic mesenchymal condensations of high cell density, and differentiate into osteoblasts or chondrocytes [24]. Neural crest cells give rise to the branchial arch derivatives of the craniofacial skeleton (skull), paraxial mesoderm cells/somites contribute to the craniofacial skeleton and form most of axial skeleton (central trunk of body) and lateral plate mesoderm cells produce the limb skeleton (appendiculars) [25, 26] *(Fig. 1.6)*.

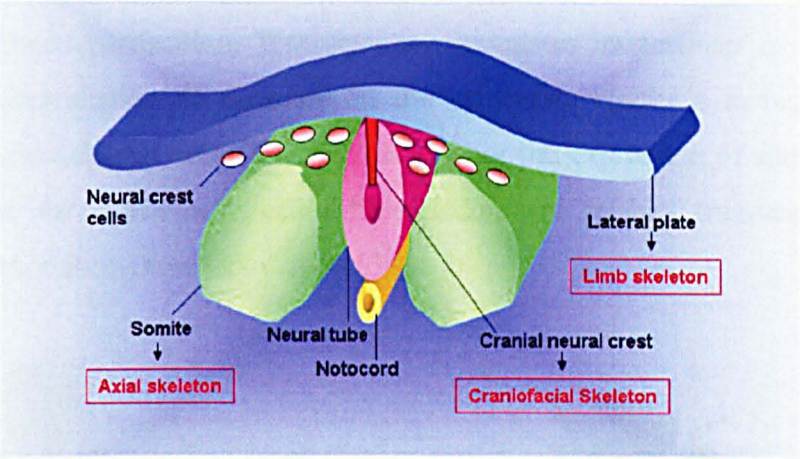

***Fig. 1.6**: Summary diagram of cross sectional embryo. Cells migrate from cranial neural crest, somites, and lateral plate mesoderm into the craniofacial, axial and limb skeleton areas which the cartilage and bone will be formed.*

1.3.1 Intramembranous Ossification

The maxilla, mandible and most of the bones in craniofacial regions are formed by intramembranous ossification in which mesenchymal cells differentiate directly into bone-forming osteoblasts [27, 28]. These cells secrete a matrix of type I collagen and other molecules forming a primary dense fibrous complex [28]. Osteoblasts synthesize phosphatase and ground substance containing a complex mix of mucopolysaccharides to cement the matrix fibers together, becoming osteoid [4, 29]. Afterwards calcium phosphate crystals are deposited in the osteoid in the mineralization process becoming bone matrix, osteoblasts are enclosed in the matrix being formed around them, and the cells become osteocytes [1, 4] *(Fig. 1.7)*. Some of the osteoblasts surrounding the initial bony trabecula also proliferate and continue to add bone to trabecula, thereby new trabeculae are formed, the center of ossification expands and trabeculae increase in thickness [25]. Bony trabecula growth and orientation are unique for each bone. When bones have grown to occupy their definitive margins and come into closer relationships with other bones, bony borders begin to form as the trabeculae become interconnected [27-29].

The differentiation of mesenchymal cells into osteoblasts or chondrocytes is regulated by a number of signaling factors and the expression of genes. In the area of intramembranous ossification, Wnt signaling stimulates intracellular events to prevent proteolytic degradation of β-catenin in the cytoplasm resulting in high levels of β-catenin in mesenchymal cells [4, 25]. This induces the expression of specific genes that are required for osteoblastic cell differentiation and inhibits transcription of genes needed for chondrocytic differentiation [30].

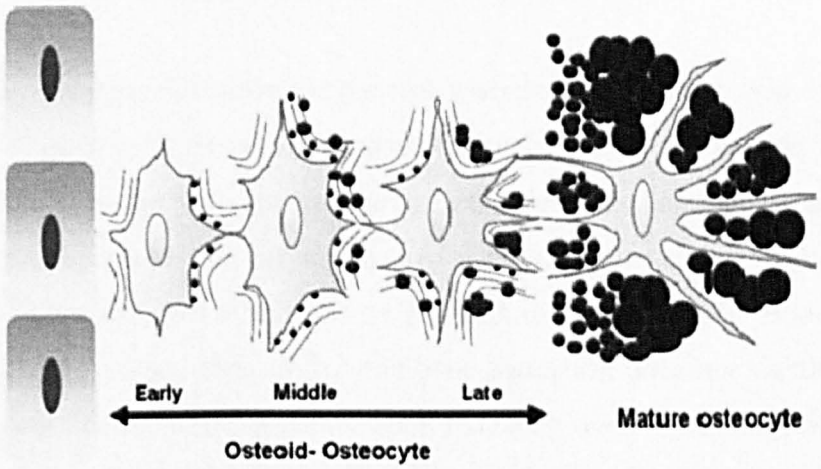

***Fig. 1.7**: A schematic of osteoblast differentiation and mineralization. The osteoblast in the osteoid-osteocyte stage becomes embedded in the nonmineralized matrix, small calcified spheres are formed along the cell membrane associated with the collagen fibers and then the late stage osteoblast converts to a dendritic osteocyte by shrinking of the cytoplasm and formation of thinner processes (Barragan-Adjemia et al. 2006).*

1.3.2 Endochondral Ossification

In regions of the axial and limb skeleton, differentiation into chondrocytes produces a framework of cartilage models which are eventually replaced by bone through the process of endochondral ossification [4]. Bone formation of this type begins through the adhesion of mesenchymal cells into clusters or condensations in the embryonic stage which then form cartilaginous templates called hypertrophic cartilage or anlagen [25]. The intercellular matrix containing characteristic cartilage matrix is formed and first appears at the center of mesenchymal condensations [4, 25, 26]. The matrix deposition spreads peripherally to the margin of the original condensation and becomes calcified hypertrophic cartilage. Ossification and deposition of bone matrix

occurs with invasion of the calcified hypertrophic cartilage, apoptosis of chondrocytes and degradation of cartilage matrix [26]. Transcriptional factors such as SOX9, RUNX2-I (also known as Cbfa1, Osf2 and AML3) have been found to play important roles in mesenchymal condensation, chondrocyte differentiation and endochondral bone forming processes [25, 26].

1.4 Bone modeling and remodeling

Bone modeling describes the process whereby bones are shaped or reshaped by the actions of the osteoblast-osteoclast complex such as during growth or in the adult to change the shape of the bone in response to mechanical load (mechanical adaptation) [2, 3, 6, 21]. The radius in the playing arm of a tennis player has a thicker cortex and greater diameter than the other side as a result of modeling [7]. Bone modeling is distinguished from remodelling in that the bone formation does not tightly follow prior bone resorption. In the adult skeleton, bone modeling occurs less frequently than bone remodeling [31].

The bone remodeling cycle consists of four phases: activation, resorption, reversal and formation. Activation is the initial event that transforms a previously quiescent bone surface into a remodeling one involving the recruitment of osteoclast precursors from cells in the monocyte-macrophage lineage in the circulation, infiltration of the bone lining cell layer, and fusion of the mononuclear cells to form multinucleated preosteoclasts [7]. During the resorption phase, acidification of the resorbing compartment is accompanied by secretion of lysosomal enzymes as well as matrix metalloproteases. The acidic solution effectively dissolves and digests the mineral and organic phases of the matrix, creating saucer-shaped resorption cavities called Howship's lacunae on the surface of bone. In the reversal phase, the osteoclasts release growth factors from the bone matrix and these factors act as chemo-attractants for osteoblast precursors and stimulate osteoblast proliferation and differentiation [7, 32]. The formation phase is the process in which the osteoblasts initially synthesize the organic matrix and then regulate its mineralization resulting in new bone deposition.

1.4.1 Interaction of bone-forming and bone-resorbing cells

A molecular basis for these processes was discovered in the form of osteoprotegrin (OPG), secreted by osteoblasts, and receptor/activator of NF-κB ligand (RANK-L, also known as OPG-L), surface-bound molecule expressed on osteoblasts and immune cells. These can bind to (RANK), a transmembranous receptor expressed on osteoclast precursor cells. Interaction between RANK-L and RANK initiates a signaling and gene expression cascade resulting in the promotion of osteoclast formation, consequentially, bone resorption. OPG acts as a soluble competitive binding partner for RANK-L, which inhibits osteoclast formation [7, 33] *(Fig. 1.8)*.

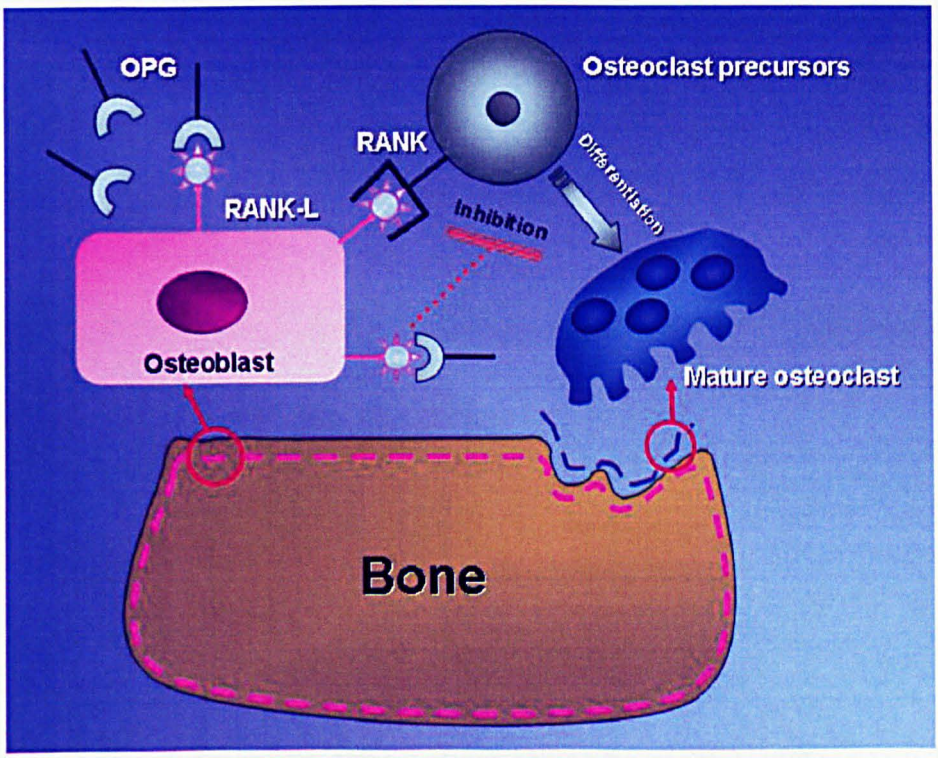

***Fig. 1.8**: A schematic of osteoblast-osteoclast interaction. The interaction between RANK-L on the surface of mature osteoblasts and RANK receptor on osteoclast precursor cells induces proliferation and differentiation of osteoclasts and can be inhibited by soluble protein OPG.*

1.5 Extracellular matrix and biomineralization of bone

Bone matrix has two components: a mineral inorganic part, composed of hydroxyapatite which contributes 65–70% to the matrix and an organic part, composed of collagen, glycoproteins, proteoglycans, sialoproteins, bone gla proteins, that comprises the remaining 25–30% of the total matrix including cells 2-5% [20-22]. The new synthesized matrix, osteoid, consists about 94% collagen [2, 3, 8, 22]. Type I collagen (>95%) is the principle collagen in mineralized bone, together with type V collagen (5%). Collagen fibril formation is initiated when collagen filaments, short chains which twist into triple helices, assemble extracellulary into striated fibrils to form the osteoid [8] *(Fig. 1.9)*. The collagen fibrils in bone are stabilized by intermolecular cross-linking involving lysines and modified lysines that form pyridinium ring structures. These cross-links are responsible for the high tensile strength of collagen fibers [10, 34]. The mineral crystals of calcium hydroxyapatite ($Ca_{10}[PO_4]_6[OH]_2$) within the collagen fibrils are believed to form initially within the gap region between collagen filaments [34, 35].

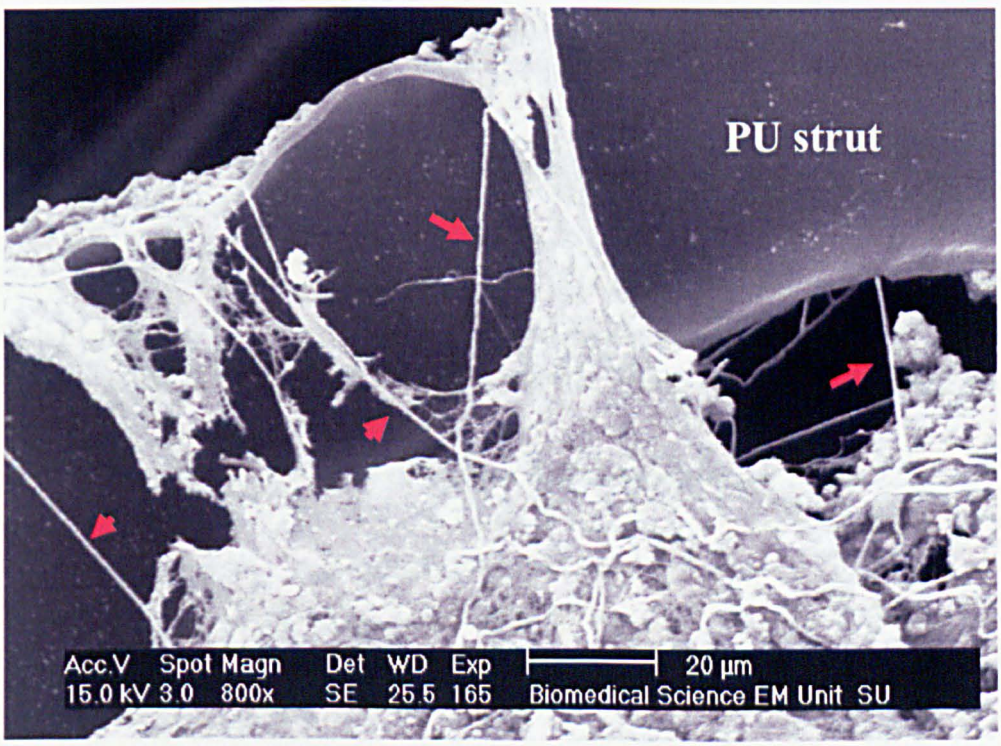

***Fig. 1.9**: Scanning electron micrograph of osteoblasts forming osteoid on PU scaffold. Collagen fibrils assemble extracellulary into fibers to form the osteoid on a polyurethane scaffold. (Head of arrows point to the fibers of collagen).*

Osteocalcin (OCN), also known as gla protein, was the first noncollagenous bone protein to be characterized. It is a small 5.8-kDa acidic protein which is modified by vitaminK-dependent carboxylating enzymes that convert glutamic acids into γ-carboxyglutamic acids (gla group) interacting with hydroxyapatite [5, 6]. Osteopontin (OPN) and Bone sialoprotein (BSP) are chemically similar molecules sharing a number of biochemical and biophysical properties. These proteins are ~34-kDa proteins with highly glycosylated and phosphorylated sites binding with the proteoglycan Hyaluronic acid (HA). Although, their structures are similar, they have different functional roles. BSP is essentially restricted to mineralizing tissues, whereas OPN has more general distribution that reflects a broader biological role [36]. OPN has also been shown to play an important role in both cell attachment and mechanotransduction responses of osteoblasts *in vitro*, and has also been indentified as an early marker of osteoblast differentiation [10]. The other components of the bone organic phase are summarized in *Table 1.2*. Both bone matrix components and signaling factors can affect bone at all stages of development [37]. Some key signaling factors and their functions are summarized in *Table 1.3*.

Table 1.2. *Components of the organic phase of bone matrix.*

Bone extracellular matrix components	Suggested functions and properties
Collagen I	Provides framework for skeletal structure and matrix calcification [34].
Biglican Decorin	Proteoglycan; affects collagen fiber growth and diameter; involved in the process of matrix mineralization [6].
Osteonectin	Glycoprotein; binds Ca^{2+} and collagen; nucleates hydroxyapatite [6].
Thrombospondin	Trimetric glycoprotein synthesis modulated by TGF-β; binds calcium, hydroxyapatite, osteonectin and other cell surface proteins; mediates cell adhesion [6]. Organizes extracellular matrix components [6].
Fibronectin	Extracellular polypeptide modulated synthesis by TGF-β with binding regions for collagen and fibrin [6]. Osteoblast attachment to substrate [6].
Osteopontin	Acidic sialoprotein; Cell attachment to matrix; involved in bone remodelling [10, 36].
Bone Sialoprotein	Sialoprotein; Cell attachment for shorter period than osteopontin [36].
Osteocalcin	Skeletal gla protein; late marker of osteogenic phenotype; involved in bone remodelling; it may also be involved in the control of mineralization through its inhibition [5, 6].

Alkaline Phosphatase	Cell-linked polypeptide; secreted from osteoblasts, promotes crystal formation in bone matrix [38, 39].
Proteoglycans I and II	Biglycan and Decorin; Affect collagen fiber growth and diameter of the fiber [6].

Table 1.2. *Components of the organic phase of bone matrix.*

Table 1.3. *Signalling factors and their functions influence bone formation.*

Signalling Factors	Functions
Bone Morphogenic proteins (BMP) [40-43]	Stimulates proliferation of osteoblasts. Causes increased matrix production. Induces MSC differentiation to osteoblasts.
Dentin matrix protein-1 (DMP1) [4]	Mineralization regulator. Induces MSC differentiation to osteoblasts. Stimulates differentiation of osteoblasts.
Fibroblast growth factors (FGF) [2, 3, 5]	Stimulates proliferation of MSCs and osteoblasts.
Platelet-derived growth factors (PDGF) [2, 3, 5]	Stimulates proliferation of osteoblasts.
Insulin-like growth factors (IGF) [44]	Stimulates proliferation of osteoblast.
Transforming growth factor-β (TGF-β) [2, 3, 5]	Induces proliferation of osteoblasts. Enhances bone resorption.
Parathyroid hormone (PTH) [45]	Causes the release of calcium from bone matrix. Induces osteoclast differentiation. Inhibits osteoblast function.
Dexamethasone (DEX) [46, 47]	Promotes the differentiation of osteoblasts.
Prostaglandin E2 (PGE_2) [2, 5, 48, 49]	Encourages the proliferation of osteoblasts. Induces the differentiation of osteoblasts. Induces alkaline phosphatase activity. Induces collagen synthesis. Inhibits osteoclast function.
Nitric oxide (NO) [50, 51]	Enhances PGE_2 release. Stimulates osteoblast proliferation. Inhibits osteoclast resorptive activity.
adenosine 3', 5'-cyclic monophosphate (cAMP) [2, 3, 5]	Enhances the growth and proliferation of osteoblasts.
Extracellular signal-regulated kinase (ERK) [21, 52, 53]	Induces the differentiations of osteoblasts. Enhances calcium deposition.

1.6 Bone mechanobiology

The primary responsibility of the skeleton is to withstand load bearing. Depending on its position in the skeleton, a bone needs a certain amount of loading to maintain its normal structure. Without adequate loading (e.g. in the microgravity of a space ship or in immobile limbs of a paralysed or bedridden patient), bone is weakened and may fracture when reloaded [54].

Bone can withstand extremely high loads, and will remain strong even following several million cycles of loading. When a force is applied to any material, such as bone, it deforms. The amount of deformation in the material relative to its original length, is the strain. The types of strain; compressive, tensile and shear (torsion), are classified based on the direction of forces applied to the material. The strain can be measured as a percentage (change in length/original length x 100). When muscle contracts, the tendon can strain as much as 5% in tension during intense activities. Compressive strains in bone during peak activities are about 0.3% strain, and bone begins to fail at about 0.7% strain (7000 microstrain) [55].

To quote Janmey and McCulloch, "mechanotransduction is the process by which cells convert mechanical stimuli into biochemical responses. It may not be a finite single process but may be a series of interrelated process that involve the recruitment of cell attachment, cytoskeleton, and signaling proteins" [56]. Mechanotransduction plays an important role in the physiology of many tissues including bone. A reduction in bone formation, bone mineral content and bone matrix production occurs during spaceflight [54]. In contrast, loading from exercise has the potential to increase bone mass [57]. The cyclic loading of a bone such as the femur or tibia during walking produces oscillating fluid shear forces in the lacunocanalicular network. Besides subjecting the osteocytes to shear forces, the loading induced compression pumps waste out of the network and directs oxygenated and nutrient fluid from the blood back to the network [58-63].

Mechanical loads *in vivo* cause deformation in bone that induces fluid flow within the bone canaliculae and deform the cells embedded in bone matrix. The cells produce second messengers which may stimulate osteoprogenitor cells to differentiate into osteoblasts resulting in new bone production and may inhibit osteoclast functions

resulting in reduced bone resorption *(Fig. 1.10)* [55]. Bone cells *in vitro* culture are also stimulated to produce second messengers when exposed to mechanical loads. However, the levels of strain used in most of these studies were 5-100 times the normal strain levels that are measured on the surface of a long bone [57, 64]. For example; the mRNA expression of osteopontin in osteoblast precursor cells during early stages of bone formation is increased three to four fold in cultured MC3T3-E1 osteoblast-like cells after mechanical loading [65]. However, osteopontin has been upregulated by mechanical strain only in supraphysiological, >3,000 μstrain or 0.3%, (typical strains incurred in bone exercise are <2,000 μstrain or 0.2% deformation [66]) whereas fluid shear on the osteoblast at physiological shear levels (1-3 Pa) produces the same response [67].

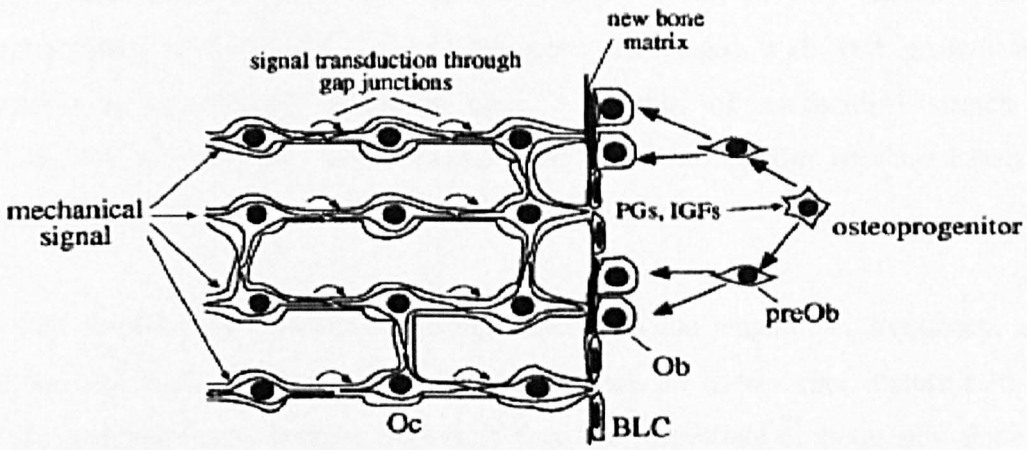

***Fig. 1.10**: Signal transduction pathways of bone cells after a mechanical stimulus. Mechanical signals stimulate osteoprogenitor cells to differentiate into osteoblasts resulting in new bone production (suggested by R. L. Duncan et al. 1995).*

Mechanical strain has been shown to alter osteoblast cell shape and increase the filamentous actin (F-actin) stress fibers which also align in the direction of load [57]. This observation would suggest that different directions of mechanical strain would produce different cellular responses, which is supported by the fact that bone matrix orientation is different in regions of compressive and regions of tension loading [68]. In an *in vivo* mouse osteoinductive tooth movement model by Pavlin and Gluhak-Heinrich, the progression of the osteoblast phenotype in the intact mouse periodontium was several-fold faster compared with that in static cultured cells without the initial proliferative response, suggesting that the mechanical signal may be targeting osteoblasts precursors to respond to an environmental challenge [11].

Osteocytes are thought to be the strain sensors of bone, which measure skeletal activity from the effects of movement of extracellular fluid caused by their bones being bent and squeezed during various activities such as walking and running [49]. *In vitro* studies have demonstrated that osteocytes respond to mechanical strain by increasing cellular levels of second messengers such as nitric oxide (NO) stimulating osteoblast proliferation [57] and leading to enhanced prostaglandin E_2 (PGE_2) release [69]. PGE_2 plays an important role in the functional adaptation of bone to mechanical load by inducing cell proliferation [6, 22, 51], alkaline phosphatase activity [70] and collagen synthesis [71] in cultured bone cells, and increasing periosteal and endosteal bone formation and overall bone mass *in vivo* [70]. Mechanical force also directly stimulates osteoblast release of inositol trisphosphate (IP3), calcium^{2+}, and adenosine 3', 5'-cyclic monophosphate (cAMP) which have been shown previously to play crucial roles in bone remodeling [72]. cAMP which has been associated with cell growth and proliferation is significantly increased after 5 minutes of mechanical stretch in osteoblasts [49, 57, 65, 69, 73]. However, the exact mechanism of stimulation is unknown.

Cell response to mechanical loading depend on the magnitude, frequency, and rate of applied load. Many studies have shown that the strain rate, determined by magnitude and frequency, is more important than the magnitude or frequency alone to induce bone formation [21]. Mechanically induced bone formation *in vivo* was not increased when loading was applied at less than 0.5 Hz, but increased four times when loading frequency was about 2 Hz [50, 74]. NO increased rapidly (a very early indicator of mechanical response) within 5 min in response to mechanical stress in bone cells [57]. Bacabac et al. (2004) suggested that low-magnitude, high-frequency mechanical stimuli may be as stimulatory as high-magnitude, low-frequency stimuli [50].

Not only are fully differentiated bone cells responsive to mechanical stimulations but also *in vitro* studies have shown that mesenchymal stem cells (MSCs) are also able to sense mechanical loads in 2-D [63, 66]. Previous studies have demonstrated that human MSCs, cultured in osteogenic medium in 2-D, decreased their growth and increased their production of mineralized matrix resulting in a more osteogenic phenotype in response to the mechanical stimulus [21, 22, 75].

As described above, a number of *in vitro* studies have been developed to apply 2-D mechanical strains and fluid flows to stimulate bone cells and MSCs in culture [50]. However, these studies may not represent the ideal environments to investigate mechanotransduction in bone cells and MSCs because they lack the 3-D cellular network and structure of real bone. Therefore, cells cultured in 3-D scaffolds provide a better physiological model for studying bone cell mechanotransduction than do cells cultured in 2-D monolayer on glass or plastic substrates. To create engineered bone tissue capable of functional load bearing, adequate mechanical properties need to be acheived. The load bearing ability of tissue engineered bone can be enhanced during the tissue engineering process, if the effects of mechanical stimulation are taken into consideration. Therefore, it is essential, in bone tissue engineering, to understand how mechanical conditions affect the formation of bone matrix components by the cells in 3-D environments in order to enhance proliferation of cells, to reduce the length of time required to grow bone tissues and to generate stronger tissues which will adapt functionally to mechanical loads minimizing the side effects of pharmaceuticals that would be experienced by patient.

1.6.1 Techniques for mechanical stimulation of cells in vitro

Many techniques *in vitro* have been used to stimulate cultured osteoblasts. For instance, broad frequency vibration [76], electromagnetic fields [77], fluid shear stress [78, 79], mechanical compressive force [22, 37, 80-84]. These techniques have induced a variety of different proliferative and differentiative responses in bone cells [85, 86]. Previous studies *in vivo* have shown that static loading of bone tissue does not cause an increase in bone formation, but cyclic loading can increase it significantly [22, 37, 77-86]. However, as each laboratory has a unique method to apply mechanical loading to cells it is very difficult to tell which stimulus is the most relevant.

1.6.1.1 Compressive loading systems

Hydrostatic pressure has been frequently used for compression of cells and tissues [21, 75, 87]. The stimulus delivered is spatially and directionally homogeneous. The waveform and magnitude of loading inputs can be easily controlled and monitored. Since there is no direct contact from loading platen, there is no concern regarding local

specimen compaction but the stimulus can cause very high values of pO2 and pCO2 in the culture medium [88].

An alternative approach is direct platen contact. This loading has proven attractive for cartilage stimulation [89]. El Haj et al. (1990) developed a culture system for axial compression of 10 mm core biopsies of cancellous bone, a device noteworthy for its provision for continuous nutrient delivery to the test specimen by means of an auxillatory pump that circulated fluid through portals in the axial compression platens [90].

1.6.1.2 Longitudinal stretch systems

This type of loading systems utilizes controlled uniaxial distention of deformable substrates. It involves compressive strain of the culture surface in a direction perpendicular to that of the tension [86, 91]. Ignatius et al. (2005) have investigated the effect of cyclic uniaxial longitudinal stretch system on a human osteoblastic precursor cell line (hFOB 1.19) in three-dimensional Coll matrices. They have found that cyclic stretching of cell seeded Coll matrices at a magnitude occurring in healing bone increased cell proliferation and slightly elevated the expression of nearly all investigated genes over unstrained controls at various time points [86].

1.6.1.3 Fluid shear systems

It is thought that during normal body movement *in vivo*, mechanical loads cause deformation in bone that creates fluid flow within the bone canaliculae and may apply stretch to bone cell membranes. Fluid flow in the bone lacunar-canalicular network is believed to be one of the potential stimuli that trigger mechanotransduction in bone. Shear stress is driven by movement of pericellular fluid through the canaliculi and over the cell surface. Bone cells *in vitro* culture can also be stimulated to produce second messengers when exposed to fluid flow [48, 81, 92, 93].

Although fluid movement induced shear stress has been recognized to act as a stimulus for cells resulting in bone remodeling *in vivo* the cellular mechanisms by which bone cells translate the loading induced signal into biochemical responses and

matrix production remained poorly understood. Jacobs et al. (1998) have modified the traditional parallel plate flow chamber system to induce oscillatory fluid flow (OFF) over the surface of cells. They suggested that OFF may be the most representative of physiological fluid flow in bone *in vivo* [94]. The developed system is based on the concept that the lacunar-canalicular network experiences pressurization in response to matrix deformation and this leads to flow along pressure gradients when bone is loaded and the flow and pressure gradients are reversed when loading is removed, thus, the fluid motion in bone is oscillatory in nature.

1.6.1.4 Combined substrate strain and fluid shear stress systems.

Since the mechanisms of action of fluid shear stresses versus substrate strain in principle may be very different and difficult to separate in normal bone, experimental designs have sometimes included both modalities to address how these two forces potentially interact [66, 87, 95-97]. The fluid flow in this system could be generated directly by flow perfusion or indirectly by substrate strain induced fluid flow or both. Owan et al. (1997) reported a four-point bending system that produced uniform levels of physiological strain and fluid forces on the cells, and modulated fluid shear stress independently of substrate strain [66]. Although these systems are thought to mimic the environment that bones are loaded *in vivo*, they are more complicated than other systems mentioned above.

1.6.2 Role of primary cilia in bone

The non-motile primary cilium is a hair-like solitary cellular structure consisting of a membrane continuous with the cell membrane [7, 32] *(Fig. 1.11 and 1.12)*. It has been known to cell biologists for over a hundred years since it was first discovered by Zimmermann in 1898 [98], but it was ignored or forgotten. No attention was paid to the primary cilium in osteoblasts and osteocytes between 1972 and 2003. Since 2003, it has been proposed by Whitfield that the primary cilium could be a mechanosensor in bone by sensing the movement of lacunocanalicular fluid [99].

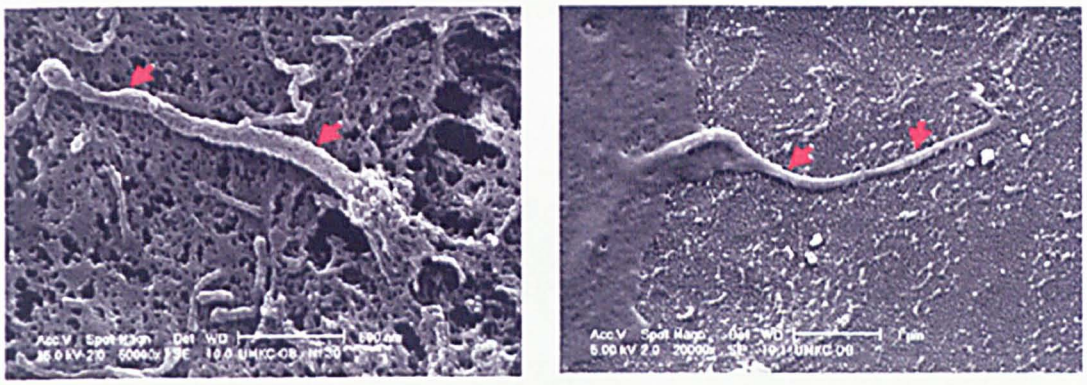

***Fig. 1.11**: Primary cilia on kidney cells. Scanning electron micrographs of primary cilium in a kidney cell (left) and an osteocyte (right) (Whitfiled 2007).*

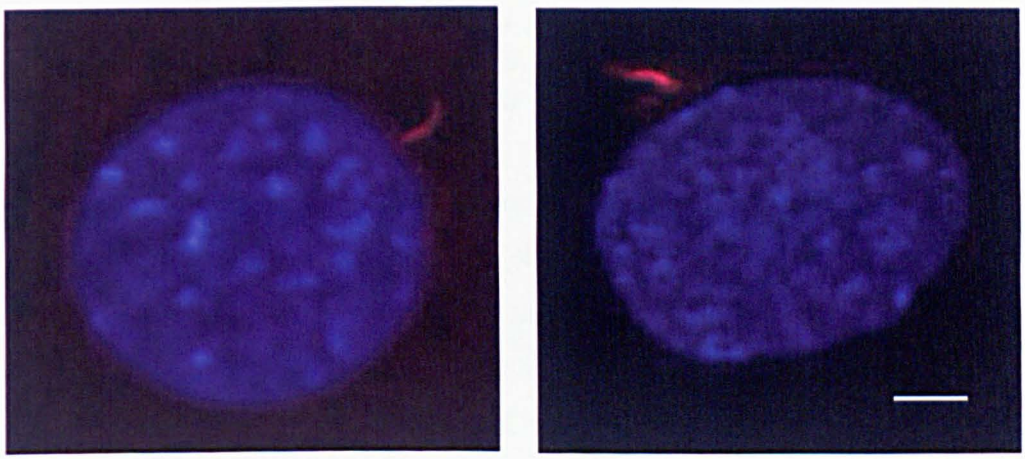

***Fig. 1.12**: Primary cilium on osteoblastic cells. An anti-acetylated α-tubulin (red) was used to stain the primary cilia on MC3T3-E1 osteoblastic cell (left) and a MLO-A5 osteoblastic-osteocytic cell (right). DNA in the nucleous is stained with DAPI (blue) (scale bar: 5 μm).*

The primary cilium extends from the mother centriole of the pair of barrel-shaped centrioles which are embedded within a protein-dense matrix known as pericentriolar matrix of centrosomes [100]. It has 9+0 pattern of elastic axial filaments (axoneme), nine peripheral microtubule pairs and the absence of the central microtubule seen in motile 9+2 cilia [101] *(Fig. 1.13)*. The relationship between the centrosome and the cilium suggests that these structures share functions and components. Only one cilium per cell is formed normally through the G0, S and G2 phases of the cell cycle. It can be formed in several hours after mitosis in proliferating cultured cells (2-4 hr after cell division in fibroblasts) [102] and starts to appear several days after the cells have reached confluence in culture. It can be seen 72 hr after it is removed by a chemical agent such as choral hydrate, cilia are about 3-5 μm long 96 hr after destruction [103].

A typical cilia is approximately 5 μm long (but up to 30 μm can be seen on cells from a kangkaroo rat kidney) [104].

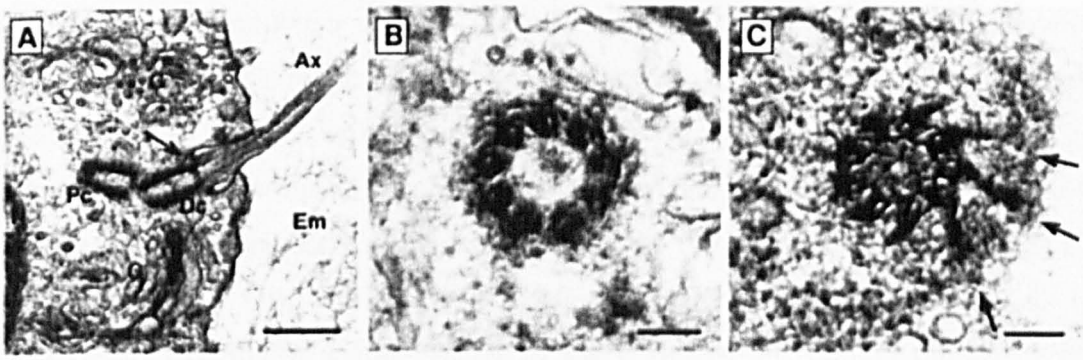

***Fig. 1.13**: Electron micrograph of diplosomal centriloes and centrosomes of chondrocytes. A, the realationship between the primary cilium (Ax), the distal (Dc), and proximal (Pc) centriole. Bar 500 nm. B, cross section of the proximal centriole. Bar 100 nm. C, Distal tip of basal body. Bar 100 nm (Poole et al. 1997).*

Primary cilia are unable to synthesize the various ciliary proteins, thus all the proteins needed for their formation and elongation have to be transported from cytoplasm of cells known as the intraciliary transport (ICT) or the intraflagella transport (IFT) system [105]. The ICT system has been described as macromolecular rafts localized between the cilia membrane and the outer doublet of microtubules and transported from the basal bodies toward the distal tip of the cilium and back towards the basal bodies [104]. The IFT88/polaris (~95-KDa) is known as an ICT protein localized to the basal body and the axoneme of cilia from *Chlamydomonas* to mammals [104, 106, 107]. Altered level of IFT88/polaris concentration influence the G1-S cell cycle progression [108-111]. *In vivo*, lack of ICT proteins, such as IFT88/polaris which is the protein encoded by Tg737, or mutation of ICT protein's genes, such as Tg737 (~3.2-Kb), results in the malformation and malfunction of primary cilia [112]. Complete knockout of the mouse Tg737 gene results in a phenotype with multiple renal, pancreatic, hepatic cysts, hydrocephalus, cartilage and bone malformations, cleft palate and supernumerary teeth [107, 109].

Primary cilia have been shown to be present in almost all vertebrate cells [101] and have recently become the focus of research interest because they are involved in human diseases and developmental abnormalities, including polycystic kidney disease, hepatic and pancreatic defects, blindness and obesity, as well as skeletal patterning

abnormalities and left-right body axis asymmetry [102, 104]. Loss of normal primary cilia function or aberrations in genes controlling either their structure development or function impacts on clinical disorders. They function both as a mechanosensor and chemosensor in renal tubular epithelia [104, 108, 113] and have recently been shown in the human kidney cell to be a fluid flowmeter, when they are bent, they can send extracellular Ca^{2+} signals into the cell and beyond to neighboring cells through gap junctions [114]. Praetorius et al. (2003) have shown that the flow response created by an increase of intracellular Ca^{2+} was dependent on the presence of primary cilia in kidney cells [115, 116]. Several ICT proteins have been found to relate to the pathogenesis of polycystic kidney disease including polycystin-1 (PC1) and Polycystin-2 (PC2). In mouse embryonic kidney cells, primary cilia act as antennae to sense fluid movement induced shear stress [114, 117]. PC1 acts as a sensory molecule that transmits the signal from extracellular fluid to PC2 which produces initial Ca^{2+} influx from extracellular environment to activate intracellular receptor. This results in massive calcium release and then regulates subcellular activities inside the cell that contribute to tissue development [104].

Since the bending of a kidney cell's primary cilium enables the cell to sense fluid flow, the bending of an osteocyte's primary cilium by moving extracellular fluid is likely to do the same thing [99, 117]. The primary cilia in chondrocytes have been shown to interact with the collagen fibers of the matrix in such a way that deformation of the matrix may induce acute bending of primary cilia [105]. This suggests that the potential for the primary cilium to act as force sensor may not only be limited to fluid shear stress but it may also act in cell-matrix or cell-cell mechanosensing in response to matrix deformation. Xiao et al. (2006) have reported that MC3T3-E1 osteoblastic cells and MLO-Y4 osteocytic cells express the Tg737 and Kif3a genes which are required for the PC1 and PC2 cilial proteins found previously in kidney cells [100]. They also have found that these cells need PC1 to activate the P1 promoter of the gene for the RUNX2 transcription factor (runt-related transcription factor 2), which targets the osteoblastic genes for Type I collagen (α1 procollagen), osteocalcin and osteopontin, resulting in an increase of osteoblast differentiation. Moreover, knockout mice lacking PC1 have reduced trabecular bone volume and density, reduced cortical bone thickness, and decreased bone mineral apposition rate.

Malone et al. (2007) have shown that the primary cilium of osteoblastic cells can deflect during fluid flow and proposed that primary cilia might be sensory organelles that translate extracellular chemical and mechanical cues into cellular responses in bone [118] *(Fig. 1.14)*. Using an siRNA transfection technique to knockdown primary cilia together with oscillatory fluid flow induced shear stress, they have shown that primary cilia are required for flow-induced increases in OPN mRNA levels in MC3T3-E1 cells, for increases in PGE_2 release and COX2 mRNA levels in both MLO-Y4 and MC3T3-E1 cells and that cilia modulate the increase in the ratio of OPG/RANKL mRNA that occurs after fluid flow in MLO-Y4. This suggests that primary cilia play a role in osteogenic responses to flow in both osteoblasts and osteocytes, and play an antiresorptive role in osteocytes. Unlike in kidney cells where the Ca^{2+} influx depends on the presence of primary cilia during flow [117], they have found that Ca^{2+} influx in bone cells is independent of primary cilia. It is possible that kidney and bone cells differ in their primary cilium-mediated responses to fluid flow causing different cellular responses.

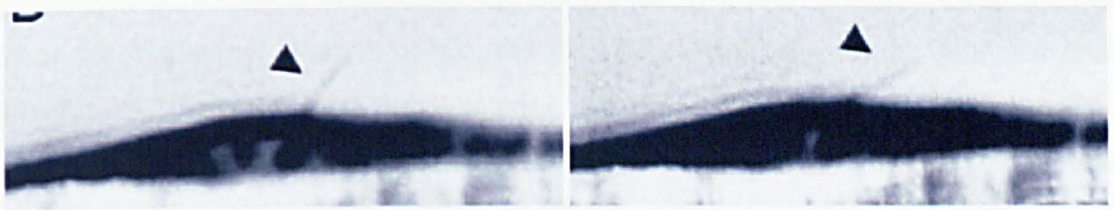

***Fig. 1.14**: Movement of a primary cilium on bone cells. Images were captured from a movie which show the side view of a primary cilium (arrowheads) extending from the apical surface of an MC3T3-E1 osteoblastic cell in a parallel plate flow chamber. Left: before the application of flow Right: during the application of steady fluid flow from left to right with about 0.03 Pa (Malone et al. 2007).*

1.7 Bone tissue engineering

Bone tissue engineering is based on the understanding of tissue formation and regeneration, and aims to induce new functional tissues by integrating knowledge from physics, chemistry, engineering, materials science, biology, and medicine [5].

There are a number of cases per year that require bone-graft procedures to replace bone defects. In Europe, the number of grafting procedures was reported to be

287,300 in the year 2000, with a predicted increase to 479,079 in the year 2005 [21, 22, 37, 48, 50, 51, 69, 74, 75, 77-80, 82-85, 96, 119-122]. Current treatments in the field of bone regenerative medicine are based on many types of bone grafts or alternatives to these, metals and ceramics. However, current therapies still have many limitations not only with the surgical techniques, but also the declining availability of donor organs and post-surgical effects [123].

Autologous bone grafts where bone is taken from another part of the patient's own body, has been the gold standard of bone replacement for many years because it provides osteogenic cells as well as essential osteoinductive factors needed for bone healing and regeneration [4, 5, 124]. Although it has a relatively good success rate, the number of cases in which it can be used is restricted, mainly due to the limited amount of the autograft that can be obtained from the donor site. Allograft, bone taken from others, could be an alternative. However, the rate of graft incorporation is lower than with the autograft. Allograft bone introduces the possibilities of immune rejection and of pathogen transmission from donor to host [4, 5, 125]. Sterilization procedures also reduce the mechanical strength of allograft [5, 126]. Metal and ceramic bone and joint replacements present several disadvantages. Although metals can provide immediate mechanical support at the site of the defect, they exhibit poor overall integration with the tissue at the implantation site, and can fail because of infection or fatigue loading [127]. Stiff metal implants, which do not have the same elasticity as surrounding bone, cause stress shielding leading to marginal bone loss around implants [5]. On the other hand ceramics are brittle and thus they cannot be used in locations of significant torsion, bending, or shear stress [128-130]. As a result of these limitations to current therapies, bone tissue engineering is emerging as a potential alternative. The field is making advances in engineering new bone tissues and the hope is that we will be able to regenerate or replace damaged and/or aging tissues without needing donated human tissue.

To engineer new bones, we need cells that will ultimately form bone, these could be osteoblasts or undifferentiated stem cells. To induce bone formation we also need signalling factors e.g. chemical, electrical and mechanical factors [4, 5, 125]. A 3-D biocompatible scaffold must be used as temporary matrix to allow new tissue to grow in a 3-D manner [4-6, 86, 125, 131]. The basic technique for tissue engineering

starts with a scaffold material such as polymer, which is then seeded with living cells and supplemented with signalling factors and grown in a controlled environment. When the cells multiply, they fill up the scaffold and grow into three-dimensional tissue. In theory, once implanted into the body, the cells will recreate their specific tissue functions *(Fig. 1.15)*. Blood vessels attach themselves to the new tissue, the scaffold dissolves, and the newly-grown tissue eventually integrates with its surroundings.

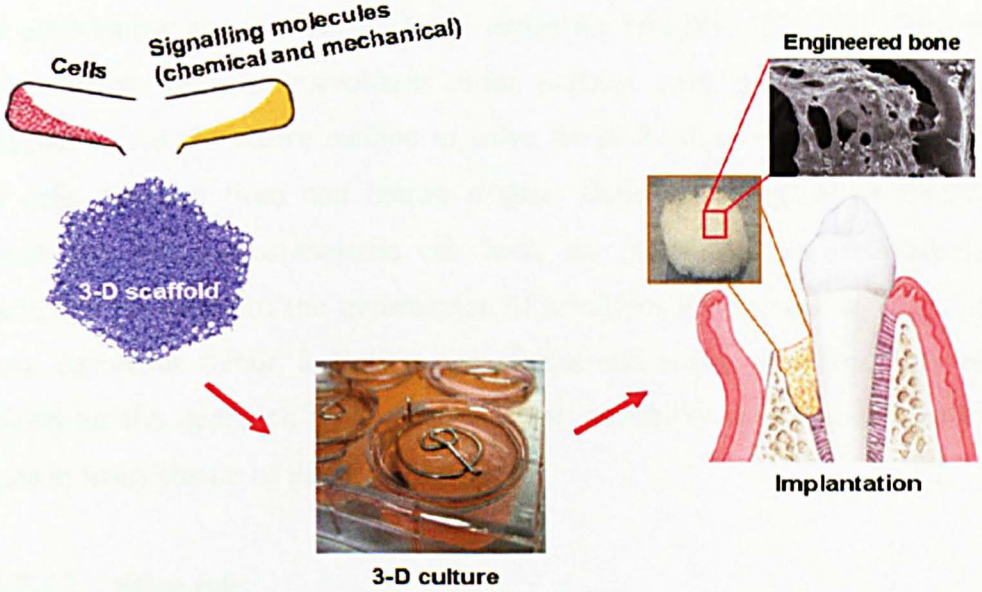

***Fig. 1.15**: Diagram of the principle concepts of bone tissue engineering.*

However, 3-D bone tissue engineering still has many problems to overcome. These limitations include limited cell in-growth into scaffolds, leading to a shell of cells around the surface of the scaffold instead of desired uniform 3-D cell distribution. It is thought that this occurs because of limited nutrient and waste exchange inside the scaffold before implantation [4, 5, 81, 131]. The correct molecular and macroscopic architecture of the engineered tissue is likely to be important for proper tissue function. The outcome of implanted engineered bone tissue will ultimately be governed by the clinical variables of each patient such as gender, habit, age, health, systemic conditions and anatomy [4, 5]. In addition, the different regions of the body will have different functional loads and vascularity. Therefore, controlling these environments to generate tissue formation, cell function, differentiation, and angiogenesis is a huge challenge for clinical application of bone tissue engineering.

1.7.1 Cells for bone tissue engineering

1.7.1.1 Osteoblasts

The isolation of autologous osteoblasts from the patients is one of the best cell choices in theory because of their non immunogenicity. However, there are several limitations of this methodology including (i) it takes time during surgery , (ii) few cells survive after biopsy and (iii) there is a low expansion rate [81, 132, 133]. Furthermore, in bone related diseases, osteoblasts from patients may not be appropriate for transplantation. An alternative method to solve the problem of low cell numbers is the use of cells obtained from non human origins. Genetically engineered animal cells, osteoblast like cells or osteoblastic cell lines, are much used *in vitro* studies [5]. However, the possibility of the transmission of infectious agents such as virus, immune rejection, cancerous tumor formation and ethical and social problems have reduced enthusiasm for this approach [23]. One promising possibility is to use stem cells which are found in many tissues of the body [5, 23].

1.7.1.2 Stem cells

Stem cells are undifferentiated cells with a high proliferation capability, the ability to self renew and the ability to differentiate into multi lineage of tissues [5, 23, 134]. However, stem cells have varying degrees of differentiation potential. The most primitive derive from the zygote (fertilized oocyte) in the embryonic stage [135], also known as embryonic stem cells (ESCs). The stem cells found in fully differentiated tissue are called adult stem cells (ASCs) [136].

Embryonic stem cells

Undifferentiated ESCs have the potential to differentiate into many kinds of cells. For instance, cardiomyocytes, haematopoietic cells, endothelial cells, neurons, chondrocyte, adypocytes, hepatocytes, pancreatic islets and so on *(Fig. 1.16)* [136]. Previous studies have shown that ESCs can differentiate to osteoblasts in the presence of dexamethasone [5]. However, the criticisms against their use because of ethical and

social questions are probably the most difficult barrier to the use of ESCs in regenerative medicine.

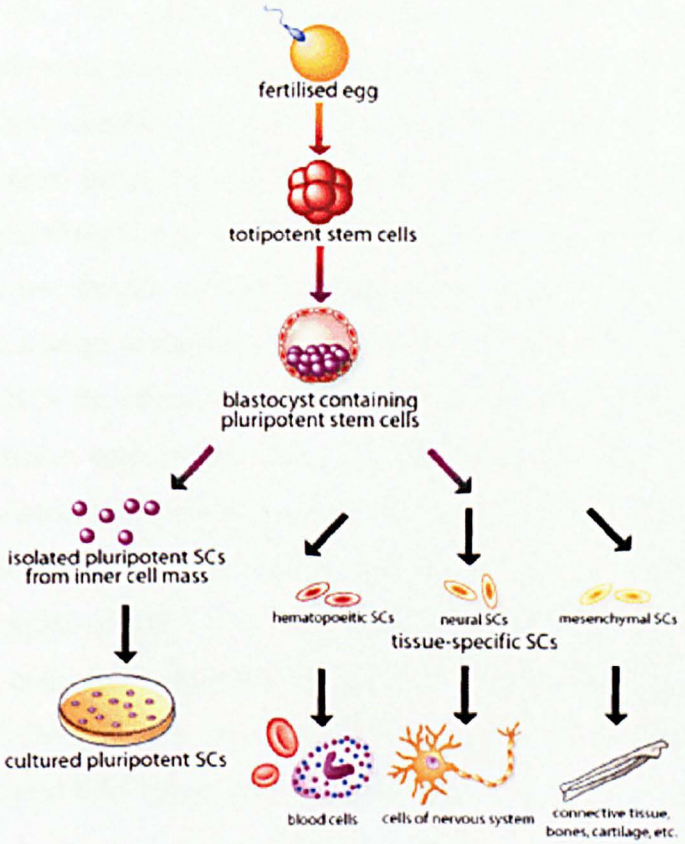

Fig. 1.16: *Pluripotent of embryonic stem cells. Embryonic stem cells originate as inner mass cells within a blastocyst. The stem cells can become many types of tissues in the body. (Picture from http://www.scq.ubc.ca/stem-cell-bioengineering/ ; April 2009).*

Adult stem cells

ASCs can be found in the bone marrow, periosteum, cartilage, muscle, fat, nervous system, blood, skin, and possibly, liver and pancreas [20]. In the bone tissue engineering field there has been a special interest in the marrow stromal cells located in the bone marrow, also known as Mesenchymal stem cells (MSCs) [5, 14, 15, 23]. Since their discovery in bone marrow MSCs have been found in other tissues such as adipose tissue and periosteum, but bone marrow is still the most exploited source of these cells [15, 23, 137]. A number of studies both *in vitro* and *in vivo* have stated that bone marrow contains an osteogenic precursor cell that can result in new bone matrix formation [22].

MSCs were demonstrated to rapidly proliferate *in vitro* and form fibroblast-like colonies in tissue culture plastic called colony-forming units fibroblastic (CFU-f) [14, 15, 21, 75, 132, 136, 138, 139]. MSCs have been shown to differentiate into bone, cartilage, fat, muscle skin, tendon and other tissues of mesenchymal origin when placed in appropriate culture conditions *(Fig. 1.17)* [5, 15]. Although ESCs have the potential to provide an unlimited supply of osteoprogeniter cells for transplantation, they have a high risk of teratoma formation [140, 141]. In contrast, autologous MSCs derived from patient's bone marrow should not face these problems and can be more easily induced into the osteogenic lineage compared with ESCs [142]. It seems that MSCs have several advantages over ESCs for use in bone tissue engineering. Although MSCs have many potential uses in tissue engineering, there are still some limitations that need to be addressed. For instance, the percentage of MSCs present in bone marrow is very low about 1 in 100,000 cells [14] and it also has been shown that the number as well as the differentiation potential of MSCs was decreased when isolated from elderly patients [14]. Therefore, it may not be clinically realistic to use autologous MSCs to repair large bone defects until the problems of expansion are overcome. Alternatively, ways of using allogenic donated MSCs may need to be devised.

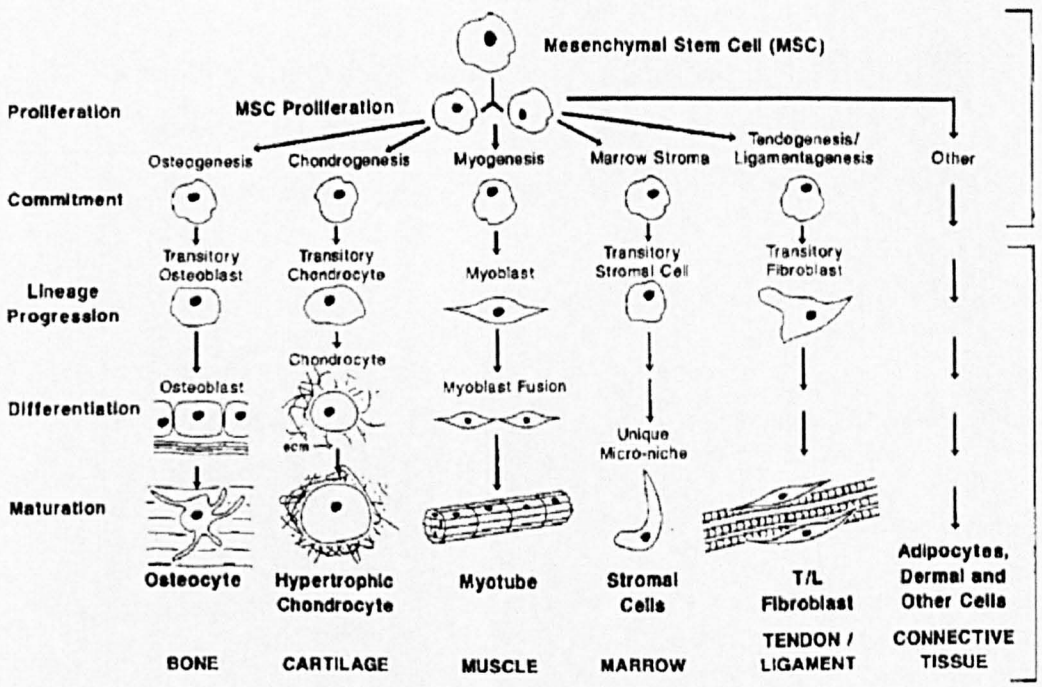

***Fig. 1.17**: Multipotent of mesenchymal stem cells. Mesenchymal stem cells have the potential to differentiate into many types of tissues including bone (Caplan 2005).*

1.7.2 Scaffolds for bone tissue engineering

Any bone tissue consists of matrices and cells. *In vivo*, the matrix is a 3-D scaffold for cells and provides them with a tissue specific environment and architecture [14, 15]. Furthermore, it serves as a reservoir of water, nutrients and any essential factors for cell growth. Not only is an appropriate 3-D matrix an essential component for bone tissue *in vivo* but also an essential component *in vitro* for new engineered bone tissue. Scaffolds in bone tissue engineering provide cells with 3-D matrix upon which to adhere, proliferate and produce matrix. They can also function as delivery vehicles for cells when implanted. However, it is important to realize that the properties of a scaffold *in vitro* may influence cell survival, signaling, growth or even gene expression of cells [5]. Some scaffolds used for bone tissue engineering are summarized in *Table 1.4*.

To obtain an appropriate scaffold for engineered bone tissue, the consideration of scaffold properties, e.g. biocompatibility, porosity, pore size, surface properties, osteoinductivity, mechanical properties and biodegradability, are important. Ideally, a scaffold for bone tissue engineering should have the following characteristics:

- 3-D and highly porous with an interconnected pore network for cell growth, nutrients and waste product transportation [5].
- Biocompatible and controllable biodegradability [124, 126, 131, 143-146].
- Suitable surface for cell attachment, proliferation and differentiation [124, 126, 143-148].
- Sufficient mechanical properties to match and bear load at the site of implantation [124, 131, 143-145].

Table 1.4. Natural and synthetic polymers used for bone tissue engineering applications.

Material	Origin	Characteristics
Collagen [149, 150]	Natural	Low immune response Good substrate for cell adhesion Low mechanical properties
Collagen-glycosaminoglycan (CG) [151-154]	Natural	Supports osteogenesis and chondrogenesis of MSCs Low mechanical properties High biodegradability and biocompatibility Can be produced with a wide range of homogeneous pore sizes
Chitosan [155]	Natural	Hemostatic Promotes osteoconduction and wound healing
Starch [5]	Natural	Thermoplastic behavior Good substrate for cell adhesion Non-cytotoxic and biocompatible Bone bonding behavior when reinforced with hydroxyapatite Scaffolds based on these materials have good mechanical properties
Hyaluronic acid (HA) [156, 157]	Natural	Minimal immunogenicity Chemotactic when combined with appropriate agents Scaffolds with low mechanical properties
Poly(hydroxybutyrate) [5, 158]	Natural	Natural occurring b-hydroxyacid Adequate substrate for bone growth Usefullness is limited due to brittle nature
Demineralized bone [138]	Natural	Promotes osteogenic differentiation of bone marrow stromal cells Good mechanical properties Good biocompatibility
Titanium [159, 160]	Synthetic	Promotes bone growth both *in vivo* and *in vitro* High biocompatibility No biodegradability Excellent mechanical properties
Poly(L-lactic acid) (PLLA) [161-164] **and poly(D,L-lactic-co-glycolic acid) (PLGA)** [148, 163-165]	Synthetic	Improves the distribution of calcified ECM Low mechanical properties Promotes growth and osteoblastic function Controllable biodegradability Degradation by hydrolysis Generates an inflammatory response in animal studies

Poly(a-hydroxy acids) [5]	Synthetic	Extensively studied aliphatic polyesters Degradation by hydrolysis It can present problems regarding biocompatibility and cytotoxicity in the surrounding area of the implantation site
Poly(e-caprolactone) [166]	Synthetic	Aliphatic polyester Degraded by hydrolysis Slow degrading Degradation products incorporated in the tricarboxylic acid cycle Good mechanical properties
Ceramic e.g. bioactive glass [167-170], **calcium hydroxyapatite ceramic** [171] **and tricalcium phosphate ceramic scaffold** [172]	Synthetic	Good bone bonding properties Degradable and nondegradable good strength but low toughness and brittle Enhances bone apposition Osteoconductivity Creates a strong bone/implant interface
Polyurethane (PU) [126, 146, 147, 173-177]	Synthetic	High biocompatibility Degradable and non degradable Promotes tissue ingrowth Supports attachment and proliferation of chondrocytes Promotes the expression and deposition of extracellular matrix proteins Supports cell proliferation and the differentiation of MSC into osteoblasts Excellent mechanical properties

Table 1.4. *Natural and synthetic polymers used for bone tissue engineering applications.*

1.7.2.1 Polyurethane (PU) scaffolds

Polyurethanes (PUs) are a popular group of biomaterials applied to medical devices that have been suggested for use in bone tissue engineering because of their excellent mechanical properties, biocompatibility and easy handling during *in vitro* culture and *in vivo* implantation [5]. Furthermore, PUs have been also shown *in vivo* to support cell growth and proliferation by increasing tissue ingrowth rates [173].

The components of PU can be represented by three basic segments described by the following general form [176]:

$$P - (D(CD)_n - P)_n$$

*P = the polyol, called the soft segment, terminated by hydroxyl groups (-OH)**

*D = the diisocyanate, low molecular weight compound, can react either P and C***

*C = the chain extender, small molecule with either hydroxyl or amine end group***

** Conventional polyols are usually polyethers or polyesters.*

*** The combination of D and C segments is called the hard segment of the polymer.*

Although, traditionally PUs have been widely used for their excellent mechanical properties and moderately good blood compatibility [178], they have also been singled out as being problematic in term of their low biodegradation. Once PUs were implanted, several sources were found to contribute to their degradation. For example, the aliphatic ester linkages in polyester-urethanes are known to be susceptible to hydrolytic degradation [179], whereas polyether-urethane materials are known to be susceptible to degradative phenomenon involving crack formation and propagation [180]. Enzymes in the physiological environment such as hydrolytic enzymes are another factor contributing to PU degradation [181]. The most often reported case of *in vivo* PU degradation is that associated with the PU-covered silicone breast implants. It has been found that the PU foam was missing (with only the basal layer of the PU foam still being visible by SEM [182]. This was evidence that a biodegradation process was occurring which resulted in substantial amounts of material being removed.

While many researchers have used PUs as long-term implant materials and have attempt to shield them from the biodegradation processes [178, 179, 181, 182], many recent works have utilized the flexible chemistry and diverse mechanical properties of PU materials to design degradable polymers for bone tissue engineering [144, 146, 181, 183]. The rate of degradation of PUs is also affected by biomaterial chemical structure, morphology and composition [178]. The surface composition of PUs varies because of the mobility of soft segments [126]. *In vivo*, the degradation of PUs is closely related to surface organization of PUs [178] and the degradation rate is twice as rapid compared with degradation *in vitro* [178]. Furthermore, there is evidence that the hard segment

may also influence the biodegradability of PUs [146] so that finding the appropriate compositions of the hard/soft segment ratio may improve controllable degradable properties for use in bone tissue engineering [183].

Biodegradable PU can be produced using variety of techniques, including electrospinning, carbon dioxide foaming, wet spinning, salt leaching and thermally induced phase separation [174]. Previous studies have shown that biodegradable PUs can support the ingrowth of cells and tissue, and undergo controlled degradation to noncytotoxic decomposition products [144, 146, 181, 183]. PU chemistry can be exploited to prepare a variety of materials, including segmented elastomers, elastomeric foam and injectable foam [174]. Due to their tunable biological, mechanical, and chemical properties, biodegradable PUs present compelling future opportunities as scaffolds for bone regeneration and tissue engineering.

However, besides the choice of adequate materials, the macro and micro-structural properties of the materials such as porosity, pore size, surface properties and mechanical properties are also important. These properties affect not only cell survival, signalling, reorganization and growth but also their gene expression and the preservation, or not, of their phenotype [184]. From a review of experimental and clinical studies it can be concluded that an appropriate 3-D scaffold is an essential component for a tissue engineering strategy and that the ideal scaffold and matrix material for bone tissue engineering has not been well developed. Advances in biomaterials may support the establishment of functional scaffolds for bone tissue engineering research and the clinical application of engineered bone tissues.

1.7.3 Bioreactors for bone tissue engineering.

Over the past few years, bioreactors have been designed and used to modulate mass transfer, which is essential both for nutrient supply and waste product elimination to maintain cell viability within large 3-D constructs. In addition, bioreactors should permit the development of efficient cell seeding strategies that can provide uniform cell distribution within large scaffolds, apply mechanical conditioning to the cells, and

provide the automated and controlled tissue mass culture needed to manufacture reproducible tissue engineered constructs [185, 186].

From a bone tissue engineering perspective, static culture does not mimic the dynamic conditions, mechanical and hydrostatic pressure, found in bone *in vivo* [5]. Bioreactors were developed to better mimic these conditions and have been widely used in *in vitro* studies [5, 132]. The use of static flasks and magnetically stirred flasks into which the seeded scaffolds can be suspended (spinner flask) was reported as a first generation bioreactor [187] in which turbulence can be induced around the construct [186]. Although, turbulence has a beneficial effect on nutrient and waste product transfer, it is very difficult to control the shear stress on such cell-seeded scaffolds.

One of the most popular bioreactors in use is the Rotating-wall perfused vessel (RWPV) or Rotary cell culture system (RCCS) which was first developed by the NASA Johnson Space Center based on the concept of space flight or anti-gravity to keep cells from falling to the bottom of the vessel under the action of gravity and to provide fluid flow perfusion within the vessel [186, 187]. However, the growth of bone tissue culture in RWPV was found to be non-uniform, always lower at the center than at the edges and the local fluid-dynamic shear stress being maximum at the edges [188]. Many studies have shown that the mechanical stress plays an important role in bone tissue growth and differentiation [73, 80, 84, 120], but it seems that RWPV does not provide enough mechanical stimulus to support this properly. Many studies have shown reduced bone cell growth and differentiation in space flight and anti-gravity environments [57, 186, 189].

Other designs are based on perfused columns or chambers in which the tissue matrices are fixed and there is continuous medium recirculation [92, 186, 190, 191]. In these systems, physical conditioning of the tissue-engineered constructs relies upon hydrodynamic and fluid flow induced shear forces. In addition, the presence of dynamic mechanical forces during cultivating stimulates tissue development by providing stimuli at variety of frequencies and loading.

Most dynamic culture systems reported use the dynamic seeding process together with continuous flow perfusion. However, these systems are much more

complicated than static cultures and also can increase cost and time of processing. In addition, turbulence or high shear stress produced by fluid flow from bioreactors could remove attached cells from the scaffold struts [92].

1.8 Overall hypothesis

The molecular mechanisms underlying the effect of mechanical stimulation on bone cell function, matrix production, mineralization and mechanotransduction responses have yet to be determined. The majority of studies have been carried out in 2-D culture systems in which cells are subjected to fluid flow and/or stretch. However, most cell types *in vivo* exist in 3-D configurations. Moreover, the type and appropriate amount of physical stimuli needed to improve tissue formation remains speculative. Factor such as level and direction of mechanical strain, dynamic versus static regimens, as well as oscillation frequency, amplitude, and cycle form may be critical for the tissue remodeling response.

For these reasons, the optimization of functional stimulation systems for bone growth in response to mechanical stimulation was carried out in this report. We hypothesized that (i) the commercial industrial grade of PU foam is biocompatible and can be used in 3-D *in vitro* static culture of bone cells (chapter 3), (ii) dynamic mechanical stimulus can improve cell growth and matrix production during 3-D static culture (chapter4), (iii) mechanical dynamic compressive loading will have the ability to stimulate osteogenic differentiation of hMSC in the same way as treatment with DEX (chapter 6), (iv) if the primary cilia were sensors for mechanical forces such as fluid flow or strain induced shear stress, then mature cells lacking a cilium would become unresponsive, unable to upregulate matrix protein gene expression and would not increase matrix production in response to mechanical stimulation (chapter 5). The overall aims of our studies are not only to provide tissue engineering solutions but also to develop an important *in vitro* model system for the enhancement of understanding into mechanicotransduction, and the relationship between physical conditions, cellular function, tissue development and tissue properties.

CHAPTER TWO: Materials and Methods

2.1 Materials

1. Scaffold: interconnected open pore Polyether Polyurethane (PU) foam grade XE1700V (Caligen Foam Ltd, Lancashire, UK (kindly donated by Professor Anthony J. Ryan, Department of Chemistry University of Sheffield, UK).
2. Osteoblastic cells: MLO-A5 (kindly donated by Professor Lynda Bonewald, University of Missouri Kansas City USA, under an MTA agreement with The University of Texas Health Science Center at San Antonio).
3. Human fibroblast cells were isolated from skin obtained from abdominoplasty or breast reduction operation (According to local ethically approved guidelined, NHS Trust, Sheffield, UK) and kept in Kroto Research Institute's tissue bank, University of Sheffield (licensing number 12179).
4. Bone marrow mononuclear cells (StemCell Technologies Inc.,London, UK or Lonza Biologics, Cambridge, UK).
5. MLO-A5 basal culture media: Alpha minimum essential medium (α-MEM) (from Invitrogen, Paisley, UK) supplemented with 5% fetal bovine serum (FBS, HyClone, Cramlington, UK), 5% bovine calf serum (BCS) (HyClone, Cramlington, UK), 1% penicillin/streptomycin (P/S) (final concentrations: 100 units/ml) and 0.25% fungizone (F) (Sigma Aldrich, Dorset, UK).
6. MG63 and human fibroblast basal culture media: Dulbecco's Modified Eagle's Medium (DMEM) (Biosera, East Sussex, UK) supplemented with 10% fetal calf serum (FCS) (Sigma Aldrich, Dorset, UK), 1% P/S, 0.25% F and 1% glutamine (final concentrations: 100 μg/ml) (Sigma Aldrich, Dorset, UK).
7. MC3T3-E1 basal culture media: α-MEM supplemented with 10% FCS, 1% P/S and 0.25% F.
8. hMSC basal culture media: α-MEM supplemented with 10% fetal calf serum (FCS), 1% P/S, 0.25% F and 1% glutamine.
9. hMSC osteogenic differentiation media: hMSC basal culture media supplemented with dexamethasone at final concentration 10 nM, ascorbic acid-2-phosphate (AA) 50 μg/ml. and 5mM of β-glycerophosphate (βGP) (Sigma Aldrich, Dorset, UK).

10. Osteogenic media A: Any basal culture media supplemented with 50 μg/ml of AA (Sigma Aldrich, Dorset, UK).
11. Osteogenic media B: Any basal culture media supplemented with 50 μg/ml of AA and 2mM of βGP .
12. Loading media: DMEM supplemented with 2% fetal calf serum (FCS), 1% P/S and 0.25% F.
13. Medical grade stainless steel rings (internal diameter 1 cm).
14. Medical grade stainless steel wires (diameter 1 mm).
15. MTT (Sigma Aldrich, Dorset, UK).
16. MTS (CellTiter 96® AQ_{ueous} One Solution Reagent) (Promega, Southampton, UK).
17. DAPI [4'-6-Diamidino-2-phenylindole] (Sigma Aldrich, Dorset, UK).
18. Propidium iodide (PI) (Sigma Aldrich, Dorset, UK)
19. Mechanical testing machine ELF3200 (ElectroForce Systems Group, BOSE, Minnesota, USA).
20. Biodynamic chamber (ElectroForce Systems Group, BOSE, Minnesota, USA).
21. Oscillatory fluid flow chamber provided by Professor Christopher Jacobs, Columbia University, New York City, USA, to use in The Cell and Molecular Biomechanics Laboratory (CMBL) at Stanford University, California, USA [94].
22. Interlaken sevohydrolic loading machine (Interlaken model 3350, Minnesota, USA).
23. Inverted stage fluorescence microscope (Image express, Axon Instrument, California, USA) at excitation wavelength 365 nm.
24. Sirius red (direct red dye)(Sigma Aldrich, Dorset, UK) .
25. Alizarin red (Sigma Aldrich, Dorset, UK).
26. Mouse antibody to Acetylated alpha tubulin [6-11B-1] (2mg/ml) (Abcam plc, Cambridge, UK).
27. FITC-conjugated rabbit anti-mouse immunoglobulins (green) or Rhodamine-conjugated goat anti-mouse immunoglobulins (red) (400mg/L) (DAKO, California, USA).
28. High-Capacity cDNA Reverse Transcription Kits (Applied Biosystems, California, USA).

29. Pre-Developed TaqMan®Assay Reagents (Applied Biosystems, California, USA).
30. Primer and probes for Real time quantitative RT-PCR of 18S, OPN, DMP1, COL1 (Applied Biosystems, California, USA).
31. TriReagent (Sigma Aldrich, Missouri, USA).
32. X-tremeGENE siRNA (small interfering ribonucleic acid) transfection reagent (Roche Molecular system, California, USA).
33. siRNA targeting polaris protein (Invitrogen, California,USA). (sequence: 5'-CCAGAAACAGATGAGGACGACCTTT-3').
34. Scrambled control siRNA (Invitrogen, California,USA).
35. ABI Prism 7900 detection system for Real time RT-PCR (Applied Biosystems, California, USA).
36. Dynabeads® mRNA DIRECT™ Kit (Invitrogen, Paisley, UK).
37. The JumpStart™ RED HT RT-PCR kit (Sigma Aldrich, Dorset, UK).
38. RNA primer sequences for RT-PCR (MWG biotech, London, UK).
39. FlashGel™ system (Lonza, Berkshire, UK).
40. Thermal cycler-Techne TC-312 (Techne, Cambridge, UK).
41. Zeiss LSM510 META confocal microscope system (Carl Zeiss AG, Oberkochen, Ger).
42. Scanning Electron microscopy (SEM) (Phillips/FEI XL-20 SEM) at an accelerating voltage of 10-15 kV.
43. Dynex microtiter® plate reader (Dynex Technologies Ltd., West Sussex, UK).
44. NanoDrop ND-1000 UV/Vis Spectrophotometer (NanoDrop products, Wilmington, USA).
45. ImageJ software (National Institutes of Health, Maryland, USA).
46. Bio image intelligent quantifier version 3.2.1 (Bio image Systems Inc., Michigan, USA).
47. WinTest software (BOSE, MN, USA).
48. All other chemicals were from Sigma Aldrich (Dorset, UK) unless otherwise stated.

2.2 Methods

2.2.1 Cell preparation

2.2.1.1 Osteoblastic cell lines and human fibroblast cells

MLO-A5 osteoblastic cell lines are immortalized cells grown from mouse long bone, established by Kato et al. (2001) [192]. Cells were isolated from long bones of seven 14-day-old osteocalcin promoter-driven T-antigen transgenic mice. MLO-A5 cells represent the postosteoblast-preosteocyte cells that exhibit intermediate characteristics between these cells and are thought to behave similary to the cells that are responsible for mineralization in bone. Kato et al. have also described that MLO-A5 cells as spontaneously producing more bone like matrix faster in culture than other osteoblastic cell lines, even without the additional chemical factors normally added to induce cell differentiation and matrix production. However, they had never been used in mechanotransduction studies prior to this study.

Standard define medium was used to expand all cell types. The cells were cultured in T75 flasks at 37°C in a humidified atmosphere with 5% CO_2 and examined daily, observing the morphology, the colour of the media and the density of the cells. The media was changed every 3 days. Osteogenic medium was used to study bone matrix growth and mineralization.

2.2.1.2 Human Mesenchymal Stem cells (hMSC)

Frozen human mononuclear cells from bone marrow, which contain hematopoeitic cells and mesenchymal stem cells were obtained from donors and purchased through registered companies shown in chapter 6. To maximize recovery of the cells from freezing when thawing, the cells were warmed very quickly by placing the vial directly from the dry ice container into a 37°C distilled water bath. As soon as the last ice crystal was melted, the cells were immediately diluted into prewarmed basal culture media. The number of viable cells was counted using a hemocytometer and trypan blue dye, which is excluded by live cells but accumulates in dead cells.

Mononuclear cells were plated in T25 flask with a minimum of 10^5 per flask. 1 mg/ml of DNAse I in PBS was used to reduce cell clumping. 3 ml of basal media was added every 3 days for 10 days before changing the media to allow hMSCs to adhere to the plastic surface, this stage was termed passage 0 (P0). After the P0 cells had adhered, the non adherent hematopoietic cells were washed away leaving fibroblast-like cells with a spindle-like morphology which form the colonies called fibroblastic colony forming units (CFU-f) *(Fig. 2.1)*. After P0, their morphology changes from a spindle-like morphology to a larger, flatter phenotype [3] *(Fig. 2.2)*. When the P0 cells had reached 80% confluence, the cells were passaged into P1 with density $5x10^5$ cells in T75 flask in 10 ml of media; cells were only used between P1 to P4 in order to retain their multipotentiality. It has been noted by Wall et al. (2007) that growth rate and calcium deposition of hMSCs decreases from passage 4 [193].

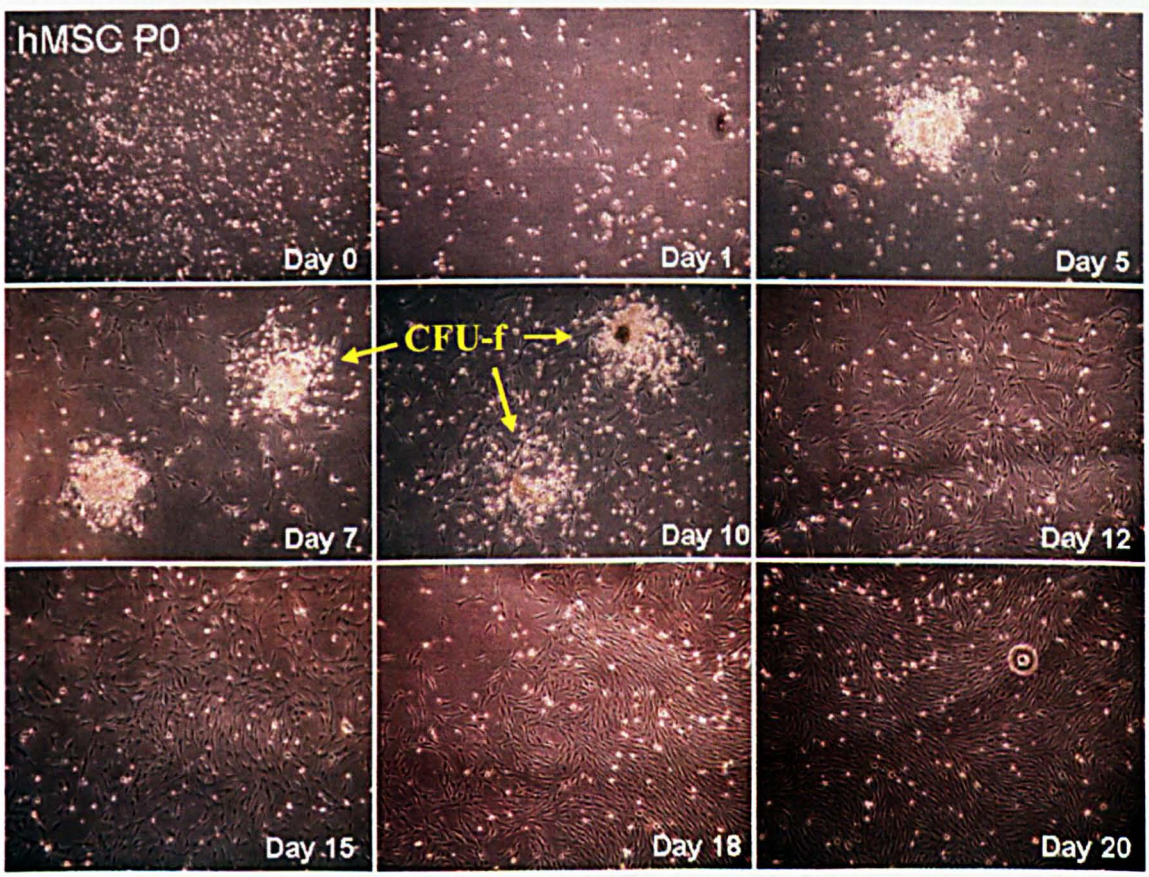

***Fig. 2.1**: Light micrographs of hMSC P0. The adherent fibroblast-like cells have a spindle-like morphology and form fibroblastic colony forming units (CFU-f) (arrow) over 20 days (x4).*

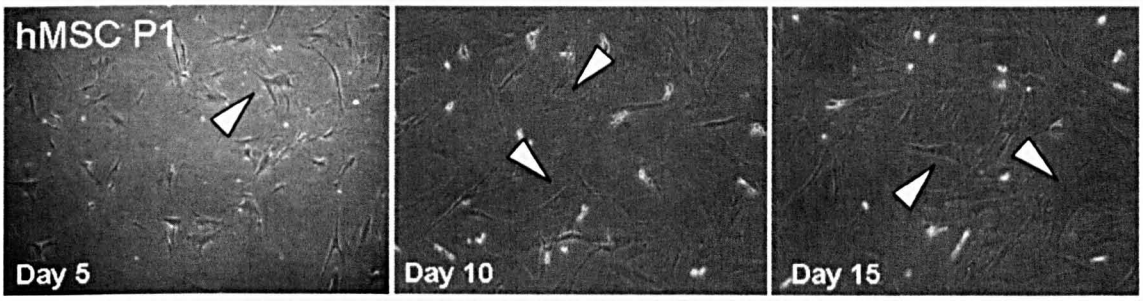

***Fig. 2.2**: Light micrographs of hMSC P1.* Some cells change from a spindle-like morphology seen in P0 to a larger, flatter phenotype (arrow head) (x10).

2.2.2 Scaffold preparation

The polymer scaffolds used in this study were based on polyether polyurethane (PU). The foam was synthesised from a 3500mw ether polyol and Toluene Diisocyanate (TDI) using water and methylene chloride as blowing agents with a siloxane silicone stabiliser and an amine catalyst (BDMAEE). To characterise the average strut and pore size of the scaffold, 45 struts and 45 pores were randomly selected from SEM images. Strut width was designated as width at the narrowest portion and average pore size was designated as the mean of the widest part of the pore and the width at 90 degrees to this. All widths measured using ImageJ (National Institutes of Health, USA) image analysis package. The pore size of the foam varies between 150-1000 μm (about 400 μm in average). The strut width is about 65 μm in average (43-96 μm) *(Fig. 2.3)*. The mechanical properties were tested by a single cycle of loading to 50% strain in 4 at 0.2 mm/sec using mechanical testing machine ELF3200. Force and displacement data was recorded by WinTest software. Properties of the polyurethane foam used as a scaffold is shown in *Table 2.1*.

All samples were cut to a cylindrical shape with diameters of 10 mm and heights of 10 mm *(Fig. 2.4)* and were subsequently sterilized using 70% ethanol and left overnight at room temperature in a sterile 20 ml tube. Prior to cell seeding, the scaffolds were washed with phosphate buffered saline (PBS) 5 times by shaking the tube and were immersed in culture media for 10 minutes under the laminar flow hood. The scaffolds were removed from the media, gently squeezed to remove excess media and placed in 1 cm internal diameter stainless steel rings (produced in the department of

engineering materials) which act as a holder and support while initial cell attachment occurs *(Fig. 2.5)*.

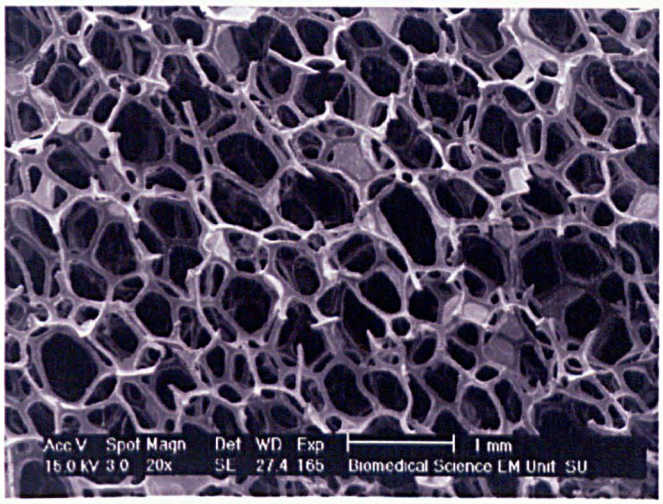

***Fig. 2.3**: Scanning electron micrograph of a PU scaffold. The average pore diameters of PU are between 150-1000 μm. The strut width is between 43-96 μm as measured from SEM images.*

***Table 2.1**: Properties of the polyurethane foam used as a scaffold. *properties specified by vendor, + Properties measured in the laboratory.*

Properties of the polyurethane scaffold	
Density (Kg/M^3)*	15-18
Tensile strength (kPa)*	80
Elongation at break (%)*	100
50% compression set (%)*	10
40% CLD hardness*	1.5-3
Porosity L/min*	120-250
Young's modulus of elasticity (kPa)$^+$	2.87 ± 0.02
Strut width (μm)$^+$	43-96
Pore size (μm)$^+$	150-1000

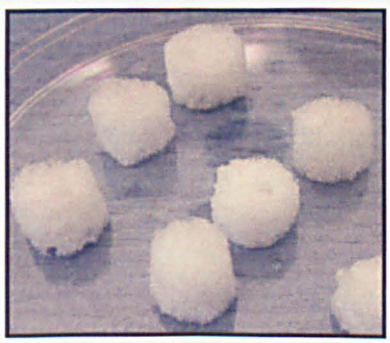

***Fig. 2.4**: Cylindrical PU scaffolds. Size of PU is 10 mm of diameters and 10 mm of heights.*

***Fig. 2.5**: Sterilized PU scaffolds. The scaffolds were pre-soaked with basal media in 1 cm internal diameter stainless steel rings.*

2.2.3 Cell seeding and culture in 3-D scaffolds

Cells were passaged under standard culture conditions in basal medium. At 80% confluence, the adherent cells were enzymatically released using trypsin/EDTA, pelleted by centrifugation at 1200 revolutions per minute (rpm) for 5 minutes and resuspended in 1 mL medium. 10 µl of cell suspension was mixed with 10 µl of trypan blue dye. Cell numbers were determined using a hemocytometer.

Static culture was used in this experiment to exclude the effects of other mechanical factors from bioreactors that may interfere with the effects of compressive mechanical stimulation applied in this study. The optimum cell density and volume of cell suspension were determined as described in chapter 3. 2.5×10^5 cells in 100 µl was added onto the top of each sterile scaffold in a well plate and, after incubating for 1 hour for initial attachment; sufficient basal culture media was added to cover the scaffolds and stainless steel rings *(Fig. 2.6A)*. Cells were allowed to attach overnight in a cell culture incubator. Subsequently, cell-seeded scaffolds were removed from the stainless steel rings and held in the media by stainless steel wire holders made from LEOWIRE® (0.8 mm in diameter, cat. No. c0400-80, Leone orthodontic and implantology, Florence, Italy) to ensure the scaffolds were kept fully immersed in the media, and then fresh media was added to cover the scaffolds *(Fig. 2.6B)*. The cell-seeded scaffolds were cultured in the incubator for the experimental period and were supplied with fresh media every 3 days. Cell seeded scaffolds were monitored for cell viability (MTT and MTS), loaded by dynamic compression or further investigated at specific time points depending on the experimental design.

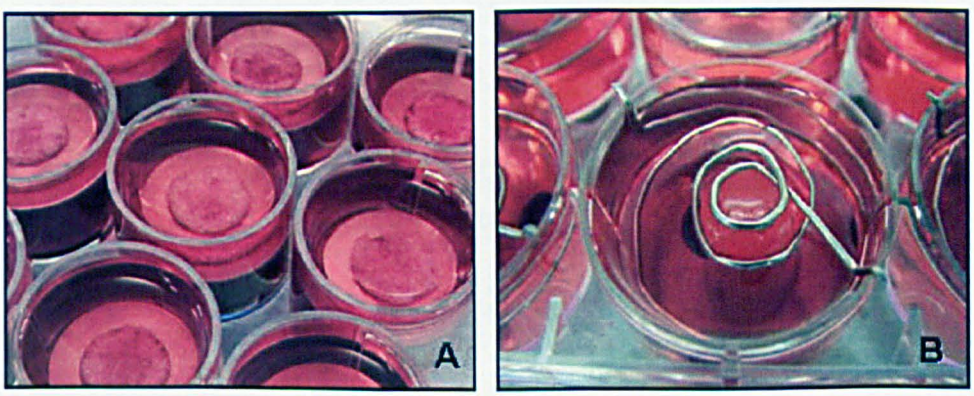

***Fig. 2.6**: Steps of cell seeding on PU scaffold. Cells were seeded in scaffolds retained in steel ring, and then sufficient media was added to cover the scaffolds after 1 hr incubation (A). On day 1 of culture the rings were removed and the scaffolds were held down by a spiral stainless steel holder (B).*

2.2.4 Application of mechanical loading

Dynamic cyclic compression was performed in a BioDynamic™ chamber mounted on a ELF3200 mechanical testing machine. The biodynamic chamber and all circuit components were sterilized by autoclave *(Fig. 2.7)*. Under the laminar flow hood, the sample to be loaded was removed from the well plate and placed into the chamber, between two compressive platens. The chamber was filled with 200 ml of loading media and then was mounted onto the mechanical testing machine *(Fig. 2.8)*. The cell seeded scaffolds were dynamically loaded in compression using a sine wave at 1Hz, 5% strain (displacement of -0.5 mm.) for different periods of time in culture. The loading force and displacement data were automatically recorded by WinTest software provided by the company. During loading, a paired-unloaded sample was kept in a sterile media-filled T75 flask in the same conditions as the loaded sample with the exception of mechanical stimulation, at room temperature. Between loading cycles, both loaded and non-loaded control samples were cultured in an incubator under standard conditions. The mechanical properties of the scaffold were tested by a single cycle of loading to 50% strain in air at 0.2 mm/sec immediately prior to the following assays.

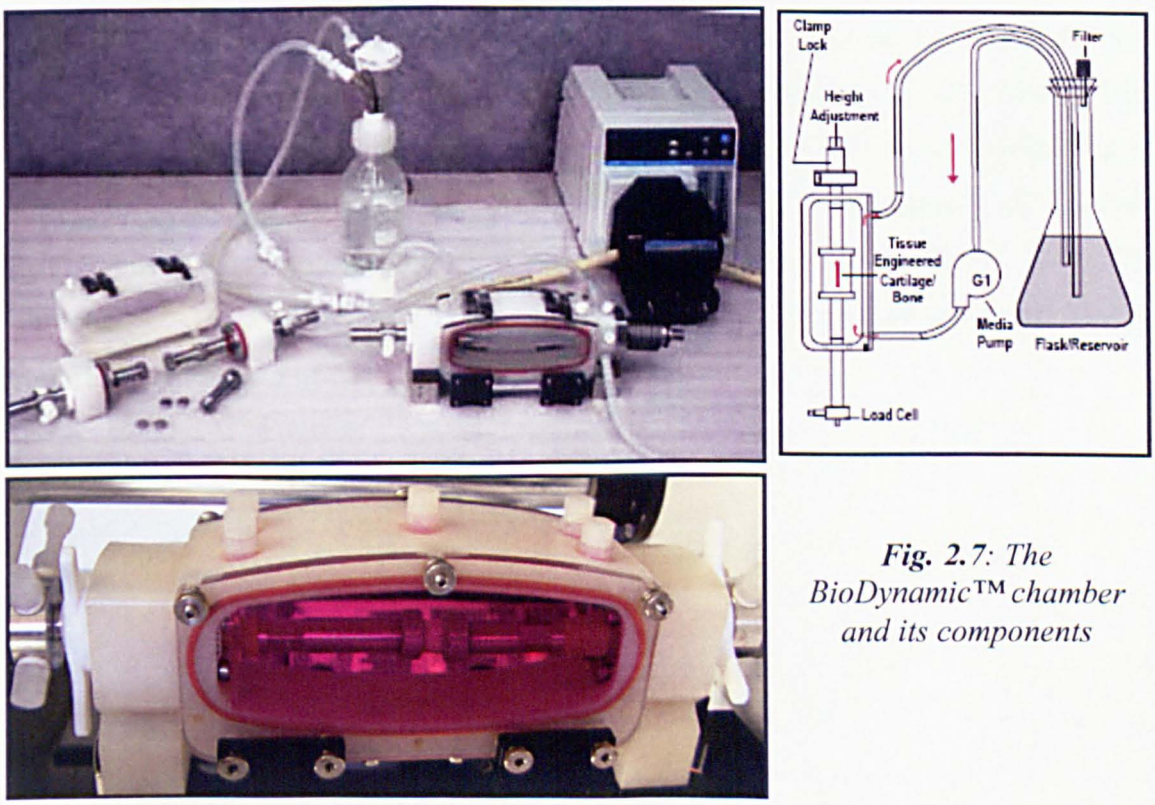

***Fig. 2.7**: The BioDynamic™ chamber and its components*

***Fig. 2.8**: The Biodynamic chamber mounted onto the mechanical testing machine (BOSE, ELF 3200). Data was recorded by WinTest software.*

2.2.5 Cell viability

2.2.5.1 MTT assay

MTT (A3-(4,5-dimethylthiazol-2-yl)-2,5-diphenyltetrazolium bromide) assay is one of the most frequently used methods for measuring cell growth and viability. The yellow MTT solution is reduced by active mitochondria in live cells to a dark blue or purple formazan insoluble salt *(Fig. 2.9)*. Subsequently, the optical density of dissolved salt supernatant is measured by using a plate reader at wavelength 540 nm. [194] The absorbance is directly related to the amount of formazan salt formed and is assumed to represent the number of live cells.

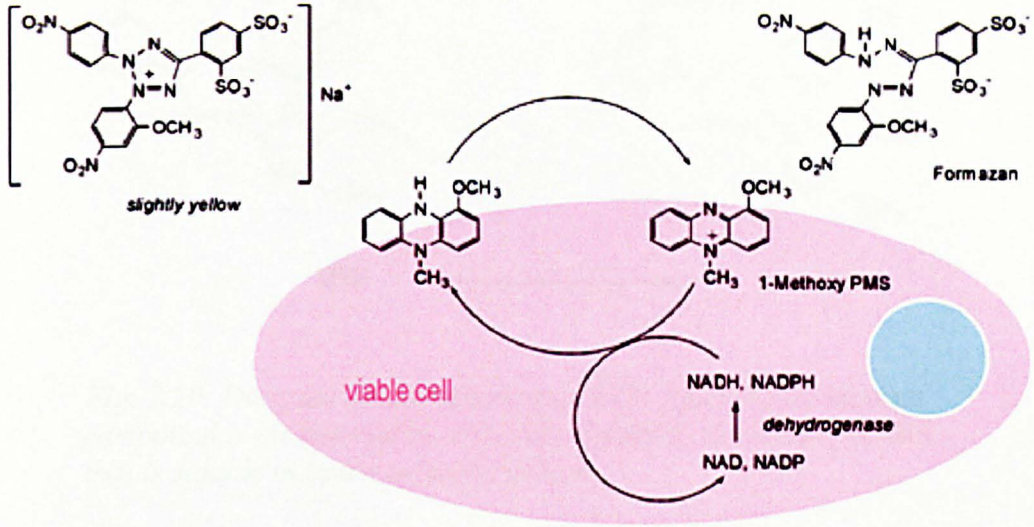

***Fig. 2.9**: A schematic representation of the reduction of MTT to formazan. This reduction takes place only when mitochondrial dehydroxygenase enzyme in live cells is active. The MTT terazolium compound is bioreduced by cells into a colored insoluble formazan (blue or purple) and therefore conversion is often used as a measure of viable (living) cells.*

In the first procedure, cell-seeded scaffolds were washed with PBS and incubated with 1mg/ml MTT in PBS for 40 minutes at 37°C, the solution was then removed and the insoluble formazan salt was dissolved with 0.125% acidified isopropanol. Finally, the absorbance of the resulting solution was determined using a plate reader.

2.2.5.2 MTS assay

MTS (3-(4,5-dimethylthiazol-2-yl)-5-(3-carboxymethoxyphenyl)-2-(4-sulfophenyl)-2H-tetrazolium) assay is another colorimetric method to determine the number of viable cells in culture [195]. Similarly to the MTT assay, the yellow MTS tetrazolium compound is reduced by live cells into a pink formazan product that is soluble in culture medium *(Fig. 2.10)*. This conversion is also presumably accomplished by NADPH or NADH produced by dehydrogenase enzymes in metabolically active cells.

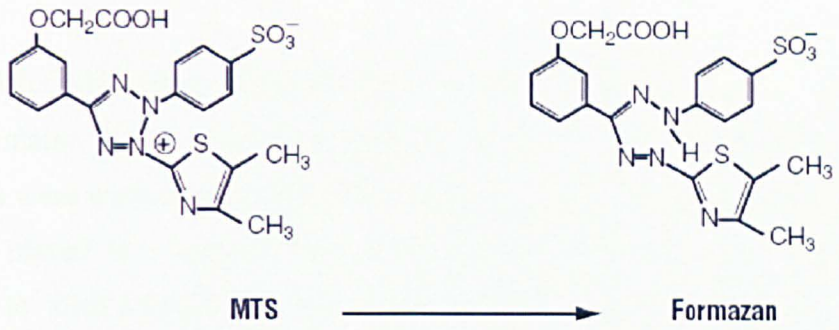

***Fig. 2.10**: Diagram of bioreduction of MTS. The MTS terazolium compound is bioreduced by cells into a colored formazan product that is soluble in tissue culture* medium.

Firstly, the media was removed. The cell-seeded scaffolds were washed with PBS until there was no colour in the solution, because the visible colour of formazan product from MTS and culture media has nearly the same wavelength that may lead to data errors when quantifying the optical density. Cell-seeded scaffolds were then placed in the 10 mm diameter stainless steel rings. Assays were performed by adding 0.5 ml of 1:10 MTS in PBS mixture directly to the scaffolds and to an empty scaffold for the blank control, incubating for 3 hours at 37°C (30-45 mins in 2-D monolayer), then 200 µl samples of the solution were pipetted out from the scaffolds and absorbance read at 490nm with a 96-well plate reader *(Fig. 2.11)*. The quantity of formazan product as measured by the plate reader is directly proportional to the number of living cells in the scaffolds (the relative number of viable cells)

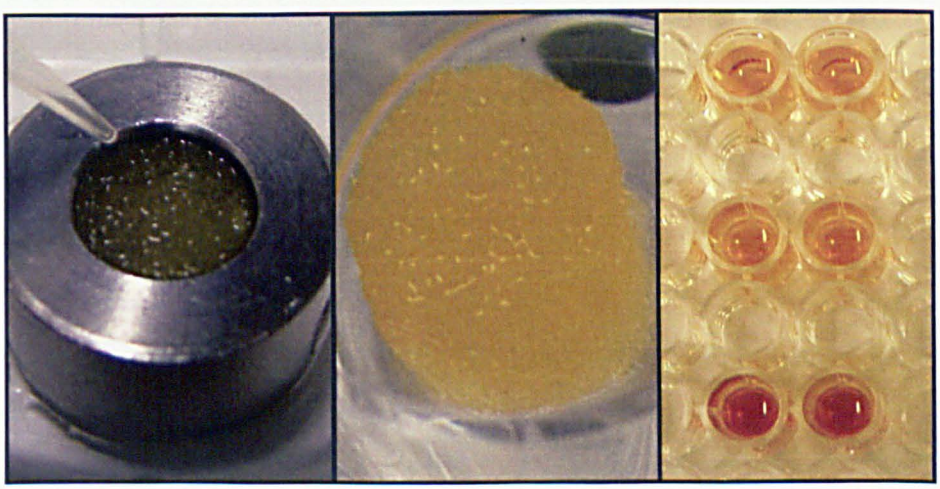

***Fig. 2.11**: Steps of MTS assay in 3-D experiments. MTS solution was added directly into a cell-seeded scaffold placed in the ring, Scaffolds were incubated for 3 hours at 37°C, and then the optical density was read at 490nm with a 96-well plate reader.*

2.2.6 *Calcium and collagen staining*

After MTS assay, scaffolds were washed three times with PBS then fixed with 10% formalin for 10 minutes at room temperature. The solution was removed and scaffolds were washed with PBS 3 times, cut into 5-6 pieces and all pieces from a single scaffold placed in a well of a six-well plate. Alizarin red, a dye that combines with calcium to form a bright red colour [196], was dissolved in distilled water 1 mg/ml, adjusted to pH 5.5 with ammonium hydroxide and 5 ml added to each well, samples were placed under mild shaking for 30 minutes at room temperature. The dye was then removed and samples were washed with distilled water. The cultures were air-dried in a fume hood and observed qualitatively under light microscopy. For quantitative analysis, the samples in each well were destained with 5% perchloric acid, under mild shaking for 15 minutes. Optical density was then measured at 490 nm using a 96-well plate reader. After Alizarin red destaining, all samples were washed with distilled water and air-dried. Sirius red dye (a strong anionic dye used for measuring collagen which reacts with sulphonic acid group on collagen molecules and aligns itself paralleled to the long collagen molecules [197]) in saturated picric acid solution (1mg/ml) was added to each well and placed under mild shaking for 18 hours. The dye solution was removed and each well was washed four times with distilled water to remove unbound dye until no more red colouring was eluted, then air-dried. The bound dye was observed qualitatively under light microscopy. For quantitative analysis, the scaffolds in each well were destained with 0.2 M NaOH/Methanol, in a 1:1 ratio, under mild shaking for 15 minutes. Optical density was then measured at 490 nm using 96-well plate reader.

2.2.7 *Messenger ribonucleic acid (mRNA) isolation and reverse transcriptase polymerase chain reaction (RT-PCR)*

mRNA is a copy of the nucleotide sequence of DNA. It transfers the coding information contained in DNA to the sites of protein synthesis. mRNA can be extracted from blood, tissues or other biologic samples and is very easily degraded by RNases, therefore, complimentary DNA (cDNA) derived from mRNA is a preferred to be used as a template in the polymerase chain reaction.

The polymerase chain reaction (PCR) is a method to amplify a specific nucleic acid sequence. The reaction must be heated to denature the double-stranded deoxyrybonucleic acid (DNA) product after each round of synthesis. The DNA polymerase isolated from hot-spring bacterium *Thermophilus aquaticus* known as "Taq polymerase" is needed for PCR [198]. It can withstand the high temperatures in the DNA denaturation step and remain stable in the reaction tube during the PCR procedure. There are three main steps in PCR which is done in an automated thermo cycler. The first step is *Denaturation* in which the original double-strand DNA is separated to single strand. Then, primers (specific sequences of the genes of interest) anneal to the complementary regions in the DNA template strands in the *Annealing* step. Finally, The DNA polymerase activates synthesis of a complementary strand which is extended by adding nucleotides in the *Extension* step.

Each cycle stimulates the primers to bind to original sequences and to synthesize new sequences. The cycle of heating and cooling is repeated until sufficient copies have been synthesized to enable detection. The reaction products are separated and visualized by gel electrophoresis *(Fig. 2.12)*.

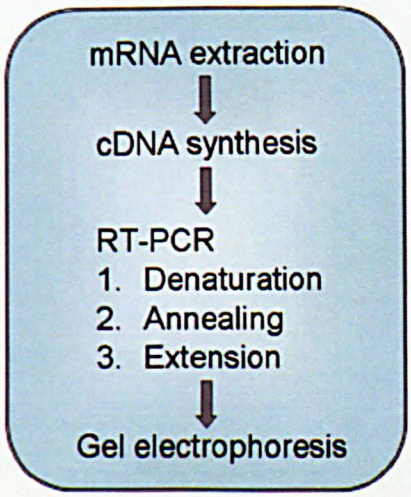

***Fig. 2.12**: Steps of measuring gene expression. mRNA extraction and RT-PCR. techniques were used to measure gene expression.*

Cell seeded scaffolds were grown and loaded as described above. At selective time points after loading, cellular mRNA was extracted using the Dynabeads® mRNA DIRECT™ Kit that is designed to isolate highly pure and intact poly A^+ tail of mRNA directly from cells and tissues. It can bind up to 2µg of poly A^+ mRNA per mg of beads *(Fig. 2.13)*. According to the manufacturer's instructions, 500 µl lysis/binding buffer

was added to break the structure of the cells, and release the DNA, RNA and protein. RNase inhibitor in the lysis/binding buffer was used to prevent the enzyme from degrading the RNA. 50µl of resuspended beads was transferred into 1.5 ml. microcentrifuge tubes, and placed on a magnet. The supernatant was removed after the solution had become clear. 50µl lysis/binding buffer was added to prepared beads to prevent drying of beads which may lower their capcity. The beads and cell lysates were mixed for 5 mins on the roller mixer to allow the poly A^+ tail of mRNA to specifically hybridize to poly T tail from the prepared dynabeads, while DNA, other RNAs and protein could not. The suspension was then washed with buffers provided in the kit. The mRNA bound beads were removed from the solution by placing on a magnet. Finally, mRNA was eluted from the beads by adding 300 µl of 10 mM Tris-HCl and incubating at 70°C for 2 min. The tube was placed immediately on the magnet and the supernatant containing the mRNA was transferred to a new RNase-free tube. According to manufactures instructions, this protocol should elute about 30 ng/µl mRNA. The mRNA samples were stored at -80°C.

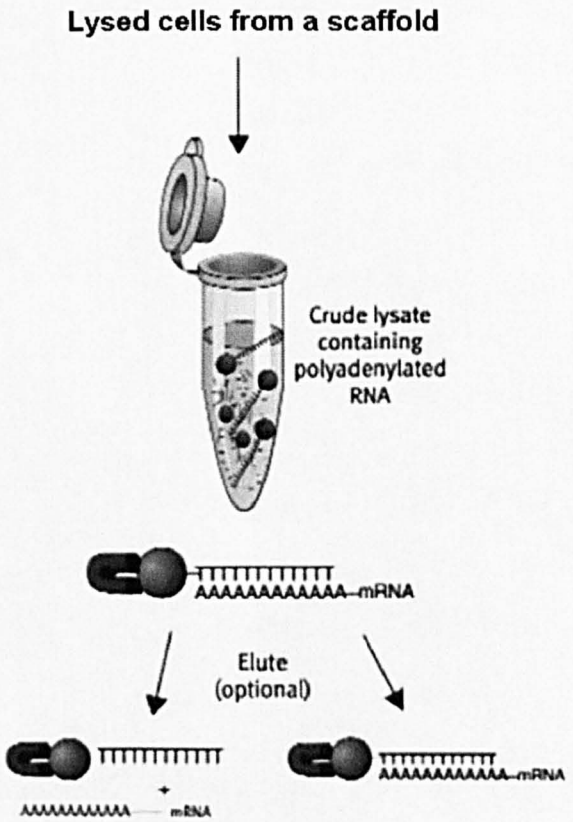

***Fig. 2.13**: Outline of the protocol for isolating mRNA from samples using Dynabeads® mRNA DIRECT™ Kit*

The isolated mRNA was reversely transcribed and amplified using the JumpStart™ RED HT RT-PCR kit. Primer sequences of target genes were shown in *Table 2.2.*

***Table 2.2**: Primer sequences used for RT-PCR.*

mRNA	Base pairs		Primer sequences
Mouse GAPDH	195	Forward	5'-CCA TGG AGA AGG CCG GGG-3'
		Reverse	5'-CAA AGT TGT CAT GGA TGA CC-3'
Mouse type I collagen	184	Forward	5'-AAT GGT GAG ACG TGG AAA CCC GAG-3'
		Reverse	5'-CGA CTC CTA CAT CTT CTG AGT TTG G-3'
Mouse osteopontin	765	Forward	5'-GAC CAT GAG ATT GGC AGT GAT TTG-3'
		Reverse	5'-TGA TGT TCC AGG CTG GCT TTG-3'
Mouse osteocalcin	240	Forward	5'-GAC AAA GCC TTC ATG TCC AAG C-3'
		Reverse	5'-AAA GCC GAG CTG CCA GAG TTT G-3'
Mouse beta actin	639	Forward	5'-TTG AGA CCT TCA ACA CCC CAG-3'
		Reverse	5'-ACT TGC GCT CAG GAG GAG CAA-3'
Mouse Bone sialoprotein	699	Forward	5'-AAT GGA GAC GGC GAT AGT TC-3'
		Reverse	5'-GTC CTC ATA AGC TCG GTA AG-3'
Human GAPDH	702	Forward	5'-GGG CTG CTT TTA ACT CTG GT-3'
		Reverse	5'-TGG CAG GTT TTT CTA GAC GG -3'
Human Osteopontin	416	Forward	5'-AGC CAG GAC TCC ATT GAC TCG AAC-3'
		Reverse	5'-GTT TCA GCA CTC TGG TCA TCC AGC-3'
Human RUNX2	125	Forward	5'-AGA TGA TGA CAC TGC CAC CTC TG-3'
		Reverse	5'-GGG ATG AAA TGC TTG GGA ACT GC-3'
Human Alkaline phosphatase	162	Forward	5'-ACC ATT CCC ACG TCT TCA CAT TTG-3'
		Reverse	5'-AGA CAT TCT CTC GTT CAC CGC C-3'
Human Type I collagen alpha 2	461	Forward	5'-GGA CAC AAT GGA TTG CAA GG-3'
		Reverse	5'-TAA CCA CTG CTC CAC TCT GG-3'

GAPDH was used as a house keeping gene, which is always expressed because it codes for proteins that are constantly required by the cell. It is essential to a cell and should be present under any conditions. In addition, it is assumed that its expression is unaffected by experimental conditions. The proteins it codes are generally involved in

the basic functions necessary for the sustenance or maintenance of the cell [199]. All primers in this project were obtained from published articles [192, 200] and were confirmed by NCBI blast (http://blast.ncbi.nlm.nih.gov/Blast.cgi). To mix up master mix for one-step RT-PCR reaction, the following reagents were added to a thin-walled 200 µl PCR microcentrifuge tube on ice *(Table 2.3)*.

***Table 2.3**: Master mix reagents and their final concentration for one step RT-PCR.*

Volume	Reagent	Final concentration
36 µl	PCR reagent Water	To make 50 µl total volume
5 µl	10 x PCR buffer	1 x
3 µl	25 mM $MgCl_2$	3 mM
1 µl	Deoxynucleotide mix	200 µM
1 µl	RNase inhibitor	0.4 units/µl
1 µl	mRNA sample	2 pg/µL to 20 ng/µl
1 µl	Specific primer (Forward+Reverse)	0.4-1 µM each primer
1 µl	Enhanced avian myeloblastosis virus reverse transcriptase (eAMV-RT)	0.04 units/µl
1 µl	JumpStart Accu Taq LA DNA polymerase	0.05 units/µl

The thermo cycler was set up for the temperature, time and number of cycles as shown in *Table 2.4*. RT-PCR products were visualized by electrophoresis on a FlashGel™ system. The DNA marker obtained from the kit was used to provide accurate size estimation of bands. 7 µl of distilled water was use to activate the gel before adding 3 µl of DNA samples or marker into each well of FlashGel™ Cassette. The gel cassette was then mounted to the FlashGel™ Dock, which provided 260V voltage and Ultraviolet (UV) light, and was run for 5-7 min until separated bands were seen clearly. Bands were imaged by using digital camera with super macro lens (Fuji S7000). The relative band density of the RT-PCR products was quantified using Bio image intelligent quantifier version 3.2.1 and then normalized to GAPDH.

***Table 2.4**: Thermal Cycling parameters for RT-PCR.*

Procedure	Temperature	Time
For 1 cycle		
First strand synthesis	47°C	50 min.
Denaturation/ RT inactivation	94°C	2 min.
For 28 cycles		
Denaturation	94°C	15 sec.
Annealing	58.5°C	30 sec.
Extension	68°C	1 min.
Final extension	68°C	5 min.
Hold	4°C	

2.2.8 Quantitative (real time) reverse transcriptase polymerase chain reaction (qRT-PCR)

Real time RT-PCR is a technique for collecting data during the PCR process. It combines amplification and detection into a single step by using a variety of different fluorescent chemistries that correlate the PCR product to fluorescent intensity [201]. After mRNA isolation, cDNA is first synthesized and used as a PCR template. The fluorescence data is collected on a real time PCR machine to generate the output data used for analysis. Then, the data is divided by its normalization factors, including multiple housekeeping genes.

At selected time points after mechanical stimulation, total RNA was extracted using TriReagent which is a mixture of guanidine thiocyanate and phenol in a mono-phase solution. It effectively dissolves DNA, RNA, and protein on homogenization or lysis of tissue samples. 1 ml of TriReagent was used per 10 cm^2 culture plate surface area for momolayer cells. Cells were scraped out from the substrate and the cell lysate was passed several times through a pipette to form a homogenous lysate and allowed to stand at room temperature for 5 min. Then, 200 µl of chloroform per ml of TriReagent used was added into samples. Samples were shaken vigorously for 15 sec, allowed to stand for 10 min at room temperature and centrifuged at 12,000 x g for 15 min at 4°C. The centrifugation separated the mixture into 3 phases: a red organic phase containing

protein, an interphase containing DNA and a colorless upper aqueous phase containing RNA. The upper aqueous solution was then transferred to 1.5 ml microcentrifuge tube and 0.5 ml of isopropanol per ml of TriReagent used was added to each sample. Samples were allowed to stand for 5 min. at room temperature and then were centrifuged at 12,000 x g for 10 min. at 4°C. The RNA precipitate was seen to form a pellet on the side and bottom of the tube, the supernatant was removed and the pellet was washed by adding 1ml of 75% ethanol per 1 ml of TriReagent used in the previous step. Samples were centrifuged at 7,500 g for 5 min at 4°C and then briefly dried for 10 min by air drying. Finally, 30 µl of DEPC RNAase free water was added to the tube. The amount of mRNA was measured by using NanoDrop ND-1000 UV/Vis Spectrophotometer.

The complementary DNA (cDNA) was synthesized using High-Capacity cDNA Reverse Transcription Kits according to the manufacturer's instructions. cDNA samples were then amplified by real time PCR using Pre-Developed Taqman®Assay Reagents to detect the expression of target sequences in cDNA samples. Primers used in this study were commercially available from Applied Biosystems, California, USA Real-time quantitative RT-PCR was performed by using ABI Prism 7900 detection system. Amplification curves for control and experimental genes (COL1, OPN, DMP1) were recorded, and relative gene levels between samples were quantified by using the relative standard curve method (ABI Prism 7700 User Bulletin 2; Applied Biosystems). All samples were normalized to endogenous control 18S rRNA. All samples and standards were run in triplicate.

2.2.9 Alkaline phosphatase (ALP) activities

ALP is an enzyme involved in bone mineralization and its activity is known to increase as cells develop along the osteogenic lineage. An ALP assay was used to measures the amount of the enzyme ALP in biological samples. [47]. Total ALP was measured spectrophotometrically with p-nitrophenyl phosphate as a substrate and normalized to relative cell number by MTS assay. Cell assay buffer was made up by mixing 1.5 M Tris (adjust pH to 9.0 with conc. HCl), 1 mM $ZnCl_2$ and 1mM Mg Cl_2 in ddH_2O. Samples were washed 2 times with PBS and then 200 µL (300 µl for 3D sample) of cell digestion buffer, containing 1:10 of cell assay buffer in ddH_2O and 1% Tritron X-100,

was added to the sample. The plate was scraped or the scaffold was squeezed for 1 min, then the extracted solution was transferred to a 1.5 ml microcentrifuge tube, vortexed, centrifuged briefly and incubated for 30 min. at 37°C and then overnight at 4°C. 10 µl (V_{sample}) of extracted solution was mixed with 190 µl of ALP solution containing 37.1 mg p-nitrophenol phosphate in 20 ml of cell assay buffer. The mixture then was vortexed for 15 second, centrifuged briefly. 200 µl (V_{total}) of mixture was transferred into a well of a 96 well plate and incubated for 10 min at room temperature. The plate was read using a plate reader with wavelength of 410 nm at 1 min and 5 min. ALP level was expressed as nmol of p-nitrophenol where 17 nmol (K) equals 1 absorbance value (A_{410}) The ALP activity was calculated using the following formula [42, 47].

$$\text{ALP activity (nmol per min)} = \Delta A_{410} * K * V_{total} / V_{sample}$$
$$= \Delta A_{410} * 17 * 200 / 10$$

2.2.10 Fluorescence microscopy of DAPI stained cells (DNA staining)

DAPI is known to form fluorescent complexes with natural double-stranded DNA, showing fluorescence specificity for AT, AU and IC clusters. Because of this property, DAPI is a useful tool in various cytochemical investigations. When DAPI binds to DNA, it is fluorescent under the blue wavelength [202, 203].

Cell-seeded scaffolds were fixed in 10% formalin solution for 10 minutes at room temperature, and then washed with PBS 3 times allowing the cells to keep their structures and preventing degradation. Subsequently, each fixed scaffold was cut to 5-6 pieces (average thickness ~ 1.5-2 mm/piece). DAPI solution, 1:1000 DAPI in PBS, was added to each well to cover scaffold pieces. The well plate was then covered with aluminium foil and incubated for 30 mins. The DAPI was removed and replaced by PBS and cells were imaged on an Axon Instruments ImageExpress inverted stage microscope using a 10× objective and standard DAPI filter set.

2.2.11 Hyaluronic acid glycocalyx staining

Cells were cultured in 6 well plates until 70% confluent. Media was removed and cells washed with 1.5ml PBS and fixed using 10% Formalin for 30 minutes. Cells

were washed and unreactive binding site blocked using 3% BSA in PBS for 1 hour. Biotinylated Hyaluronic Acid Binding Protein (HABP 5μg/ml, Merck UK) was added and samples incubated for 3 hours. Cells were washed and FITC-Streptavidin (λ_{ex}=490nm, λ_{em}=523nm) was added for 30 minutes (2.5μg/ml). Samples were imaged and analysed using the Zeiss LSM510 META confocal microscope system (Oberkochen, Ger) with ×63 water dipping lens.

2.2.12 Primary cilia staining

Primary cilia have axonemes containing tubulin, therefore they can be detected by immunostaining with anti-tubulin antibodies. Alpha tubulin immunostaining shows the microtubular cytoskeleton, which is specific and especially dense around the centrosome region in which primary cilia occur [102].

Samples were washed with PBS 3 times and fixed in 3.7% formaldehyde solution for 10 min. Cells were permeablised by using 0.1% tritron X-100 solution and then incubated in primary blocking solution, containing 1% Albumin bovine serum and 0.2% Igepal in PBS, for 1 hrs (2-D) or 2hr (3-D) at room temperature. Samples were incubated with the primary antibody solution (1:2000 of 2 mg/ml mouse antibody to Acetylated alpha tubulin in Primary blocking solution) for 24 hrs at 4°C and then were washed with primary blocking solution 3 times (5 min/wash on shaker). The secondary antibody, 1:30 of FITC-conjugated rabbit anti-mouse immunoglobulins (studies performed in Sheffield) or Rhodamine-conjugated goat anti-mouse immunoglobulins (studies performed in Stanford) in primary blocking solution was applied to samples for 1 hr at room temperature and protected from light for all subsequent steps. Samples were washed again with primary blocking solution 3 times (5 min/wash on shaker). The DAPI solution (1:1000 DAPI in PBS) or PI solution (1mg/10ml in PBS) was added to samples for 30 min (DAPI) or 15 min (PI) then washed 3 times with PBS. Cells were imaged by using confocal microscopy.

2.2.13 Primary cilia removal by chloral hydrate

Primary cilia develop from the cell's mother centriole and are anchored to the basal body. It has previously been shown that long-term incubation with chloral hydrate

removes cilia from *Paramecium caudatum* [204] *(Fig. 2.14)*, from the early embryo phase of the sea urchin [205], from MDCK cells (madin-Darby Canine Kidney Cells) [115, 116] and bone cells [118]. Chloral hydrate destabilizes the junction between the cilium and the basal body probably through disassembly of microtubules [205]. Praetorius and Spring 2002 have shown that when deciliated MDCK cells were allowed to recover in normal cell culture medium for several days (96 hours), the primary cilia grew back and the flow-induced Ca^{2+} response returned.

Deciliation in this study was achieved by incubating samples in culture media containing 4 mM chloral hydrate for 24 hours. The loading experiments were performed immediately after samples were washed 3 times with PBS and 1 time with normal culture medium.

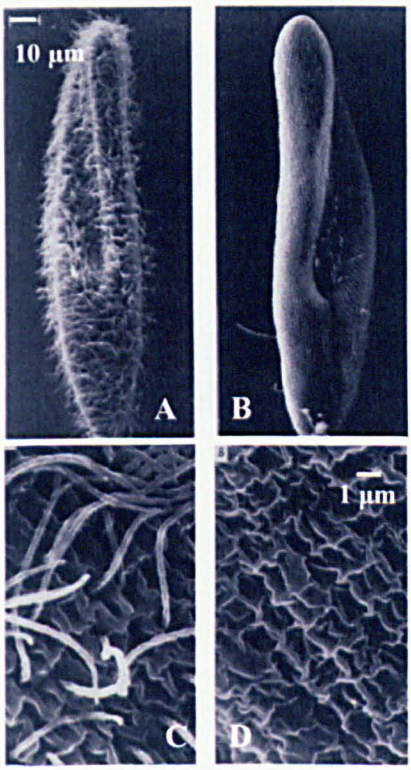

***Fig. 2.14**: Scanning electron micrographs of cilia on paramecium. The images show control (A and C) and deciliated paramecium after 20 hours incubation with 4 mM chloral hydrate (B and D) (Dunlap, 1977).*

2.2.14 Knockdown primary cilia by Small interfering RNA (siRNA) transfection of polaris protein

Small interfering RNA (siRNA) transfection is the method of choice to target specific genes for silencing. siRNA can bind with RNA –induced silencing complex (RISC) inside the cell. This multi-protein complex together with RNase activity can

guide the target mRNA to degradation [206]. Since intraciliary transport (ICT) proteins such as polaris, polycystin and tg737 have been reported to be important proteins for the biogenesis and function of primary cilia [100, 118], they are widely used to study the effects of abrogation of primary cilia on many kind of mammalian cells by knocking down these proteins or silencing their mRNAs [115].

One day prior to transfection (day 0), cells were seeded on each glass slide (38 mm x 10 mm) at density of 50,000 cells per slide. This should give 20-30% confluency at day 1. The slide was washed with PBS and vacuumed with the tip of pipette so that there were no media or PBS left. To prepare the transfection reagent, 10 μL of X-tremeGene siRNA transfection reagent was directly added into 90 μL of serum free Opti-MEM1 medium (without antibiotics) and then mixed well by pipetting up and down for 30 sec. 10 μL of siRNA targeting polaris or 10 μL of scrambled control siRNA in 90 μL of Opti-MEM1 (20 μM) was mixed with the prepared transfection reagent immediately after diluting (within 5 min). The mixture was incubated for 20 min and 800μL of media was then added into the mixture. 1 mL of solution was dropped into each slide placed in petri dish, incubated for 4 hrs and then 9 ml of media was added to the petri dish. The medium was changed 24 hrs after transfection and fluid flow experiments were performed 48 hrs after transfection.

2.2.15 Oscillatory fluid flow

The parallel plate flow chamber has been used successfully to study cellular responses to fluid flow induced shear stress in *in vitro* 2-D studies [94, 118]. The device was developed and previously described by Jacobs et al. (1998) [94] (kindly provided for use at Stanford University, USA by Professor Christopher Jacobs). Briefly, the customised parallel plate flow chamber was made up of a polycarbonate manifold with the inlet and outlet ports, a glass microscope slide with cell attached and a gasket held together by vacuum pressure *(Fig. 2.15)*.

To study the effects of fluid flow in the present study, 50,000 MLO-A5 cells were seeded on a fibronectin coated glass slide and cultured for 3 days. Before loading, the glass slide was mounted to the parallel plate flow chamber which was used to apply oscillatory laminar fluid flow with a period of 1 Hz and a surface shear stress of 2 Pa at

the chamber wall *(Fig. 2.15)*. The fluid volume in the chamber measures 56 mm x 24 mm x 0.28 mm. Oscillatory flow was supplied with an Interlaken sevohydrolic loading machine connected to Hamilton glass syringe and chamber *(Fig. 2.15)*. All chambers were kept in an incubator under standard conditions during the loading period. A control set was kept in the same conditions as an experimental set to ensure that any differences detected were not due to the disruption of the cells incurred by chamber mounting.

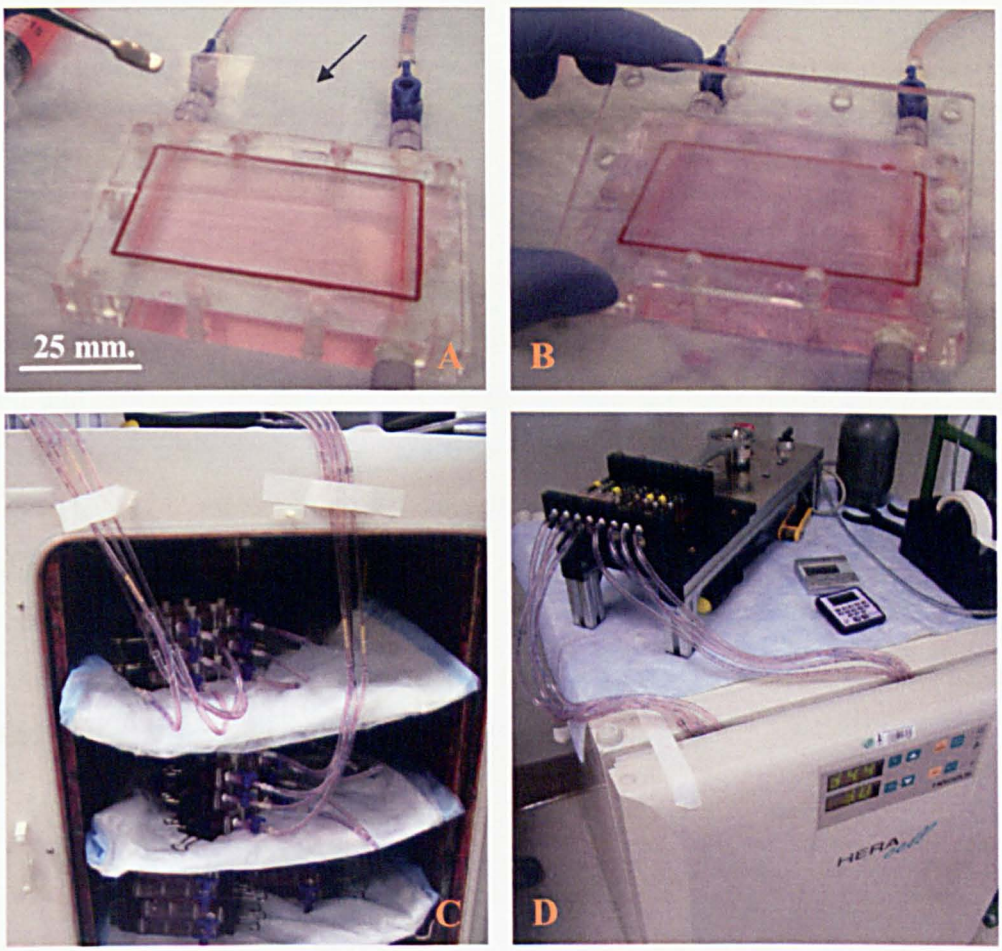

***Fig. 2.15**: The parallel plate flow chamber and its components. The chamber consists of a glass slide with cells attached (A), polycarbonate manifold and gasket (B). The components were held together by vacuum and kept in an incubator during loading with standard conditions for cell culture (C). The inlet and outlet ports were connected to the actuator (D) which generates oscillatory laminar fluid flow with a period of 1 Hz and an estimated maximum cell surface shear stress of 2 Pa.*

2.2.16 Scanning Electron microscopy (SEM)

To examine matrix production by cells, cells seeded scaffolds were fixed with 2.5% glutaraldehyde in 0.1 M sodium cacodylate buffer for 30 minutes at room temperature, and post fixed with 2% osmium tetra oxide for 1 hour. The samples were dehydrated in a graded series of ethanol up to 100% and freeze dried. Samples were mounted onto the 12.5 mm stubs and sputter coated with gold, and then observed with a scanning electron microscope (Phillips/FEI XL-20 SEM) at an accelerating voltage of 10-15 kV.

2.2.17 Statistical analyses

All 20 day experiments were repeated three times with a minimum of N = 2 per condition, per repeat (N=6). RNA experiments were repeated three times. Cell viability, calcium and collagen per cell, and mechanical properties were tested by two sample *t*-test. Differences were considered statistically significant if the *p*-value was less than 0.05 ($p<0.05$). To allow for cell numbers, data was normalized to MTS values. Normalized loaded samples (divided by the non-loaded controls within the experiment) were compared to control samples using a Mann-Whitney test with 95% confidence level. All statistical tests were performed using Minitab software. Two-way ANOVA was used to test differences between multiple treatments.

CHAPTER THREE: Optimizing a three dimensional (3-D) model *in vitro* to study mechanobiology of bone constructs.

3.1 Introduction

Mechanical loading is an important regulatory factor in bone homeostasis, and plays an essential role in maintaining the structure and mass of bone throughout a lifetime [64]. A better understanding of cellular and molecular responses of bone cells is the key to further improvements of therapeutic approaches in orthopaedics, orthodontics, periodontics, bone repair, bone regeneration and implantology. Mechanical force is also known as an osteoinductive factor that plays an important role in bone growth and repair *in vivo* [120]. Many *in vitro* studies have shown that osteoblasts and osteocytes respond to mechanical loads such as stretch and fluid-flow induced shear stresses, with initiation of signalling pathways [48]. The underlying mechanisms by which bone cells respond to mechanical signals are difficult to investigate in a 3-D environment, because of difficulties in analysis [176, 195]. Due to the limitations of *in vivo* models, previous studies on mechanical regulation of bone cells mostly focused on proliferative responses and cell-associated genes responses, rather than on the stimulation of cell differentiation and matrix production [44, 207-209]. There has been an increased awareness of the need for improvement and development of 3-D *in vitro* models to mimic the 3-D environment, as found in intact bone tissue, and to validate 2-D *in vitro* results. However, a critical barrier to the development of 3-D bone models *in vitro* is the limited transport of nutrients and metabolites throughout scaffolds *(Fig. 3.1)*. Many previous studies have shown adverse effects on cell survival, cell proliferation and cell differentiation when cells are cultured in 3-D scaffolds by static culture techniques [81, 132, 133]. In 3-D static culture, although more media is used to cover all surfaces of the scaffold, the transportation of nutrients and waste products is limited. This depends on many factors such as the pore size and porosity (volume/volume) of the scaffold, the scaffold material and the overall size of the scaffold [210]. Therefore, the aims of this chapter were to optimize a model

system by which bone cells could survive in 3-D static culture and their responses to mechanical stimuli could be examined *in vitro* in a 3-D environment.

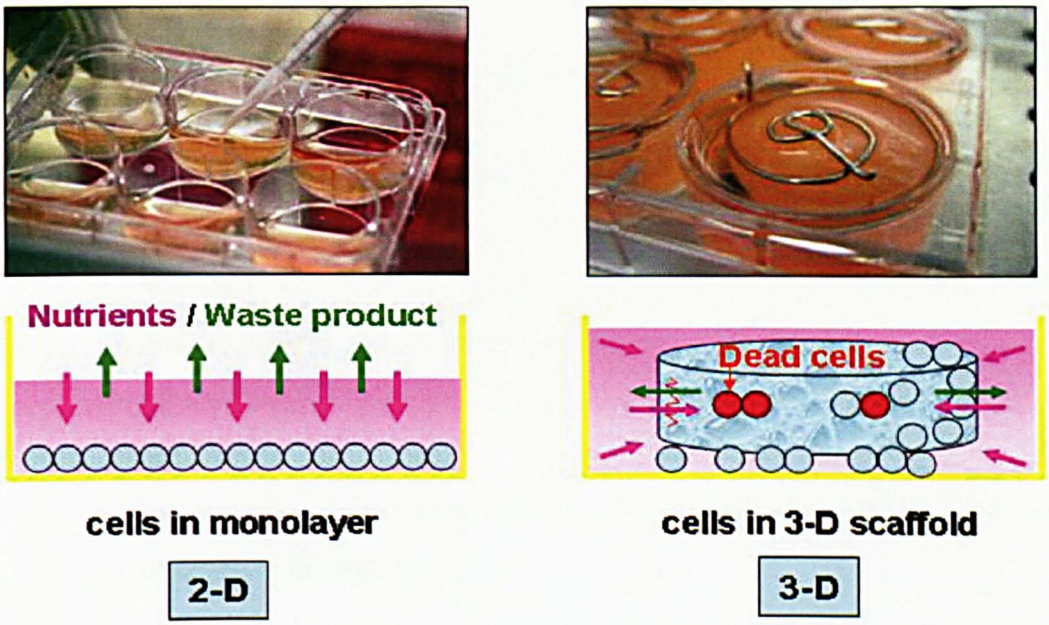

***Fig. 3.1**: Differences between 2-D and 3-D cultures. In 2-D culture, cells grow in monolayer in which they can get nutrients directly from media. In 3-D static culture, although more media is used to cover all surfaces of the scaffold, the transportation of nutrients and the exchange of waste products is limited. Therefore, viable cells usually stay more at the edges than the centre of the scaffold. Moreover, the leakage of cell suspension during seeding might cause cells to grow on the surface of the plate rather than growing on the scaffold.*

In this chapter, we optimized a biomechanical 3-D model in which cells can grow and survive in 3-D polyurethane (PU) scaffolds. PU scaffolds have sufficient elasticity, resiliency, and stiffness to deal with *in vitro* mechanical loading, and also are biocompatible with bone cells [126, 144, 146, 147, 176, 183, 211]. This is the first time that a non-degradable industrial grade of PU foam was reported to be used as supporting scaffold for *in vitro* bone tissue engineering. The advantages of using this type of foam are that it is highly porous and has high elasticity and mechanical stability which allow it to retain a supporting role even at high strain levels. A non-degradable PU maintains its properties over time and does not leach degradation products into the culture. This scaffold is also highly reproducible, thus eliminating scaffold variability as a confounding variable in our experiments. Although, other porous materials have been investigated for bone tissue engineering from naturally derived materials to synthetic polymers and ceramics [81, 92, 161], few scaffolds have adequate mechanical properties for repetitive direct strain on the scaffold material [212]. Our hypotheses in this chapter are that the commercial industrial

grade of PU foam is biocompatible and can be used in 3-D *in vitro* static culture of bone cells including MLO-A5 osteoblastic cell which had never been cultured in a 3-D environment prior to these studies.

The experiments described in this chapter are divided into 3 stages.

1. Studying the effects of different osteogenic media on osteoblastic cell growth and differentiation in 2-D culture.
2. Studying the relationship between the capacity of the novel PU scaffold and the volume of cell culture media.
3. Monitoring the viability of cells in the scaffold (comparing MTT and MTS).
4. Investigating the potential of the 3-D static culture system to be a model of engineered bone tissue.

3.2 Studying the effects of different osteogenic media on osteoblastic cell growth and differentiation in 2-D culture.

Kato et al. (2001) have shown that the newly developed osteoblastic cell line, MLO-A5, can mineralise faster, even in the absence of β-glycerophosphate (βGP), than other osteoblastic cells including MC3T3-E1 cells which have been widely used in bone *in vitro* experiments [192]. A low concentration of βGP (2mM) was recommended by Chung et al. (1992) to use as osteogenic supplements in culture to minimise the chance of non-cell specific calcium phosphate deposits [213]. Our hypothesis in these experiments was that MLO-A5 cells can mineralise faster than MC3T3-E1 cells and non-mineralising human fibroblast cells (negative control) even in a low concentration of βGP.

To test this hypothesis, MLO-A5, MC3T3-E1 and human fibroblast cells (a negative control) were seeded at 7.5×10^3 cells per well in 12 well plates supplied with 3 different media, (i) normal culture media, (ii) osteogenic media A containing AA and (iii) osteogenic media B containing AA and βGP. Cells were cultured in the incubator for 14 days and were supplied with fresh media on days 3, 6, 9, 12. Cells were assayed for cell viability (MTS), collagen and calcium production at day 7 and day 14.

3.2.1 Results

MTS assay showed that by day 14 the relative number of MLO-A5 cells was slightly decreased but not significantly from day 7 in all media types. In contrast, the proliferation of MC3T3-E1 cells and human fibroblasts increased over 14 days. Quantitative data showed that the number of viable MC3T3-E1 cells was less at day 7 in osteogenic media compared with basal media but higher at day 14 *(Fig. 3.3)*. Although, Sirius red staining showed that collagen produced by MLO-A5 and MC3T3-E1 cells increased greatly between days 7 and 14 in both osteogenic media A and B, the collagen level of MC3T3-E1 was higher than that of MLO-A5 cells at day 14, about 2 times in osteogenic media A and 3 times in osteogenic media B, indicating that collagen production by MC3T3-E1 cells was more responsive to osteogenic media *(Fig. 3.4)*. The calcium content of MLO-A5 cells increased rapidly and significantly at day 14 from day 7 when cultured in osteogenic media B *(Fig. 3.5)*. This result also was supported by qualitative data from light microscopy which indicated that much more calcium was produced by MLO-A5 cells *(Fig. 3.2)*.

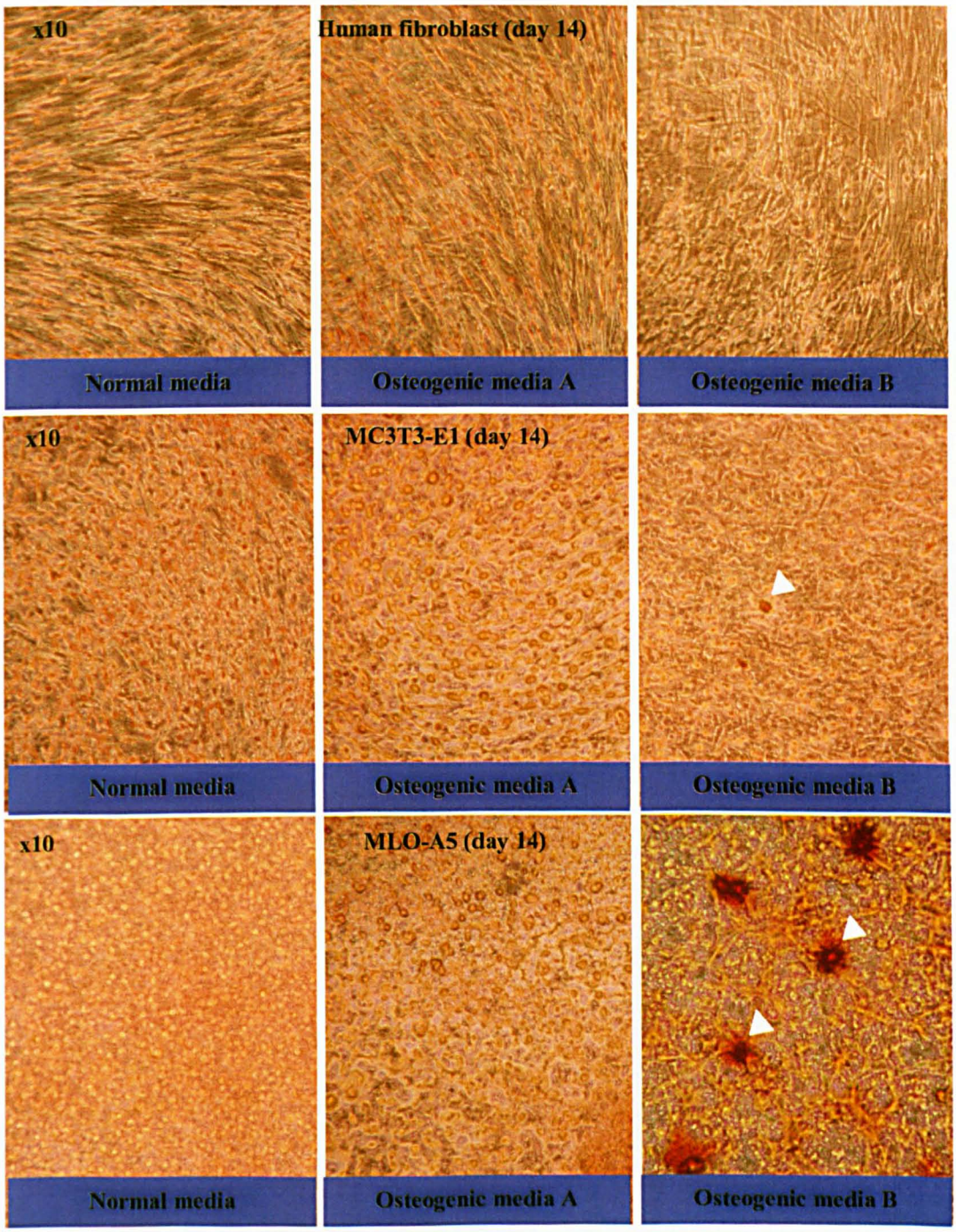

***Fig. 3.2**: Light micrographs of calcium staining. Calcium deposits were stained using alizarin red. White arrow head indicated that calcium production from MLO-A5 cells at day 14 was much more than that from other cells.*

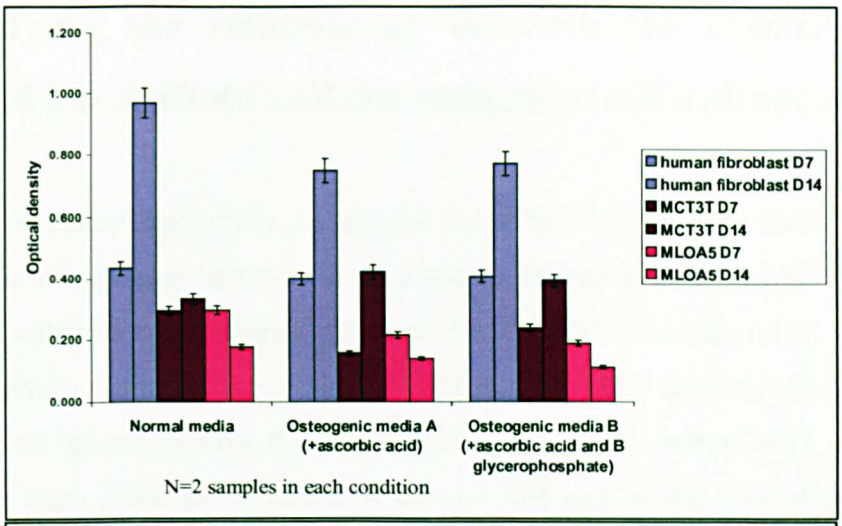

***Fig. 3.3**: Quantitative cell viability of human fibroblasts, MCT3T-E1s and MLO-A5s cultured in 3 different media.*

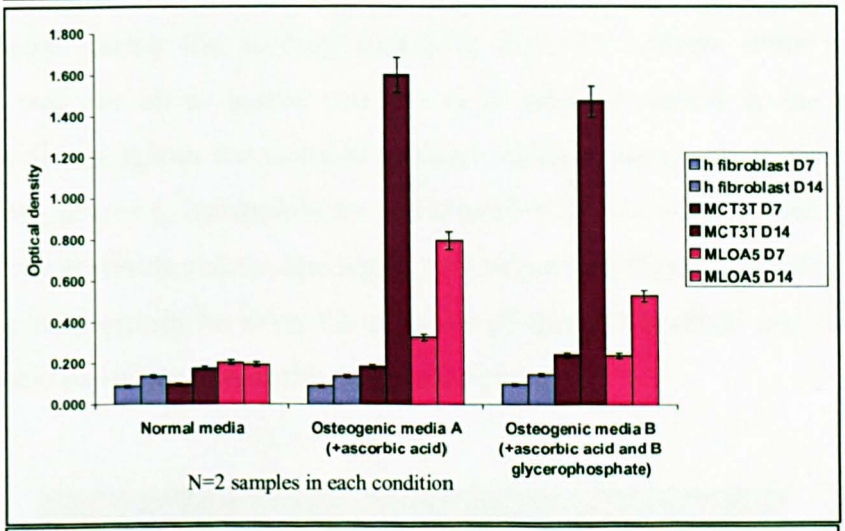

***Fig. 3.4**: Quantitative collagen staining of human fibroblasts, MCT3T-E1s and MLO-A5s cultured in 3 different media.*

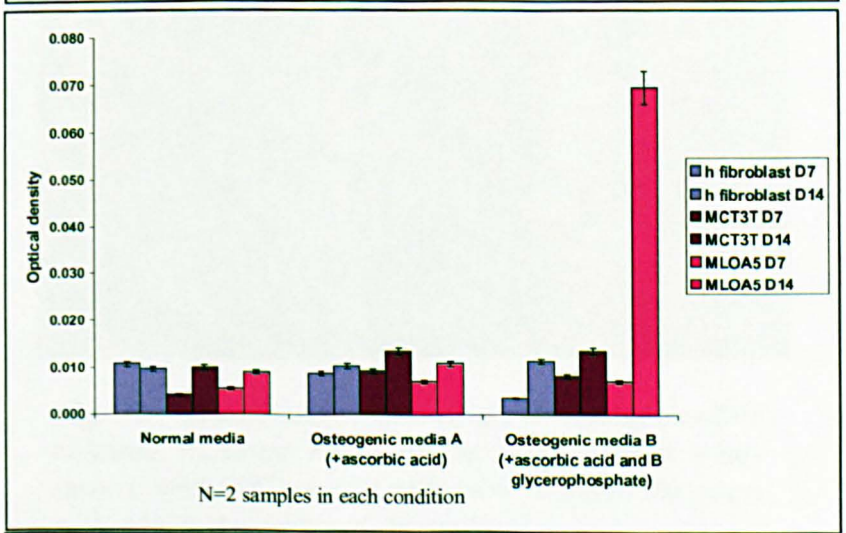

***Fig. 3.5**: Quantitative calcium staining of human fibroblasts, MCT3T-E1s and MLO-A5s cultured in 3 different media.*

3.3 Studying the relationship between the capacity of the novel PU scaffold and the volume of cell culture media.

In our preliminary study, to test the biocompatibility of the novel PU scaffold which has not been used in tissue culture before, human fibroblast cells ($5x10^4$) were seeded and cultured in a 2-D well plate and the 3-D PU (diameter of 10 mm, hight of 10mm) in static conditions for 5 days. In 3-D culture, MTT staining showed that cells can survive on the scaffold but the purple formazan insoluble salt of MTT indicated that viable cells were found at the edges of the scaffold and on the surface of the culture plate rather than the centre of the scaffold. The possible reasons for this outcome are not only limited nutrient transportation to the center of scaffold but also the leakage of cell suspension during the seeding step *(Fig 3.1)*. To address these problems, an experiment was set up to assure that the cells initially seeded in the scaffold can distribute well throughout the scaffold without leakage during the static seeding step. The pore size, porosity, hydrophilicity and overall size of a scaffold can influence the capacity of the scaffolds and the leaking of cell suspension from the scaffold. Therefore, study of the relationship between the capacity of this PU scaffold and the volume of initial cells-media suspension in this stage is essential.

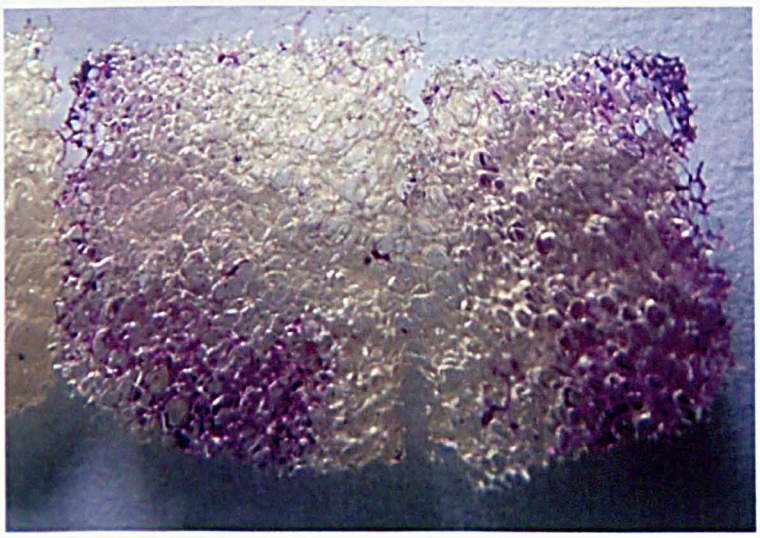

***Fig. 3.6**: Transverse section of a cell-seeded scaffold cultured in static condition in a preliminary study stained with MTT. Active cells were found at the edges rather than the centre of the scaffold.*

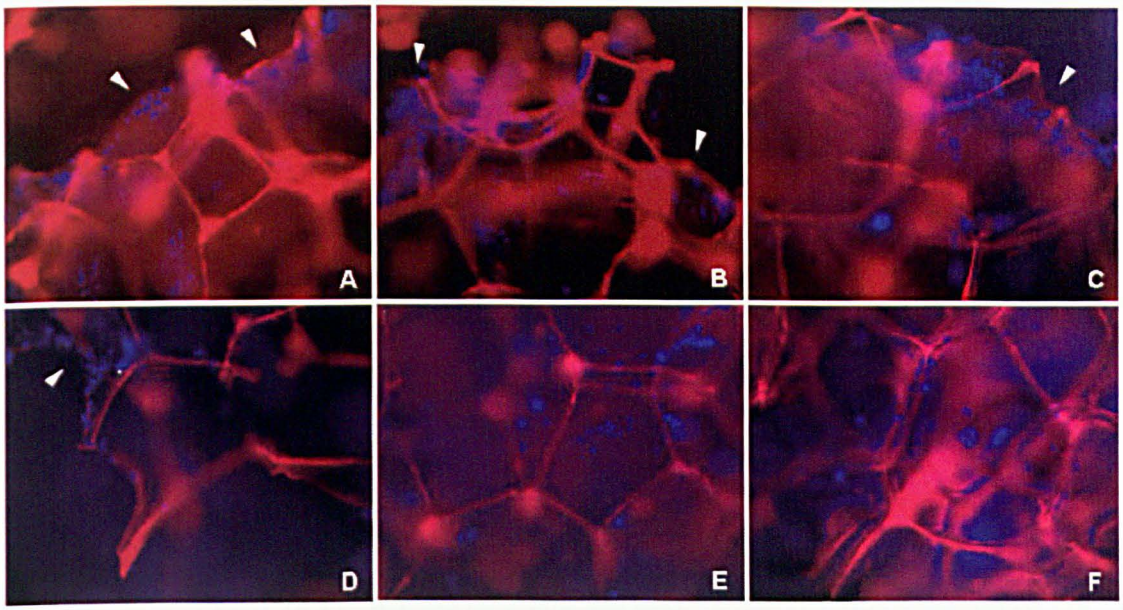

***Fig. 3.7**: Fluorescence images of stained nuclei of cells on PU. The Stained nuclei using DAPI staining are shown in blue color. The cells attach to scaffold struts and distribute more around the edge (white arrow head, A-D) than the deeper part (E-F) of the scaffold (5 days culture). The red color shows auto fluorescence of scaffold struts.*

To study the relationship between the capacity of this novel PU scaffold and the volume of the initial cell-media suspension, scaffolds were cut to fit into stainless steel rings, 10 mm thick and 10 mm diameter *(Fig. 3.8)*. The stainless steel ring is non resorbable material that is easy to sterilise. It has been used successfully in a skin 3-D model in our lab to hold the cell-media suspension on the thin scaffold [214]. In this bone model, the ring was not only used to hold the cell suspension during the seeding step but also was adapted to keep the foam in place during the initial attachment period to prevent floating of the cell-seeded foams on the surface of the media. 3 different volumes of cell-media suspension; 100 µl, 150 µl and 200 µl, were seeded into the middle or on the top of dry or wet scaffolds *(Fig. 3.9 and 3.10)*. White filter paper was used to detect the leakage of suspension from scaffolds *(Fig. 3.11)*.

3.3.1 Results

The optimum volume of cell suspension to ensure uniformity of suspension perfusion through the scaffold without leakage from the scaffold is 100µl for this size of cylindrical PU foam *(Fig. 3.12 and 3.13)*. According to this result, if the size of scaffold is changed, the new optimal volume will be obtained from the following formula.

Optimal volume of cell suspension (µl) = $\frac{2r^2h}{5}$

- r = radius of polyurethane foam (mm.)
- h = height of polyurethane foam

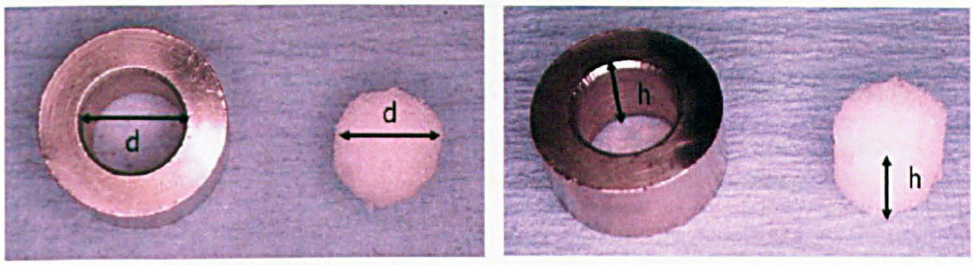

***Fig. 3.8**: Size of a PU scaffold. The scaffold was cut to fit into a stainless steel ring used to hold a scaffold in the cell seeding procedure; Diameter (d) = 10 mm (r = 5 mm), Height (h) = 10 mm, Capacity = $\pi r^2 h$ = 785.71 $mm^3 \approx 0.786$ ml.*

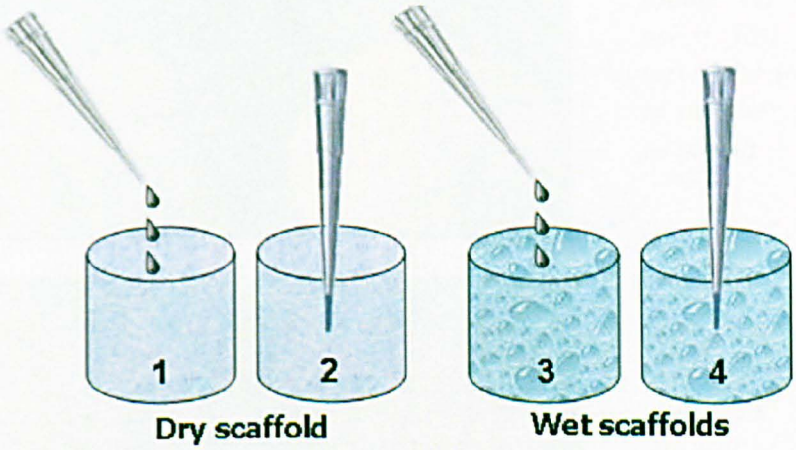

***Fig. 3.9**: Injection methods of cell suspension media into scaffolds. The media was injected on top or inside of wet or dry scaffolds with 3 different volumes; 100 µl, 150 µl, 200 µl.*

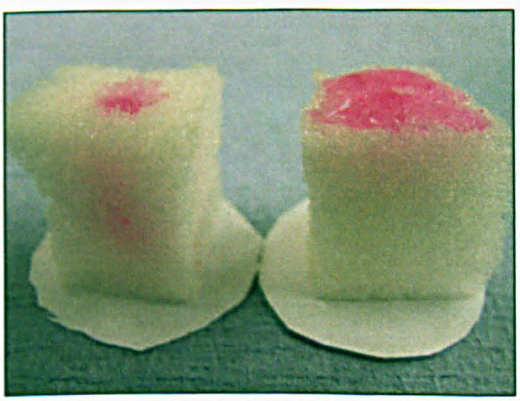

***Fig. 3.10**: Absorption of media on dry PU scaffold. The media was injected inside (left) and on the top of scaffolds (right).*

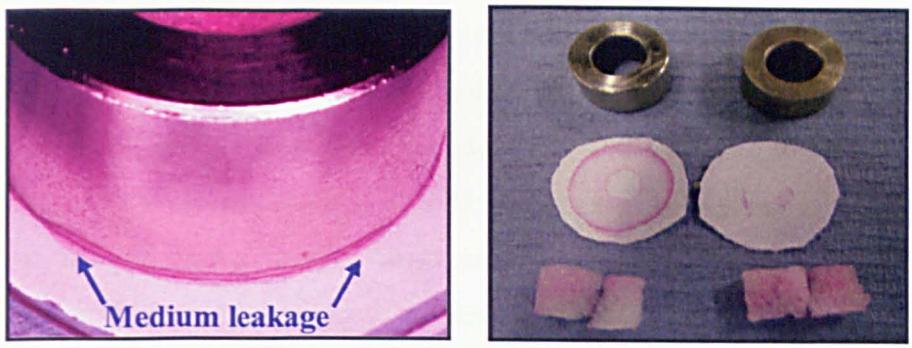

Fig. 3.11: White papers under the scaffold-stainless steel rings. The leakage of culture medium was shown on the papers.

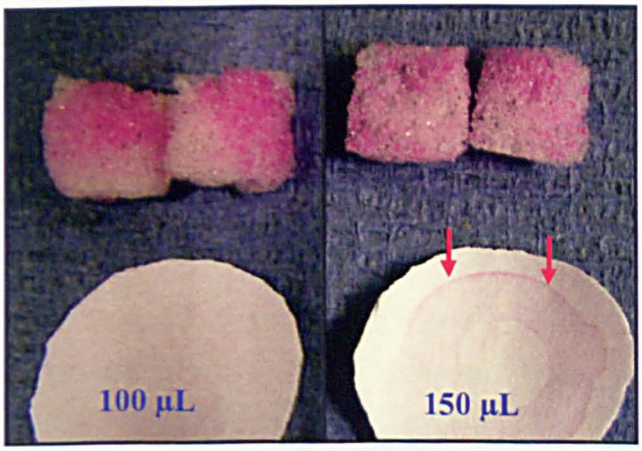

Fig. 3.12: Media leakage on white papers. Media was found on the paper after using 150 µl media on the top of the wet scaffold but not in another sample using 100 µl media.

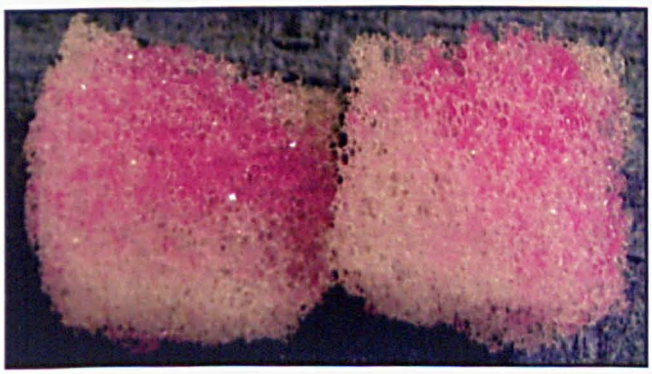

Fig.3.13: The distribution of 100 µl culture medium around the scaffold.

3.4 Monitoring the viability of cells in the scaffold (comparing MTT and MTS)

As previously mentioned, the concentration of initial seeding cell number may affect the cell distribution and viability on scaffolds. In this experiment, we used the established amount of cell-media suspension, calculated and tested from the experiment

in stage 2, to seed cells into scaffolds with varying numbers of cells suspended in 100 µl of media to see the distribution of cells on scaffolds. MLO-A5 cells were seeded at $125x10^3$ and $250x10^3$ cells per 2-D plate and $500x10^3$ and $1000x10^3$ cells per 3-D scaffold. Samples were assayed for cell viability at 3 hr and 5 days after seeding using the MTT and MTS assay. In the present study, MTT was also used to confirm that cells survived and uniformly proliferated in 3-D scaffolds in all groups by indicating the distribution of dark blue or purple formazan crystals all around whole scaffolds and when cut in half *(Fig. 3.15)*. However, we found that MTT cannot appropriately be used to quantify cell viability in this 3-D system because dissolving and removing the formazan crystal properly from scaffolds is very difficult, which may lead to data errors reading the absorbance on plate reader *(Fig. 3.14)*. MTS was an alternative method to quantify relative cell number because it easily releases the pink soluble formazan salt across the cell membrane into surrounding media.

3.4.1 Results

This study, comparing MTT and MTS, showed that the absorbance values from the MTT assay were different between 2-D and 3-D, giving an apparently lower cell numbers in 3-D. In contrast, The MTS assay showed that the relative cell numbers in 2-D and 3-D were similar *(Fig. 3.16)*. The observation of MTT staining showed the darker blue formazan crystals on scaffolds of the day 5 samples compared with the 3 hr samples indicating more cells on the scaffold *(Fig. 3.14)*. However, when the stain was eluted, the absorbance data did not show higher relative number of cells at day 5 compared with 3 hr indicating that the stain was not completely removed from the scaffold by dissolving MTT.

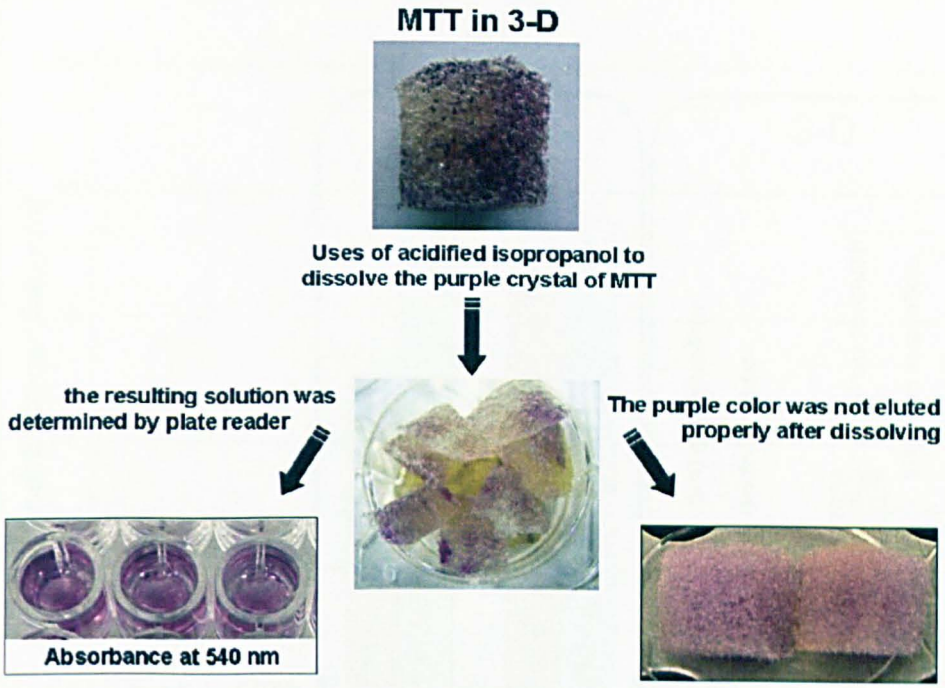

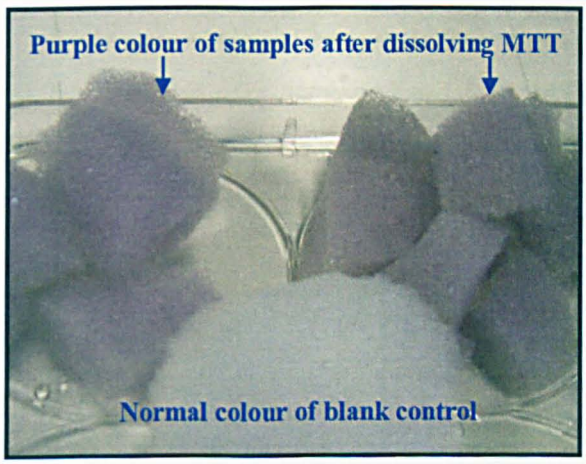

Fig. 3.14: Steps of MTT quantitation. Acidified isopropanol was used to dissolve dark blue colour of formazan salt which was not removed properly from cell-seeded scaffolds. The purple colour was still shown on samples compared with a blank control scaffold.

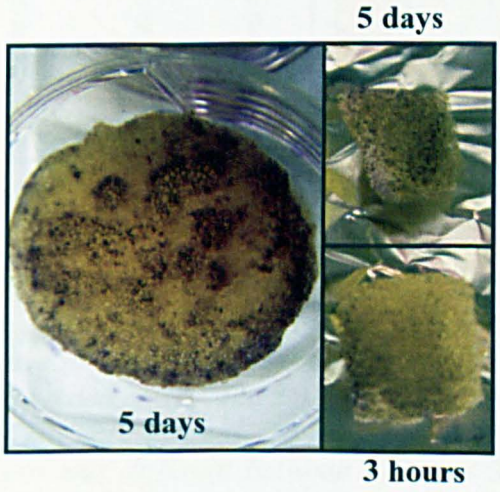

***Fig. 3.15**: The dark blue formazan crystals from MTT assay. The crystals indicate more cells on the scaffold at day 5 compared with 3 hr after seeding.*

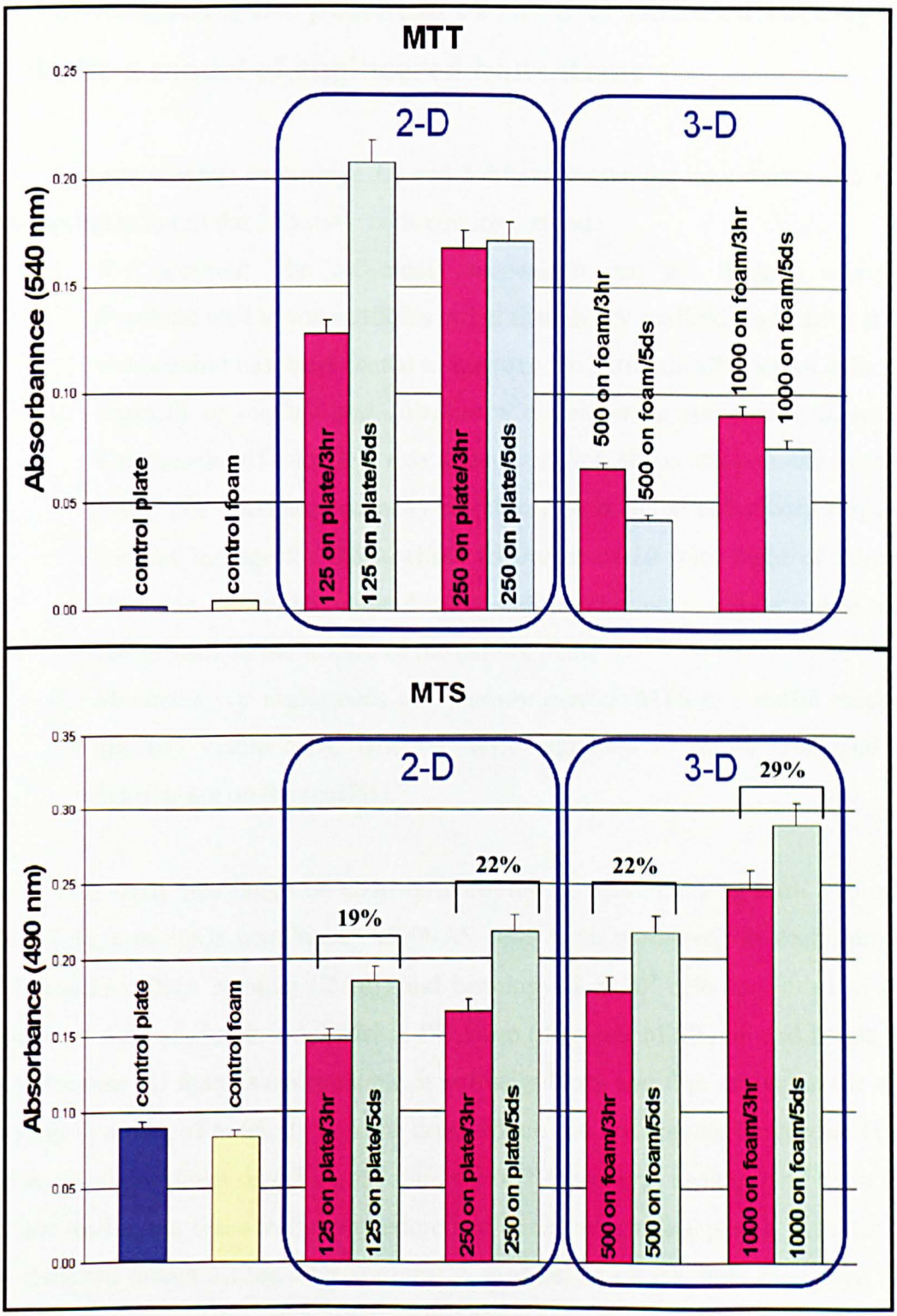

***Fig. 3.16**: The bar chart comparing MTT and MTS assay. Data indicates the relative number of viable cells by reading the optical density of formazan product. Cells seeded in 2-D and 3-D conditions at 125, 250, 500 and 1000×10^3 cells/well or scaffold, were assayed at 3 hrs and 5 days of culture. In the MTT assay, the viability pattern was different between 2-D and 3-D, there was an apparent reduction in value in 3-D. In contrast, in the MTS assay, there were similar increases of viable cells between 3 hrs and 5 days in both 2-D and 3-D. (N=2 in each condition, control is the plate or scaffold only with no cells present).*

3.5 Investigating the potential of the 3-D static culture system to be a model of engineered bone tissue

The experiments from stage 3.3 and 3.4 have shown the importance of 3 factors in the optimization of the 3-D static cells culture method.

1. *Wet scaffold*: The cell-media suspension can get through easily and distribute well in wet scaffolds rather than in dry scaffolds indicating that the wet scaffold has the potential to improve the initial distribution of cells.
2. *Capacity of scaffold and distribution of cell-media suspension on scaffold*: The capacity of a scaffold may depend on size, shape and porosity of this PU foam. The maximum capacity which can hold initial cell-media suspension without leakage for this scaffold (diameter of 10 mm, hight of 10mm) is 100 µl to insure the required initial cell number on scaffolds and to reduce cell growth on the surface of the culture plate.
3. *Monitoring of viable cells over culture period*: MTS is a useful method to quantify viable cells, whereas MTT can help to locate cells and their distribution on the scaffold.

This study was based on short-term culture, to optimize long-term 3-D culture over 15 days in static conditions, MLO-A5 cells were monitored in scaffolds using MTT staining, DNA staining (DAPI) and histology. $2.5x10^5$ cells in 100 µl of media suspension were seeded in a cylindrical PU foam (diameter of 10 mm and height of 10 mm). Because PU foam is hydrophobic, it normally floats and flips around in the media, resulting in a lack of nutrients in some areas which can not contact the media. For this reason, a stainless steel ring (internal diameter of 10 mm) was used to hold the scaffold in place during the cell seeding procedure and initial attachment period. After the ring was removed (about 12 hrs after seeding), a medical grade stainless steel wire holder was used to immerse the cell-seeded scaffold in the media over the culture period. The media was changed every 3 days with 10 ml of fresh media, fully covering a whole scaffold in a 6 well plate, to provide sufficient nutrients.

3.5.1 Results

MTT staining showed that cells distributed well in the scaffold and remained viable over 20 days of culture. Viable cells were present throughout the scaffold *(Fig. 3.17)*. DNA staining by DAPI was used to observe the distribution of cell nuclei along the scaffold struts. Nuclear staining by DAPI and fluorescence microscopy indicated that cells were contained within the scaffold pores by day 5 but did not show visual evidence of adhesion to the sides of the scaffold pores. However by days 10 and 15 of culture, clusters of cells were found lining the walls of the scaffold pores and cells appeared to be embedded in extracellular matrix *(Fig. 3.18)* as confirmed by the later experiments in the next chapter. Histology sections also confirmed cell attachment on the scaffold struts by days 10 *(Fig. 3.19)*.

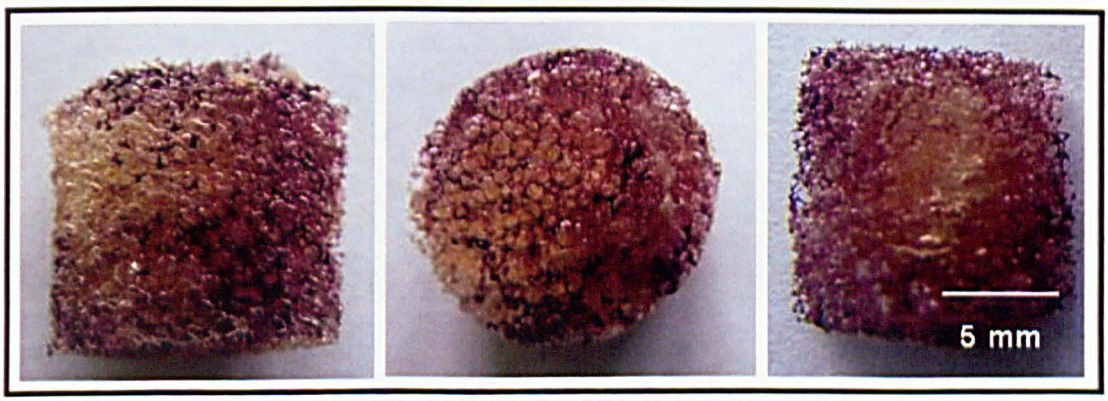

***Fig. 3.17**: Stained scaffold using MTT. Active cells were found throughout the scaffold at day 20 of culture (left: intact scaffold side view, centre: intact scaffold top view, right: transverse section of scaffold).*

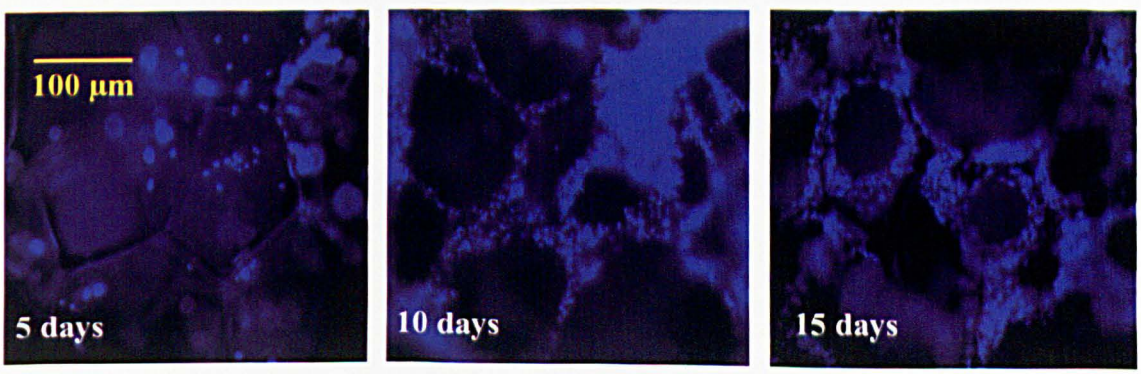

***Fig. 3.18**: Fluorescence images of DNA staining on PU scaffolds. DNA of cells was stained by DAPI (blue). Clusters of cells are found lining the walls of the scaffold pores and appear to be embedded in extracellular matrix by days 10 and 15 of culture (×20 fluorescence microscope).*

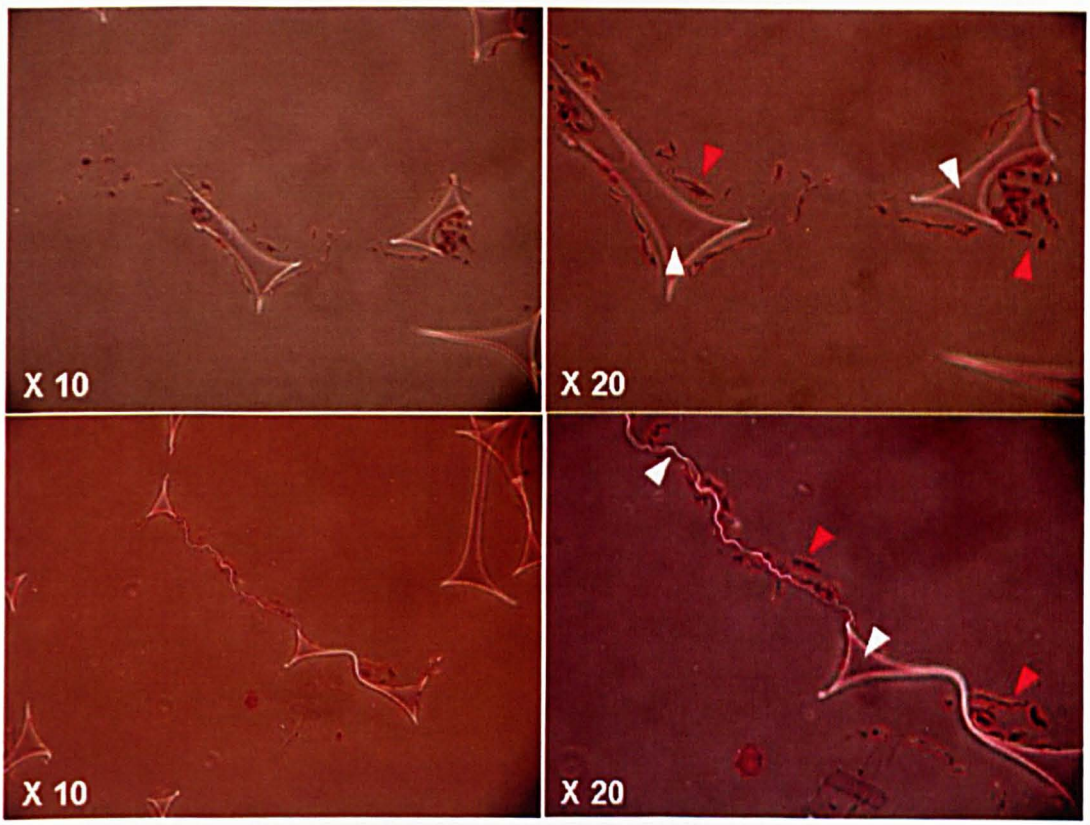

***Fig. 3.19**: Histology sections of cell-seeded scaffolds on day 10 of culture. Cells (red arrow head) were found attached to and lining the scaffold struts (white arrow head).*

3.6 Discussion

We have demonstrated for the first time in this chapter that MLO-A5 osteoblastic cells can be cultured on an industrially produced PU foam which has not previously been reported for use in 3-D tissue culture before. We optimized a non-dynamic method to culture cells in this novel PU scaffold as a model system by which bone cells could survive in 3-D static culture and their responses to stimuli could be examined *in vitro* in a 3-D environment. The systems has less complicated equipment and techniques compared to dynamic seeding and culture system making it easy to use and operate in the laboratory. In addition, cells are not pre stimulated by any mechanical stimuli during seeding and culture which enables the researcher to study selected mechanical stimuli and mechanotransduction in bone tissue constructs. We suggest that 3-D bone engineered constructs can mimic the bone environment providing a better physiological model than cells cultured in 2-D monolayer. The model could be used for bone engineered tissue implantation and other *in vitro* studies of bone in 3-D environments including a better understanding of the mechanically controlled tissue differentiation process.

Important keys factors in our static culture model are (i) *The scaffold material* which is biocompatible and has good properties such as wide pores, high porosity and good elasticity to provide enough media perfusion for nutrients and waste product transportation throughout scaffolds, (ii) *The appropriate proportion between the size of scaffolds and initial cell number in cell-media suspension* (initial cell concentration) in the seeding step which can help to distribute and maintain cells in the scaffold during the initial attachment. (iii) *Scaffold holders*, stainless steel rings and wire holders, help to stabilise and immerse the cell-seeded scaffold in the media without contacting the surface of the culture plate over the culture period, (iv) *Pre-soaked scaffolds* with culture media containing serum which improves the hydrophilicity of the scaffold. (v) *Type of cells* which can rapidly grow and spread on scaffolds. Although, this non-dynamic model showed acceptable results, the model did not show perfect distribution of cells in the center of scaffold as seen in the transverse section of scaffold stained by MTT *(Fig. 3.17)*. However, alternative techniques such as mechanical stimuli to induce media flow and/or perfusion bioreactor culture could be added to the culture system to improve the growth, migration and distribution of cells.

MLO-A5 cells represent the late stages of osteoblasts/pre osteocytes. To my knowledge, these cells have never been used in 3-D cultures before. MLO-A5s were chosen for this study because of their reported ability to produce matrix rapidly. In stage 4 of this chapter, we have tested and confirmed that MLO-A5 cells can mineralize faster than other osteoblast-like cells when supplemented with low concentration of βGP in 2-D culture, therefore a low concentration of βGP (2 mM) was chosen for use in our 3-D model (in the next chapter) as also recommended by Chung et al. (1992) to minimise the chance of non-cell specific calcium phosphate deposits [213]. However, culturing the cell-seeded scaffold constructs in the standard concentration of 5mM βGP, which is widely used in many studies, may accelerate mineralization further.

Ignatius et al. (2005) demonstrated that low initial cell seeding densities ($7x10^3$ cells/cm^2) on 3-D rectangular collagen gels led to better cell proliferation and viability than high densities ($1.7x10^4$ cells/cm^2), indicating that low initial cell concentration might result in a better adaptation towards 3-D culture conditions [86]. However higher initial seeding cell concentrations were used in most previous studies ($1.2x10^5$ - $6x10^7$ cells/cm^2) [81, 92, 215, 216] including in our present study ($5.3x10^4$ cells/cm^2; calculated using total scaffold surface, struts plus pores) to gain sufficient detectable matrix production by cells.

Metabolic assays such as MTT and MTS are widely used to evaluate cell viability or cell proliferation in 2-D studies [217]. However, cells at different densities exhibit different metabolic activity levels in 2-D and 3-D [195]. The quantification of cell number by dissolving MTT formazan salt in 2-D and 3-D has shown different trends in our study. The results in 3-D from the MTT assay are also much different from MTS in the same group of samples. Although the purple formazan salt of MTT was clearly present throughout the scaffolds, this was not reflected in the optical density. Both MTT and MTS solutions may not be able to reach all of the cells in the interior regions of scaffolds and the metabolic products may not be properly removed from the scaffolds in the supernatant. Many studies have shown that the accuracy of metabolic assays in 3-D is dependent on the efficiency of metabolite diffusion into and out of constructs [195, 218]. It seems that using an MTT assay to quantify cell proliferation is more erroneous than the MTS assay because of the difficulty in removing insoluble

metabolic products from cells and scaffolds. We suggest that MTS, or a similar method in which the product is soluble, will be a better method to quantify relative cell number rather than MTT.

Although we had more viable cells from MTS by 5 days compared with 3 hrs, it is not possible to calculate a proliferation rate based on this result because, as well as cells proliferating in the scaffold, some cells may have died or stopped proliferating. The MTS can only report the final relative amount of viable cells which have result from a combination of proliferation, differentiation, apoptosis and necrosis. Interestingly, when double the number of cells was seeded, this did not result in double the number of viable cells by MTS assay at 3 hrs. This may be because some cells could not stick on the surface of the scaffolds at 3 hrs, some cells could not access the limited surface area of the scaffold or the MTS assay may have a non-linear relationship with cell number. The final number of viable cells at day 5 also did not indicate double the amount of cells, this may be because the higher amount of cells per surface area inhibited proliferation or also due to a non-linear relationship.

Many people have shown that other formulations of polyurethanes are biocompatible both *in vitro* [126, 144, 146, 147, 176, 183, 211] and *in vivo* [219, 220] but the PU used in the present study is an industrial type of PU which has not previously been reported to be used for tissue culture. Although, there is limited use of PU scaffolds in bone tissue engineering because of their long-term *in vivo* lack of biodegradation [178], they were chosen for use in the present study because they have sufficient elasticity, resiliency and stiffness to deal with *in vitro* mechanical loading, and also are highly reproducible and cost-effective. In this chapter, we demonstrated that this PU was biocompatible with human fibroblasts and MLO-A5 mouse osteoblastic cells. These results are in agreement with the study of Guelcher et al. (2006) in which MG-63 osteoblastic cells were seeded in PU foams under dynamic conditions, they showed that PU foams had no signs of cytotoxicity and supported the attachment of cells. They have demonstrated that not only were high cell viabilities found using MG-63, but also using MC3T3 cells in the similar PU foams [174]. In addition, Fassina et al. (2005) have shown that PU foam can support cell proliferation and calcified matrix deposition of SAOS-2 human osteoblastic cells [126]. This suggests that PU has the ability to support many cell types. PU, however, is

hydrophobic polymer in which cell culture media does not penetrate easily when dry. In our study, we demonstrated that PU becomes more hydrophilic when sterilized in alcohol overnight and pre soaked with culture media before cell seeding. It is possible that pre soaking with culture media containing serum also allows cells to easily attach to the protein of the serum.

Although this new industrial grade PU scaffold shows the potential to be used in bone tissue culture, it may not be an ideal material for tissue implantation if degradation is required. However, Professor Anthony J. Ryan in Department of Chemistry University of Sheffield is developing degradable polyurethane scaffolds for further refinement of our system where we hope to allow scaffold degradation to occur as bone matrix is produced [221]. Chemical and structural modifications in the near future are being performed in several laboratories to discover whether it is possible to improve the final biochemical characteristics of PU scaffolds for bone tissue engineering applications including injectable PU scaffold [174, 222] and PU/ carbon nanotube foams [223].

The permeability of media through scaffolds is another important factor in tissue engineering since the appropriate fluid mobility allows maximal nutrient influx to support cells in scaffolds *in vitro* as well as *in vivo* wound sites. O' Brien et al. (2007) have shown that there are a number of factors that influence the permeability of foams such as porosity, pore interconnectivity, pore size and orientation, fenestration size and shape and surface area. They have found that scaffold permeability increases with increasing pore size (from 96 to 151 microns) and high porosity (>90%), and decreases with increasing compressive strain (from 0 to 40% strain). In addition, the porosity of foams can also decrease under compression [210]. The scaffold used in our 3-D model has a high mean pore size (mean±SD of 384±151 microns) which was recommended for bone tissue engineering (>300 microns) by Karageorgiou et al. (2005) [212] and has a high elasticity in both wet and dry conditions (chapter 2) which may help to increase the scaffold permeability and also to maintain the shape preventing pore closing and permanent deformation of the scaffold under high compressive force.

Many previous studies have shown that it is difficult to distribute cells within the scaffold with adequate uniformity and supply them with sufficient nutrients to support

growth, function, and viability throughout the constructs in 3-D static culture [81, 132, 133, 224-227]. Cell seeding of scaffolds is the first step in establishing 3-D culture and plays a crucial role in determining the progression of tissue formation [225]. The initial cell density and initial cell distribution within the scaffold affects the uniformity of cells in engineered tissue constructs [226]. However, in our 3-D static culture system, we showed that cells migrated and distributed well in the novel industrial grade PU scaffold and remained viable over 20 days of culture. Viable cells were present throughout the scaffold as shown by MTT staining and produced extracellular matrix in which they embedded.

3.7 Summary

- We have tested our hypotheses that the novel industrial grade PU scaffold is biocompatible and has good properties such as wide pore size and good elasticity to provide enough media perfusion for nutrient and waste product transportation throughout scaffolds.
- Cells can survive and distribute well throughout scaffolds in static condition over 15 days of culture period.
- The appropriate proportion between the size of the scaffolds and initial cell number in cell-media suspensions (initial cell concentration) in the seeding step of the model system can help to distribute and maintain cells in the scaffold during the initial attachment step.
- Stainless steel holders help to stabilise and immerse the cell-seeded scaffolds in media without contacting the surface of the culture plate over culture periods.
- Pre-soaked scaffolds with culture media containing serum can improve the hydrophilicity of the scaffolds.
- The MTT assay can help to locate cell distribution on scaffolds, whereas the MTS assay is a better method to quantify relative number of viable cells in 3-D scaffolds.
- MLO-A5 cells can mineralize faster than other cells when supplemented with low concentration of βGP (2 mM) in 2-D culture. They could be used for studying the effects of mechanical loading on the transitional stage of osteoblatic-osteocytic differentiation in culture.
- The optimized model system has the potential to be used in *in vitro* studies of bone in 3-D environments including a better understanding of the mechanically controlled tissue differentiation process and matrix maturation.

CHAPTER FOUR: Stimulation of bone matrix production and mineralization in bone tissue constructs using mechanical loading.

4.1 Introduction

Bone is believed to respond to mechanical loading via the mechanotransduction process, in which bone cells detect mechanical stimuli and convert them into biochemical signals [57]. Exploration of the mechanisms by which this occurs have centred on the role of the osteocyte in mature bone which is the cell best placed to sense changes in strain in mature bone matrix [64, 93]. In most models of bone mechanotransduction the osteocyte senses load and passes signals to the bone lining osteoblasts and/or bone resorbing osteoclasts. However, all bone cell types respond to mechanical load *in vitro* [228] and developing bone, which does not contain mature osteocytes, is also known to respond strongly to mechanical signals, for example during fracture healing [229, 230] and implant integration [231]. It is highly likely that the osteoid matrix also contains mechanically responsive cells which may signal to neighbouring cells and/ or respond directly with a bone forming response.

Many studies have provided evidence to support the paradigm that bone formation is stimulated *in vivo* by strain [232, 233] and strain induced fluid flow [234]. However, understanding how osteoblasts and their precursors respond to mechanical loads has been complicated by the routine use of 2-D substrates for mechanobiological investigations. Crucial mechanobiological parameters differ when cells are rounded, similar to the *in vivo* 3-D environment where cells are embedded in their own matrix, rather than flattened on a 2-D surface. Bacabac et al. (2008) have shown that cell function and mechanical properties are closely related to morphology. They suggest that a rounded cell morphology leads to a less stiff cytoskeleton compared to a flattened cell morphology [235]. In addition, Cukierman et al (2001) have provided evidence that focal cell-matrix adhesion complex formation in 2-D and 3-D configurations is different, in terms of structure, localization, and function. 3-D-matrix interactions can enhance cell biological activities and focus integrin distribution into discrete points [236]. Jarrahy et al. (2005) have also shown that osteoblastic cells responded to osteogenic differentiation at a slower rate when cultured on 3-D scaffolds by

downregulating both alkaline phosphatase and osteocalcin relative to 2-D culture [237]. These works have demonstrated the importance of dimensionality in interactions controlling communication between cells and the matrix. Mechanical forces may be transmitted to cells differently when cells are on a 2-D surface or within a 3-D matrix, and cells in a 3-D matrix may experience mechanical signaling that is unique compared with that in 2-D environments. However, the mechanisms underlying these differences are still unclear.

3-D bone tissue engineering models used as mechanobiological test system have the potential to provide data to improve bioreactor conditions for engineered bone tissue as discussed in the research community [238]. Some researchers are already using developments in 3-D culture to apply mechanical forces previously applied in 2-D to 3-D culture systems e.g. substrate strain [86, 138, 149, 239] and oscillatory fluid flow [81, 92, 215] as summarized in *Table 4.1*. These studies have looked for either short term signaling outcomes such as release of the endocrine factor PGE_2 [81, 92], mRNA expression of the growth factor and osteogenic markers [86, 92, 149, 215], or matrix protein production [138, 239].

***Table 4.1**: A table of various studies of osteoblastic cells, showing responses of cells to mechanical loading in 3-D environments.*

Group	Cells	Type of stimulation	Outcome
Jaasma and O'Brien (2008) [92]	MC3T3-E1	Intermittent flow perfusion (collagen-GAG scaffold)	Upregulation of PGE_2 release and COL1, COX-2, OPN mRNA.
Tanaka et al. (2005) [215]	MC3T3-E1	Strain induced oscillatory fluid flow (OFF) (decellularized bone scaffold)	Upregulation of c-fos, COX-2, OPN mRNA.
Vance et al. (2005) [81]	MC3T3-E1	OFF perfusion (porous calcium phosphate scaffold)	Upregulation of PGE_2 release.
Ignatius et al. (2005) [86]	Human fetal osteoblastic cell line	Cyclic stretching (collagen gel on silicon dish)	Upregulation of Runx-2, ALP, OPN, OCN, COL1, histone H4 mRNA.

In addition, many research groups have indicated that matrix production and mineralization by bone marrow-derived mesenchymal stem cells may be increased by short periods of cyclic strain *in vitro*, e.g. in a 4-point bending model [138], uniaxial cyclic tensile strain [149] and cyclic longitudinal strain [240] (to be discussed further in chapter 6).

Mechanical stimulation in 3-D bioreactors for tissue engineering which can generate mechanical stimuli and provide nutrients through scaffolds may help to enhance bone formation, reduce the time needed to grow tissues and improve the mechanical properties of bone tissue constructs. In addition, they also show great promise as a tool to study bone cell mechanotransduction mechanism in a 3-D environment *in vitro*. In the previous chapter, we optimized a 3-D static culture system and tested the hypotheses that the novel industrial grade PU scaffold is biocompatible and can be used to culture MLO-A5 osteoblastic cells in a 3-D static culture model. Cells were shown to survive and distribute well throughout scaffolds in static condition over 20 days of culture. Images from fluorescence microscopy indicated that cells were embedded in their extracellular matrix along struts of scaffolds suggesting that this newly developed 3-D culture model has the potential to be used for further investigations of extracellular matrix and its mineralization in 3-D scaffolds.

In this chapter, our hypothesis is that intermittent short period of dynamic mechanical stimulus can improve cell growth and matrix production during 3-D static culture. The principal aim of this study was to examine whether mechanical loading would improve cell growth and accelerate matrix maturation and mineralization by MLO-A5 cells in a 3-D environment. Therefore, intermittent mechanical compressive loading and osteogenic supplements were added to the 3-D model developed in the previous chapter to study the effects of mechanical stimuli on bone matrix maturation and mineralization in tissue engineered bone constructs.

To test the hypothesis in this chapter, the experiments were divided into 3 stages:

- Stage 1: investigation into the effects of different mechanical loading regimens by varying loading times and culture periods on osteoblastic cells in 3-D constructs.

- Stage 2: using optimized short bouts of compressive loading to accelerate matrix maturation and mineralization in 3-D constructs.
- Stage 3: studying the effects of different compressive strains (2.5% and 10%) on matrix production and mineralization of osteoblastic cells in 3-D constructs.

4.2 Investigation into the effects of different mechanical loading regimens by varying loading times and culture periods on osteoblastic cells in 3-D constructs.

The aim of these experiments is to study different loading regimens by which the production of extracellular matrix by MLO-A5 cells could be stimulated by monitoring cell viability and collagen production. To study the effects of varying loading times and periods, MLO-A5 osteoblastic cells were statically seeded at densities of $2.5x10^5$ cells per scaffold in polyurethane (PU) foam cylinders, 10 mm height and 10 mm diameter, using the seeding and culture methods described in chapters 2 and 3. The cell-seeded scaffolds were cultured in standard culture media supplemented with AA (without βGP). Dynamic loading under cyclic compression was applied in a sterilised biodynamic chamber at 1Hz and 5% strain under 6 different regimens. Loading was applied for 0.5, 1 or 2 hours (loading period) per day and repeated 2 or 3 times (loading time) over the experimental period *(Fig. 4.1)*. Between loading cycles, scaffolds were cultured statically in an incubator in standard conditions. Cell-seeded scaffolds were assayed at 2 or 5 days after the final load (post loading time) for cell viability by MTS assay and collagen content by Sirius red staining and colourimetry *(Fig. 4.1)*.

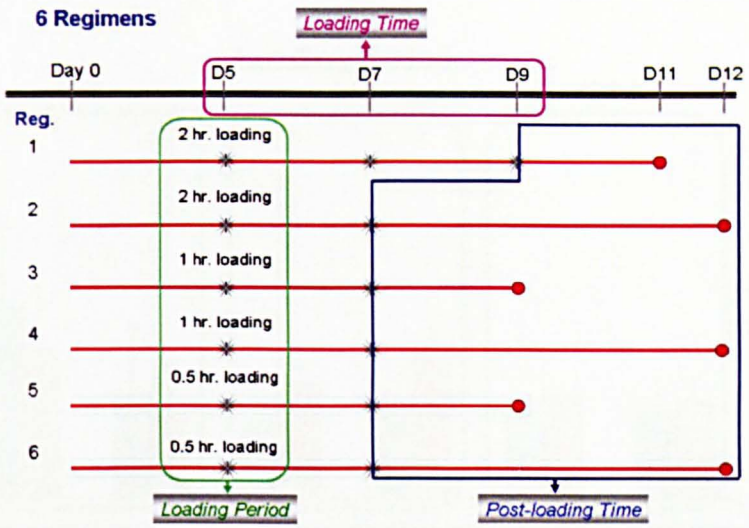

***Fig. 4.1**: Time lines between 6 different regimens. Loading period (0.5, 2 or 2 hr), loading time (2 or 3 times) and post loading time (2 or 5 days) were tested. Red dots show the day that samples were assayed. Stars show the days that samples were dynamically loaded with 5% strain, 1 Hz. (N=4 for reg 1,2,4 and 6, N=2 for reg 3 and 5).*

4.2.1 Results

Cell viability

MTS assay showed that MLO-A5 cells survived in all loaded scaffolds. Relative cell number in loaded samples increased when loading was applied for 0.5 hr and 1 hr, but was slightly less in the 2hr loading group compared with the nonloaded group *(Fig. 4.2)*. Although there was no statistically significant changes in cell viability within the loaded group between 2 days and 5 days after the final load, relative viable cell number significantly increased 5 days after the final load in loaded samples which had been loaded for 1 hr (regimen 4) compared with nonloaded samples ($p<0.05$) *(Fig. 4.3)*.

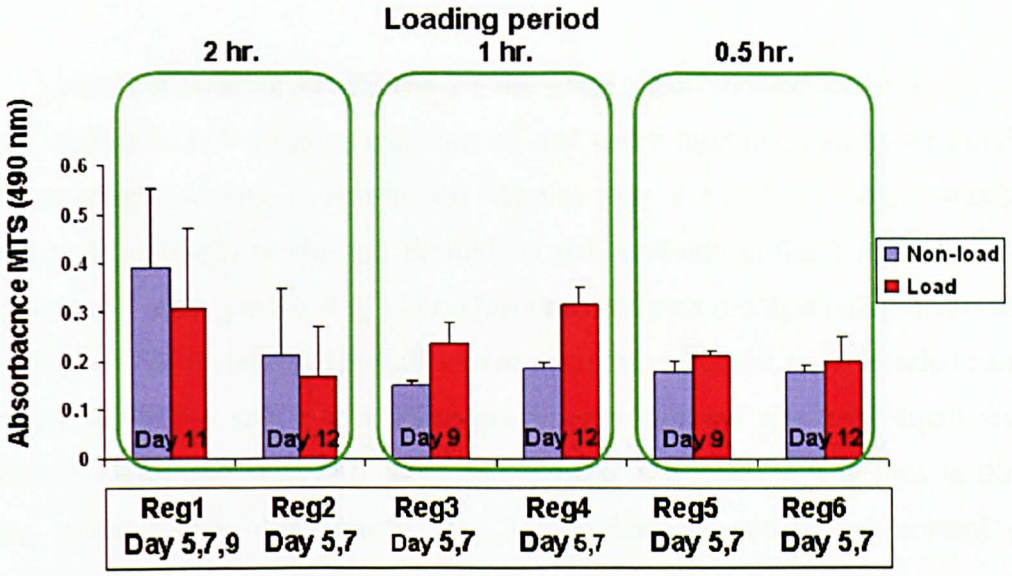

Fig. 4.2: Cell viability from MTS of 6 different regimens. Cell numbers increased in the loaded 1 hr and 0.5 hr groups but there were fewer viable cells in the loaded 2 hr group compared with non-loaded samples.

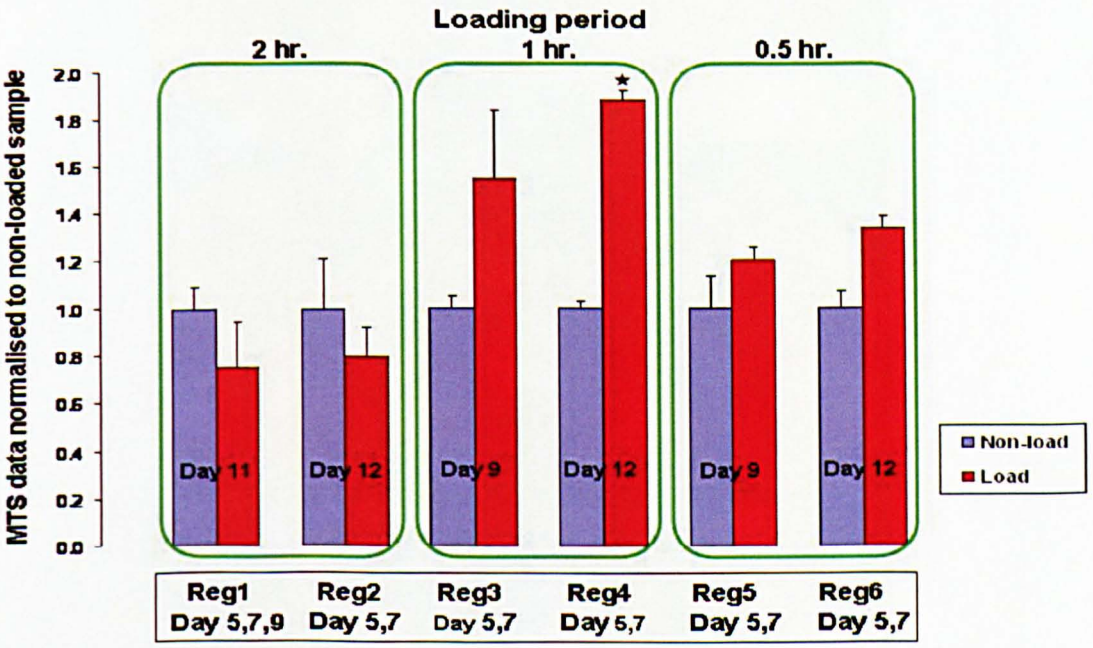

Fig. 4.3: Normalised data of 6 regimens from MTS assay. Relative viable cell number significantly increased 5 days after the last load in samples which had been loaded for 1 hr compared with nonloaded samples (Regimen 4) (two sample t-test, $p<0.05$).

Collagen content

Sirius red staining at the end of the experiment showed that the amount of collagen produced in both gross examination and under light microscopy was higher in loaded samples compared to non-loaded samples *(Fig. 4.4 and 4.5)*. There was higher uniformity of collagen production throughout the scaffolds in the 2 hr loading group compared with other groups *(Fig. 4.4)*. Quantitative Sirius red destaining demonstrated that collagen content increased in all loaded samples compared to nonloaded samples. However, in the 0.5 and 1 hr loading groups, the increase was very small and not statistically significant. The only large and significant difference was seen in the 2 hr loading group which was significantly higher than its non-loaded control group ($p<0.01$) *(Fig. 4.6, 4.7 and 4.8)*.

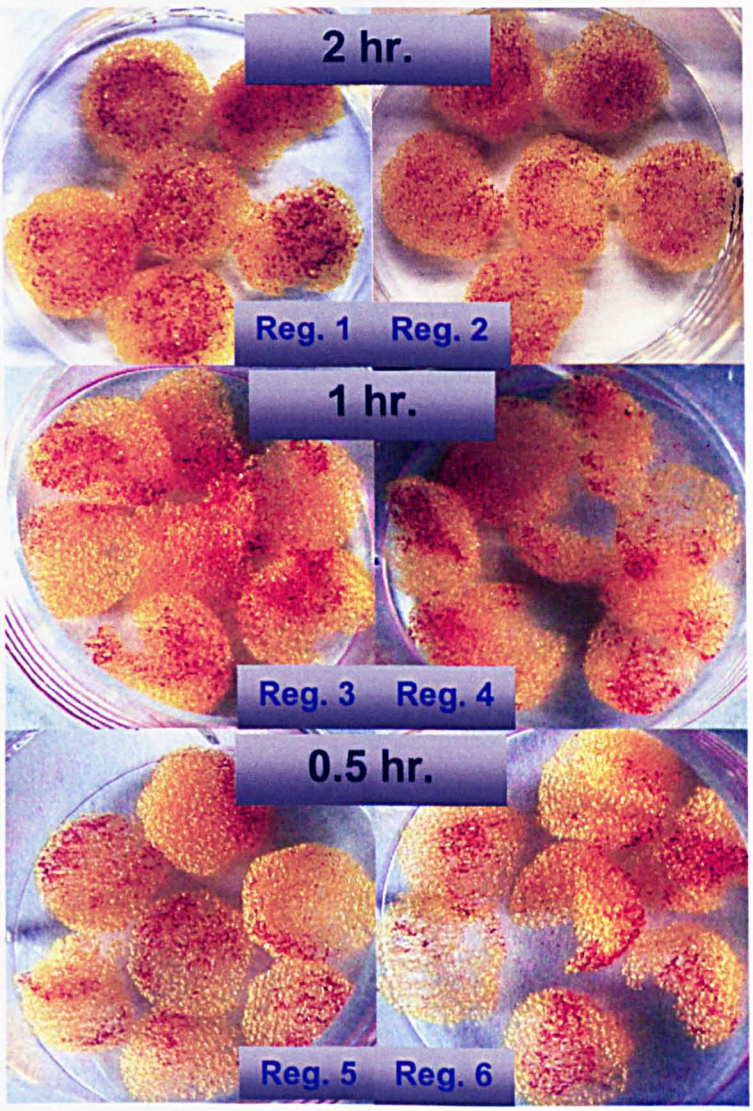

***Fig. 4.4**: Sirius red stained sections of whole scaffolds from 6 regimens. As seen in the photographs, there was higher uniformity of collagen production (red) throughout the scaffolds in the 2 hr loading group compared with other groups.*

***Fig. 4.5**: Sirius red staining at the end of the experiment from regimen 1. The amount of collagen in scaffold sections by digital photograph and light microscopy appeared higher in loaded samples compared to nonloaded samples.*

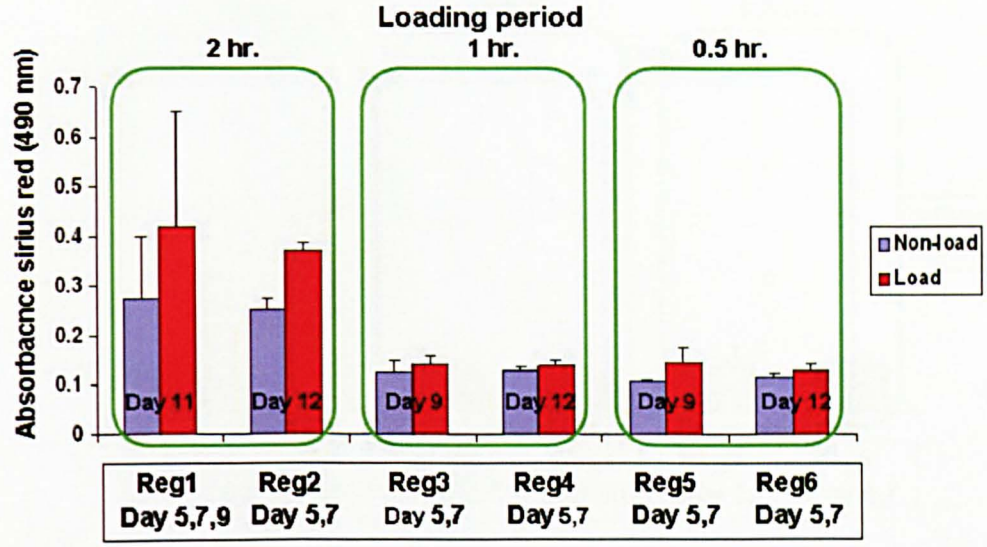

Fig. 4.6: Destaining of Sirius red of 6 regimens. Collagen per scaffold was about the same for the 1 hr and 0.5 hr loading groups but was higher in the 2 hr loading group compared with non-loaded samples.

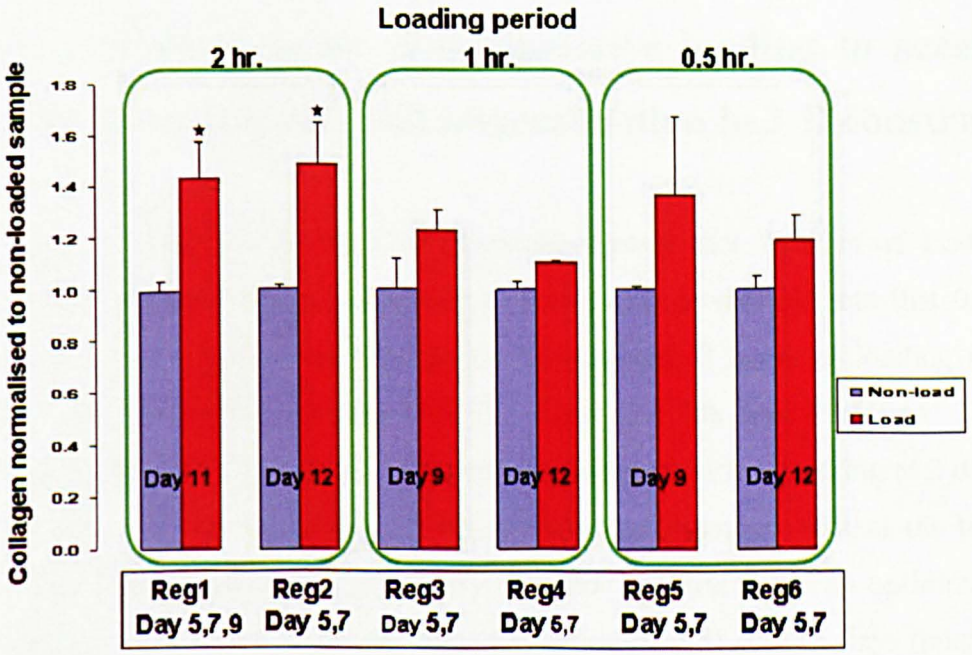

Fig. 4.7: Quantitative Sirius red normalised to non-loaded samples. Data demonstrated that collagen content was slightly but not significantly increased in the 1 hr and 0.5 hr groups. It was significantly higher in both regimens in which 2 hr of loading was applied (two sample t-test, $p<0.01$).

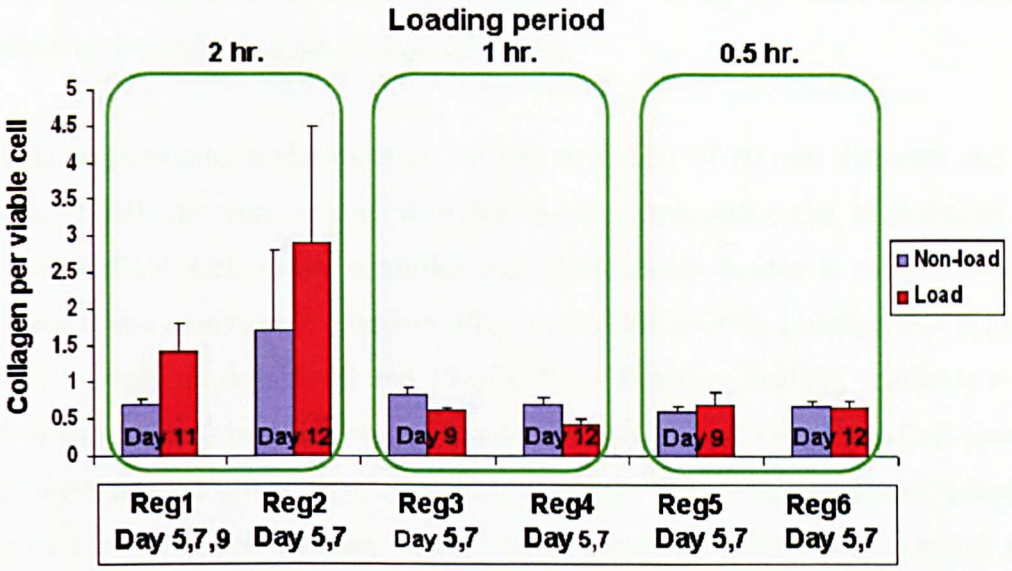

Fig. 4.8: Collagen data normalized to relative cell number. Collagen per cell remained the same in all loaded groups except the 2 hr loading groups where loaded samples contained more collagen per cell with high sample variability, compared with non-loaded samples.

4.3 Use of short bouts of compressive loading to accelerate matrix production and mineralization in 3-D constructs.

Results from the previous experiments showed that 2 hours of loading can significantly improve collagen distribution throughout the scaffold, but that 0.5 and 1 hour of loading do not at the time points investigated. 2 hours of loading can also increase collagen production measured at 5 days after the final load (reg. 2) with a greater difference from the non-loaded control compared with measuring at 2 days (reg. 1). Therefore, for the second set of experiments, we hypothesised that the bone-like matrix production and mineralization in 3-D tissue constructs can be optimized using 5% dynamic compressive strain for 2 hours (loading period) every 5 days (post loading time or resting time). The results from the 2-D study in chapter 3 also showed that calcium production by MLO-A5 cells increased significantly at day 14 compared with day 7. To investigate matrix mineralization, longer culture periods (more than 14 days) were required to provide enough time for the cells to produce detectable mineralized matrix in 3-D constructs. Therefore, the aims of these experiments were to examine the

effects of combining intermittent cyclic compressive loading on mineralized matrix production in 3-D scaffolds over 20 days of culture.

3-D polyurethane scaffolds were cut into cylinders of 10 mm diameter and 10 mm height. Scaffolds were seeded with MLO-A5 osteoblastic cells at densities of $2.5x10^5$ per scaffold. Cell-seeded scaffolds were dynamically loaded in compression at 1Hz, 5% strain in a biodynamic chamber (Bose Electroforce3200). Loading was applied for 2 hours per day on days 5, 10 and 15 of culture. Between loading, scaffolds were cultured in an incubator in standard conditions for up to 20 days *(Fig. 4.9)*. Cell-seeded scaffolds were assayed on days 10, 15 and 20 of culture for scaffold stiffness (young's modulus of elasticity), cell viability (MTS assay), calcium (Alizarin red staining) and collagen content (Sirius red staining). Separate samples were used for SEM and micro-computed tomography (micro-CT) of both loaded and non-loaded samples at the end of experiment. SEM was performed as described in chapter 2. For micro-CT, fixed samples were sent to the laboratory of Prof. Ralph Müller, Institute for Biomechanics, Eidgenössische Technische Hochschule (ETH), Zurich. Images were recorded and analyzed by Thomas Kohler and Martin Stauber.

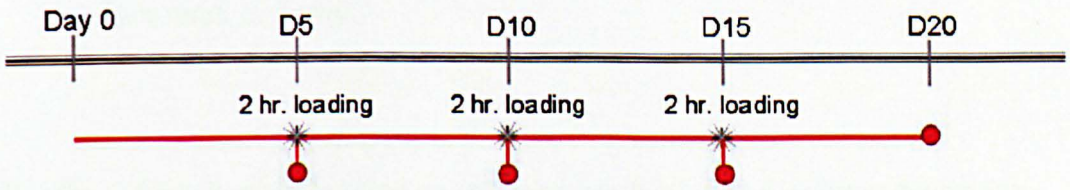

***Fig. 4.9**: Experimental design to study effects of scaffold compression on bone cells. The experiments consist of 2 hr loading periods, 3 short bouts of loading time (every 5 days) and a post loading time of 5 days. Red dots indicate the day on which samples were assayed.*

4.3.1 Results

The effect of mechanical loading on cell viability

After just 1 bout of 2hrs of loading on day 5, there were significantly more metabolically active cells as indicated by MTS on day 10 *(Fig. 4.12)*, however this

difference was not present in samples collected on days 15 or 20. Loading appears to accelerate cell proliferation in the short term (5 days after the first load) but in both groups cell number ceases to increase after day 15 (10 days after the first load). MTT staining showed that the dark blue crystals indicating viable cells were better distributed throughout scaffolds in loaded groups compared with non-loaded groups at day 20 *(Fig. 4.10)*.

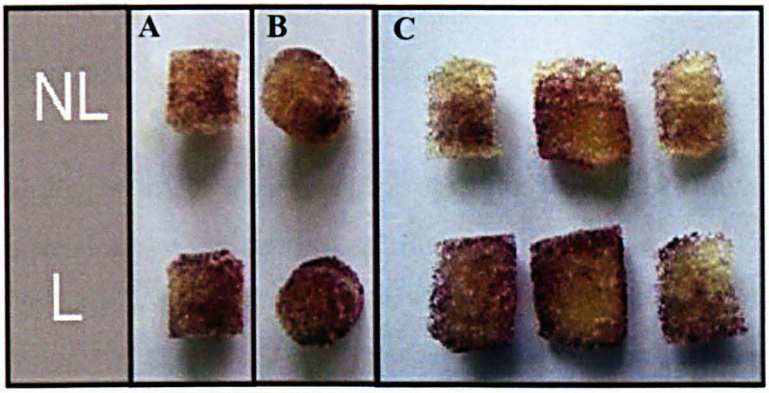

Fig. 4.10: *Viable cells on a scaffold up to 20 days of culture. MTT staining was used to loacate active cells (dark blue) on scaffolds. Cells survived and migrated throughout scaffolds in both load and non-load groups. (A: intact scaffold side view, B: intact scaffold top view, C: transverse section of scaffold, NL: Non-load, L: Load).*

The effect of mechanical loading on collagen production and calcium deposition

All scaffolds showed evidence of matrix production as indicated by Sirius red and Alizarin red staining from day 10 of culture. By day 20 loaded scaffolds contained significantly more total calcium and collagen compared to non-loaded controls as indicated by the intensity of red staining. The stain was more evenly distributed throughout the scaffold in loaded samples *(Fig. 4.11A and 4.11B)*. Both stains were quantified by colorimetry. Total collagen content was significantly, consistently 2 times higher ($p<0.05$) in loaded than non-loaded samples at all time points *(Fig. 4.12)*. Calcium content was significantly higher in loaded samples on days 15 and 20 only ($p<0.05$) *(Fig. 4.12)*.

When data were normalized to MTS levels to allow for cell number effects, collagen content per cell increased steadily over the time in culture with a more rapid increase in loaded samples throughout the culture period *(Fig. 4.13C)*. Calcium content per viable cell was low in non-loaded samples and barely increased over time *(Fig. 4.13C)*. In contrast, in loaded samples calcium content was slightly higher by day 15 and increased rapidly between days 15 and 20. The amount of calcium per relative viable cell number also increased by approximately 5 times ($p<0.05$), in the loaded group at the end of the experiment *(Fig. 4.13B)*.

Scaffold stiffness (Young's modulus of elasticity)

Alongside the increase in matrix production, scaffold stiffness increased in both loaded and non-loaded samples during culture, with a more rapid change in loaded samples. Empty scaffolds maintained a constant modulus over 20 days immersion in media, indicating the properties of the scaffold did not change during culture *(Fig. 4.13D)*. Stiffness was significantly (2 fold) higher in loaded samples by the end of experiments (~3.9 vs 6.2 KPa, $p<0.01$).

mRNA expression (RT-PCR)

In order to examine more immediate responses to loading, gene expression of matrix proteins; type I collagen (COL1), osteopontin (OPN) and osteocalcin (OCN), were measured 12 hrs after a single bout of 2 hrs loading or control treatment. Loaded samples showed higher levels of COL1 mRNA (about 3 fold) as measured by band density relative to GAPDH, a result consistent with increased collagen protein by Sirius red staining. OPN mRNA levels showed a 2 fold increase in loaded samples compared to nonloaded, with OCN showing a 2.5 fold increase, though the semi-quantitative density differences were not statistically significant *(Fig. 4.14)*. A parallel study performed by an undergraduate in our lab under my supervision showed that mouse OPN transcript levels of MC3T3-E1 osteoblastic cells were also higher after 2 hr of dynamic compressive loading. mRNA levels in samples collected 24 hr after loading were approximately 4 times higher than non-loaded samples using GAPDH as a control *(Fig. 4.15)*.

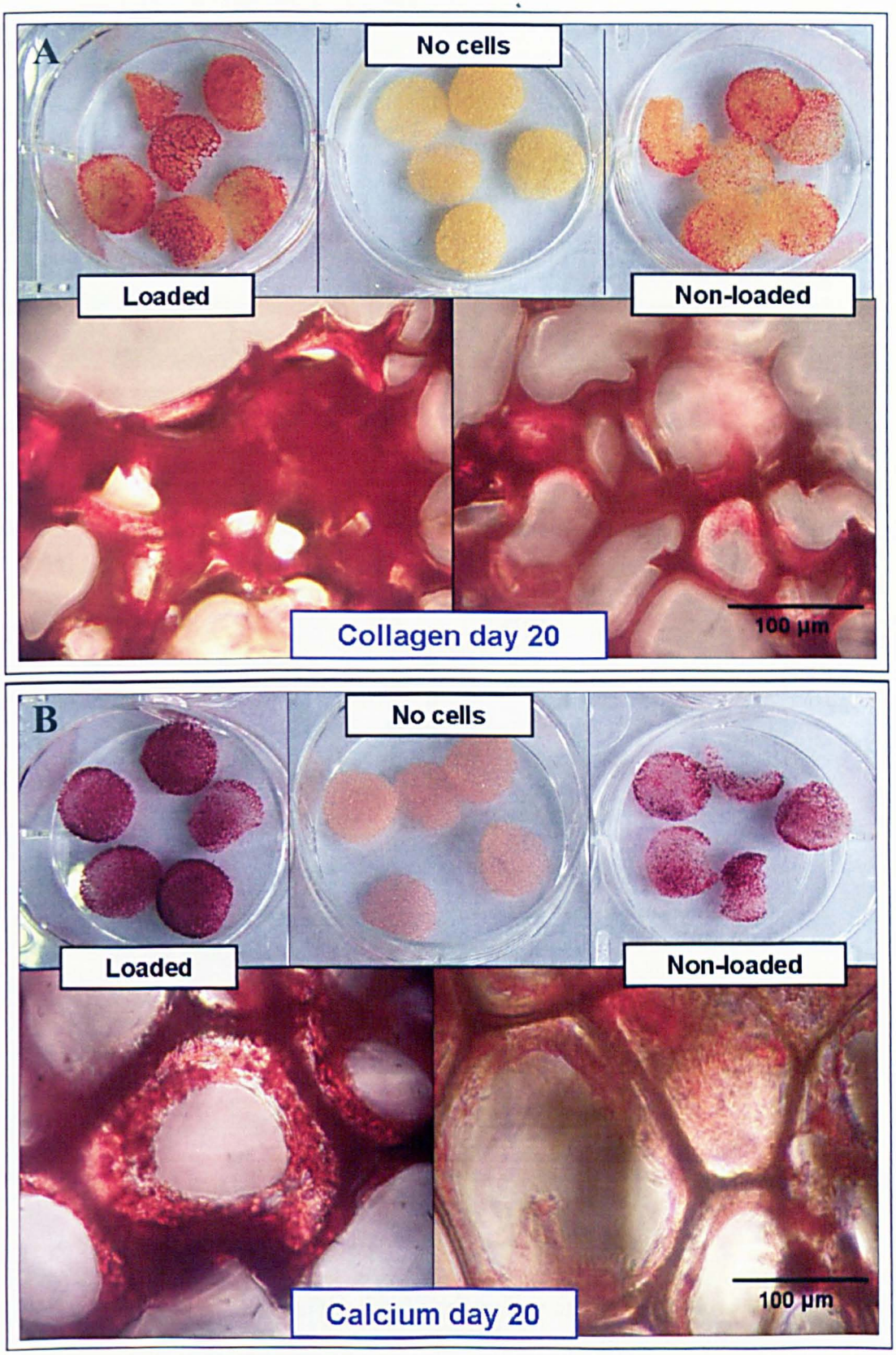

Fig. 4.11: *Calcium and collagen in the scaffolds. Appearance of representative loaded, empty and non-loaded scaffolds, one scaffold per well, cut into cross sections and stained with Sirius red (collagen)(A) and Alizarin red (calcium) (B), light micrographs of a random area of the scaffold are shown below. (pubished in Bone 2009).*

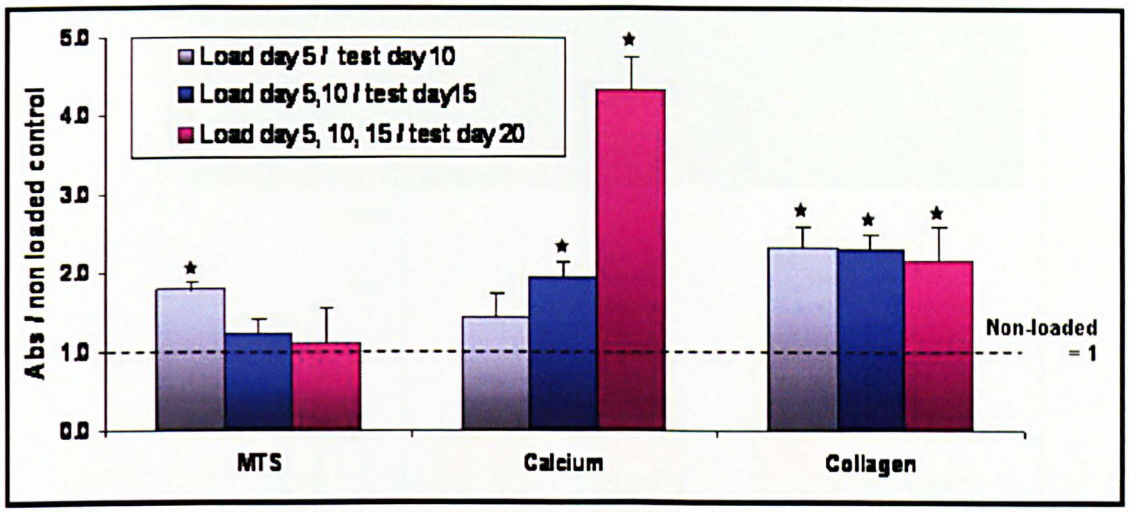

*Fig. 4.12: MTS, Alizarin red and Sirius red absorbance per loaded. Mean ± SD was normalised to its paired non-loaded scaffold scaffold at day 10, 15 and 20 of cultures. (n=6, *=p<0.05 for MannWhitney test). (pubished in Bone 2009).*

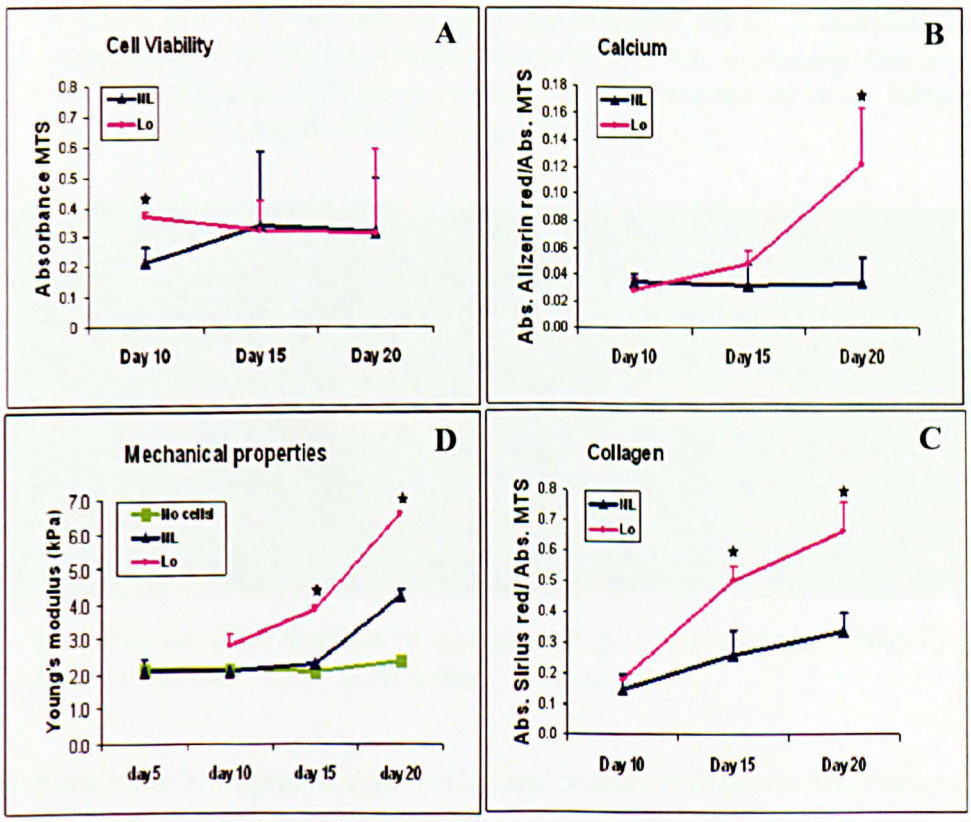

*Fig. 4.13: Changes over time in cell viability, calcium per viable cells, collagen per viable cells and mechanical properties of the scaffolds. Mean ± S.D. (A) Colourimetric absorbance of MTS (N=6). (B) Colourimetric absorbance of Alizarin red / respective MTS value (N=6). (C) Colourimetric absorbance of Sirius red / respective MTS value (N=6). (D) Young's modulus of elasticity under a single compressive load to 50% strain (N=4) *p<0.05 Student's t-test (NL=Non load, L=Load). (published in Bone 2009).*

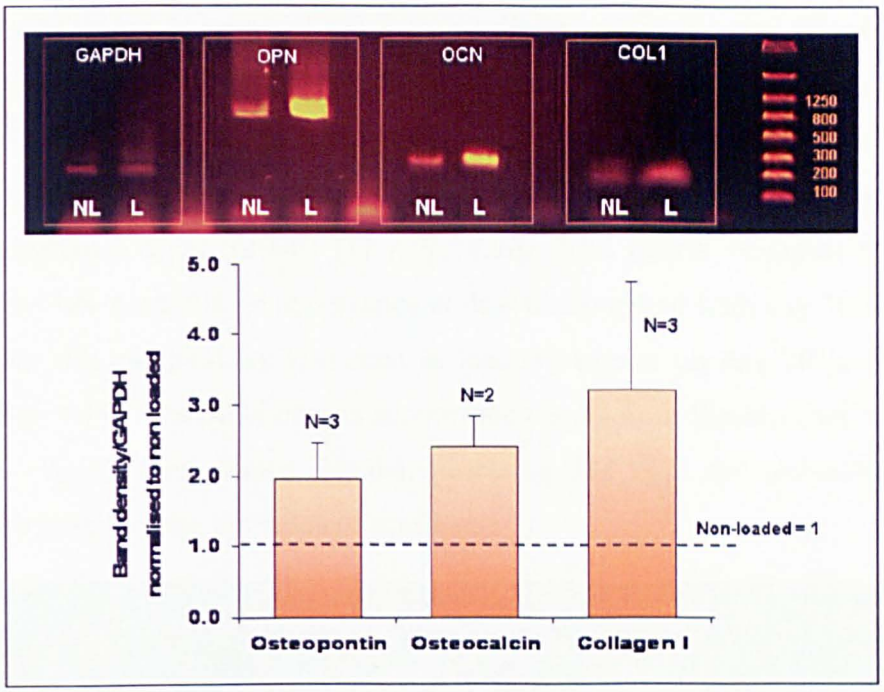

Fig. 4.14: *mRNA expression of Col1 OPN and OCN 12 hrs after a single bout of 2 hrs of loading. An example gel of 3 independent experiments is shown. Loaded samples showed increased levels of Col1, OPN and OCN gene expression as measured by band density relative to GAPDH. (NL=Non-load, L=Load).*

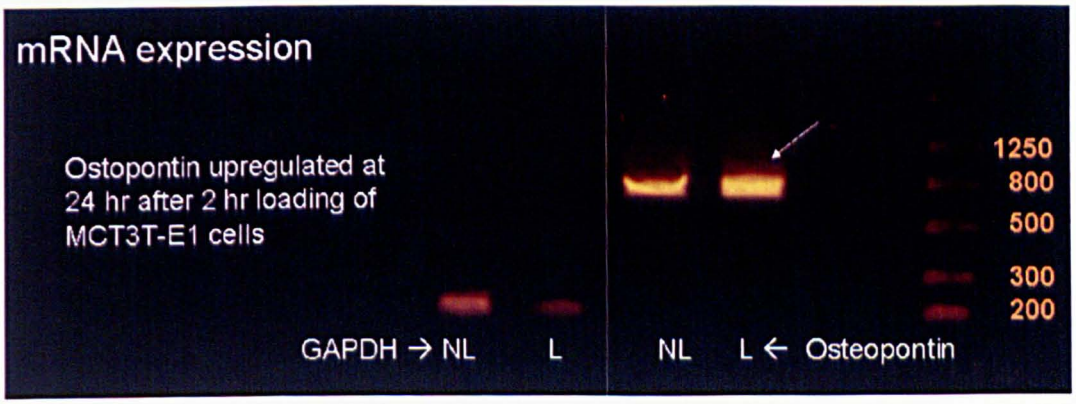

Fig. 4.15: *RT-PCR analysis of osteopontin gene expression of MC3T3 at 24 hr after 2 hr loading. (NL= non-loaded, L= loaded).*

Micro Computed Tomography (micro-CT) and Scanning Electron Microscopy (SEM)

Images from micro-CT confirmed the Alizarin red data, indicating larger amounts of mineralized matrix throughout the scaffolds in loaded compared to non-loaded samples *(Fig. 4.16 and 4.17)*. The quantitative data from micro-CT showed that the percentage of bone volume density (BV/TV) per scaffold increased about 2 fold in loaded samples (0.12%) compared with non-loaded samples (0.06%) *(Fig. 4.16)*. SEM

further confirms the presence of thick extracellular matrix by day 20 of culture in nonloaded samples. The preliminary study culturing non-loaded cell-seeded scaffolds in static conditions over 40 days showed that, by day 30, the matrix contains fibers and spherical nodules, the nodules having the appearance of calcospherulites as described by Barragan-Adjemian et al. (2006) [1] *(Fig. 4.18)*. The matrix becomes thicker and smoother and has a multilayer appearance at day 40 compared with day 20 *(Fig. 4.18)*. Interestingly, this morphology was seen in loaded samples on day 20 in the present regimen *(Fig. 4.19)*. The SEM images support the results from fluorescence microscopy (shown in *Fig. 3.14* of chapter 3), demonstrating that cells are embedded in their extracellular matrix along the struts of scaffolds.

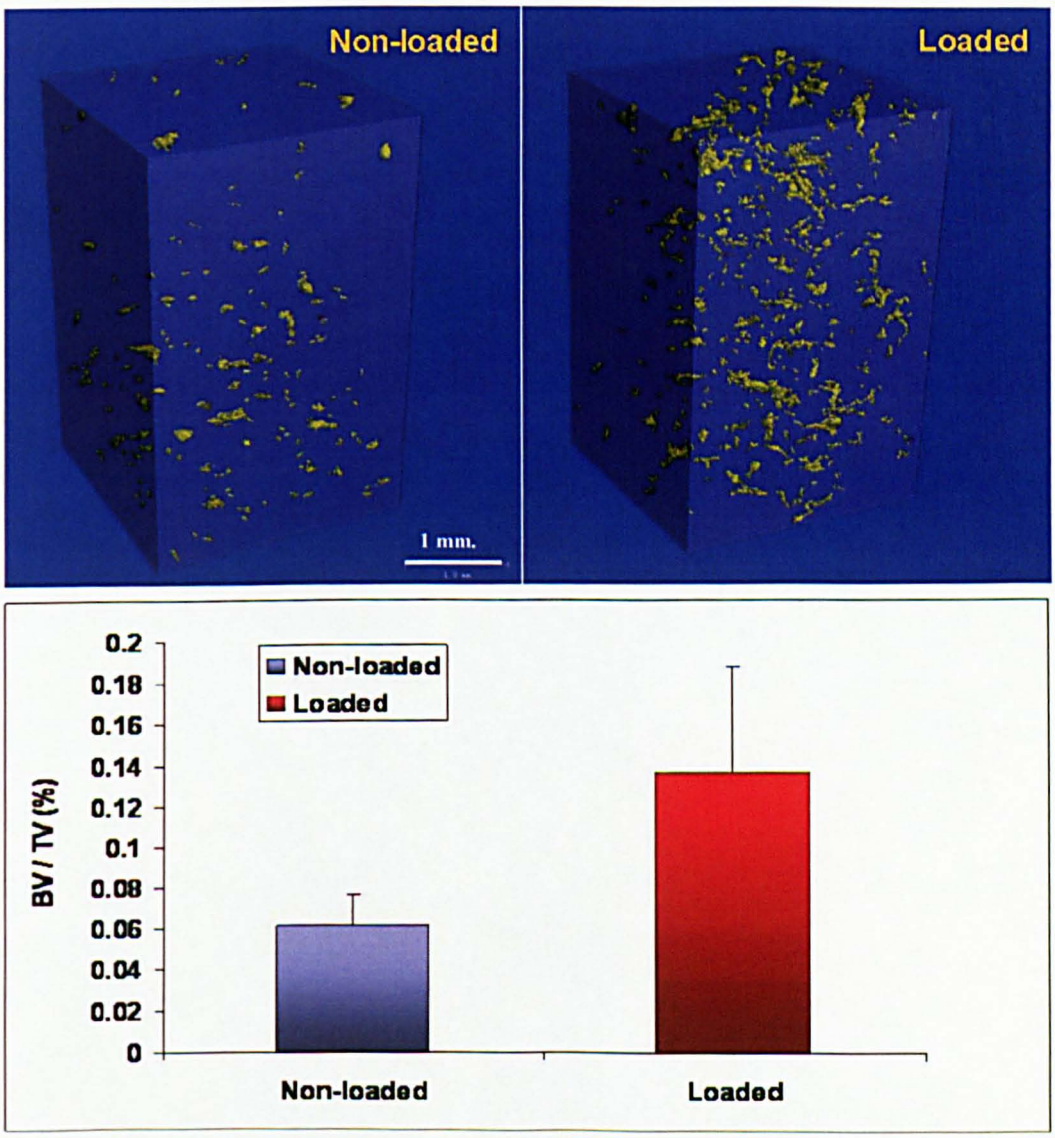

***Fig. 4.16**: 3-D micro-CT images of mineralised matrix in the center of scaffolds. The distribution and uniformity of mineralized matrix in the center of scaffolds. The mineralized tissue in loaded samples was increased about 2 fold compared with non-loaded samples (N=2).*

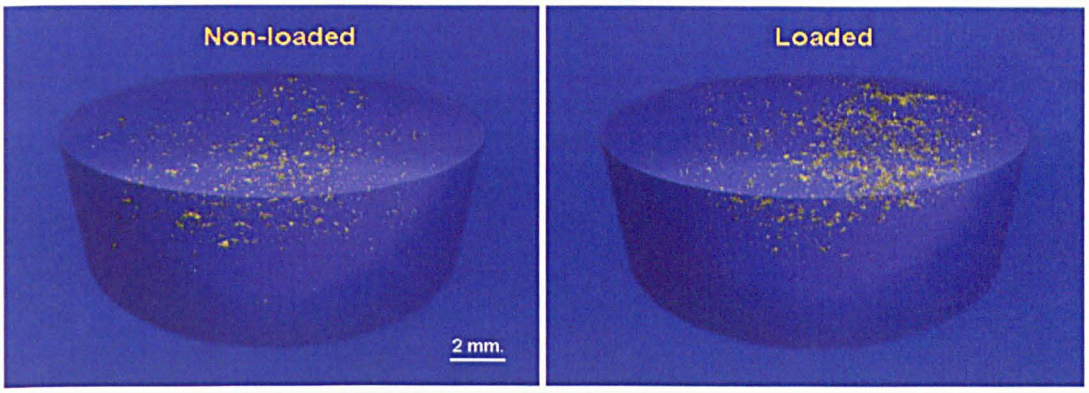

Fig. 4.17: 3-D micro-CT images of the whole scaffolds. The distribution of mineralized matrix, the field of view is wider than the scaffold and including the fluid-filled sample holding chamber.

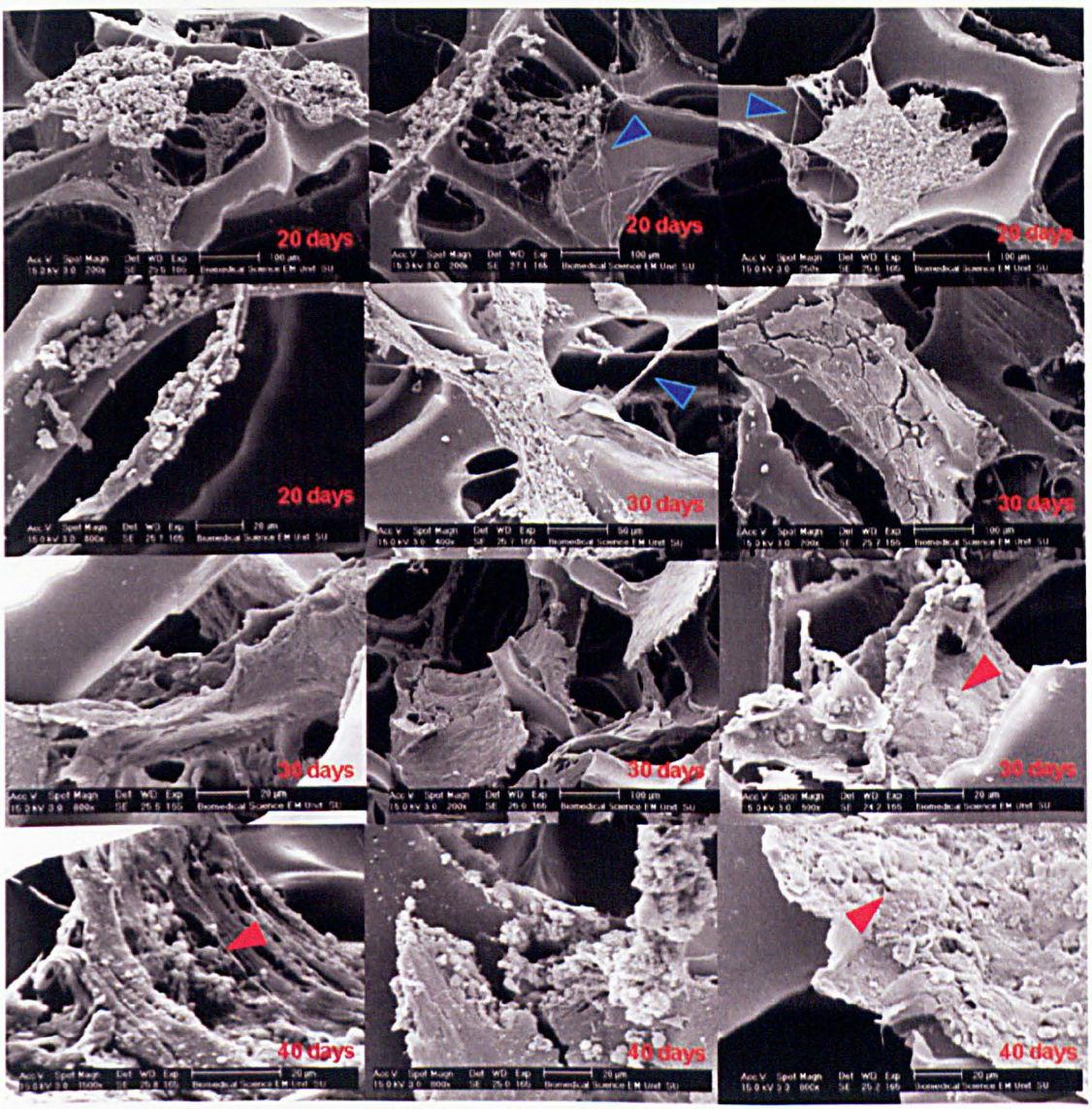

Fig. 4.18: Scanning electron micrographs of non-loaded cell and matrix in static culture over 40 days. Cells were embedded in thick matrix which contained both fibrous (blue arrow head) and spherical structures (red arrow head) indicative of collagen and calcospherulites respectively.

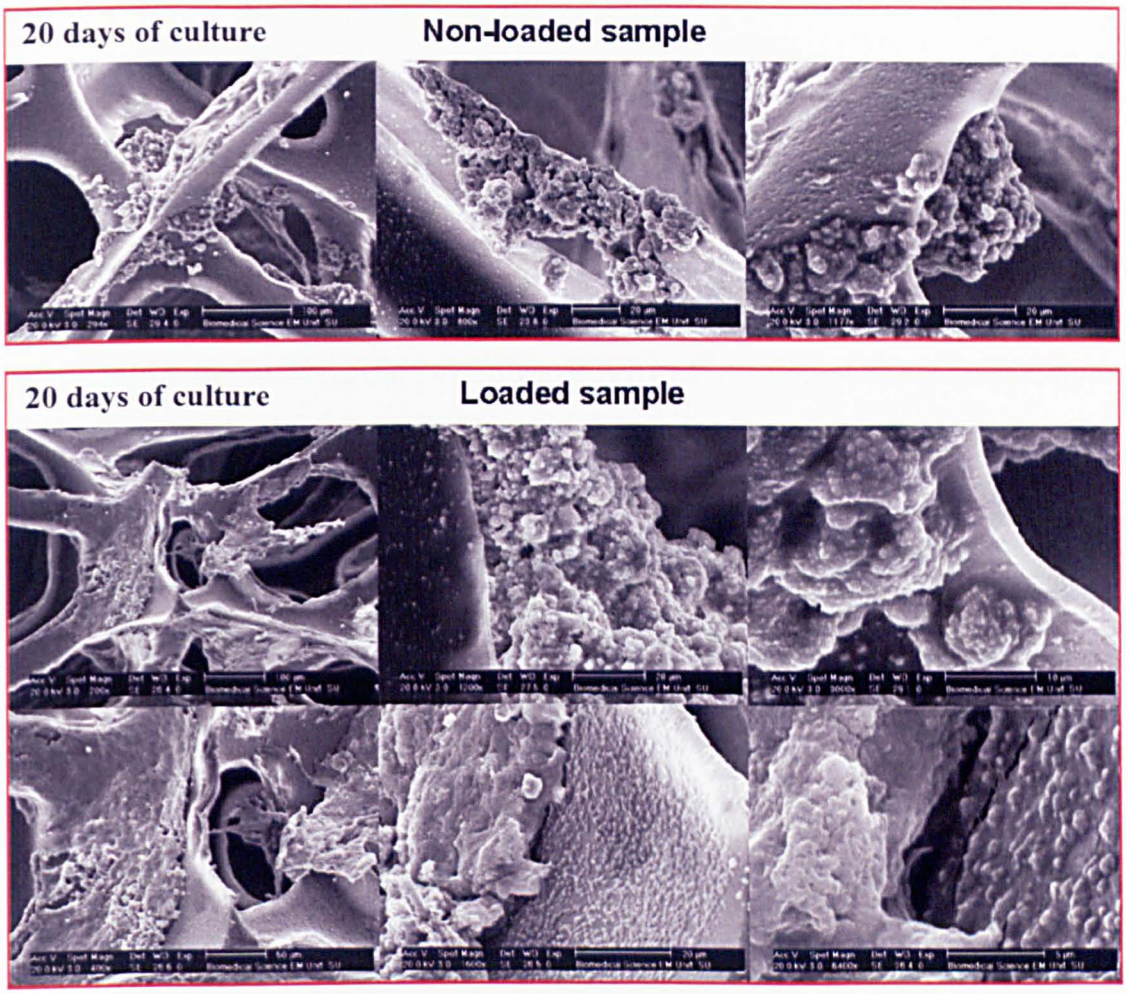

Fig. 4.19: Scanning electron micrographs at day 20 of culture, after 3 short bouts of loading (5% strain, 1Hz, 2 hr) were applied every 5 days. The matrix becomes thicker, smoother and more mature in loaded samples by day 20, more similar to that seen in non-loaded samples at day 40 (Fig. 19), than in non-loaded samples at the same time point.

4.4 Studying the effects of different compressive strains (2.5% and 10%) on matrix production and mineralization of osteoblastic cells in 3-D constructs.

Previous sections have shown that matrix production and mineralization in 3-D tissue constructs can be optimized using 5% dynamic compressive strain for 2 hr, applied every 5 days with 3 bouts of loading over 20 days of culture (day 5, 10 and 15). These experiments aimed to test the effects of 2 different compressive strains (2.5% and

10%) on matrix production and mineralization in 3-D constructs, using the previously developed regimen.

PU scaffolds (10 mm diameter and 10 mm height) were seeded with MLO-A5 osteoblastic cells at densities of $2.5x10^5$ per scaffold. Cell-seeded scaffolds were dynamically loaded in compression at 1Hz, 2.5% or 10% strain in a biodynamic chamber (Bose Electroforce3200) *(Fig. 4.20)*. Loading was applied for 2 hours per day at day 5, 10 and 15 of a 20 day culture period. Cell-seeded scaffolds were assayed on days 10, 15 and 20 of culture for cell viability by MTS assay, collagen content by Sirius red staining and calcium by Alizarin red staining.

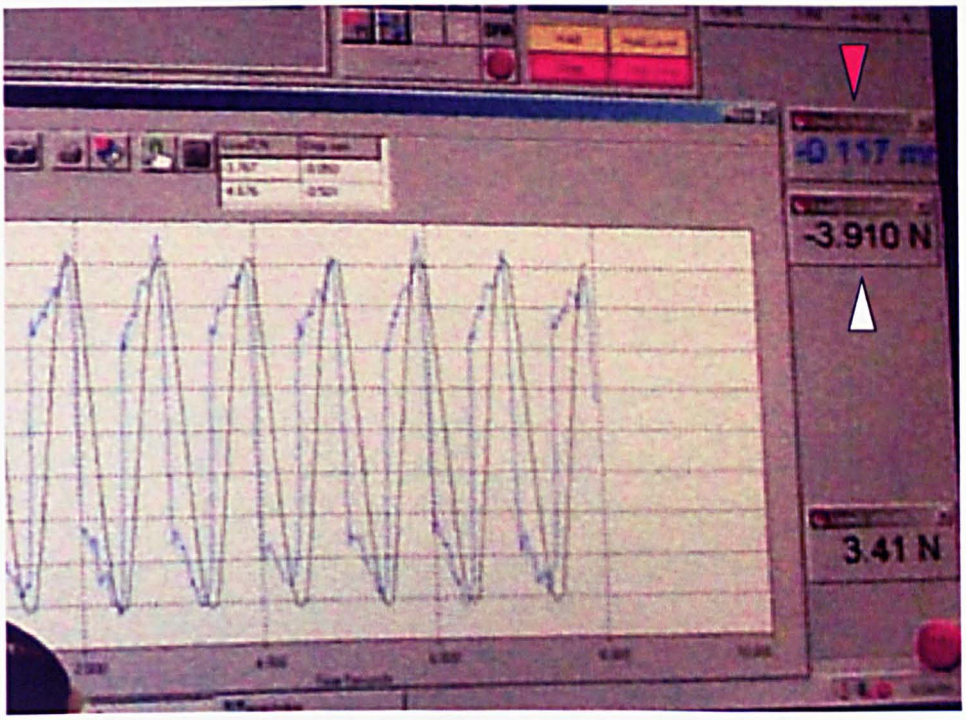

***Fig. 4.20**: Cyclic compression on a cell-seeded scaffold. Load with with 10% strain (white arrow head) and deformation (red arrow head) were monitored by Wintest software (BOSE, ElectroForce 3200).*

4.4.1 Results

Cell viability

MTS assay indicated that MLO-A5 cells survived in scaffolds loaded at both 2.5% and 10% strains. Relative cell number was slightly less in all loaded samples compared with non-loaded groups *(Fig. 4.21)*.

Collagen and calcium content

Sirius red and Alizarin red staining at the end of the experiment showed that the amount of collagen and calcium examined in scaffold sections and under light microscopy were slightly higher in loaded compared to non-loaded samples *(Fig. 4.22 and 4.23)*. Sirius red destaining quantitative data demonstrated that collagen content increased in 10% strain loaded samples compared to nonloaded samples (about 70% increase) *(Fig. 4.21)*. Interestingly, light micrographs of calcium staining in many areas on these loaded scaffolds (with 10% strain) showed that the calcium distribution was more clumped and twisted around the bundles of fibers rather than being spread over patches of matrix *(Fig. 4.24)*. This experiment indicated that 5% strain was close to the optimum strain to be applied in this system, as 2.5% strain was not seen to affect matrix production and 10% strain seemed to cause a slight decrease in cell number and had unexplained effects on matrix distribution.

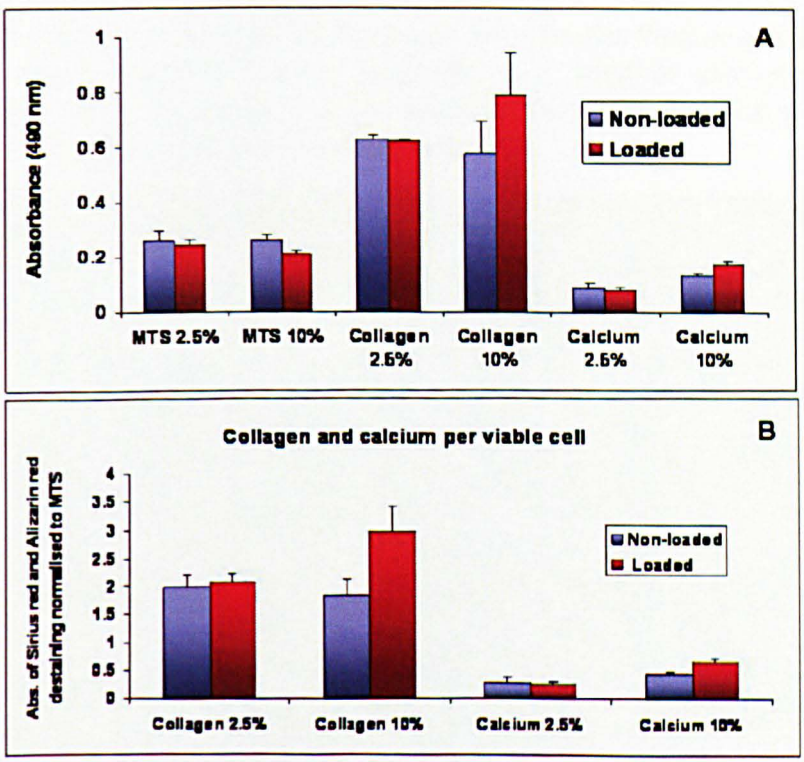

Fig. 4.21: *Cell viability, calcium and collagen in the scaffolds. (A) Mean ± SD of MTS (cell viability), Alizarin red (calcium) and Sirius red (collagen) absorbance per scaffold at day 20 (n=2). (B) Mean ± SD of collagen and calcium normalized to cell viability shows that collagen per viable cell increased in 10% strain loaded samples compared to non-loaded samples (about 70%) but calcium did not increase markedly.*

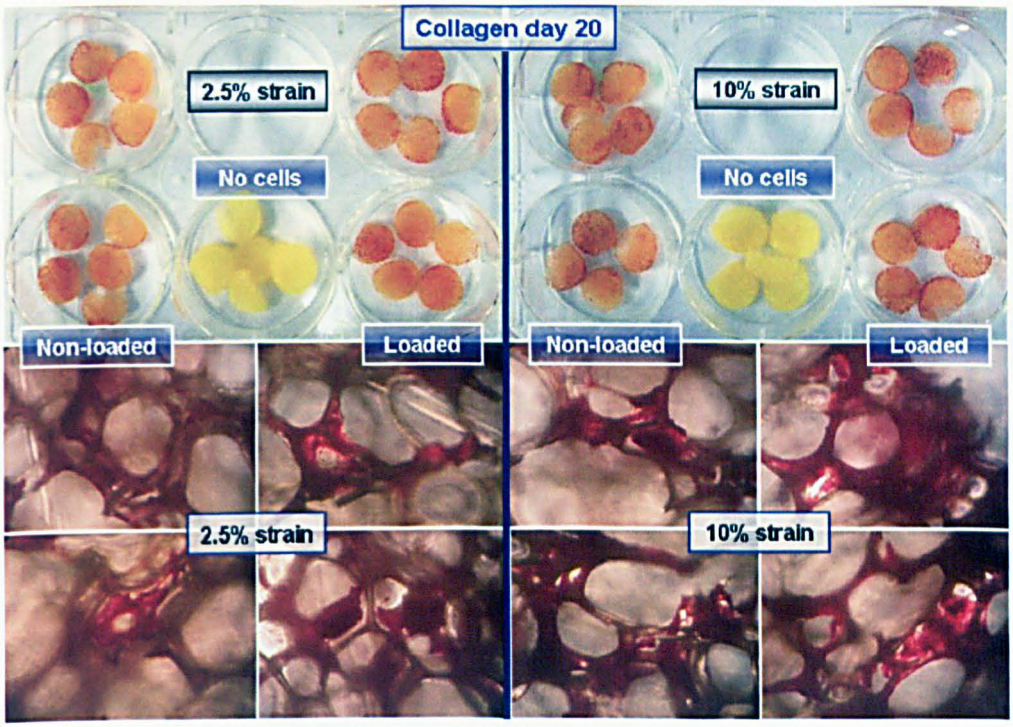

Fig. 4.22: Sirius red stained scaffold sections. The distribution of collagen in loaded, empty and non-loaded scaffolds, one scaffold per well. Light micrographs of a random area of the scaffolds show comparisons of collagen production between 2 different loading strains.

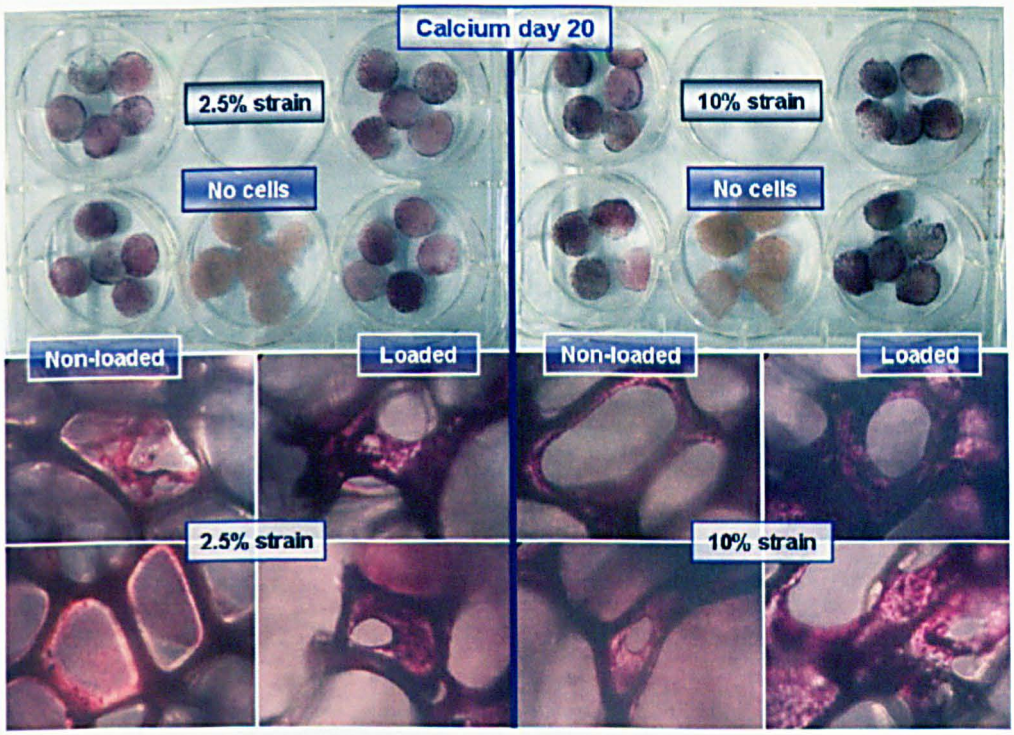

Fig. 4.23: Alizarin red stained scaffold sections. Light micrographs of the scaffolds (one scaffold per well) show calcium deposition (red) in loaded and non-loaded samples at 2 different loading strains.

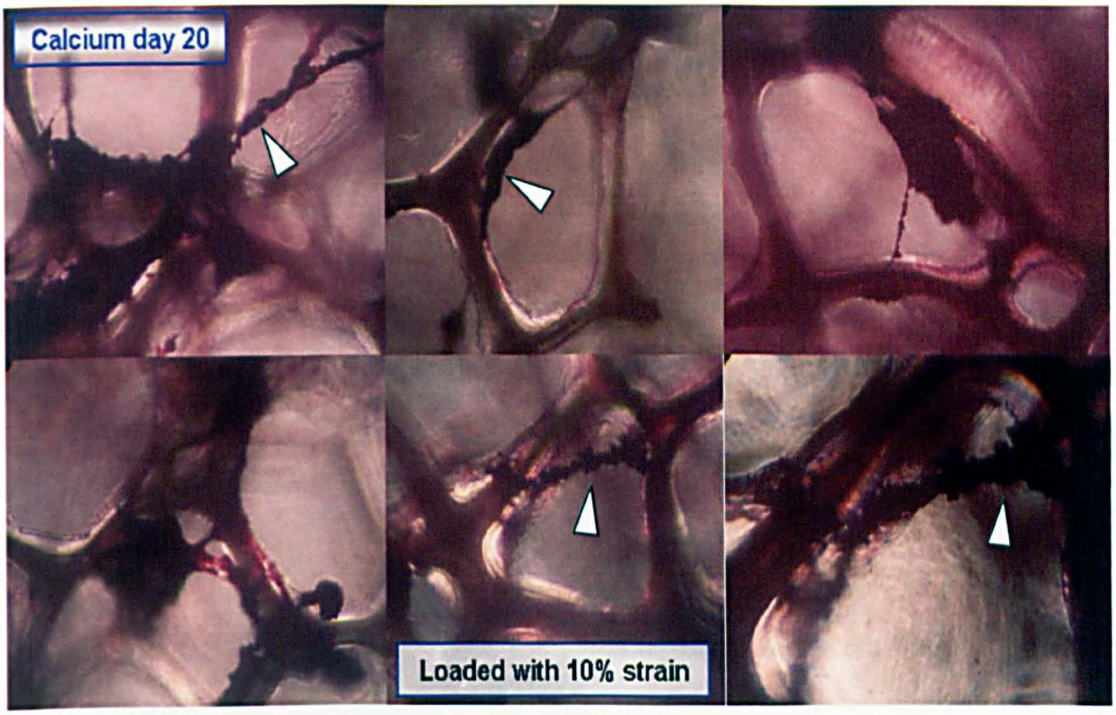

Fig. 4.24: *Light micrographs of the 10% strain loaded scaffolds. Calcium was stained using Alizarin red. The deposition of calcium was more clumped and twisted around the bundle of fibers rather than spread on the patch of matrix (arrow head).*

4.5 Discussion

- ***In vitro 3-D mechanical stimulation as a potential model system for bone tissue engineering.***

2-D and 3-D static culture does not mimic the dynamic conditions, mechanical and hydrostatic pressure, found in bone *in vivo* [5, 217]. Many dynamic 3-D culture systems reported, combine a dynamic seeding process together with continuous flow perfusion in bioreactors. These culture methods are more complicated, costly and time consuming than static culture. The turbulent flow incurred in many styles of dynamic bioreactor, e.g. spinner flasks and rotating wall vessels can interfere with studies of specific magnitudes of mechanical stimulation on bone engineered constructs. In addition, turbulence or high shear stress produced by fluid flow from bioreactors could remove attached cells from the scaffold [92]. In this chapter, we have shown that intermittent short periods of compressive loading can improve cells growth and their matrix production during 3-D static culture suggesting that the cells are responding to the mechanical compression stimulus either by directly sensing the substrate strain or the fluid shear stress caused by media movement through the porous scaffold. As the loading period is short it is likely that the stimulation of matrix growth does not occur during the loading period but that the loading initiates a cascade of events that result in an upregulation of survival and matrix producing genes.

Jassma and O' Brien (2008) found that dynamic culture in a flow bioreactor stimulated the production of early stage bone formation markers and led to better cellular infiltration into the construct compared with samples grown in static conditions. Although dynamic culture in a bioreactor can lead to better cellular infiltration into the construct, histological analysis revealed that a monolayer of cells found on scaffold surfaces under static culture was no longer present in the bioreactor culture resulting in scaffolds containing 40-52% fewer cells than the static group [92]. It is possible that the combination of dynamic and static culture could be an alternative method in bone tissue engineering to maintain cell proliferation and improve matrix production by cells. For long term culture, the appropriate periods of mechanical stimulation or fluid flow (dynamic) should be performed together with appropriate resting periods of static culture. Dynamic processes will allow sufficient nutrients and waste product exchange

for cells and also provide mechanical stimulation for bone formation whereas appropriate recovery periods in static culture may be required to allow sufficient time for cell proliferation in the construct.

- ***Mechanical stimulation of bone cells.***

Bone cell shear stress, induced by fluid flow in the porous spaces of bone, is believed to be an important mechanical stimulus in *in vivo* [57, 64, 241]. To imitate fluid flow induced shear *in vitro*, osteoblastic cells are usually cultured in monolayer on slides or discs which are mounted in parallel plate flow chambers, where the cells are exposed to fluid flow [48]. For example, Donahue et al. (2003) have shown that MC3T3-E1 osteoblastic cells in 2-D environment responded to oscillating fluid flow induced shear stress with both an increase in intracellular calcium concentration and an increase in PGE_2 production [242]. In 3-D study, Cartmell et al. (2003) have shown that osteoblastic cells exposed to a low flow rate (0.01 ml/min) had the greatest viability and proliferation whereas gene expression of Runx2, osteocalcin and alkaline phosphatase increased as the flow rate increased from 0.01 to 0.2 ml/min. This suggests that the larger stress upregulated gene expression but it was detrimental to cell viability and proliferation when load was applied continuously for 1 week [133]. However, these can not replicate the mechanical stimulus in a 3-D configuration where the more rounded morphology of cells in 3-D supports a less stiff cytoskeleton compared the with flattened cellular morphology found in a 2-D environment [235] Structure, localization, and function of cell-matrix focal adhesions are also different between 2-D and 3-D [236]. In addition, cells behave very differently when cultured in 3-D compared with in monolayer, not only in terms of their morphology and adhesion but also in their biological response to biophysical factors [81, 237, 243].

Pavlin and Gluhak-Heinrich have shown in an *in vivo* animal model that the progression of the osteoblastic phenotype in response to mechanical loading was several fold faster compared with that *in vitro*, but they observed no effect on cell proliferation [11]. This suggests that the mechanical signal may be targeting osteoblast precursors in the state of readiness to respond to an environmental challenge, without affecting the initial proliferative responses. However, King et al. (1991) have reported that bone formation in 2-D *in vitro* was achieved by both proliferation and increased function of

each individual osteoblast [244]. This result is in agreement with our 3-D study in which the mechanical loading can stimulate osteoblasts to produce bone matrix production after the initial proliferative response (increase of cell viability at 5 days after the first bout of loading) *(Fig. 4.13C)*.

- ***Differences of mechanical loading regimens.***

In this chapter, 2.5%, 5% and 10% maximum global strains were applied in the biodynamic chamber, this induced both substrate mediated strain and fluid flow induced shear stress. We showed that 5% scaffold strain was the most effective to induce matrix production and calcium deposition. However, at this stage we do not know which local strains the cells experience or what the shear stress is in the scaffold pores. We showed that different loading regimens (by varying the length of the loading and culture periods) can affect relative cell number and matrix production. A 1 hr loading period increased cell viability while a 2 hr loading period upregulated collagen production. Neither relative cell number nor collagen production is affected by increasing the number of loading periods from 2 to 3 times over 12 days of culture. There were no major changes in relative cell number and collagen production between 2 days and 5 days of post loading time *(Fig. 4.6-4.8)*. Although many authors investigated the effects of varying frequency of mechanical strain on bone cells and found that this factor is associated with cell proliferation, matrix production and gene expression [21, 81, 138, 245], we showed in the present study that varying the magnitude and loading time can also affect cell viability and matrix maturation of osteoblastic cells.

In adult bone tissue, matrix production occurs during tissue repair and in response to mechanical load [218]. Duncan et al. (1995) have shown that mechanically induced bone formation in an *in vivo* study is not increased if loading is applied at less than 0.5 Hz, but increases four times when loading frequency is about 2 Hz [57]. Compressive load and bending force have also been previously shown to play an important role in bone growth, repair and remodeling *in vivo* [6, 64, 120]. Maximum strains incurred in bone during exercise are about 0.005-0.2% strain (50-2000 μstrain) depending on types, positions and areas of bone [241] however, there is some controversy about what local strain bone cells themselves experience [246, 247]. Although low strain magnitudes (<0.2%) are routinely generated within the human

skeletal system during vigorous activities, many signaling factors have been upregulated by mechanical strain only at more than 0.2% strain suggested to be "supraphysiological" conditions [241]. Therefore, to study the effects of mechanical load *in vitro* on osteoblastic cells, the levels, frequencies of strain and strain rate used in most previous studies are 5-100 times the habitual strain levels that are found on the surface of living bone [48, 57, 120, 138]. For example, uniaxial 5% strain, 1 Hz [240], and equibiaxial 3% strain, 0.25 Hz strain [21] have been also shown to induce mineralisation of human MSCs in *in vitro* monolayer experiments. This is also the case for our present study in which maximum high global strains (2.5%, 5% and 10%) were applied to PU foam scaffolds at a frequency of 1 Hz. [248]. However, the high strain we applied can not be easily compared with previous monolayer studies where cells are strained directly, because the deformation of foam structures is highly complex [249] and results in local variations in both substrate strain and strain induced fluid flow.

In our studies, the high strains applied to a soft matrix (scaffold of 2 kPa) are more similar to the environment in facture healing or implant osseointegration than to whole bone loading, in which the matrix is much stiffer (10-30 GPa) and global strains are lower (<0.2%). Fibrous tissue around an implant has been measured to be 2 MPa [250], whereas the granulation tissue present at the beginning of fracture healing has been estimated to be 2 kPa [251] which is similar to the stiffness of the PU scaffold used in this study. In addition, 5% strain has also been suggested to be optimal for intramembranous bone formation in a healing fracture [248]. Therefore, cells on a scaffold of low stiffness such as PU might be a good model for testing fracture healing intervention.

The frequency of loading cycles applied in the present study was 1Hz which is the frequency most commonly used in bone cell mechanotransduction studies as it replicates walking pace. However, observations that high frequency, low magnitude loading induces bone formation *in vivo* [252] may also apply to *in vitro* bioreactor loading. Studies in our laboratory indicated that matrix production by MSCs was also upregulated by high frequency loading [253].

Different animal loading *in vivo* studies have compared loading regimens and shown that the effects of mechanical loading on bone cells are dependent upon the

magnitude, duration, and rate of the applied load. Duncan et al. (1995) suggested that loading must be cyclic to stimulate new bone formation and longer duration, lower amplitude loading has the same effect on bone formation as loads with short duration and high amplitude [57]. It has been also shown that the duration of loading, number of loading periods and recovery periods influence the osteogenic response to mechanical loading [254]. Mechanical loading protocols are more osteogenic if the load cycles are divided into short bouts, separated by adequate resting periods, than if the cycles are applied in a single continuous loading [255]. It has also been demonstrated that a short period of loading contribute to the mechanosensitive response in *in vitro* 2-D studies [242, 256]. Our *in vitro* 3-D mechanical loading system demonstrated that 2 hr short bouts of dynamic compressive loading with 5 days resting period for 20 days cultures enhanced bone matrix production and mineralization in engineered tissue constructs. This has interesting similarities (short bout of cyclic loadings) and differences (higher loads and longer resting periods) to *in vivo* studies. In the current system, we can reduce complicated procedures of continuous loading, and the associated costs and laboratory time needed to engineer bone tissues if intermittent short bout of loading can maintain as good outcomes as continuous loading. In addition, high mechanical forces, frequency and magnitudes which may be harmful to living tissue *in vivo* can be generated safely in this *in vitro* model.

- ***Bone matrix maturation.***

Researchers have recognized the importance of understanding the differentiation of osteoblasts into mature matrix-synthesizing cells during the osteogenic response to mechanical loading. Osteogenic differentiation can be induced *in vitro* by many techniques. The most popular method is using cell culture medium supplemented with differentiation factors such as chemical compounds. Osteogenic differentiation, however, may also be induced by electrical and mechanical signals. Bone cells are usually shown to need ascorbic acid (AA) in order to produce collagen and beta-glycerophosphate (βGP) to make mineral. Kato et al. (2001) showed that MLO-A5 osteoblastic cells will produce matrix and mineralize even in the absence of AA and βGP [192]. Therefore, MLO-A5 cells have the potential to produce enough matrix and mineralize in a short time frame such with minimal supplements that mechanically modulated changes could be readily detected in a 3-D model. The results in this chapter

revealed that calcium content in the constructs is sensitive to short bouts of dynamic cyclic compressive force in a time-dependent manner *(Fig. 4.13B)*, in short-term culture, even when cell-seeded scaffolds were supplemented with low concentration of β-GP (2mM). However, higher concentrations of β-GP may cause greater change in mineralization.

Oxygen (O_2) level and nutrient distribution are important factors for the development of many tissues. *In vivo*, nutrients and O_2 are provided by blood vessels covering the surface and penetrating into the center of living bone, whereas *in vitro* they are provided by culture media surrounding the scaffold. In *in vitro* 3-D cultures, where the media can not easily get through to cells in the center of the construct, less nutrients and O_2 are delivered to those cells. Zahm et al. (2008) have shown that mineralization and alkaline phosphatase activity of MLO-A5 osteoblastic and MLO-Y4 osteocytic cells in both 2-D monolayer and 3-D alginate scaffold is lower when in grown 2% O_2 (hypoxia) compared to 20% O_2 (normoxia) suggesting that that a low concentration of O_2 decreased the mineralization potential of bone cells at both early and late stages of maturation [257]. In our study, we showed that good matrix distribution and mineralization can be seen through out the scaffold even in the centre. The mineral distribution seemed to be improved by mechanical loading (Fig 4.11 and 4.16), however, in our system, O_2 distribution and nutrient flow would only be improved during a short period of the total culture time. Therefore, it is unlikely that the results are due to higher oxygen tension in the loaded scaffolds, unless a short period of higher oxygen results in long-term changes in matrix production.

In our system, the observation that many cells seem to be embedded in ECM rather than attached to the scaffold wall as shown in SEM and fluorescence images is important when considering how well this culture system mimics the biological environment. It has been argued that cells seeded on scaffolds with large pores (100 of microns) are not truly in a 3-D environment because the pore is so large that the cell is effectively attached to a 2-D surface [258]. A biomimetic environment should have cells surrounded by matrix fibers to which they attach in all directions. However, scaffolds with pores smaller than 100 microns do not allow adequate nutrient diffusion for cell survival [212]. Our culture system allows nutrient diffusion via the highly porous scaffold while supporting a rapid matrix forming response, so that the cells are

interacting with their own ECM rather than the synthetic material. In addition, cell-ECM interactions *in vitro* have been shown to be crucial in encouraging mineralized matrix formation in engineered tissue scaffolds [84].

- ***Gene expression of bone matrix proteins***

In bone matrix, as well as collagen and mineral, there are small amounts of extracellular matrix proteins which can be bound to or associated with mineral crystals and collagen fibers. The presence of mRNA for these molecules is a marker of osteogenesis or matrix production. Characterization of osteogenic markers such as Osteocalcin (OCN) and Osteopontin (OPN) was performed to provide an increased understanding of matrix formation with mechanical stimulation [37]. OPN has been shown to play an important role in both cell attachment and mechanotransduction responses of osteoblasts *in vitro*, and has also been indentified as an early marker of osteoblast differentiation [37]. OCN and OPN are normally expressed at maximum levels in the post-proliferative period of osteogenesis [86].

It has been shown that OCN expression was stimulated several days prior to mineralization [259, 260] suggesting that the expression of OCN coincides with the onset of mineralization. Several studies compared osteoblastic cells in 2-D and 3-D cultures and found OCN production only in 3-D culture [86, 261]. Teeth movement models in mice have also provided evidence that the OCN gene is mechanically induced in osteoblasts many days before the mineralization stage, since its high expression could be followed from the early stage of matrix deposition (48 hr after mechanical stimulus) [262]. However, our study has shown that OCN can be induced more rapidly than 48 hr after mechanical compression (12 hr) in our 3-D engineered tissue model.

Harter et al. (1995) have shown that mechanical strain *in vitro* also increased the transcription of OPN and COL1 genes [263]. In animal models under physiologic loading, an early response of ALP was detected after 24 hrs of loading, followed by a stimulation of OCN and COL1 between 24 and 48 hrs, and deposition of osteoid after 72 hr. They also showed that the responses of osteoblast-associated genes to mechanical loading were 10- to 20-fold greater than the increase in cell number, indicating that the induction of differentiation and an increase of cell function are the primary responses to

osteogenic loading [11]. Our study showed that the levels of OPN and OCN mRNA in MLO-A5 cells in a 3-D scaffold in both loaded and non-loaded samples was similar at 4 hrs after stimulation but it was decreased rapidly in non-loaded samples by 12 hrs, while it was upregulated and remained high up to 24 hrs after loading indicating that dynamic compression can stimulate longer term effects on mRNA expression of these matrix proteins *(Fig. 4.14 and 4.15)*.

Gerstenfeld et al. (1999) and Toma et al. (1997) have shown that OPN was identified *in vivo* as a signaling molecule in bone remodeling [264] and a mechanically responsive gene in osteoblasts [265]. However, Denhardt et al (2001) have shown that the increase of OPN mRNA level *in vivo* was observed in only osteocytes exposed to mechanical stimulus but was inhibited in osteoblasts [266]. In the present study, we observed the increase of OPN, OCN and COL1 gene expression in late stage osteoblasts induced to synthise bone matrix in 3-D *in vitro*. The expression of COL1 mRNA and collagen production in our study also supports earlier studies which have reported high level collagen synthesis from the early to the late stage of osteoblast development [260, 267]. The results indicate that cyclic dynamic compressive loading in osteoblastic-seeded constructs can increase the level of mRNA for matrix proteins from the late stage of osteoblasts toward the maturation stage of osteocytes as well as collagen production and mineral deposition. Interestingly, Ghosh-Choudhury et al. (1996) have shown that collagen induction at the mRNA level occured in osteoblasts after they have reached confluence or after subjecting them to BMP-2 stimuli, but the induction was lost after 5 days of culture [259]. This may indicate that the 5 day gap between loading times with the appropriate loading periods in our study may help to re-trigger the increase in mRNA expression of matrix protein resulting in collagen production over the culture period, up to 20 days.

Kaspar et al. (2000) have shown that cyclic stretching of primary human osteoblasts seeded on silicone disc (2-D) at a magnitude occurring in physiologically loaded bone tissue (0.1% strain) increased COL1 mRNA expression while OCN was reduced [97]. However, in our present study, using cyclic compression on osteoblastic cells-seeded scaffold with a high compressive strain (5%) showed upregulation not only of the mRNA expression of COL1 but also OCN and OPN. This suggests that a higher global strain magnitude, which can be easily generated and controlled in the laboratory,

has the potential to increase osteoblastic activities related to matrix production, matrix mineralization and maturation for bone tissue engineering.

4.6 Summary

- We optimized a method, in which intermittent dynamic loading is applied to the static 3-D culture previously described. The biodynamic chamber and mechanical testing machine used here can apply a large range of strains, strain rates, frequencies and loading durations to a cell-seeded scaffold.
- This model system of osteoid-like matrix grown in 3-D culture in a mechanically controllable environment should be a useful tool for investigations on bone mechanotransduction and optimisation of mechanical loading regimens for tissue engineering, fracture repair and implant integration.
- MLO-A5 rapidly mineralising osteoblasts are mechanosensitive and respond to different loading regimens, varying in loading magnitude and duration of loading time, inserted into a static culture period with marked increases in matrix production, maturation and mineralization.
- A global maximum strain of 5% was the most effective to induce matrix production and calcium deposition compared with 2.5% and 10% strain.
- Bouts of 2 hrs of loading can increase collagen production while 1 hr loading can increase cell viability.
- The short bouts of dynamic compression with 5 days of resting period can stimulate longer term effects (12-24 hrs) on mRNA matrix protein expression compared with non-loaded conditions. This indicates that the 5 day gap between loading times with the appropriate loading periods in our study may help to retrigger the increase in matrix protein mRNA expression resulting in collagen production over the culture period, up to 20 days.
- The intermittent short period of compressive loading can accelerate cell growth and matrix production during 3-D static culture suggesting that the cells are responding to the mechanical compression stimulus either by directly sensing or the substrate strain or the fluid shear stress induced by flow through the porous scaffold.

CHAPTER FIVE: The role of the primary cilia in mediating mechanically induced increases in matrix production.

5.1 Introduction

Bone tissue alters its mass and structure in response to chemical and mechanical stimulation both *in vivo* and *in vitro*. The role of mechanical forces in regulating bone tissue has long been recognized. It is thought that during normal body movement *in vivo*, mechanical loads cause deformation in bone that creates fluid flow within the bone canaliculae and may apply stretch to bone cell membranes. Fluid flow in the bone lacunar-canalicular network is believed to be one of the potential stimuli that trigger mechanotransduction in bone. Shear stresses driven by movement of pericellular fluid through the canaliculi and over the cell surface, cell processes and cell body in normal bone has been estimated as 0.8-3.0 Pa at the cell membrane. It is thought that this shear stress is sensed by osteocytes [268] which produce second messengers to stimulate osteoprogenitor cells to differentiate into osteoblasts resulting in new bone production and/or inhibit osteoclast function resulting in reduced bone resorption [57, 64]. Bone cells *in vitro* culture can also be stimulated to produce second messengers when exposed to mechanical loads [48, 81, 92, 93], however it is not known whether this is by similar mechanisms as *in vivo*.

Although fluid movement induced shear stress has been recognized to act as a stimulus for cells resulting in bone remodeling *in vivo* the cellular mechanisms by which bone cells translate the loading induced signal into biochemical responses and matrix production remained poorly understood. Jacobs et al. (1998) have modified the traditional parallel plate flow chamber system to induce oscillatory fluid flow (OFF) over the surface of cells. They suggested that OFF may be the most representative of physiological fluid flow in bone *in vivo* [94]. The developed system is based on the concept that the lacunar-canalicular network experiences pressurization in response to matrix deformation and this leads to flow along pressure gradients when bone is loaded and the flow and pressure gradients are reversed when loading is removed, thus, the fluid motion in bone is oscillatory in nature.

The capacity of engineered bone tissue to alter its mass and structure in response to chemical and mechanical stimulation has been reported over the last few years. However, just as with bone *in vivo* the mechanisms by which bone cells in tissue engineered bone transduce mechanical signals are poorly understood. In chapter 4, I showed that bouts of dynamic cyclic compressive loading induce matrix production by osteoblasts. When a cell-seeded porous scaffold is dynamically compressed, the cells are subjected to both direct strain by deformation of the matrix/scaffold and fluid-flow induced shear stress by movement of the surrounding media through the scaffold pores. In collaboration with the Cell and Molecular Biomechanics Laboratory at Stanford University, USA, an investigation into the mechanism by which osteoblasts sense fluid flow was conducted under the supervision of Professor Christopher Jacobs.

Interestingly, primary cilia, which are known mechanical sensing organelles of kidney cells, have recently been shown to be potential mechanosensors in bone. The non-motile primary cilium is a hair-like solitary cellular structure surrounded by a membrane continuous with the cell membrane [55, 100, 102-104, 114, 117]. It has been known to cell biologists for over hundred years since it was first discovered by Zimmermann in 1898 [98] , but it was ignored or forgotten because of its unknown functions. The primary cilia of osteoblasts and osteocytes were first reported in 1972 but no attention was paid to them until 2003 when Whitfield proposed that the solitary cilium could be a mechanosensing organelle in bone by detecting pulsing lacunocanalicular fluid [99]. As the bending of the primary cilium of kidney cells can cause the cell to sense fluid flow (see more detail in chapter1), the bending of an osteocyte's primary cilium in response to the movement of extracellular fluid is likely to do the same thing [99]. The primary cilia in chondrocytes has been shown to interact with the collagen fibers of the extracellular matrix and this interaction may be responsible for the acute bending of the primary cilia of chondrocytes under load [105]. This suggests that the potential for the primary cilium to act as a force sensor may not only be limited to fluid shear stress but it may also act in cell-matrix or cell-cell mechanosensing.

Based on Prof. Jacobs works, I hypothesized that if the primary cilia were sensors for mechanical forces such as fluid flow or strain induced shear stress, then mature cells lacking a cilium would become unresponsive, unable to upregulate matrix

protein gene expression and would not increase matrix production in response to mechanical stimulation. To test this hypothesis, siRNA transfection was used to silence the gene expression of an essential protein (polaris) for primary cilia biogenesis and function [118]. In further experiments, chloral hydrate which is believed to destabilize the junction between the cilium and the basal body by disassembly of microtubules [205] was used to disrupt primary cilia formation. To imitate the fluid flow induced shear stress *in vitro*, osteoblastic cells are usually cultured in monolayer on slides or discs which are mounted in parallel plate flow chambers, where the cells are exposed to fluid flow [48] *(Fig. 5.1)*. Therefore to study the effects of primary cilia on mechanically responsive bone matrix production *in vitro*, oscillatory fluid flow-induced shear stress was applied in a parallel plate in a 2-D study.

However, these 2-D studies can not represent well the mechanical environment in a 3-D configuration in real bone tissue which contains a complex mix of forces including deformation strains in multiple directions and fluid flow induced shear stress. It is possible that strain induced bone deformation could affect the movement of primary cilia in mature 3-D matrix in which cilia are embedded and bound to matrix protein. This may be a more relevant mechanism than the idea that fluid flow causes primary cilia to deflect freely, which is more relevant to a 2-D environment. To mimic a 3-D environment for primary cilia I used our developed 3-D loading system (refered to chapter 3 and 4), based on substrate strain generated by external forces. As discussed this strain is also likely to induce fluid flow through the scaffold pores that creates fluid shear stresses on bone cells *(Fig. 5.2)*. Therefore, in our system cells will feel a combination of deformation and fluid flow induced forces as they do in bone and osteoid *in vivo*.

In this chapter, the experiments were divided into 3 stages.

Stage 1: Detection of primary cilia on MLO-A5 cells in both 2-D and 3-D using fluorescence staining and confocal microscopy.

Stage 2: Studying the potential role for primary cilia in bone matrix production in a 2-D environment.

Stage 3: Investigating whether the primary cilium is involved in mechanical responses of bone tissue formation in 3-D constructs.

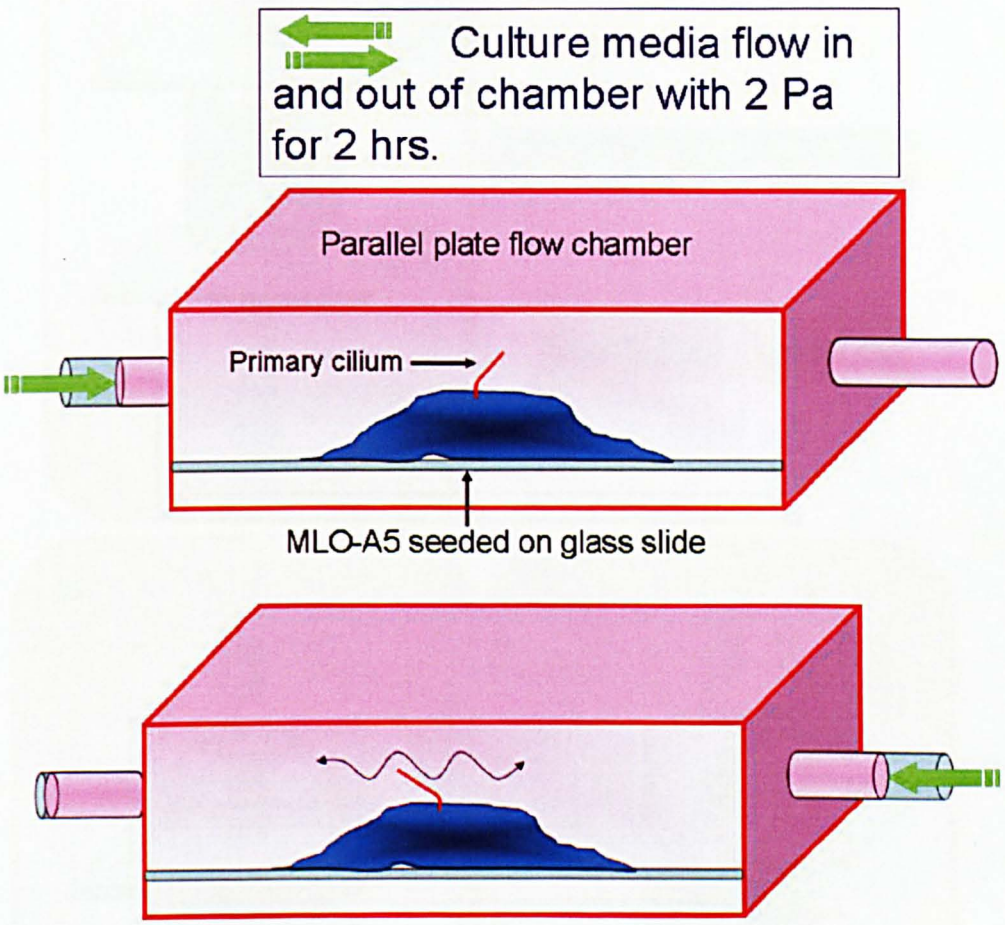

***Fig. 5.1**: A schematic of shear stress on the bending cilium mediating mechanosensation by primary cilia. The parallel plate flow chamber is made up of a polycarbonate manifold with inlet and outlet ports, a glass microscope slide with cells attached and a gasket held to the slide by vacuum pressure. The cell is subjected to oscillatory fluid flow with 2 Pa of wall shear stress for 2 hrs. The primary cilium may act as an antenna sensing fluid flow and the shear stress on the bending cilium could mediate mechanosensation by primary cilia.*

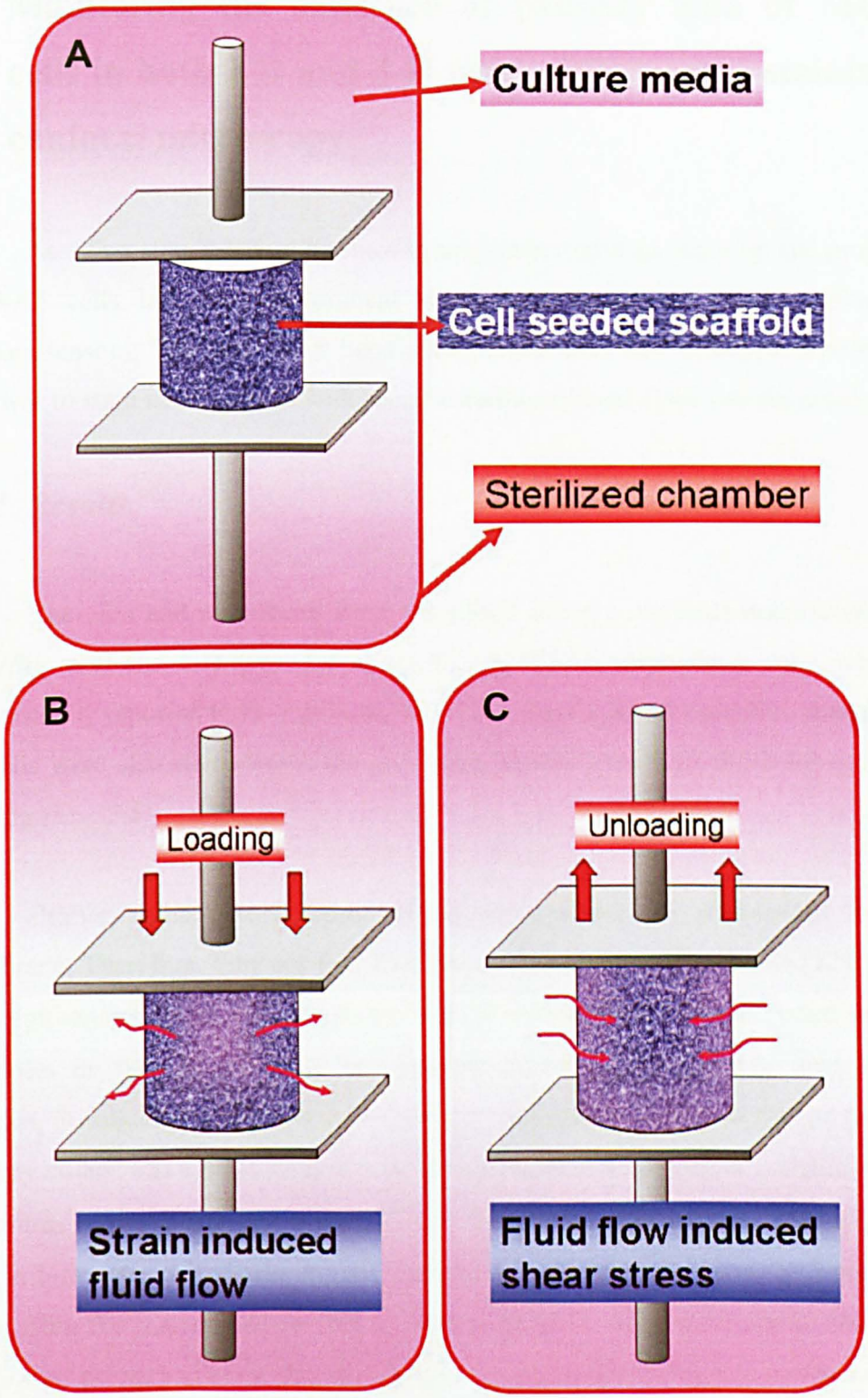

***Fig. 5.2**: A schematic diagram of strain induced fluid flow and shear stress on the 3-D PU scaffold. A cell seeded scaffold was placed in the sterilised biodynamic chamber (A). Compressed scaffold with fluid flow moving outwards (B), and relaxed scaffold with fluid flow moving inwards (C) could induce shear stress on the surface of cells in the scaffold, similar to the fluid flow that is assumed to occur in bone in vivo.*

5.2 Monitoring the existence of primary cilia of MLO-A5 cells in both 2-D and 3-D using fluorescence staining and confocal microscopy.

As a first step, it had to be shown that primary cilia do occur on and project from MLO-A5 cells into the environment where they would be capable of acting as mechanosensors. This had never been shown before for this cell type. The technique used was to stain microtubules with specific anti-acetylated alpha tubulin antibody.

5.2.1 Results

The cilia and cell nuclei were visualised using a confocal microscope in both 2-D *(Fig. 5.3)* and 3-D *(Fig. 5.4 and 5.6)*. MC3T3-E1 osteoblastic cells, which have been recently reported to have primary cilia [18], were used as a positive control. MLO-A5 cells were also stained with the secondary antibody only, to check for non-specific staining *(Fig. 5.5)*

Primary cilia extend from the centrosome and are surrounded by plasma membrane. Therefore, they are found on the surface or the edge of cells [12]. In mouse renal epithelial cells *in vivo*, the centrosome was located near the cell edge and mature centrioles in 80% of the cells had primary cilium protruding into duct lumen. In contrast, in subcultured cells in 2-D, the centrosome came closer to the nucleus, so the primary cilium was always located near the cell nucleus However, it is still unclear how the primary cilia locate and organize in 3-D cultures. I showed in these experiments that, in 3-D static culture, the mature primary cilium of MLO-A5 can be found at about 5 μm from the nucleus of the cell *in vitro (Fig. 5.7)*. This is similar to the expected position of primary cilia *in vivo* in which the primary cilia is located on the edge of the cell rather than near the nucleus of the cell.

Although primary cilia have been reported to have mechanosensory properties in many types of cells, there are not many studies that have shown how they relate to other proposed mechanosensors in bone tissue. Reilly et al have shown that the glycocalyx, a pericellular glycosaminoglycan and proteoglycan layer, may be another mechanism by

which the cells sense load induced shear stress [48]. Within the natural bone environment, the glycocalyx would extend from the cell to the mineralised matrix creating a highly hydrated molecular sieve [269]. Therefore, the localisation of the primary cilia in relation to the hyaluronan glycocalyx was also investigated using immunofluorescent staining and confocal microscopy (the hyaluronan of the glycocalyx was stained by Hayley Morris, a PhD student in our group). The confocal images showed that when the primary cilium was mature, the hyaluronan glycocalyx could be seen to spiral around the primary cilia *(Fig. 5.8)*. This shows there is an interaction between the hyaluronan glycocalyx and the primary cilium, indicating a potentially complex relationship in mechanosensation by bone cells. To my knowledge, however, there has been no reported data about how the primary cilia of bone cells might interact with the glycocalyx and the bone mineralised matrix.

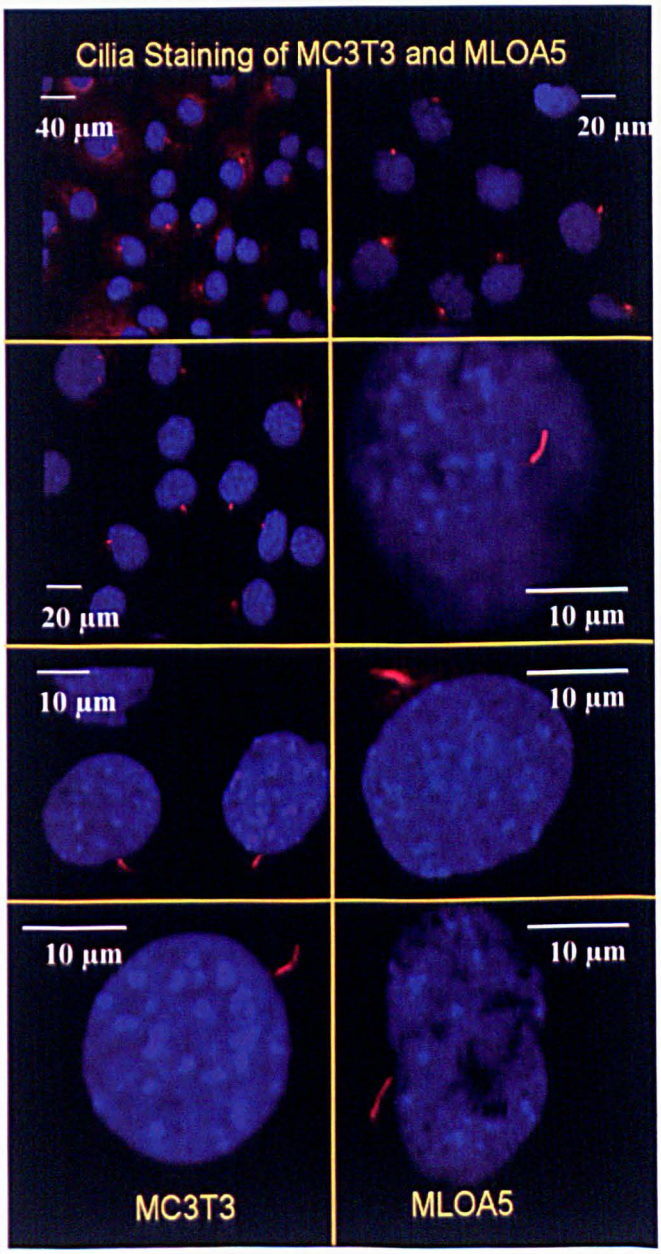

***Fig. 5.3**: Primary cilia in 2-D culture of MC3T3-E1 and MLO-A5 osteoblastic cells. The cilia (red) project from the apical surface of cells. Cell nuclei stained by DAPI were shown in blue. Primary cilia are stained with mouse primary antibody to acetylated-alpha tubulin and Rhodamine-conjugated rabbit anti-mouse immunoglobulins as a secondary antibody.*

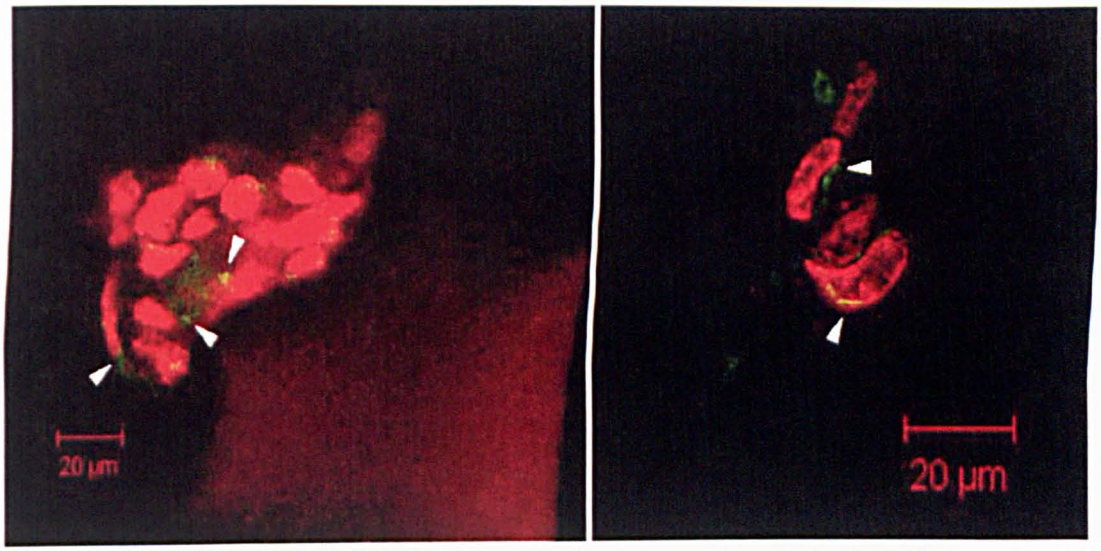

***Fig. 5.4**: Primary cilia of MLO-A5 cells on 3-D PU scaffold. They were stained by mouse primary antibody to acetylated-alpha tubulin and FITC-conjugated rabbit anti-mouse immunoglobulins as a secondary antibody show in green (arrow head). Cells also were stained with PI (red) showing the location of nuclei. Scaffold strut shows autofluorescence in red.*

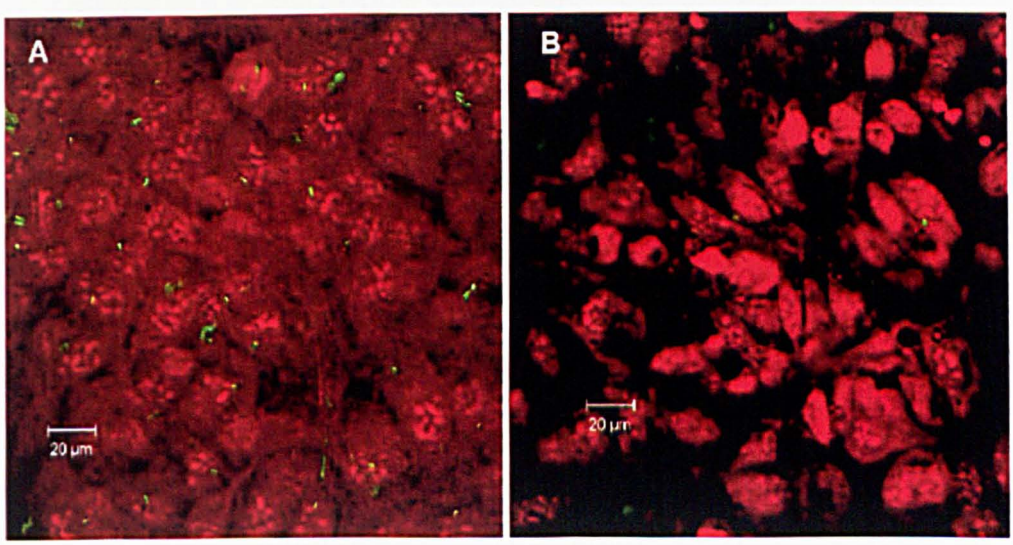

***Fig. 5.5**: Primary cilia on MLO-A5 osteoblastic cells. The cilia were stained with mouse primary antibody to acetylated-alpha tubulin and FITC-conjugated rabbit anti-mouse immunoglobulins as a secondary antibody (A). Primary cilia display fluorescence in green. Nuclei stained with Propidium iodide (PI) show in red. Cells stained with the secondary antibody (B).*

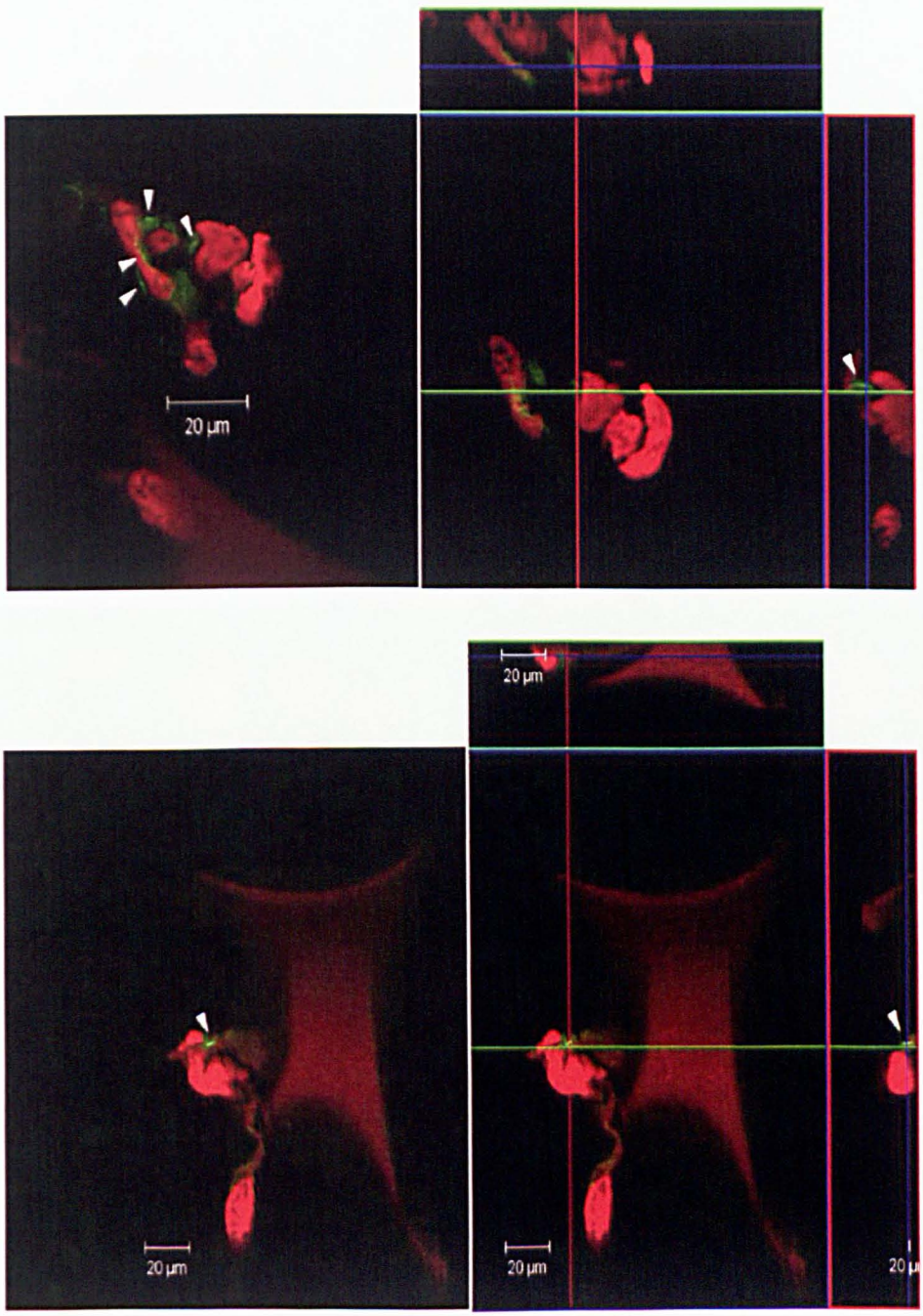

***Fig. 5.6**: Confocal images analysis from X, Y and Z planes. The images show the existence of primary cilia on the 3-D scaffold.*

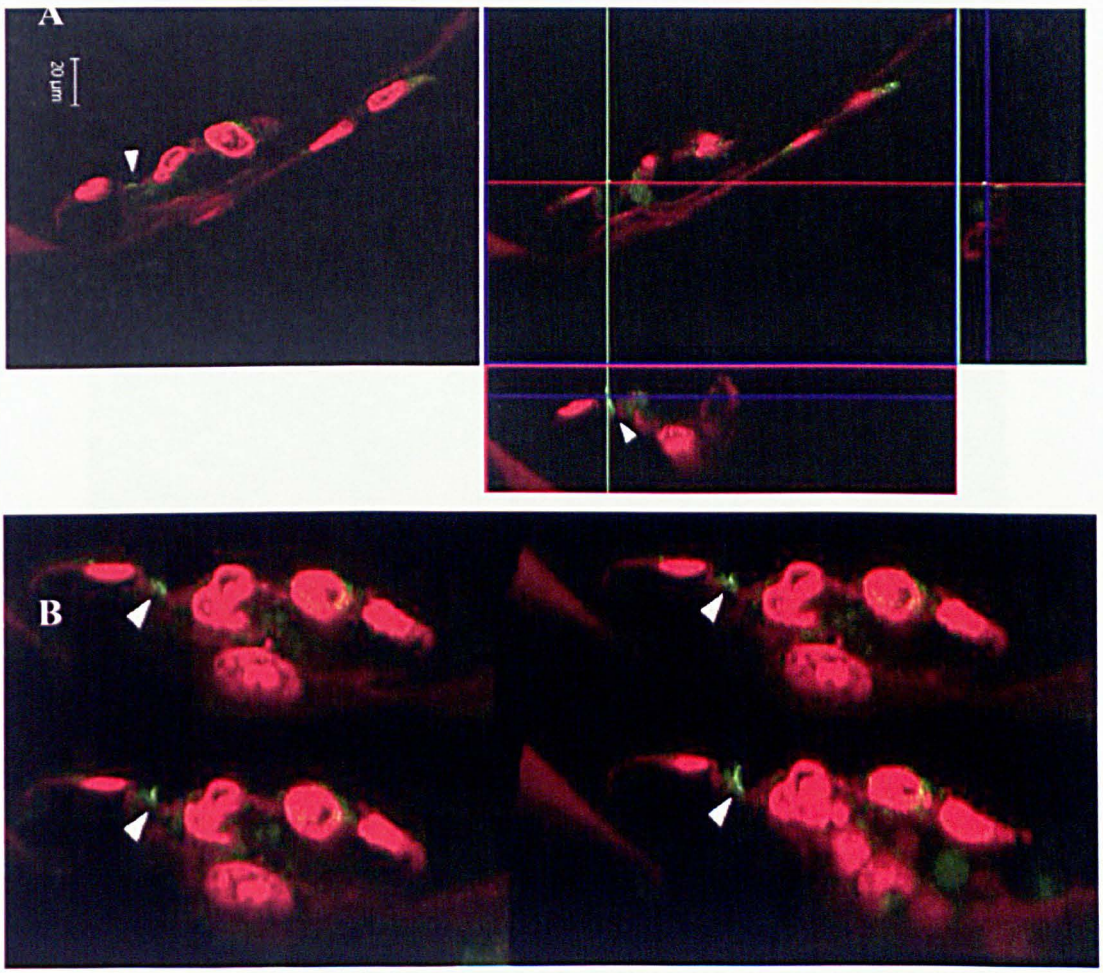

***Fig. 5.7**: Confocal images of primary cilia of MLO-A5 cells cultured in a 3-D PU scaffold. Primary cilium (green) was found at about 5 µm away from nucleus of cell (red) (A). Matched serial images at 4 different depths (B. This is similar to the expected position of primary cilia in vivo in which primary cilia are located on the surface of cells rather than near the nucleus of the cell as it is normally found in 2-D cultures.*

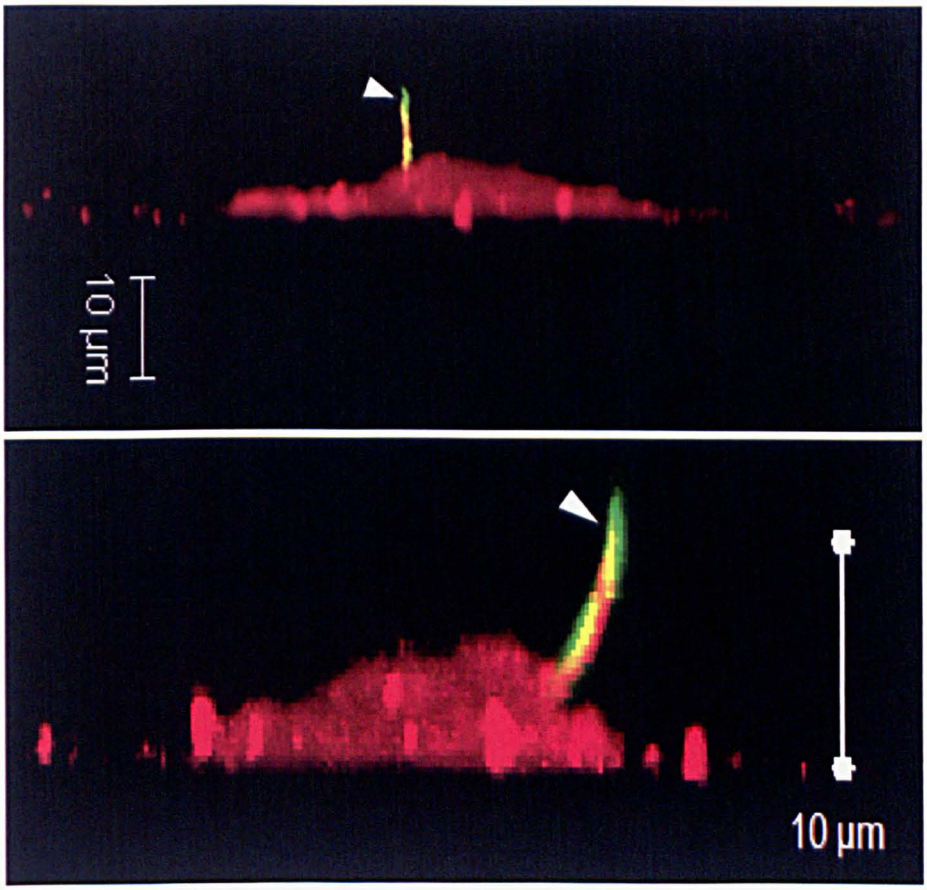

***Fig. 5.8**: Confocal images of interaction between glycocalyx and a mature primary cilium. Primary cilia of MLO-A5 cells (green, white arrow head) were stained by immunofluorescence using anti-acetylated alpha tubulin as the primary antibody. Hyaluronan glycocalyx (red) was stained using Biotinylated Hyaluronic Acid Binding Protein (HABP). The glycocalyx appears to wind round the mature primary cilium. Images were reconstructed from 120 consecutive z stacked images with a spacing of 12 µm between each optical slice. (Glycolcalyx was stained by Hayley Morris).*

5.3 Studying a potential role for primary cilia in bone matrix production in 2-D environment

The experiments in this 2-D stage of the study were conducted at the Cell and Molecular Biomechanics Laboratory at Stanford University, USA. The primary cilia of the cells were removed by knockdown of polaris protein using siRNA transfection technique. The transfection efficiency was observed by localization of fluorescent

labeling contained in the transfection reagents into cells through plasma membrane using the lipofection technique. It produced a high yield of positively transfected cells whereas the fluorescence was not seen in negative controls (no transfection) *(Fig. 5.9)*.

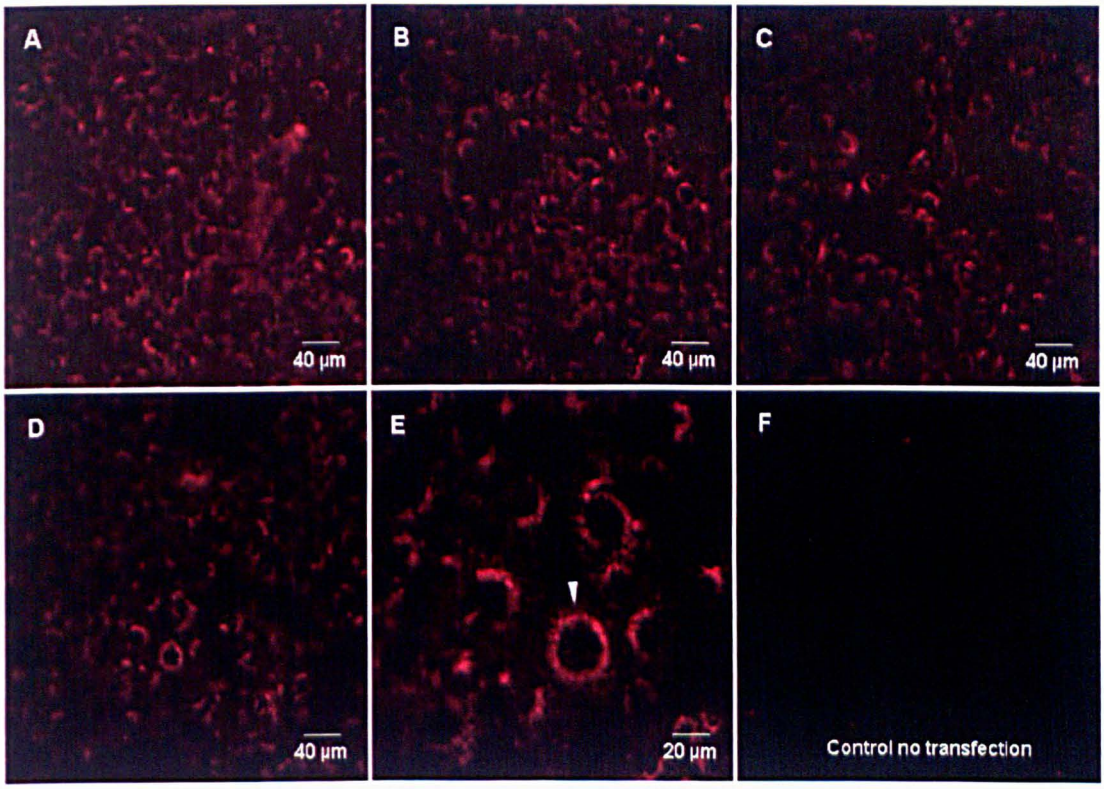

***Fig. 5.9**: MLO-A5 cells transfected with siRNA using a lipofection method. A high fluorescent yield of positively transfected cells (A-E) was shown. The fluorescence was not seen in negative (no transfection) controls (F).*

To investigate the effects of primary cilia on bone matrix production in 2-D, MLO-A5 cells were seeded on fibronectin coated slides with $5x10^4$ cells per slide and subjected to oscillatory fluid flow at 2Pa (average of normal shear stress, 0.8-3 Pa, in normal bone), for 2 hours on day 3 of culture (the method was described in chapter 2). Scrambled siRNA control (the same nucleotide composition as the target siRNA but in a scrambled sequence with no match to any mouse mRNA) and polaris knockdown mRNA was transfected into cells at day 1 of culture using the siRNA transfection technique. mRNA was isolated to assay gene expression of type I collagen (COL1), osteopontin (OPN) and Dentin matrix protein1 (DMP1), an early marker of osteoblast differentiation, using realtime RT-PCR at day 4 of culture (24 hr after flow). Calcium

and collagen production were stained by Alizarin red and Sirius red respectively at day 8 (5 days after flow) *(Fig. 5.10)*.

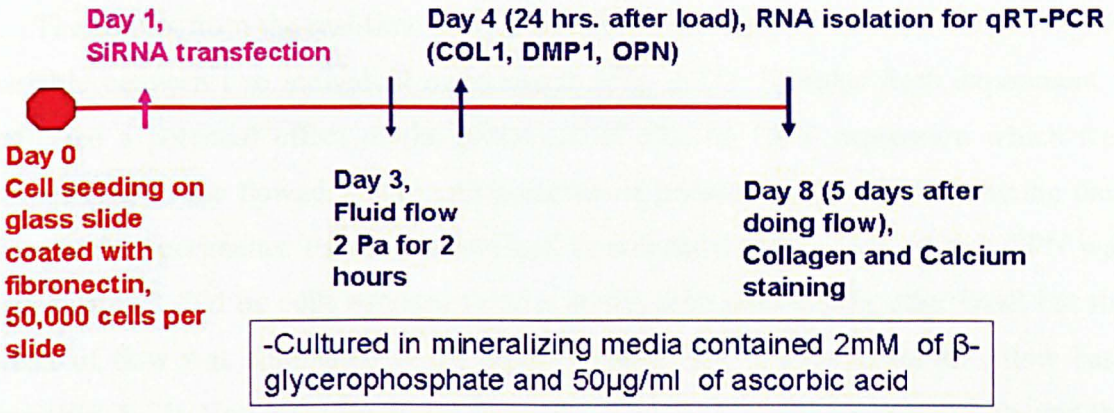

Conditions	Control	Scrambled control Si RNA	Polaris Si RNA
Nonflow	6 samples	6 samples	6 samples
Flow	6 samples	6 samples	6 samples

***Fig. 5.10**: Experimental design to study the effects of fluid shear stress on defective primary cilia in 2-D. Fluid shear stress (2 Pa) was applied on MLO-A5 cells. Bone matrix production by the cells with intact and defective primary cilia in 2-D were monitored. The experiment was repeated 2 times.*

5.3.1 Results

Collagen content as measured by Sirius red was significantly higher in cells subjected to fluid flow where the cells retained their cilia (no transfection and scrambled mRNA groups) but the flow induced increase in collagen content was eliminated in cells transfected with polaris siRNA *(Fig. 5.13 and 5.14)*. Although the siRNA transfection technique of polaris and scrambled siRNA has been used successfully in MC3T3-E1 and MLO-Y4 cells in previous study [118], the group transfected with scrambled siRNA in MLO-A5 cells in the present study did have a much smaller response to flow compared with the non-transfected group indicating either that the transfection adversely affected the cell's ability to respond to flow or the scrambled gene had some unpredicted effects on the cilia of this cell type or another aspect of mechanosensation. Calcium deposition appeared to be slightly different between the experimental groups under light microscopy, however, there were no significant differences in quantified calcium content after destaining the Alizarin red at day 8 *(Fig. 5.13 and 5.14)*. This may be because samples were assayed at a very early stage of

mineralization. The effects on calcium deposition may be clearer after longer culture periods.

The results from the real-time RCR experiments were less clear the data was highly variable between two individual experiments *(Fig. 5.11)*. Samples from experiment 1 indicated a potential effect of the prescence of cilia on OPN expression which was upregulated in the flowed group with presence of primary cilia. After combining data from both experiments, the data normalised to non-flow groups showed that OPN was upregulated 2 fold by cells exposed to flow at this time point (24 hr after flow) but the effect of flow was eliminated in the group without cilia relative to the non-flow base line *(Fig. 5.12)*, However, the scrambled group also showed no response to flow and the non cilia, non flowed cells appeared to produce as high levels of OPN mRNA as their respective flow groups. Gene expression of COL1 and DMP1 did not show the same trend as matrix production as assayed by Sirius red staining at day 8 *(Fig. 5.14)*, at this time point of day 4 *(Fig. 5.12)*. Overall these real-time PCR results indicate there were major problems with performing the technique and they are too variable to draw any conclusions from them.

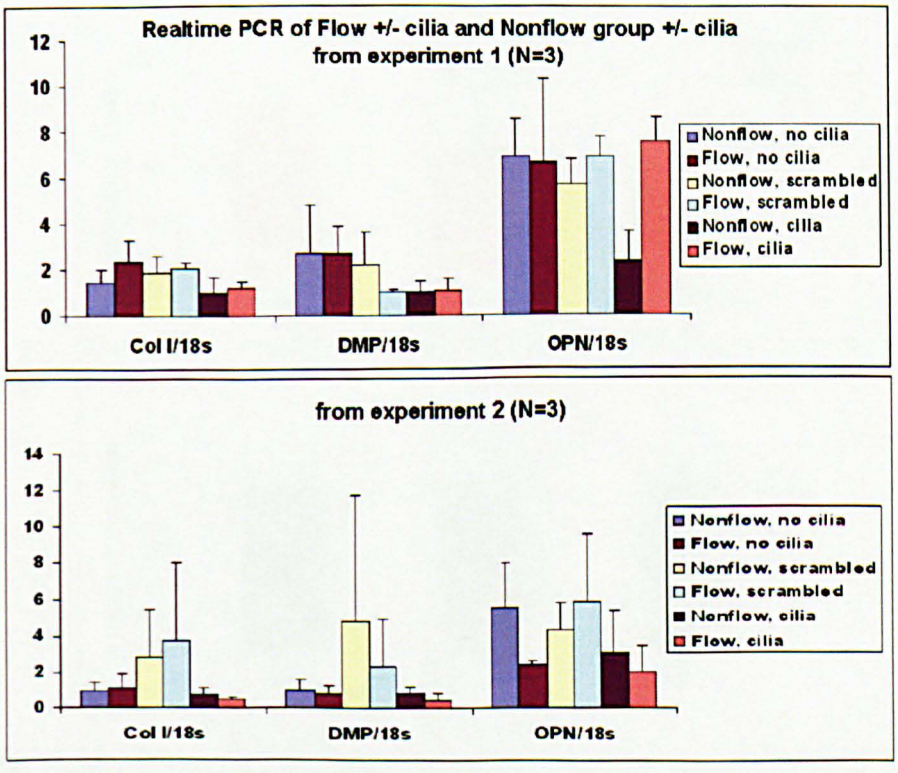

***Fig. 5.11**: Quantitative RT-PCR data. High variable results between two individual experiments were shown (Mean ± SD, N=3).*

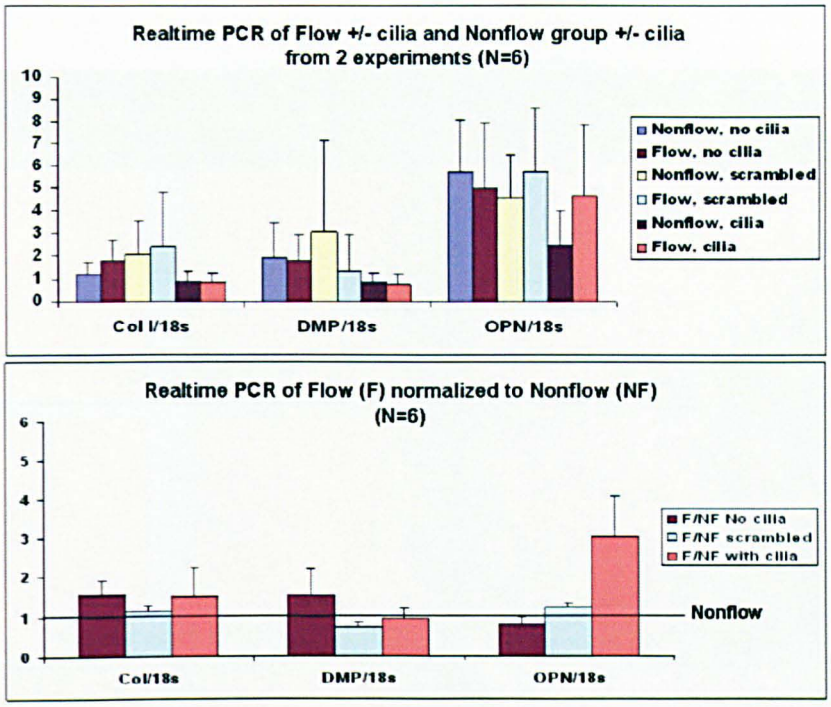

***Fig. 5.12**: The bar charts of the quantitative RT-PCR. The data was combined from both experiment (Mean ± SD, N=6) and normalized to non-flow groups (Mean ± SE, N=6). Osteopontin gene expression normalized to 18S appears to be upregulated about 2 fold in cells exposed to flow but there was no effect of flow in the knockdown group or the scrambled*

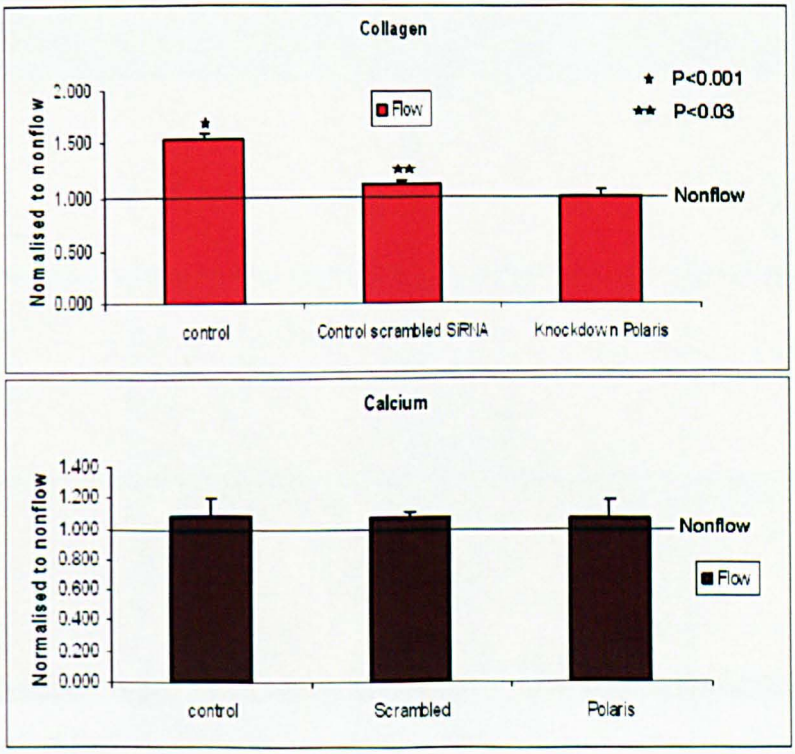

***Fig. 5.13**: Total collagen and calcium by destaining normalised to the nonflow group. Data shows significantly increasing collagen production in all control flow group (with cilia) compared with the non-flow group of the corresponding treatments, but the difference was eliminated in the absence of primary cilia. Calcium content shows no differences between groups. (paired t-test).*

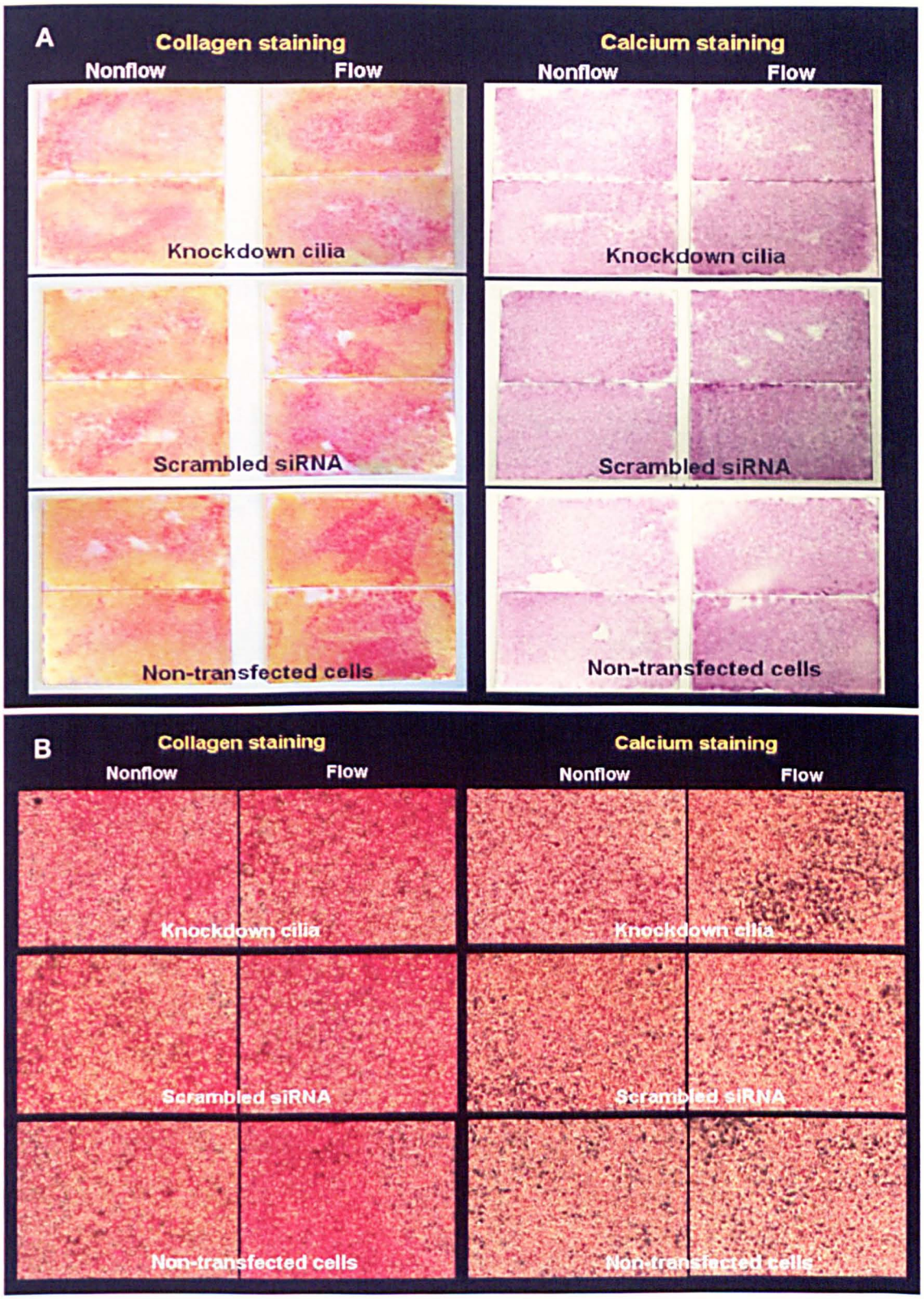

***Fig. 5.14**: Collagen and calcium staining of transfected and non-transfected cells. Images were taken from glass slides (A) and when look at under the light microscope (x4) at day 8 (B). Collagen was shown in red. Calcium deposition was stained in dark purple on glass slides or black dots under the light microscope.*

5.4 Investigating whether the primary cilium is involved in mechanical responses of bone tissue formation in 3-D constructs.

Because of the problems encountered during the 2-D experiments, alternative methods for both primary cilia removal, by using chloral hydrate, and monitoring gene expression of matrix proteins, by using bench-top RT-PCR, to study how primary cilia and mechanical conditioning stimulate tissue engineered bone formation in 3-D constructs were carried out. Although it has previously been shown that long-term incubation with chloral hydrate removes cilia from *Paramecium caudatum* [204], from the early embryo phase of the sea urchin [205], from MDCK cells [115, 116] and bone cells [118], it has never been shown in MLO-A5 cells before. In these experiments, the chloral hydrate method to remove primary cilia from MLO-A5 cells was firstly optimized. However, the mechanism of chloral hydrate deciliation is unclear. It has been proposed that it destabilizes the junction between the cilium and the basal body probably through disassembly of microtubules [205]. Dunlap (1977) suggested that the shearing forces encountered by the cell in its environment may be responsible for the actual breakage and removal of the cilia which is weakened by chloral hydrate [204]. In this stage, I show that after 6 hrs of incubation with chloral hydrate, a few cells without cilia can be detected and the primary cilia had a more condensed configuration. After 12 hrs of incubation, they changed their appearance from elongated structures to small bright dots or grossly distorted microtubule organization. After 24 hrs of incubation, the primary cilia were undetectable *(Fig. 5.15)*. 24 hrs of incubation was repeated for imaging in 3-D culture *(Fig. 5.16)*.

To study the effect of loading induced mechanosensation by primary cilia on matrix gene expression in a 3-D environment, polyurethane scaffolds were cut into cylinders of 10 mm diameter and 10 mm height. Scaffolds were seeded with MLO-A5 cells at densities of 2.5×10^5 per scaffold. Cell-seeded scaffolds were dynamically loaded in compression at 1Hz, 5% strain in a biodynamic chamber. Cell-seeded scaffolds were incubated with 4 mM chloral hydrate for 24 hr on day 9. Dynamic compressive loading (5% strain, 1 Hz) was immediately applied for 2 hours 24 hrs after chloral hydrate incubation (on day 10) so that there was not time for the primary cilia to re-grow prior

to loading. Gene expression of OPN and COL1 were measured 12 hrs after a single bout of 2 hrs of loading or control treatment.

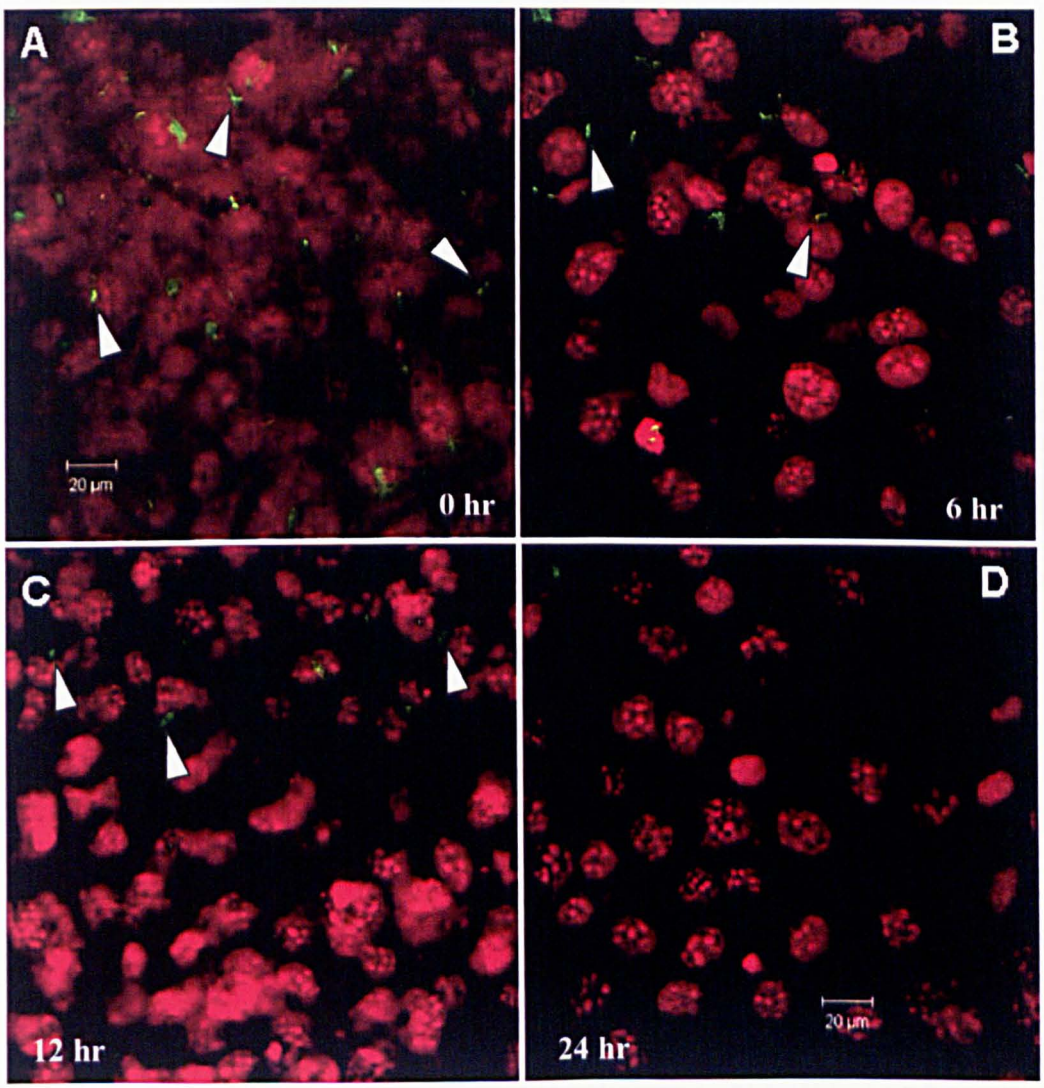

***Fig. 5.15**: Fluorescence images of MLO-A5 cells and their primary cilia from 2-D culture. The cilia were stained with anti-acetylated alpha tubulin (green). The images were taken before incubation with 4mM chloral hydrate (A), after 6 hr incubation (B), after 12 hr incubation (C) and after 24 hr incubation (D). Nuclei of cells were stained with PI (red). Arrow heads pointed primary cilia.*

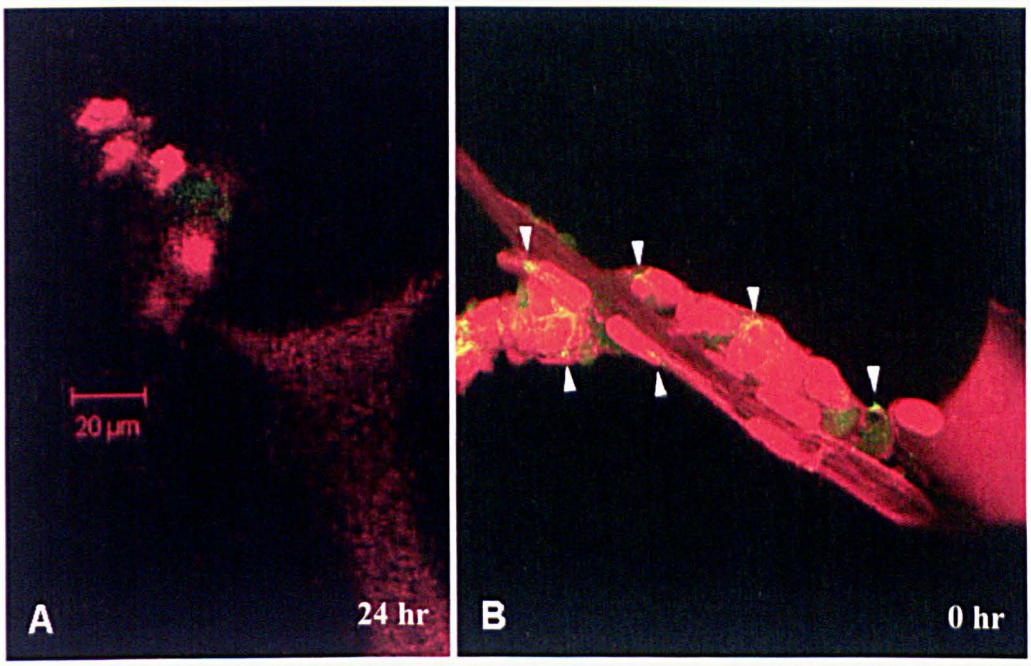

***Fig. 5.16**: Fluorescence images of primary cilia of MLO-A5 cells after 24 hr incubation with chloral hydrate in 3-D culture. The images show undetectable primary cilia after 24 hr incubation with chloral hydrate (A). Primary cilia (white arrow heads) can be observed before incubation (B).*

5.4.1 Results

Loaded samples with primary cilia present showed increased levels of OPN and COL1 gene expression (about 2.5 fold) compared with non-loaded samples as measured by band density relative to GAPDH. Data of loaded samples normalised to non-loaded samples of the same group of treatment showed that OPN expression was significantly higher in cells with cilia subjected to loading compared to cells with no cilia subjected to loading. ($p< 0.05$, two sample-t test, N=3) *(Fig. 5.17)*.

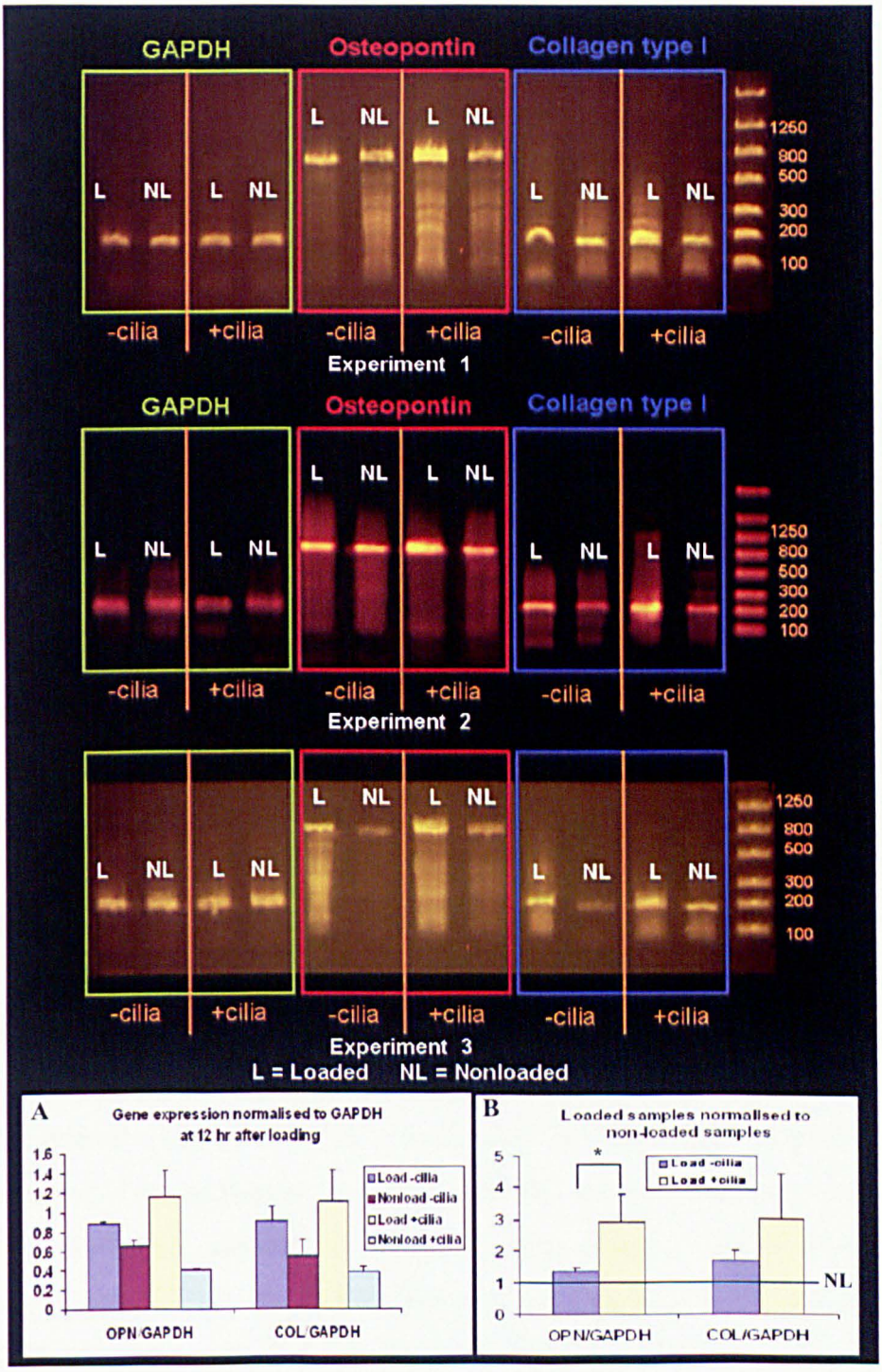

Fig. 5.17 *mRNA expression of OPN and COL1 12 hrs after a single bout of 2 hrs of loading. Gels of 3 independent experiments are shown. (A) Loaded samples with primary cilia present showed increased levels of OPN and COL1 gene expression (about 2.5 fold) as measured by band density relative to GAPDH. (B) OPN expression was significantly higher in cells with cilia subjected to loading compared to cells with no cilia subjected to loading. (*p< 0.05, 2 sample-t test, N=3).*

5.5 Discussion

This is the first time that primary cilia of MLO-A5 cells have been visualized and reported in both 2-D and 3-D environments *in vitro*. In mouse renal epithelial cells *in vivo*, the centrosome was located near the cell surface and cells had primary cilium protruding into duct lumen. In contrast, in subcultured cells in 2-D, the centrosome come closer to the nucleus, so the primary cilium was always located near the cell nucleus [103]. A similar effect was also found in our 2-D cultured cells *(Fig. 5.3)*. In this chapter, we showed that mature primary cilia in 3-D environments can be found far from the nucleus (about 5 μm) of the cell. However, we could not see the particular organization pattern of primary cilia, as seen in some tissues *in vivo* such as kidney duct lumen, in this 3-D static condition. This may because of high auto-fluorescence of the PU scaffold, some non-specific staining of microtubules or because cells do not organise when in the non-stimulated condition. Primary cilia seem located randomly in the 3-D static model, it is possible that mechanical factors such as type, direction and force of loading may play important role in cell migration and organisation *in vivo*. Therefore, in the future it would be interesting to compare the organization and localization of primary cilia in our 3-D system between static and loading conditions.

Malone et al. (2007) have demonstrated that the presence of primary cilia in MC3T3-E1 osteoblastic cells is essential for the OPN gene expression changes and PGE_2 release exhibited by these cells in response to a fluid flow stimulus indicating that primary cilia play a role in osteogenic responses to flow [118]. In our study, we also found that primary cilia were needed to upregulate OPN and COL1 gene expression in samples subjected to mechanical stimuli and that the absence of primary cilia inhibited the matrix production induced by dynamic compression of the scaffold. This is supported by our RT-PCR results from the previous chapter in which we showed that OPN, OCN and COL1 mRNA levels of MLO-A5 cells can be upregulated from 12 hr after loading. Loaded scaffolds containing cells with primary cilia present showed higher levels of COL1 and OPN mRNA (about 2.5 fold) as measured by band density relative to GAPDH compared with non-loaded controls and loaded cells with absence of primary cilia. OPN expression was significantly higher in cells with cilia subjected to loading compared to cells with no cilia subjected to loading *(Fig. 5.17)*. We suggest that the primary cilium may mediate the matrix-forming response of bone cells to

mechanical loading in our 3-D model which has implications for mechanical conditioning in bone tissue engineering.

There is evidence that matrix proteins such as collagen bind to the primary cilium in chondrocytes. When the cilium interacts with collagen, alterations occur in the plasma membrane and in the ciliary microtubules that may be responsible for the acute bending of primary cilia [105]. To my knowledge, there is no report about interactions of primary cilia and bone mineralized matrix or the proteoglycans such as glycocalyx in the interstitial fluid. We showed the potential of the 3-D model that we have optimized to study how primary cilia and bone matrices interact with each other in 3-D environments in which cells are embedded in mineralized matrices. However, the challenge of this study is to maintain the absence of primary cilia over long term culture periods to allow enough time for cells to produce mineralized matrix.

The techniques to remove primary cilia used in this chapter need to be further investigated. Primary cilia can grow back to normal when cells are returned to normal standard medium after chloral hydrate incubation. We have found that, in MC3T3-E1 and MLO-A5 experiments, cell monolayers were partially detached from the substrate if they were incubated with chloral hydrate for longer than 24 hours (up to 48 hours) suggesting the absence of primary cilia can not be maintained for long term experiments using the chloral hydrate method. Praetorius et al. (2003) have shown that long incubation of MDCK kidney cells up to 68 hr with 4mM chloral hydrate produces substantial changes in the organization of intracellular microtubules [116]. Primary cilia can be completely removed when kidney cells are incubated with chloral hydrate for 68 hr. However, flow sensing on these cells was abolished after 20 hr exposure of chloral hydrate compared with normal cells by monitoring intracellular calcium [116]. In our present study, cells were incubated with 4 mM chloral hydrate for 24 hour and loaded immediately at that time point to prevent reformation of primary cilia and the detachment of cells from the substrate. However, it was shown that chloral hydrate treatment disturbed the mitotic spindle in mouse oocyte by interfering with microtubules [166]. This might cause non specific effects on the cells in our present study.

It has been shown in previous studies that the intracellular microtubules have returned to nearly normal appearance when cells were allowed to recover for 24 hours in normal media [116] while at the same time-point the primary cilia were still not observed. Therefore, it is possible that it would be better to allow cells to recover 24 hours in normal media before loading experiments are performed to reduce any non specific effect of chloral hydrate. The prolonged incubation time required to remove the cilia in MDCK cells [270] and MC3T3-E1 cells [118] had no effect on their attachment. However, the chloral hydrate seemed to have an adverse effect on cell-substrate attachment of MLO-A5 cells by detaching cells from the surface indicating that incubation time and period can be different for each cell type. This is the first time that MLO-A5 cells were used to study flow and mechanical sensing of primary cilia in bone. Therefore, optimizing the incubation time in chloral hydrate, in which primary cilia can be removed and cells are not detached from surface, is needed. We showed that 24 hr incubation was enough to reduce flow sensing of MLOA-5 cells in 3-D by inhibiting the upregulation of mRNA gene expression of OPN and COL1.

At present, chloral hydrate is the only effective tool for removal of MLO-A5 osteoblastic cell cilia in 3-D in our lab even though its action is not solely restricted to serving the attachment of the cilium to the basal body. Other techniques such as siRNA transfection of polaris protein, are more complicated, expensive and needed to be optimized. Our 2-D experiment to study mechnosensing of primary cilia using siRNA transfection techniques showed that the scrambled siRNA had effects on all cells and inhibited their ability to respond to flow. This problem may occur because either the transfection technique inhibited cells to response to a fluid flow stimulus or the inadequate sequences of scrambled siRNA enabled it to also knockdown the primary cilia or inhibit other mechanosensory mechanisms. Even though the scrambled siRNA sequence does not have an explicit intended target, there are plenty of partially-complementary sequences with which it may interact [271, 272].

Although, the primary cilia could not be removed completely in all cells by either chloral hydrate deciliation or siRNA transfection of polaris protein techniques, the results of this study have shown that absence or changes in morphology of primary cilia can influence the function of cells subjected to mechanical forces and that the presence of intact primary cilia is required for load sensing. Praetorius et al. (2003) have

shown that flow sensing was completely abolished in deciliated MDCK cells returned to normal medium for 72 hours, a time when cilia were still not detectable by immunofluorescence but the flow response only fully recovered after 120 hours, at which time all cells exhibited cilia, and were similar to those of control cells [115, 116]. However, there is a report showing that the primary cilia of bone cells act differently from ciliated kidney cells for example, they do not transduce the external mechanical stimulus via the same Ca^2+ ion flux as in kidney cells [118].

5.6 Summary

- This is the first time that the primary cilia of MLO-A5 osteoblastic cells have been visualized and used to study flow and mechanical sensing in bone cells both in 2-D and 3-D environments *in vitro*. We presented evidence that mature primary cilia in 3-D environments can be found far from nucleus (about 5 μm) of the cell indicating they are located around the edge of cells as seen in *in vivo*.
- We presented preliminary evidence of an interaction between the hyarulonan glycocalyx and the primary cilium indicating a potentially complex relationship between these two mechanosensors in bone.
- The 2-D experiments showed that collagen production significantly increased in flow groups where the cells retained their cilia but the flow induced increase in collagen content was eliminated in cells transfected with polaris siRNA.
- Primary cilia of MLO-A5 cells can be removed by incubating with 4 mM chloral hydrate. We showed in this chapter that 24 hrs incubation was enough to reduce flow sensing of MLOA-5 cells in 3-D by inhibiting the upregulation of mRNA gene expression of OPN and COL1 in response to load.
- Loaded scaffolds containing cells with primary cilia present showed higher levels of COL1 and OPN mRNA (about 2.5 fold) as measured by band density compared with non-loaded controls and loaded cells with primary cilia removed. We suggest that the primary cilium may mediate the matrix-forming response of bone cells to mechanical loading in our 3-D model which has implications for mechanical conditioning in bone tissue engineering.

CHAPTER SIX: The effects of mechanical stimulation on hMSC for bone tissue engineering.

6.1 Introduction

A high number of bone replacements were performed in Europe in 2000 (>280,000) [123], the USA. (>500,000) and worldwide (>2.2 million) in 2005 [273]. Bone grafting procedures (both autografts and allografts) are used in order to repair bone defects in orthopedics, neurosurgery and dentistry [273]. However, they have limited availability. Autografting requires an additional surgery that can lead to donor site morbidity and pain [274] whereas allografting carries the risks of disease transmission and implant failure due to immune response, fracture, or nonunion [275]. As a result of these limitations to current therapies, bone tissue engineering is emerging as a potential alternative.

Tissue engineering, in which a patient's undifferentiated cells or stem cells are seeded onto a biocompatible scaffold in controllable environments *in vitro* is the subject of much recent focus by researchers. Advances in the field are leading to the engineering of new clinically useable tissues such as urinary bladder [276], laryngeal and tracheal tissues [277]. It is hoped that such advances will allow the regeneration or replacement of aging tissues without the need for human organs. To engineer a bone tissue replacement, cells need to be grown in a 3-D scaffold provided with sufficient nutrients and stimuli. Bioreactors for cell culture which provide mechanical and chemical stimuli can be used to induce growth and differentiation of cells, and may enhance extracellular matrix deposition and mineralization of the tissue constructs [21, 75, 138, 149, 253, 278, 279].

Stem cells are an attractive source of cells for use in tissue engineering and regenerative medicine. They differ from progenitor cells in their capacity for self-renewal and multilineage differentiation, where progenitor cells are not capable of self renewal [280]. In theory, this capacity for self renewal could provide an unlimited source of donor materials for transplantation [142]. Stem cells can be derived from the inner cell mass of an embryo blastocyst (embryonic stem cells (ESCs)) or from adult

tissues (adult stem cells (ASCs)), such as bone marrow-derived mesenchymal stem cells (MSCs) [23]. However, there is some controversy as to whether 'MSCs' are true stem cells or skeletal stem cells, able to regenerate only skeletal tissues such as bone, cartilage and marrow fat cells [281, 282]. Therefore, MSCs are also called "Bone Marrow Stromal Cells (BMSC)", a term used to describe non-blood-forming cells in bone marrow [282]. MSCs are easier to obtain and proliferate more rapidly than fully differentiated osteoblasts. However, bone tissue engineering may require pre-differentiated osteogenic progenitor cells or osteoblasts, rather than undifferentiated stem cells before implantation, in order to prevent non-specific tissue differentiation of stem cells.

To direct MSCs along the osteogenic lineage, non-protein-based chemical compounds such as Dexamethasone (DEX), a synthetic glucocorticoid, are widely used because they are easy to produce [46, 283, 284]. DEX has been shown to act at both early and late stages of osteogenic differentiation to accelerate osteoblastic maturation [46]. In continuous treatment with DEX, MSCs have been shown to increase expression of osteocalcin and bone sialoprotien [285], alkaline phosphatase activity [286] and matrix mineralization [287, 288]. However, DEX has also been shown to downregulate expression of collagen type I and enhance maturation of adipocytes in culture [289]. These effects may be reduced if DEX is used at a suitable concentration and duration during culture.

Mechanical forces have been shown previously *in vivo* to play an important role in bone formation by inducing osteoprogenitor cells in the marrow stroma to differentiate into osteoblasts at the cortical bone surface [290]. They have also been reported to regulate bone growth *in vivo* [64]. Chapter 4 described studies demonstrating that mature osteoblasts respond to mechanical loading in an *in vitro* 3-D environment by increasing bone matrix production and upregulating matrix protein gene expression [291]. This suggests that the mechanical loading system developed previously would also have the potential to induce osteogenic differentiation and bone matrix production by MSCs for use in bone tissue engineering. However, the effects of mechanical loading on differentiation of human MSC are not well understood due to the variety of mechanical stimuli and loading systems used. The hypothesis in this chapter is that mechanical dynamic compressive loading, as described in the previously

developed regimen, will have the ability to stimulate osteogenic differentiation of hMSC in the same way as treatment with DEX. Two sets of experiments were performed in this chapter as follows:

1. Verifying the effects of DEX on osteogenic differentiation of hMSCs by measuring ALP activity in 2-D.
2. Studying the effects of dynamic compressive loading and DEX treatment on osteogenic differentiation and bone matrix production of hMSCs.

6.2 Preliminary test: Verifying the effects of DEX on osteogenic differentiation of hMSCs by monitoring ALP activity in 2-D.

Prior to investigations in 3-D, a 2-D study was performed using bone marrow derived hMSCs to confirm the effects of DEX on cells over 14 days. This was achieved by monitoring ALP activity, an early marker of hMSCs differentiation along the osteogenic lineage. $2x10^4$ cells of hMSC passage 2 were seeded into a 12 well plate and cultured in standard basal media supplemented with 50μg/ml AA, 5mM βGP and 10nM DEX. Both control (no DEX) and experimental groups were cultured for 14 days. Samples were assayed on days 7 and 14 for cell viability (MTS) and osteogenic differentiation using a biochemical assay of ALP activity as described in chapter 2.

6.2.1 Results

The results showed no difference in the relative cell number of metabolically active cells in all samples, indicating that cell viability was not affected by DEX treatment over 14 days of culture *(Fig. 6.1)*. ALP activity was found to be a function of the presence of DEX treatment. Samples in culture conditions with DEX treatment demonstrated significantly higher enzyme activity (about 137% or 20 nmol/min higher) when compared to non-DEX-treated samples following 14 days of cultivation *(Fig. 6.2)*.

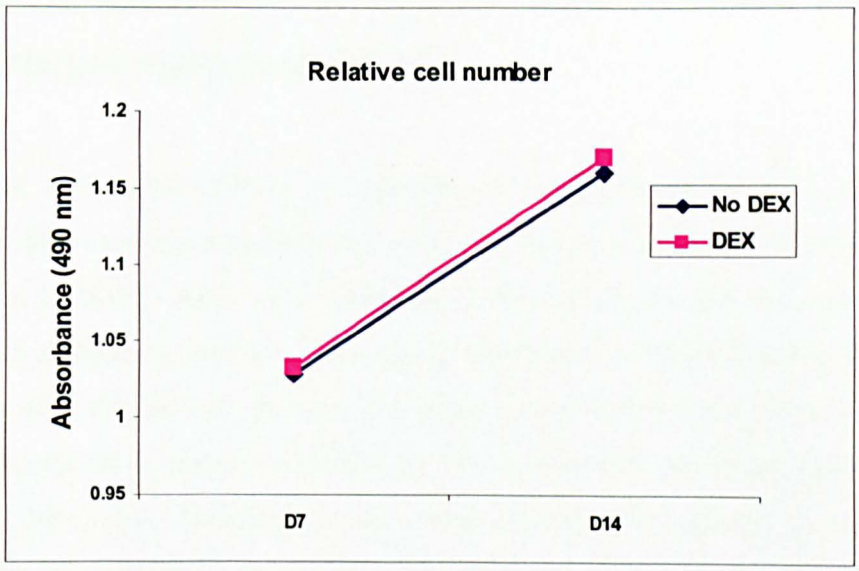

Fig. 6.1: *Change over time of relative cell number on day 7 and day14 after adding DEX. Data shows an increased number of viable cells at day 14 compared to day 7. There is no difference in relative cell number between treatment and non-treatment groups. (N=2)*

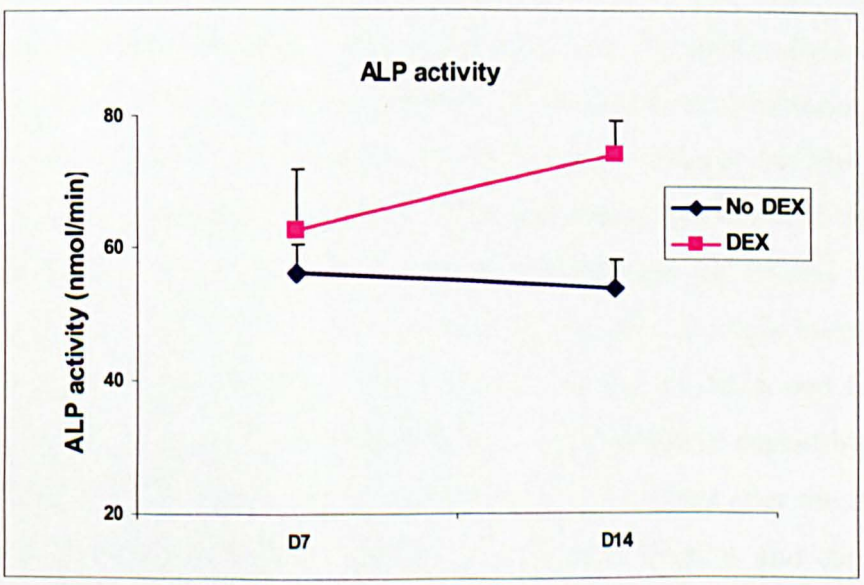

Fig. 6.2*: Change over time of ALP activity on day 7 and day 14 after adding DEX. Data shows an increase of ALP activity in DEX treated samples at day 14 compared with no DEX controls. (N=2)*

6.3 Studying the effects of dynamic compressive loading and DEX treatment on osteogenic differentiation and bone matrix production of hMSCs

These experiments aimed to investigate the effects of dynamic compressive loading and DEX treatment on differentiation and matrix production of hMSCs in 3-D. Polyurethane scaffolds were used with the loading methods and regimen described previously in chapters 3 and 4 of this report. However, a higher number of cells and smaller size of scaffolds than that in our previous experiments were chose in this study to reduce proliferation period of MSCs as MSCs normally proliferate about 4 times slower than MLO-A5 osteoblastic cells. $5x10^5$ hMSCs were seeded in polyurethane scaffolds, 10 mm diameter and 5 mm height, and cultured in standard culture media with or without 10nM DEX. Sekiya et al. (2002) have shown that MSCs expanded most rapidly by day 4 after plating [292]. Therefore, DEX and βGP in the present study were added on day 4 to modulate MSCs differentiation at this time point. Cell-seeded scaffolds were compressed at 5% global strain for 2 hours on day 9 and then every 5 days in the biodynamic chamber. The experiment was repeated 3 times (N=2 per individual experiment). 6 samples from 3 donors (A, B and D; detail of donors shown in *Table 6.1*) were tested for cell viability by MTS assay, collagen by Sirius red and calcium by Alizarin red at day 24 of culture. The gene expression of matrix protein type I collagen (COL1), osteopontin (OPN), alkaline phosphatase (ALP) and runt-related transcription factor 2 (RUNX2), were measured 12 hrs after a single bout of 2hrs of loading (day 9) or control treatment (from donor C, D and E). Stein and Lian (1993) have shown that ALP expression is upregulated in the maturation period by day 12 of culture. Therefore, ALP activity was monitored on day 12 (3 days after the first bout of loading, N=6 from donor C, D and E). The experimental timeline and conditions are shown in *Fig. 6.3*.

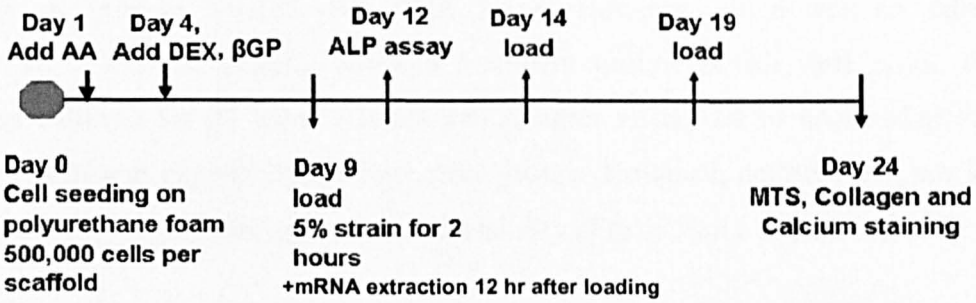

Conditions	With Dex	Without Dex
Nonload	6 samples	6 samples
load	6 samples	6 samples

***Fig. 6.3**: Experimental design to study the effects of dynamic compressive loading and DEX on osteogenic differentiation and bone matrix production of hMSCs.*

***Table 6.1**: Information on the human mononuclear cells obtained from five different donors.*

Donor (Lot No.)	Company	Date of aspiration	Age	Gender	Ethnicity	Passage number
A (PCBM1499)	Stemcell Technologies	15 Nov 06	20	Female	Caucasian	2
B (070148A)	Lonza	26 Jan 07	44	Male	Caucasian	2
C (PCBM1497)	Stemcell Technologies	14 Nov 06	23	Male	Hispanic	2
D (PCBM1376)	Stemcell Technologies	27 Mar 06	28	Male	Not known	2
E (PCBM1619)	Stemcell Technologies	13 Aug 07	23	Male	Caucasian	2

6.3.1 Results

The results show that ALP activity at day 12 (3 day after first bout of loading) in samples subjected to mechanical loading, treated with DEX or both was significantly elevated compared with static non-loaded controls without DEX *(Fig. 6.4)*.

Interestingly, ALP activity in samples subjected to loading with no DEX treatment was as high as samples treated with DEX alone. However, there was no significant difference in enzyme activity between treatment groups at this time point. For the samples cultured for 24 days, relative cell number at day 24 in non-loaded samples without DEX was slightly higher than other groups. However, neither DEX nor loading had statistically significant effects on cell viability *(Fig. 6.5 and 6.9)*.

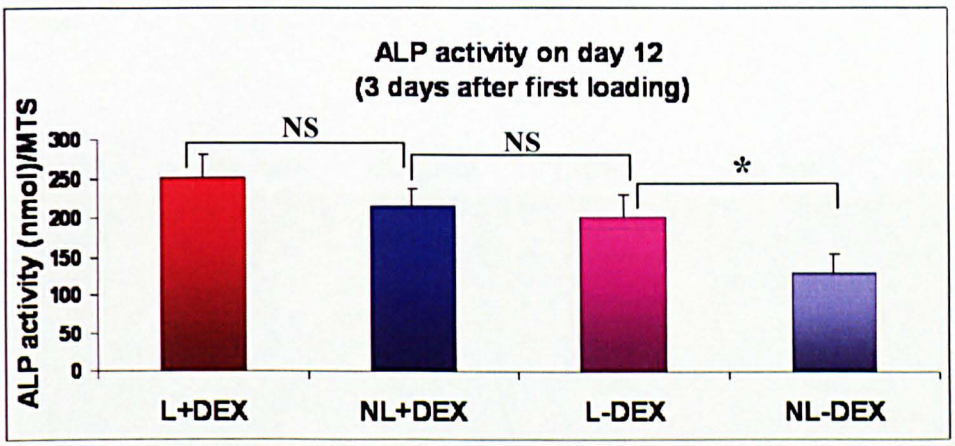

***Fig. 6.4**: ALP activity at 3 days after the first bout of loading. Data shows higher activity in all treatment groups with loading DEX or both loading and DEX treatment, compared to non-loaded without DEX (N=6). (*p<0.05, two sample-t test).*

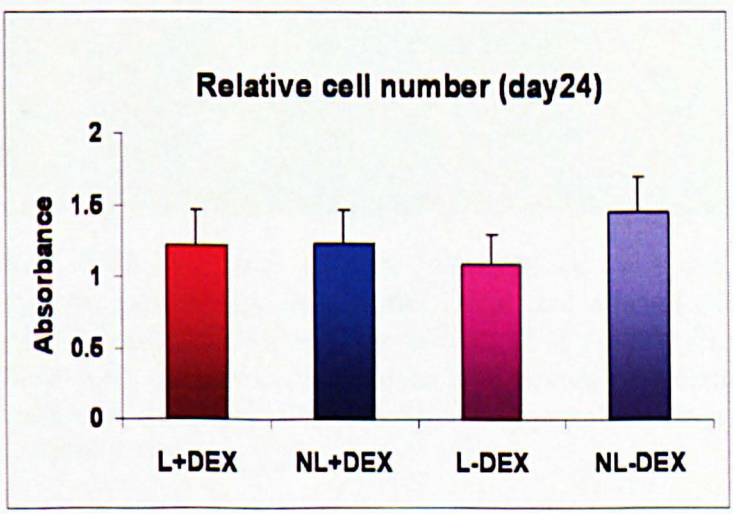

***Fig. 6.5**: The bar chart of relative cell number. Data shows slightly higher cell viability in the non-loaded without DEX group but there is no statistically significant difference at the end of experiment) (Mean ± SD, N=6)*

Collagen and calcium staining of scaffolds showed good distribution of matrix throughout the scaffold in each section *(Fig. 6.6)*. Examination of the scaffolds by light microscopy showed qualitative differences in both Sirius red staining for collagen *(Fig. 6.7)* and Alizarin red staining for calcium *(Fig. 6.8)*. Both matrix components appear higher in all treatment groups with loading, DEX or both treatments compared to non-loaded without DEX at the end of the experiment. Quantitative results from destaining showed that relative collagen content per cell was significantly increased in the loaded group compared with the non-loaded group in all conditions (paired t-test) *(Fig. 6.10B and 6.10D)*.

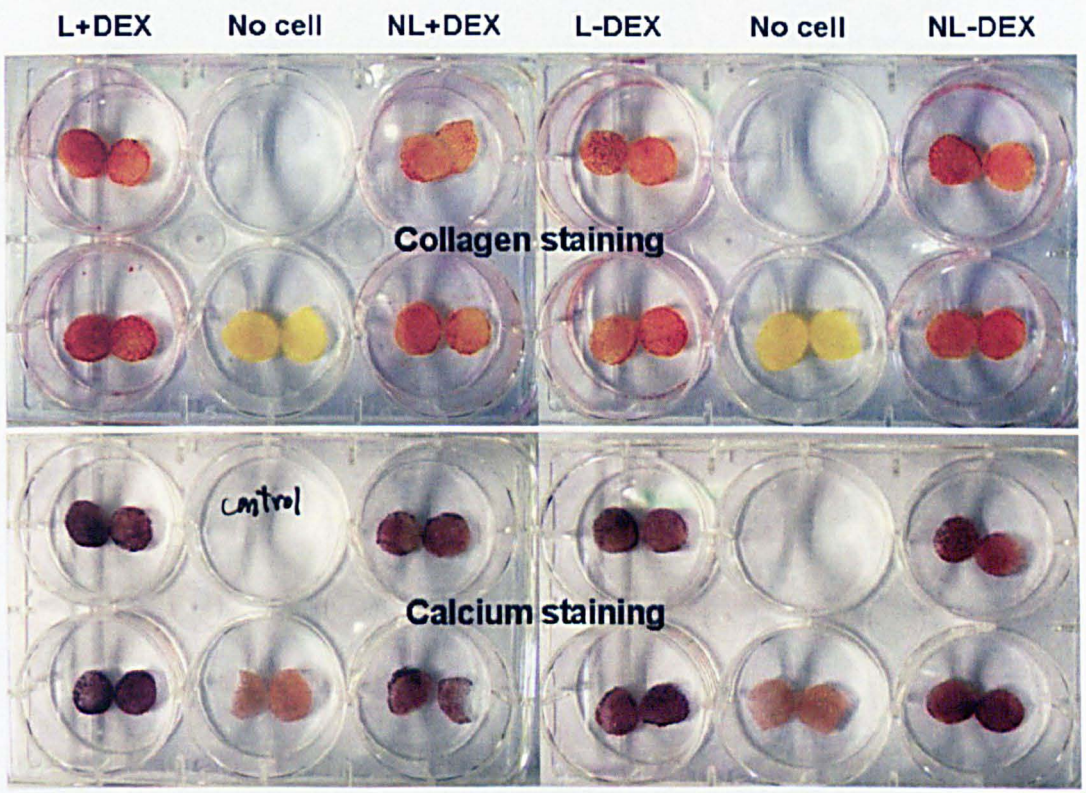

***Fig. 6.6**: Collagen and calcium staining of samples. Images show representative loaded (L), non-loaded (NL), and control (no cell) scaffolds supplemented with DEX (+DEX) or without DEX (-DEX) from donor D. One scaffold per well, cut into cross sections and stained with Sirius red (collagen) and alizarin red (calcium). Experiment was repeated 3 times with 3 different donors (Table 6.1).*

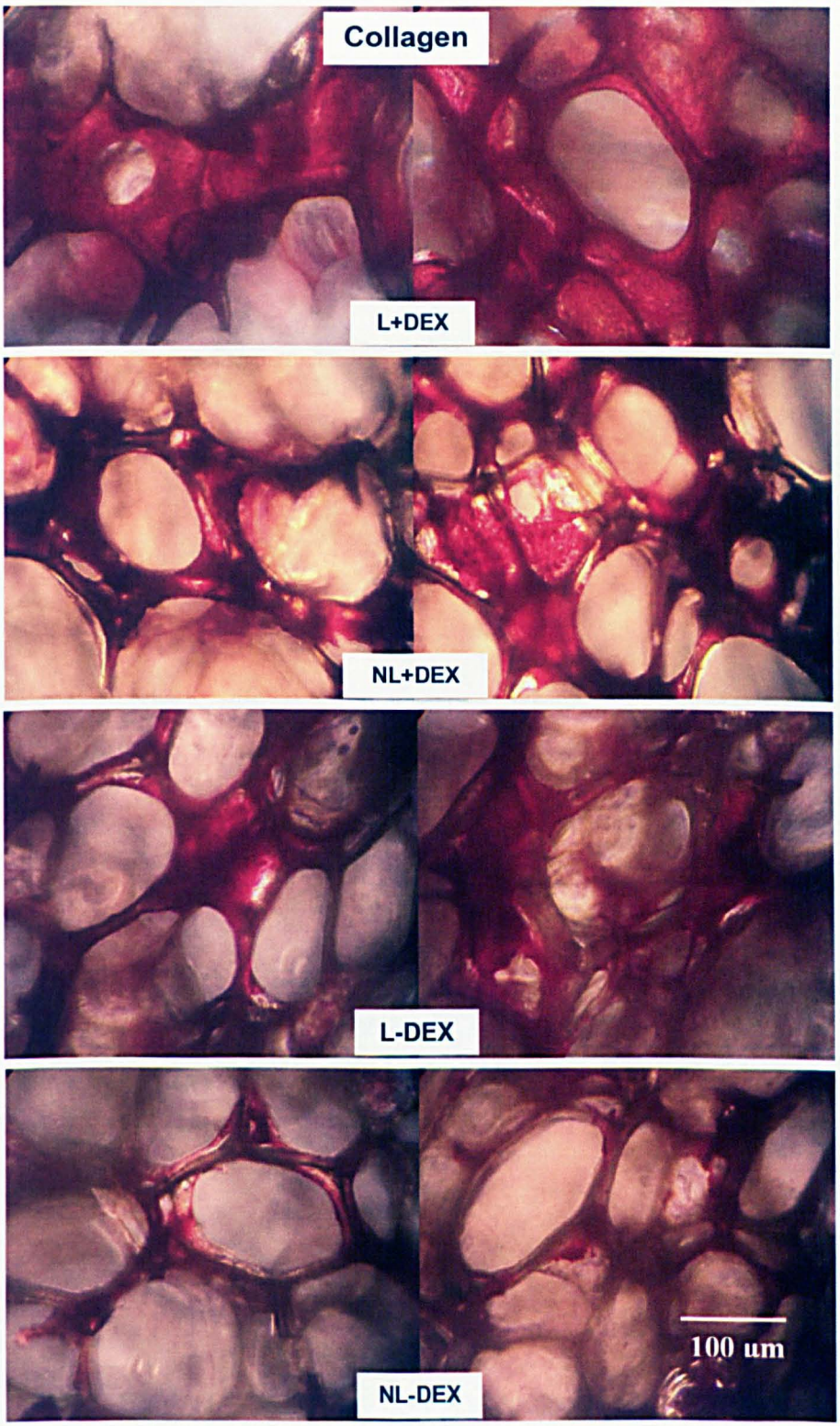

***Fig. 6.7**: Light micrographs of random areas of scaffolds stained by Sirius red at the end of the experiment. The amount of collagen in scaffold appeared higher in loaded samples supplemented with DEX compared to other groups.*

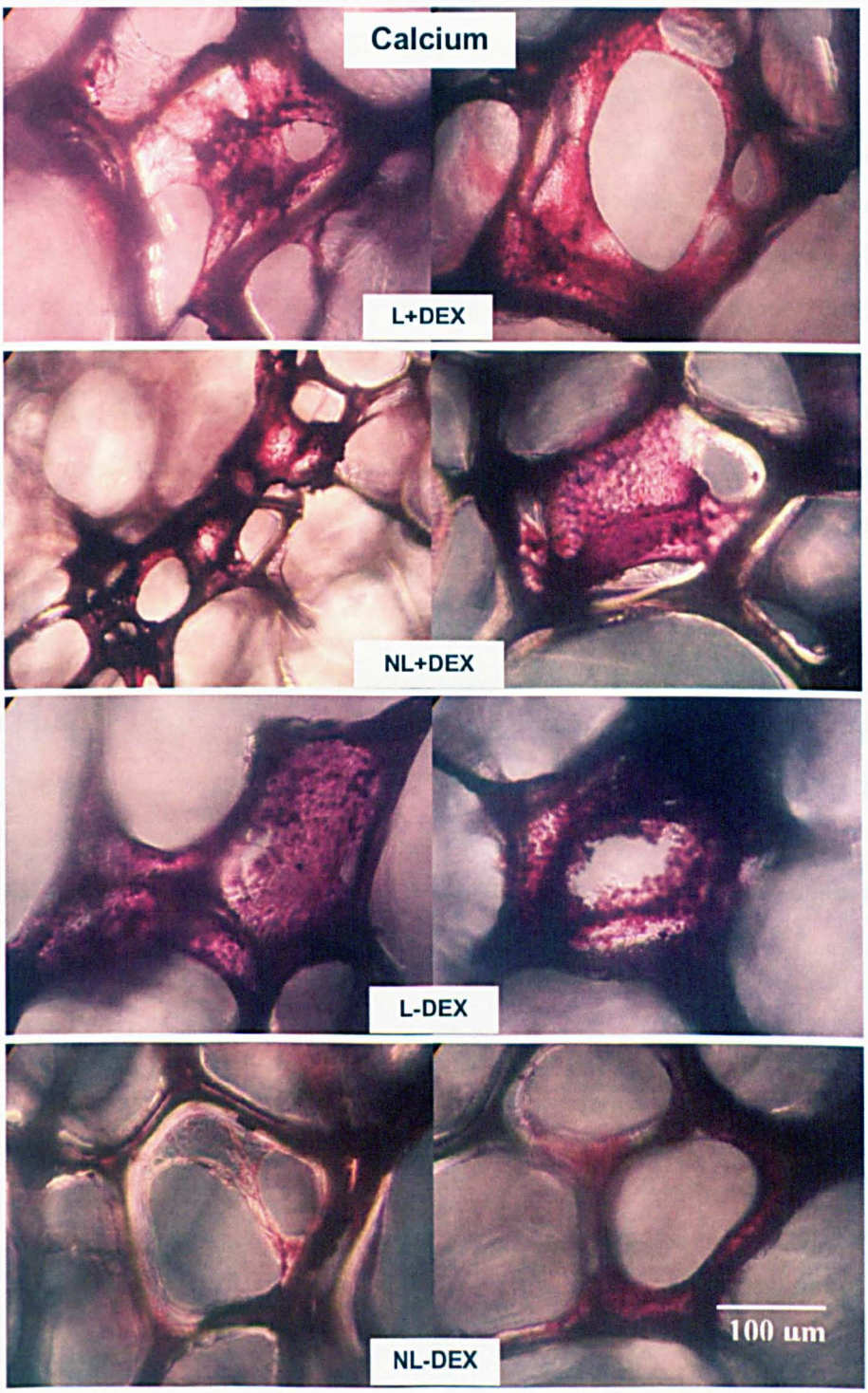

***Fig. 6.8**: Light micrographs of random areas of scaffolds stained by Alizarin red at the end of the experiment. The amount of calcium in scaffold appeared higher all treatment groups with either loading or DEX or both compared to non-loaded without DEX.*

The differences in collagen and calcium per scaffold between individual donors are shown in *Fig. 6.9*. When the data were combined, there was no difference in the amount of collagen and calcium produced in the non-loaded group supplemented with DEX and the loaded group without DEX (two sample t-test) *(Fig. 6.10)*. All values of collagen and calcium per viable cell were normalized within each donor group to the non-loaded without DEX data to reduce the variation between individual experiments. A two-way ANOVA analysis of this normalised data showed that collagen and calcium production were significantly different with loading or DEX treatment compared to non-loading or no DEX treatment *(Fig. 6.11)*. Although the combination of loading and DEX led to significant additive effects with a greater amount of collagen and calcium production than other groups, statistical analysis using two-way ANOVA showed no significant interaction between loading and DEX groups, suggesting that the two effects are independent.

mRNA expression using semiquantitative RT-PCR of OPN, COL1, RUNX2 and ALP 12hrs after a single 2hr bout of loading or control treatment showed that COL1 expression upregulated significantly after loading whereas OPN, RUNX2 and ALP upregulated significantly after DEX treatment compared to non-loading or no DEX treatment. There is no interaction between the effects of loading and DEX as measured by band density relative to GAPDH. (Two-way ANOVA, N=3) *(Fig. 6.12)*.

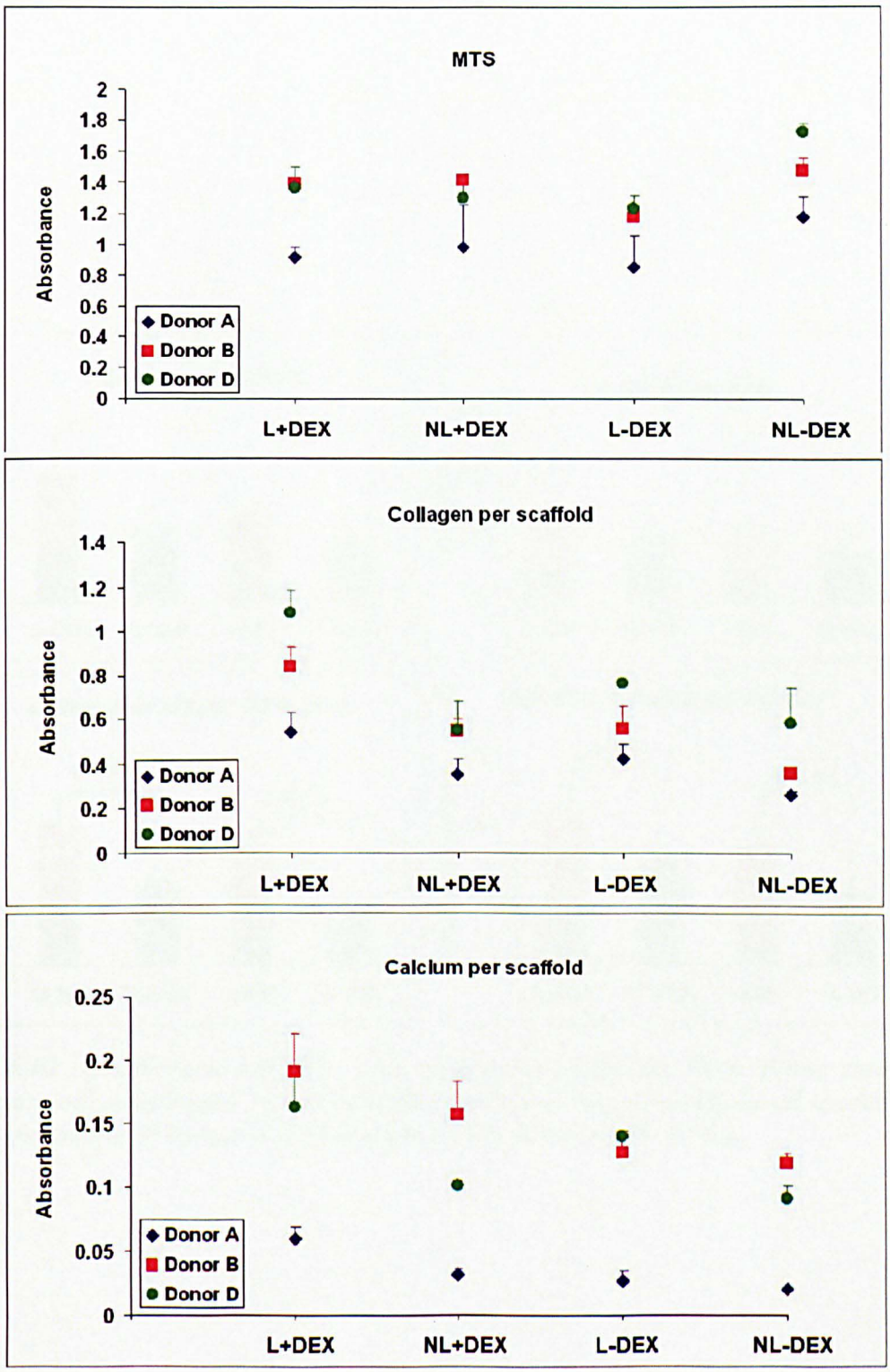

***Fig. 6.9**: Cell viability, total collagen and total calcium content per scaffold. Differences between individual donors were shown. Calcium deposition was more variable than collagen production. (N=2 per donor).*

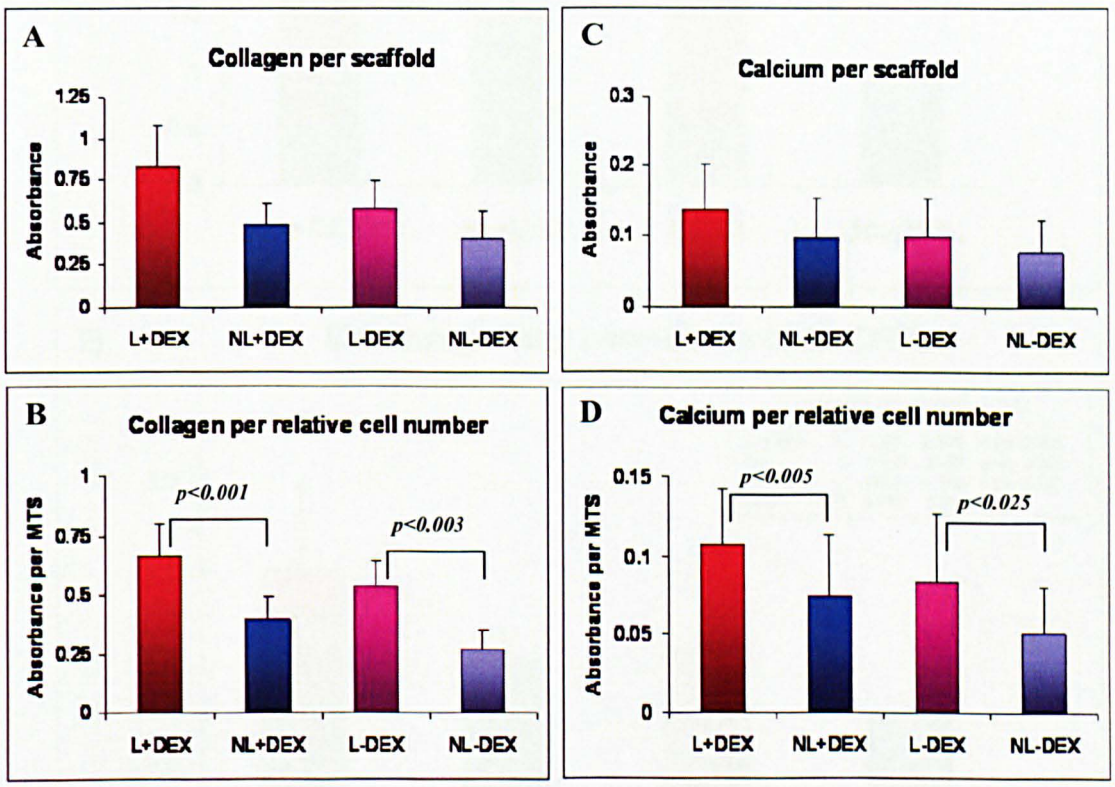

***Fig. 6.10**: Quantitative collagen and calcium in scaffolds. Data shows that collagen and calcium per viable cells (B,D) increased significantly in all loaded samples compared to non-loaded (paired t-test). (Mean ± SD, N=6.).*

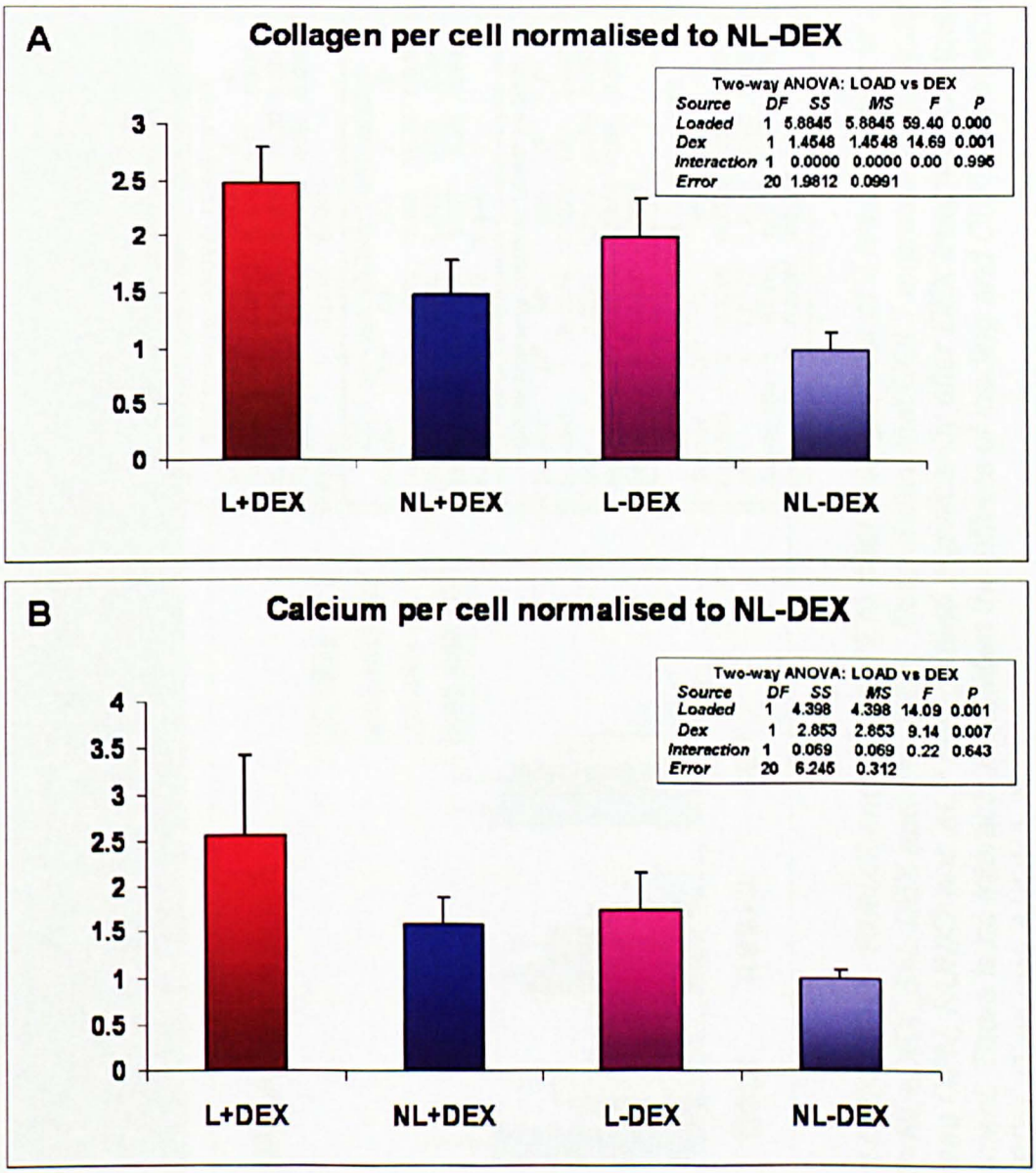

***Fig. 6.11**: Collagen and calcium per viable cell normalized to non-loaded samples supplemented with no DEX. Data shows that production increased significantly after loading or DEX treatment compared to non-loading or no DEX treatment, but there is no interaction between the effects of loading and DEX (mean ± SD, N=6, two-way ANOVA).*

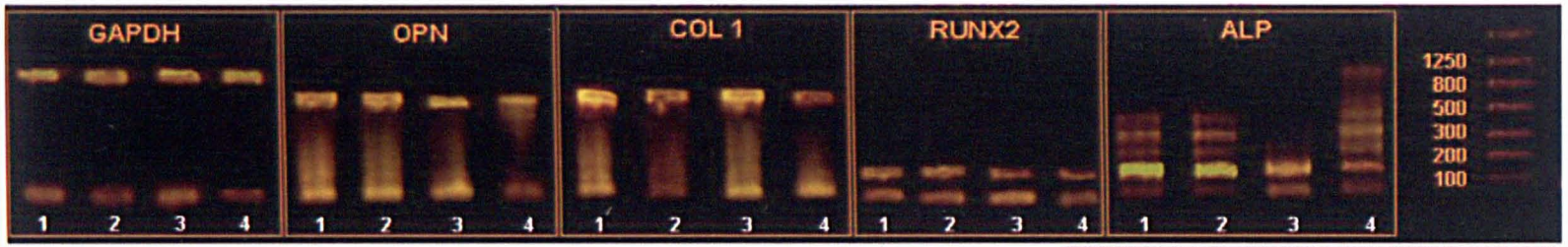

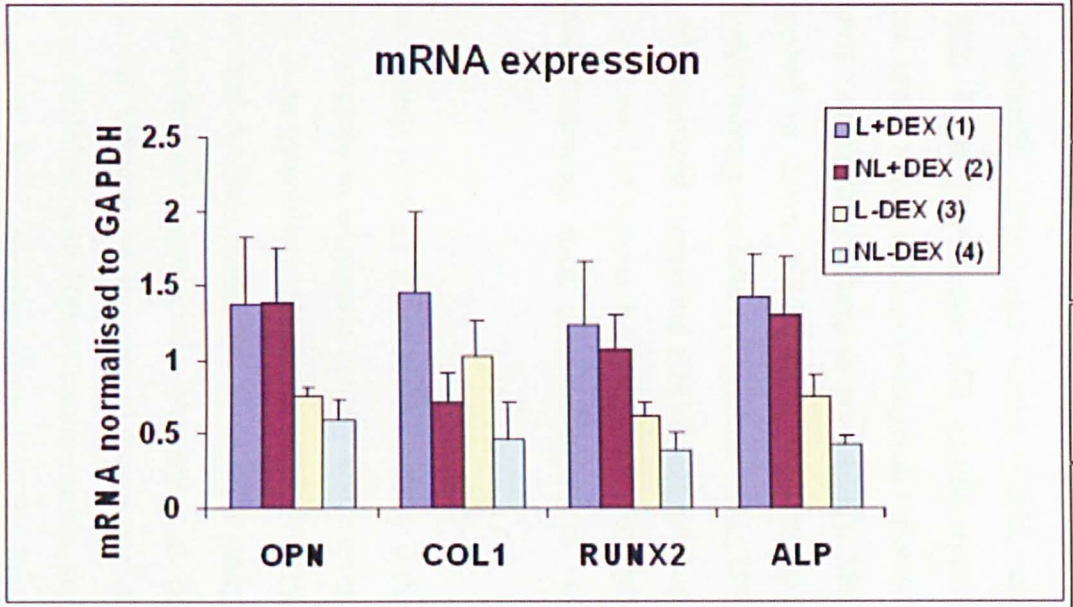

OPN two-way ANOVA: LOAD vs DEX

Source	DF	SS	MS	F	P
Loaded	1	0.0153	0.0153	0.17	0.695
Dex	1	1.5077	1.5077	16.32	0.004
Interaction	1	0.0219	0.0219	0.24	0.639
Error	8	0.7393	0.0924		

COL1 two-way ANOVA: LOAD vs DEX

Source	DF	SS	MS	F	P
Loaded	1	1.285	1.285	11.27	0.010
Dex	1	0.344	0.344	3.02	0.120
Interaction	1	0.027	0.027	0.23	0.642
Error	8	0.912	0.114		

RUNX2 two-way ANOVA: LOAD vs DEX

Source	DF	SS	MS	F	P
Loaded	1	0.1075	0.1075	1.61	0.240
Dex	1	1.2946	1.2946	19.36	0.002
Interaction	1	0.0043	0.0043	0.06	0.807
Error	8	0.5350	0.0669		

ALP two-way ANOVA: LOAD vs DEX

Source	DF	SS	MS	F	P
Loaded	1	0.1405	0.1405	2.09	0.187
Dex	1	1.7973	1.7973	26.68	0.001
Interaction	1	0.0314	0.0314	0.47	0.514
Error	8	0.5388	0.0674		

***Fig. 6.12**: mRNA expression of OPN, COL1, RUNX2 and ALP at 12 hr after a single bout of 2 hrs of loading or control treatment (1=L+DEX, 2=NL+DEX, 3=L-DEX and 4=L-DEX). Data shows that COL1 expression upregulated significantly after loading whereas OPN, RUNX2 and ALP upregulated significantly after DEX treatment compared to non-loading or no DEX treatment. There is no interaction between the effects of loading and DEX as measured by band density relative to GAPDH. (Two-way ANOVA, N=3)*

6.4 Discussion

This chapter presented a novel, *in vitro* 3-D static culture model capable of stimulating hMSCs mechanically within PU scaffolds. It also demonstrated that mechanical loading in this model has the ability to promote osteogenic differentiation of bone marrow derived hMSCs, even when cultured in the absence of dexamethansone.

Osteogenic differentiation of MSCs

Most previous studies have shown that protein-based cytokines, growth factors and extracellular matrix proteins such as BMP [283, 293], Interleukin-6 [294], Laminin-5 [53], as well as non-protein-based chemical compounds like Dexamethasone (DEX) [283], Vitamin D (Calcitriol) [295] and statins [296], can induce osteogenic differentiation of MSCs. There is evidence that undifferentiated hMSCs are highly sensitive to mechanical strain, which induces osteogenic differentiation by upregulating gene expression of early osteogenic markers *in vitro* [297]. Moreover, other physical stimuli have been applied to direct MSCs along the osteogenic lineage, including electrical fields [298], electromagnetic fields [43], ultrasound [299] and heat [39]. In the present study, a non-protein-based compound (DEX) and mechanical stimulus (dynamic compressive loading) were used to induce the osteogenesis of hMSCs. DEX was chosen because it is the most commonly used chemical agent *in vitro* to induce hMSCs differentiation.

ALP has been widely used as a marker of MSCs differentiation toward the osteogenic lineage, as increases in enzymatic activity and expression of both the gene and protein correspond to an osteoblastic phenotype [216, 300-302]. It peaks during the matrix formation phase and declines thereafter, while OPN and OCN peak in the late maturation or early mineralization phases [303]. Mauney et al. (2004) have shown that ALP activity *in vitro* was elevated by mechanical forces for cells cultured in 10nM DEX, but this effect was abolished with 100nM concentration, suggesting that DEX can inhibit this mechanism at high concentrations [302]. For this reason, 10nM concentration of DEX was chosen for use in the present study to optimize the effects of mechanical loading. This chapter tested the hypothesis that mechanical forces (short bouts of dynamic compressive loading) can induce osteogenic differentiation of hMSCs

in the same way as chemical treatment (DEX). The hypothesis was tested by monitoring ALP activity, gene expression of osteogenic markers, matrix production and mineralization. Interestingly, the effect on ALP activity in samples subjected to only loading without DEX was the same as in samples treated with only DEX. This result suggests that mechanical loading has the potential to induce osteogenic differentiation of hMSCs, and could be used as a substitute for or alongside DEX treatment.

Scaffold materials

Although there is limited use of PU scaffolds in tissue engineering due to their lack of biodegradation during long-term *in vivo* culture [178], they were chosen for use in the present study because of their elasticity, resiliency and stiffness. This allows them to withstand *in vitro* mechanical loading, while at the same time being highly reproducible and cost-effective. It was shown in the previous study that these PU scaffolds are biocompatible with MLO-A5 mouse osteoblastic cells [304]. Therefore, it was predicted that this scaffold could be a good support for MSCs. In addition, Zanetta et al (2008) have reported that PU foams can support cell adhesion and proliferation *in vitro*, sustaining MSC growth and differentiation into osteoblastic cells by observing CaP deposition in static culture [177].

Mechanical stimulation of MSCs

Mechanical loading has been shown previously to play an important role in bone formation *in vivo* by inducing osteoprogenitor cells in the marrow stroma to differentiate into osteoblasts at the cortical bone surface [290]. Arnsdorf et al (2009) have shown in a 2-D study that oscillatory fluid flow induces the upregulation of Runx2, Sox9 and PPARgamma, transcription factors involved in the osteogenic differentiation pathways of MSCs. In addition, Simmons et al (2003) and Diederichs et al (2008) have shown that 2-D cyclic strain on hMSCs seeded on silicone rubber upregulated gene expression of collagen type I and III [240], activated the extracellular signal-regulated kinase (ERK 1/2) and increased calcium deposition [21]. In tissue engineering, previous 3-D studies of dynamic culture with MSCs, using continuous flow perfusion bioreactors, have shown the upregulation of mineralised matrix deposition *(Table 6.2)* [84, 216]. The initial aim of these bioreactors was to distribute

nutrients, but a secondary effect would be the application of a fluid flow stimulus. Several 3-D studies have also demonstrated that short periods of strain applied to human bone marrow-derived MSC-seeded scaffolds induce mRNA expression and osteogenic differentiation marker level responses, e.g. tensile loading [149, 305], and 4 point bending [138] as summarized briefly in *Table 6.2*.

These results, together with the present study, suggest that mechanical stimuli play a crucial role in modulating both the osteogenic differentiation process of MSCs and their matrix maturation, including matrix production and mineralization, both *in vitro* and *in vivo*. Interestingly, Sumanasinghe et al (2006) have shown that cyclic strain can induce osteogenic differentiation of bone marrow-derived hMSCs in 3-D collagen matrices without the addition of osteogenic supplements [149]. They used a high strain rate (4 hr loading per day of 10% or 12% strain) to stimulate cells each day for 7 or 14 days, and demonstrated upregulation of BMP-2 gene expression. However, there is no investigation of long-term matrix production in the study. To my knowledge, this is the first time that a comparison of the effects of pharmaceutical agents and intermittent short bouts of dynamic compressive loading, in long-term culture up to 24 days, on osteogenic differentiation, matrix production and mineralization in 3-D has been reported.

Beresford et al. (1992) have shown that DEX can inhibit expression of collagen type I (COL1) and enhance maturation of adipocytes in culture [289]. Although we do not show inhibition of COL1 mRNA expression in our study, its Upregulation is much less than others *(Fig. 6.12)*. However, dynamic compressive loading can upregulate gene expression of COL1 significantly compared to non-loaded samples (about 2 fold). This suggests that mechanical loading could be used to stimulate collagen synthesis in situation where DEX has no effect or negative controls and could help to induce matrix production.

RUNX2 (also called Cbfa1) gene expression was performed in this study as it is specific to the early differentiation of MSCs into the osteogenic lineage, and is a modulator of bone formation by fully differentiated osteoblasts [306]. The present study showed altered levels of RUNX2 between the DEX and the non-DEX treated groups (higher in DEX treated samples), with a smaller effect on these markers between loaded

and non-loaded groups *(Fig. 6.12)*. This is interesting data which may indicate that DEX plays a more crucial role than mechanical stimulation in the early stage of osteogenic differentiation.

***Table 6.2**: A table of various studies on human bone marrow-derived MSCs showing responses of cells to mechanical loading in 3-D environments.*

Group	Type of stimulation	Culture period	Outcome
Cartmell et al. (2003) [133]	Flow perfusion on cell-seeded human trabecular bone scaffold (continuous, flow rates 0.2 ml/min)	7 days	-Upregulation of RUNX2, OCN, ALP mRNA expression
Muaney et al. (2004) [138]	4-point blending on cell-seeded demineralised bone matrix (*intermittent*, about 3% strain with rate 5mm/min for 250 cycles per day).	16 days	-Increase of ALP activity
Datta et al (2005) [84]	Flow perfusion induced fluid shear stress on cell-seeded titanium fiber mesh scaffold (*continuous*, flow rate 1.0 ml/min).	16 days	-Increase of calcium content
Sumanasinghe et al. (2006) [149]	Uniaxial cyclic tensile strain on cell-seeded collagen gel (*intermittent*, 10% and 12% strain, 4 hr per day everyday).	14 days	-Upregulation of BMP-2 gene expression
Byrne et al. (2008) [305]	Uniaxial cyclic tensile strain on cell-seeded collagen-glycosaminoglycan scaffold (*intermittent*, 5% strain for 4 hr per day on day 5, 6 and 7 of culture).	7 days	-Upregulation of OPN gene expression
Grayson et al. (2008) [216]	Medium flow induced shear stress on cell-seeded decellularized bone matrix (*continuous*, flow rate 0.85 ± 0.01 mL/s , 0.7-10 mPa).	35 days	- Greater bone volume by μCT - Increasing of total protein, ALP, BSP and OPN
Sittichockechaiwut et al. (2009) (Current results)	Cyclic dynamic compressive strain on cell-seeded polyurethane scaffold (*intermittent*, 5% strain for 2 hr per day every 5 days)	24 days	-Upregulation of ALP and COL1 gene expression - Increase of collagen and calcium content

Matrix production and mineralization

The results demonstrated that gene expression levels of collagen type I and ALP at 12 hrs after the first bout of loading paralleled the responses obtained for collagen and calcium production following 24 days of cultivation. Collagen and calcium production were significantly increased in mechanically stimulated MSCs (about 250% with DEX and 200% without DEX) when compared to non-loaded samples with no DEX *(Fig. 6.10)*. In contrast, samples treated with DEX only (no loading) displayed no significant difference in collagen and calcium production when compared to samples subjected to loading only (no DEX). This indicates that matrix synthesis and mineralization can be elevated by mechanical stimulation independent of DEX. Interestingly, the amount of collagen and calcium produced showed a significantly greater increase when loading and DEX treatment were combined, demonstrating an additive effect of the two stimuli.

Differences in stem cells obtained from different donors are also an important factor for tissue engineering and clinical applications which needs to be addressed. In these experiments, the effects of stimuli on hMSC differentiation and production follow the same trend in individual experiments, even allowing for differences between donors. However, some research has shown no consistent effects on hMSCs between different donors [167]. This suggests that the incorporation of short bouts of dynamic loading within 3-D culture may be a tool to promote osteogenic differentiation of MSCs, in combination with pharmacological agents. However, the combination of biologically active and mechanical factors needs to be carefully optimized for clinical implantation of engineered bone tissue.

Bone tissue engineering strategies

For bone tissue engineering, conventional tissue culture and cultivation methods in 2-D limit the clinical application of these cells as sufficient bulk matrix cannot be produced for implantation. Therefore, many tissue engineering strategies have been developed to culture cells in 3-D. Many previous studies have demonstrated that pre-induced osseointegration of MSC-seeded scaffolds, once implanted *in vivo,* accelerates bone defect repair by delivering a more mature osteogenic population capable of

immediate bone formation [284, 307, 308]. Yoshikawa et al. (1997) have shown that precultivation of MSC-seeded hydroxyapatite scaffolds in the presence of chemical osteogenic conditions (including dexamethasone, AA and βGP) before implantation increased the rate of osteogenesis and level of osteogenic markers of those MSCs *in vivo* [284]. Some researches believe that undifferentiatied MSCs can be seeded *in vivo*, although this may cause problems of unwanted tissue formation (for example fat tissue where bone is required). Therefore, pre-differentiation may provide a better tissue engineering strategy for clinical implantation.

Other strategies of pre-culture, including various bioreactor systems which provide primarily nutrient distribution and secondarily mechanical stimuli, have also been reported as methods for improving *in vitro* culture conditions. The aim is to promote the proliferation and osteogenic differentiation of MSC-seeded constructs before implantation, resulting in improved structure and function of the engineered bone tissue [21, 75, 138, 149, 253, 278, 279]. In the present study, it was shown that the osteogenic differentiation, matrix production and mineralization of hMSCs can be induced by short bouts of mechanical stimulus, rather than improving the nutrient distribution as in continuous flow bioreactor culture systems. However, if a less porous or larger scaffold were used, continuous perfusion may be needed to maintain cell viability in the centre of the scaffold, even when short bouts of loading are introduced.

The mechanism of osteogenic differentiation is complicated and still unclear. Understanding the mechanisms by which DEX and loading induce differentiation in human MSCs is beyond the scope of this work, which focuses on a technique to achieve osteogenic differentiation. However, Jaiswal et al. (2000) have proposed that one of the potential signal transduction pathways which may direct the differentiation of hMSCs is the mitogen-activated protein kinase (MAPK) pathway [309]. Extracellular signal-related kinase (ERK), a member of MAPK family, stimulates the differentiation of hMSC into osteoblasts via phosphorylation of the osteogenic transcription factor RUNX2/Cbfa1 [53, 309].

This study has shown that a combination of cyclic compressive loading and resting periods can improve engineered bone constructs *in vitro*. This is demonstrated by upregulation of the expression of osteogenic genes and alkaline phosphatase activity

in hMSCs, as well as increasing bone like matrix production of osteoblast-derived hMSCs, even in the absence of dexamethasone. The data suggests that a mechanical stimulus is an additional or alternative tool for establishing precultivation conditions prior to clinical implantation of tissue engineered bone, which has implications in the design of mechanical loading regimens in bioreactor culture.

6.5 Summary

- This is the first time that the effects of DEX, the standard osteogenesis stimulator, have been compared to intermittent short bouts of dynamic compressive loadings during long-term culture (up to 24 days, 3 bouts of 2 hr loading with 5% strain). Effects on osteogenic differentiation, matrix production and mineralization in 3-D were studied.
- The novel PU was shown to have sufficient properties to deal with *in vitro* mechanical loading. It was also shown to have biocompatibility with human bone marrow-derived MSCs.
- The *in vitro* 3-D static culture model developed is capable of stimulating hMSCs mechanically within novel PU scaffolds, and is able to promote osteogenic differentiation of bone marrow derived hMSCs when cultured in the absence of DEX.
- A combination of short bouts of dynamic compressive loading, which induces fluid flow in the scaffold, and several days of resting periods can improve engineered bone constructs *in vitro*. This is demonstrated by upregulation of gene expression of osteogenic differentiation, alkaline phosphatase activity of hMSCs, and increasing bone-like matrix production of osteoblasts derived from hMSCs in the same way as chemical treatment (DEX). It could be used as a substitute for DEX treatment or incorporation with DEX. The incorporation of short bouts of dynamic compressive loading and DEX treatment within this system may be a key mechanism for promoting osteogenic differentiation of MSCs in bioreactors.
- DEX appears to have an effect in the early stages of osteogenic differentiation. In contrast, loading seems to play an important role on matrix production of cells, including collagen synthesis, and could help to prevent the adverse effects of DEX on collagen synthesis.
- Dynamic compressive loading could be an additional or alternative tool for establishing precultivation conditions for clinical implantation.

CHAPTER SEVEN: Conclusions and future work

7.1 3-D model for bone tissue engineering

Recent developments in tissue engineering reviewed by Cancedda et al. (2007) [310] have highlighted the need for an understanding of how immature/ developing bone responds to mechanical load. Bone tissue engineering is usually performed with a single cell type, most commonly bone marrow derived mesenchymal stem cells (MSCs) or an osteoblastic cell line as a model system. Many researchers have shown that MSCs and osteoblasts produce mineralised ECM when cultured in three dimensional scaffolds and that mineralisation is improved by the application of mechanical forces to the growing cell/scaffold constructs using bioreactor culture [161, 278, 311, 312]. We optimised a system in which dynamic and static cultures are combined to optimize cell viability and bone matrix production. The model system can apply a large range of strains, strain rates, frequencies and loading durations to a cell-seeded highly reproducible industrially produced scaffold.

We showed that MLO-A5 rapidly mineralising osteoblasts are mechanosensitive and respond to loading regimens inserted into a static culture period with marked increases in matrix production, maturation and mineralization. This method in which osteoid-like matrix is grown in 3-D culture in a mechanically controllable environment should be a useful tool for investigations on bone mechanotransduction and optimisation of mechanical loading regimens for tissue engineering, fracture repair and implant integration.

However, further investigations of factors that affect the dynamic culture of the cells such as distribution of strain, including local (cell level) strain and force throughout scaffold, and other parameters to be used are needed to optimize overall engineered bone tissue. Although the effects of substrate strain and fluid shear stress have been investigated separately, mostly using 2-D substrates [37, 63, 94], it is very difficult to evaluate the contribution of each mechanical input within bioreactors in which it is difficult to separate both substrate strain and fluid shear stress from each.

One limitation of our system is the size of the biodynamic chamber. The amount of media used in the biodynamic chamber is at least 200 ml to cover a cell-seeded scaffold during mechanical stimulation. Therefore, detection of signalling factors released into the media such as PGE_2 and Nitric oxide was very difficult because of high dilution of the biochemical agent in the media. In addition, it increases the cost of an experiment and is complicated to use in an incubator. A smaller chamber could solve this problem.

7.2 Mechanical stimulation for bone tissue engineering

We showed that MLO-A5 osteoblastic cells *in vitro* can survive and proliferate well in a 3-D interconnected porous PU scaffolds and respond to compressive mechanical stimulation by increasing collagen matrix production and construct stiffness. Future studies are needed to investigate cell function, cell differentiation, and bone matrix formation in response to different mechanical strain rates, frequencies and stimulation by using the same model system. In the future these studies will be modified to enhance human MSCs growth, proliferation and differentiation to improve the length of time required to grow the tissue *in vitro* before implantation and to create stronger tissue that is adapted to mechanical loads by using mechanical stimulation in 3-D.

The model system we developed will be useful for further mechanotransduction studies *in vitro*. It provides good conditions to study short term effects of mechanical loading in 3-D tissue constructs. For further study or longer culture, additional techniques such as long-term, integrated bioreactor culture system might be required to optimize the differentiation of the cells and development of functional extracellular matrix and mineralization.

7.3 The mechanisms by which cells sense and respond to loading.

Mechanotransduction plays an important role in bone. The process of mechanotransduction can be divided into 3 steps.

7.3.1 Mechanocoupling

Mechanical loads in vivo cause deformations in bone and create fluid movement within the canaliculae, pumping nutrients to the osteocytes and creating fluid shear stresses on osteocyte's cell membranes [267]. Dynamic loading, associated with extracellular fluid flow and the streaming potentials within bone, is believed to be the most effective for stimulating new bone formation *in vivo* [56]. Although dynamic mechanical loading used in our system can generate strain and fluid flow induced shear stress within cell-seeded scaffolds, it is still unclear which type of stimulus causes a more significant effect on the bone cells in our studies.

7.3.2 Biochemical coupling

Although the mechanism for conversion of mechanical forces into biomechanical signals has yet to be determined, serveral likely candiates have been proposed. One possible pathway is the ECM-integrin-cytoskeletol axis [312]. Cells attach to ECM by binding to integrins and integrins attach to the actin cytoskeleton. Due to the cytoskeleton network connecting to the extracellular matrix, mechanical stimulus would be rapidly transmitted to the nucleus, possibly altering gene expression in our studies. In addition, mechanical strain may alter cell shape and cytoskeletal organization.

Since Guharay et al. (1984) have reported that ion channel can be gated by mechanical strain [313], this is likely another candidate mechanism in our studies. Alteration in ion channel activity in osteoblasts have been associated with bone cell activation by mechanical stimuli including strain and stress [314]. Walker et al. (2000) have also reported that osteoblasts experienced a large transient increase in intracellular calcium upon application of strain and increased levels of the extracellular matrix proteins osteopontin and osteocalcin within 24 h postload [315]. These data suggest that increase of intracellular calcium through activation of channels may be the initial cellular signal for osteoblastic response to mechanical strain.

7.3.3 Transmission of biochemical signal

Bone cells have been shown to respond to mechanical strain with increased levels of second messengers including intracellular calcium [315], cyclic AMP and inositol phosphates [65], ALP and insulin-like growth factor I [316]. There are 2 possible pathways by which a biochemical signal in the sensor cell is propagated to the effector cell to increase osteogenic activity and matrix production after a mechanical loading in our studies. Firstly, Osteoblasts can sense and also act as effectors of mechanical signals and may communicate the signal through cell processes connected by gap junctions. The other pathway for intercellular communication is paracrine factors to signal the effector cell to increase cell activity [57].

7.4 Primary cilia of bone cells

It is still unclear how the primary cilia of bone cells transmit external mechanical information to the inside of the cell and how they interact with the mineralized matrix of bone. We are now looking at how the primary cilia might function together with other demonstrated mechanosensors e.g. glycolalyx (the proteoglycan cell coat) in our lab. The mechanical stimulus that the primary cilia receive could be converted across their membrane and the plasma membrane of cells into a chemical signal that prompts a cellular response such as cytokine release or a change in gene expression. The data in chapter 5 support our hypothesis that both oscillatory fluid flow induced shear stress and cyclic dynamic compression can mediate mechanosensation in MLO-A5 osteoblatic cells via the primary cilium. Given the extent of matrix production around the cells (shown in SEM images in chapter 4) it seems that cells are more embedded in their own matrix in 3-D rather than located freely in a 2-D environment. We propose that the deflection of primary cilia by strain transmitted through the extra cellular matrix (ECM) or deformation of the ECM allows it to act as a mechanosensor suggesting that the primary cilia may be an important mechanism to induce bone formation during 3-D dynamic bone tissue engineering.

Future work on primary cilia should focus on (i) optimizing the siRNA transfection technique, (ii) looking at the orientation of primary cillia in a 3-D environment and their interactions with mineralized matrices before and after dynamic

loading condition, and (iii) studying whether extracellular stimuli perceived by primary cilia lead to changes in cell behavior and physiology. Although the primary cilia are can not be indentified with conventional light microscopy because of optical interference from ECM, fluorescent immunohistochemical labeling could allow us to visualize primary cilia and their interaction with the ECM. In addition, the 3-D model I developed *in vitro* could be used to investigate the structural relationship between the ECM and primary cilia. It also would be interesting to examine the specific expression of ECM receptors such as the integrin subunit β1 on the surface of primary cilia of bone cells. Integrin subunit β1 is a common transmembrane glycoproteins of most matrix-binding integrins. The functions of integrins are to mediate cell adhesion to ECM and to act as receptors, transducing signals from the cell surface to the cytoplasm [317]. Although it has been shown in a chondrocyte study that integrins help anchor the cilium to the mechanically functional collagen fibers within the ECM of cartilage [105], there is no report, to my knowledge, of the relationship between integrins, other ECM receptors and the primary cilia in bone. Furthermore, to understand the role of the cilia in mechanosensing during bone tissue engineering, the primary cilium of hMSCs and how it developes during osteogenic differentiation needs to be investigated.

7.5 Mesenchymal stem cells for bone tissue engineering

Osteogenic differentiation of stem cells *in vitro* could be enhanced by using a combination of various techniques such as protein and non-protein based compounds, physical stimuli or co-culture with osteoblasts [20, 142]. I showed that the combination of mechanical force (short bouts of cyclic compressive loading) and a chemical compound (DEX) can induce more effective stimulation of osteogenic differentiation than either stimulus alone. However, this bioreactor system is able to stimulate only a single 3-D tissue construct at a given time. To scale up the engineering of bone tissue constructs, the development of a multi-chamber bioreactor system that is easy to use, needs to be considered such as the novel 4-chamber system available from Bose *(Fig. 7.1)*.

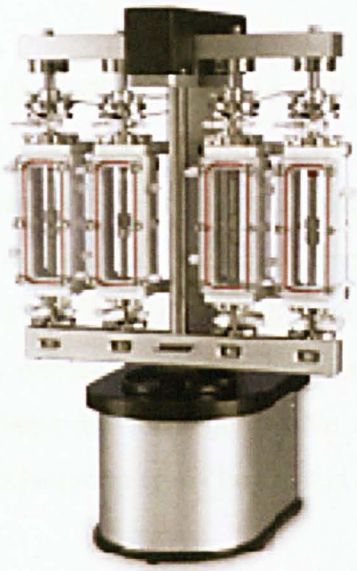

***Fig. 7.1**: The multi-chamber bioreactor system provided by BOSE Electroforce.*

Although we showed that some osteogenic markers were elevated in this study, furthur investigations of osteogenic differentiation of MSCs such as surface antigens, cytokines, and the expression of other early genes is still needed to confirm the existence of differentiated osteoblasts. In addition, histological and other methods (such as mineral analysis by FTIR) are needed to understand the structure and mechanical properties of the engineered bone tissue.

Scaffold material is an important key factor in bone tissue engineering. Some scaffold materials such as titanium [318], ceramic [319], and hydroxyapatite [284] have been demonstrated to enhance osteogenic differentiation of MSCs by accelerating bone formation and osteointegration when used for bone repair *in vivo*. However, the novel PU scaffolds used in our study have never been investigated for these effects before. There is no evidence in the literature to suggest that polyurethane has any bioactive properties, the benefit of using this scaffold probably comes from their high porosity, allowing better nutrient distribution than many other scaffolds. A parallel study comparing this scaffold with other scaffold materials would help to confirm whether the osteogenic differentiation effects in the present study come from only a combination of mechanical force and dexamethasone or an additive effect of the novel PU scaffold.

7.6 Clinical Applications

A 3-D bone-like matrix is rapidly formed by bone cells in our system, including both primary cells and cell lines. Even if this matrix containing live cells is not implantable, due to risk of disease transmission or immune rejection, it may be useful in forming an *in vitro* decellularised pre-matrix to encourage human cell growth as described by Datta et al. (2006) [84] on titantium foams. Studies such as this also help to inform the debate about how far along the differentiation pathway cells should be, prior to implantation for regenerative medicine [15], supporting the idea that bone matrix for implantation could be created *in vitro* using pre-differentiated, mature cells.

For clinical applications of stem cell therapy, minimal use of supplements containing animal or human proteins in *in vitro* culture is required to avoid contamination with pathogens and antigenicity of these proteins when they adhere onto the surface of cultured stem cells [142]. Although, serum-free and synthetic serum media have been introduced to minimize these problems [320], cells generally tend to have a lower proliferation, become apoptotic and show poor adhesion [142, 320]. Therefore, the development of effective culture protocols is still needed for clinical applications of human MSCs.

Bone repair and remodelling *in vivo* are related to the interactions between different cell types (osteoblast, osteocyte and osteoclast) via many proposed complex pathways [4, 8, 25]. Osteoclasts are involved in bone resorption resulting in changes of bone shape and size [8]. In addition, other environmental factors *in vivo* such as hormones, cytokines and systemic disease including diabetes can delay growth of new bone [8, 17, 26, 132, 293]. Little is known about how osteoclasts would respond to tissue engineered bone, but in the future it may be possible to add differentiating osteoclasts to our 3D system to examine their interaction with the newly formed matrix *in vitro*.

Our studies demonstrated that mechanical stimulation can enhance bone formation in a 3D culture system suggesting that the development of tissue engineering bioreactors, which are capable of applying controllable mechanical stimulation, can improve the production of tissue engineered bone. There are still many hurdles to be

overcome before tissue engineered bone can be routinely used clinically. The most successful applications of bone tissue engineering in this decade may be in the development of *in vitro* physiological models for studying the pathogenesis of disease and for developing molecular therapeutics. To reach the goal of the field of tissue engineering - improvement of patient's lives, all of the basic science, biotechnology, surgical technique improvements and clinical procedures need to be integrated. Short and long-term assessment of engineered tissue transplantation as well as cost-effectiveness and availability to patients remain important key factors to assure that the engineered tissue implants offer clinical advantages over the existing alternatives in the future.

7.7 Conclusions

- The 3-D model system we optimized in *chapter 3* is not only intended to inform tissue engineering solutions but could also to provide an important *in vitro* model system for the enhancement of understanding into mechanotransduction, and the relationship between physical conditions, cellular function, tissue development and tissue properties.
- The model system and loading regimens as described in *chapter 4* showed the potential to increase extracellular matrix protein expression, matrix production and mineralization of osteoblstic cells on tissue constructs.
- The methods developed were also used to study the role of primary cilia in mediating mechanically induced increases in bone matrix production in *chapter 5* and it was shown that loaded scaffolds containing cells with presence of primary cilia showed higher levels matrix protein expression compared with non-loaded controls and loaded cells with absence of primary cilia. We suggest that the primary cilium can mediate the matrix-forming response of bone cells to mechanical loading in our 3-D model which has implications for mechanical conditioning in bone tissue engineering.
- Studying the effects of mechanical stimulation on hMSCs for bone tissue engineering in *chapter 6* also showed that combination of short bouts of dynamic compressive loading, which induces fluid flow in the scaffold,

and several days of resting periods can improve engineered bone constructs *in vitro* by upregulation of gene expression of osteogenic differentiation, alkaline phosphatase activity of hMSCs, and increasing bone-like matrix production of osteoblasts derived from hMSCs in the same way as chemical treatment (DEX). This suggests that dynamic compressive loading could be an additional or alternative tool for establishing precultivation conditions for clinical implantation.

APPENDIX 1

Conferences

1. 7th Annual White Rose Tissue engineering Meeting, The University of Sheffield, UK, 21st December 2005.
2. BOSE Electroforce System user meeting, The National Physical Laboratory (NPL), London, UK 12th June 2008.
3. Tissue and Cell Engineering Society Annual Meeting (TCES), Nottingham University, UK, 2nd-4th July 2008

Oral presentations

1. BOSE Electroforce System user meeting: "Mechanical Stimulation of Bone Cells for Tissue Engineering", The University of Birmingham, UK, 8th June 2006.
2. 5th World Congress of Biomechanics (WCB): "A 3-D model for mechanical manipulation of tissue engineered bone, using Polyurethane foam and osteoblastic MLO-A5 cells", Munich, Germany, 29th July – 4th August 2006
3. 8th Annual White Rose Tissue engineering Meeting: "Osteoblastic cells response to compressive loading in 3-dimensional scaffolds: the effects of varying loading and culture periods", University of York, UK, 18th December 2006
4. BOSE Electroforce System user meeting: "Using the biodynamic chamber to stimulate bone matrix growth", Stroke-on-Trent, UK, 6th June 2007.
5. 8th international bone fluid flow workshop meeting: "The effects of varying mechanical loading regimens on collagen production by MLO-A5, late-stage osteoblasts", Stony Brook State University of New York, New York City, USA, 13th -14th September 2007.
6. Center for Biomaterials and Tissue Engineering: "Understanding how mechanical conditioning stimulates tissue engineered bone formation: a

potential role for primary cilia", Kroto Research Institute, University of Sheffield, UK, 19th January 2008.

7. 9th international bone fluid flow workshop meeting: "Oscillatory Fluid Flow mediates Mechanosensation in MLO-A5 Osteoblatic Cells via the Primary Cilium", Vrije Universiteit, Amsterdam, Netherland, 22nd-23rd May 2008.
8. The Tissue Engineering and Regenerative Medicine International Society European 2008 meeting (TERMIS-EU), "Oscillatory fluid flow (OFF) induced shear stress increased bone matrix production: The potential of primary cilia mediate mechanosensing for bone engineered tissue" Porto Conogress Center-Alfandegar, Porto, Portugal, 22nd-26th June 2008.
9. 10th Annual White Rose Biomaterials & Tissue Engineering Group Work in Progress Meeting, "Use of dynamic compressive loading to stimulate human mesenchymal stem cells (hMSCs) differentiation and matrix production in bone tissue engineering.", The Kroto Research Institute, University of Sheffield, UK, 18th December 2008

Poster presentations

1. Tissue and Cell Engineering Society Annual Meeting (TCES): "A 3-Dimensional, in vitro Model to Study the Effects of Compressive Loading on Osteoblastic Cells" The University of Sheffield, UK, 3rd -4th July 2006.
2. Bone Research Society and British Orthopedics society (BRS-BORS): " The Effects of Dynamic Compressive Loading on Osteoblastic cells in 3-Dimensional Scaffolds", University of Southampton 5th -6th July 2006.
3. American society of bone and mineral research (ASBMR) conference: "The Effects of Compressive Loading on Matrix Production by Osteoblastic Cells Cultured in Polyurethane Scaffolds", Hawaii Convention Center, Hawaii, USA,16th-19th September 2007.
4. American society of bone and mineral research (ASBMR) conference: "Collagen and Osteopontin Upregulation by Mechanical Loading of Bone Cells in Porous 3D scaffolds", Hawaii Convention Center, Hawaii, USA,16th-19th September 2007.

5. 3rd UK Mesenchymal Stem Cell Meeting, "Use of dynamic compressive loading to stimulate human mesenchymal stem cells (hMSCs) differentiation and matrix production in bone tissue engineering.", The Octagon Centre, University of Sheffield, UK, 8th January 2009.

Training and research scholars

1. Bioreactor Design and Stem Cell Processing Workshop, Co-organised by Keele University and The University of Sheffield, Buxton, 18th - 22nd June 2006.
2. IRC Modules Course in Polymer Science, The University of Sheffield, UK., 30th October 2006.
3. Excellence Exchange Scheme research scholar to do research at the Cell and Molecular Biomechanics Laboratory (CMBL), Department of Biomechanical Engineering, Stanford University, USA, 15th September - 15th December 2007.

Awards

1. Travel grant from the Royal Thai Government, Thailand, £450
2. Excellence Exchange Scheme from The University of Sheffield, £2,225
3. Young investigator travel grant from 8th international bone fluid flow workshop, USA, $500.
4. Travel grant from Tissue and Cell Engineering Society (TCES), UK, £100.
5. Young investigator travel grant from the American Society of Bone and Mineral Research (ASBMR), USA, $400.
6. Travel grant from Learned society, The University of Sheffield, £350
7. Travel grant from Department of Engineering materials, The University of Sheffield, £350
8. **Best 50 abstracts** awards from The Tissue Engineering and Regenerative Medicine International Society European 2008 meeting (TERMIS-EU), "Oscillatory fluid flow (OFF) induced shear stress increased bone matrix production: The potential of primary cilia mediate mechanosensing for bone

engineered tissue" Porto Conogress Center-Alfandegar, Porto, Portugal, 22nd-26th June 2008.

9. **First prize** of oral presentation from 10th Annual White Rose Biomaterials & Tissue Engineering Group Work in Progress Meeting, "Use of dynamic compressive loading to stimulate human mesenchymal stem cells (hMSCs) differentiation and matrix production in bone tissue engineering.", The Kroto Research Institute, University of Sheffield, UK, 18th December 2008.

Publications

1. [Abstract] "Mechanical Stimulation of Osteoblastic Cells in 3-Dimensional Polyurethane foam Scaffolds" in Journal of Bone and Mineral Research (JBMR) Vol 21 Suppl., September 2006 pp. s373.
2. [Abstract] "A 3-Dimensional, in vitro Model to Study the Effects of Compressive Loading on Osteoblastic Cells" in Journal of European cells and materials Vol. 11 suppl.3 2006 p.84.
3. Sittichockechaiwut, A., et al., Use of rapidly mineralizing osteoblasts and short periods of mechanical loading to accelerate matrix maturation in 3D scaffolds. BONE, 2009. 44(5): p. 822-829.

APPENDIX 2

European Cells and Materials Vol. 11. Suppl. 3, 2006 (page 84) ISSN 1473-2262

A 3-dimensional, in vitro model to study the effects of compressive loading on osteoblastic cells.

Anuphan Sittichokechaiwut [1], Anthony J. Ryan [2] and Gwendolen Reilly [1]

[1] Department of Engineering Materials, [2] Department of Chemistry University of Sheffield, UK

INTRODUCTION: Mechanical force is an osteoinductive factor that plays an important role in bone growth and repair in vivo[1]. Our aim was to design a model system by which bone cell responses to mechanical load could be examined in vitro in a 3D environment. Our previous study has shown that osteoblastic cells survive well and proliferate in our polyurethane (PU) open cell foam scaffolds. Cell number after 15 days of culture was four times that after 5 days of culture. Examination of cell distribution, under fluorescence microscopy, showed that cells were clearly adherent and spread out along the sides of the pores of the PU and were seen in the centre of a 25 mm diameter, 10mm high scaffold (*Fig.1*).

Fig 1: Cell distribution on PU scaffold by using Fluorescence microscopy (DAPI staining).

METHODS: MLO-A5 osteoblastic cells were seeded at densities of 250,000 cells per scaffold in cylindrical polyurethane (PU) scaffolds, 10 mm thick and 10 mm diameter. The cell seeded PU scaffolds were dynamically loaded in compression at 1Hz, 5% strain in a sterile fluid-filled chamber (*Fig.2*). Loading was applied for 2 hours per day at days 5, 7 and 9 of culture. Between loading cycles, scaffolds were cultured in an incubator in standard conditions. Cell seeded scaffolds were assayed at day 3 and day 11 for cell proliferation by MTS assay

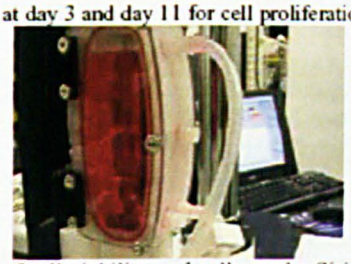

Fig. 2 Bose ElectroForce 3200 with biodynamic chamber

of cell viability and collagen by Sirius red.

RESULTS: Osteoblastic cells survived in loaded scaffold, final cell number was slightly but not significantly lower in loaded samples compared with unloaded at day 11 (*Fig 3*). In contrast, collagen content increased in loaded scaffolds. Microscopy of Sirius red stained scaffolds showed much more staining in the loaded group on day 11 (*Fig 4*). Sirius red quantification indicated that in loaded samples collagen content increased by 66% between days 3 and 11, compared with only 44% in unloaded controls. The scaffold stiffness (Young's modulus) also increased in loaded samples over time (*Fig 5*).

DISCUSSION & CONCLUSIONS: The goal of this study was to develop a model to analyse the effects of mechanical stimulation on osteoblastic cells in a 3-D system, to understand how mechanical stimulation can enhance bone tissue engineering. Although the number of viable cells decreased under our loading regimen, the amount of collagen and scaffold stiffness increased, indicating increased matrix production by cells. This model has the potential to answer questions about cell survival, distribution, matrix production and stiffness in 3-D, in response to mechanical signals.

Fig 3: Cell viability over 11 days (MTS assay)

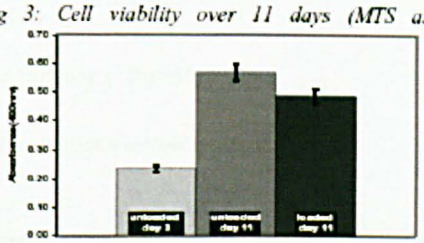

Fig. 4: Collagen on PU scaffold by using light microscopy (Sirius red staining) on day 11.

Fig 5: Stiffness (Young's modulus) of Scaffolds over 9 day on loaded specimens

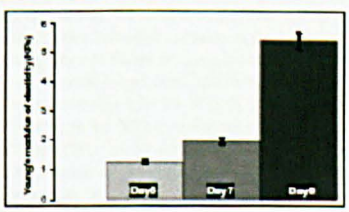

REFERENCES: [1] Carter, D.R et al (1988), J. Orthop. Res. 6(5):736-748. [2] Y. Kato et al (2001), J Bone Miner Res. 16(9):1622-33.

ACKNOWLEDGEMENTS: Dr. L. Bonewald, University of Missouri at Kansas City, UA. kindly donated MLO-A5 osteoblastic cell. Bose provided use of the ElecroForce 3200 for an evaluation period. Funding for this project was provided by the Royal Society of London, The University of Sheffield and the Thai Government.

APPENDIX 3

Bone 44 (2009) 822–829

Contents lists available at ScienceDirect

Bone

journal homepage: www.elsevier.com/locate/bone

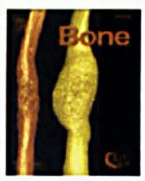

Use of rapidly mineralising osteoblasts and short periods of mechanical loading to accelerate matrix maturation in 3D scaffolds

Anuphan Sittichockechaiwut [a], Andrew M. Scutt [b], Anthony J. Ryan [c], Lynda F. Bonewald [d], Gwendolen C. Reilly [a,*]

[a] Department of Engineering Materials, Kroto Research Institute, North Campus, University of Sheffield, Broad Lane, Sheffield, S3 7HQ, UK
[b] School of Medicine and Biomedical Sciences, University of Sheffield, UK
[c] Department of Chemistry, University of Sheffield, UK
[d] Department of Oral Biology, School of Dentistry, University of Missouri-Kansas City, USA

ARTICLE INFO

Article history:
Received 3 September 2008
Revised 19 December 2008
Accepted 26 December 2008
Available online 14 January 2009

Edited by D. Burr

Keywords:
Mechanobiology
Tissue engineering
Bioreactors
Osteoid
Polyurethane

ABSTRACT

MLO-A5 cells are a fully differentiated osteoblastic cell line with the ability to rapidly synthesise mineralised extracellular matrix (ECM). We used MLO-A5 cells to develop a system for studying the mechanical modulation of bone matrix formation in 3D using a cyclic compressive loading stimulus. Polyurethane (PU) open cell foam scaffolds were seeded with MLO-A5 cells under static conditions and loaded in compression at 1 Hz, 5% strain in a sterile fluid-filled chamber. Loading was applied for only 2 h per day on days 5, 10 and 15 of culture and cell-seeded scaffolds were assayed on days 10, 15 and 20 of culture. Collagen content as assayed by Sirius red was significantly (2 fold) higher at days 15 and 20 in loaded samples compared with static controls. Calcium content as assayed by alizarin red was significantly (4 fold) higher by day 20. The number of viable cells as assayed by MTS was higher in loaded samples at day 10 but there was no difference by days 15 and 20. Loaded samples also had higher stiffness in compression by the end of the experiment. The mRNA expression of type I collagen, osteopontin and osteocalcin was higher, after a single bout of loading, in loaded than in non-loaded samples as assayed by RT-PCR. In conclusion, mineralisation by fully differentiated osteoblasts, MLO-A5s, was shown to be highly sensitive to mechanical loading, with short bouts of mechanical loading having a strong effect on mineralised matrix production. The 3D system developed will be useful for systematic investigation of the modulators of *in vitro* matrix mineralisation by osteoblasts in mechanobiology and tissue engineering studies.

Introduction

Bone responds to mechanical loading and disuse *in vivo* and many of the attempts to understand the mechanisms by which this occurs have centred on the role of the osteocyte which is the cell best placed to sense changes in strain in mature bone matrix [1,2]. However, all bone cell types respond to mechanical load *in vitro* [3] and developing bone, which does not contain mature osteocytes, is also known to respond strongly to mechanical signals, for example during fracture healing [4,5] and implant integration [6]. Understanding how osteoblasts and their precursors respond to mechanical loads has been complicated by the routine use of 2D substrates for mechanobiological investigations. Whereas it is becoming clear that crucial mechanobiological parameters such as cell stiffness [7], focal adhesion complex formation [8] and ultimately production of differentiation markers [9] differ when cells are rounded or contained in a 3D matrix, more similar to the *in vivo* environment, rather than flattened on a 2D surface.

In bone tissue engineering, much research is dedicated to finding ways to enhance mineralised matrix formation to create bone suitable for tissue regeneration and repair [10]. Many researchers have shown that both precursor osteoblasts derived from mesenchymal stem cells (MSCs) and osteoblastic cell lines produce mineralised ECM when cultured in three dimensional scaffolds and that mineralisation is improved by growing the cell/scaffold constructs in bioreactor conditions that apply flow through the scaffold [11–14]. The positive outcomes of bioreactors culture are usually ascribed to both improved nutrient transport and the mechanical forces generated, though it is difficult to separate the respective contributions of these two effects. While it is well demonstrated that some kind of dynamic culture environment improves tissue engineered bone formation, little is known about the mechanisms by which this occurs, how they relate to *in vivo* mechanisms of mechanically induced bone formation and how to optimise bioreactor culture to maximise bone production.

* Corresponding author.
E-mail address: g.reilly@sheffield.ac.uk (G.C. Reilly).

8756-3282/$ – see front matter © 2009 Elsevier Inc. All rights reserved.
doi:10.1016/j.bone.2008.12.027

Therefore, the question of how bone cells respond to mechanical forces in 3D is relevant to both an understanding of mechanotransduction in bone *in vivo* and in tissue engineered bone.

The potential for 3D tissue engineering models to be used as mechanobiological test systems and for mechanobiology to provide data for improving bioreactor conditions in tissue engineering has been discussed in the research community [15]. Some researchers are already using developments in 3D culture to apply mechanical forces previously applied in 2D to 3D MSC culture systems e.g. oscillatory fluid flow [16–18] and substrate strain [19–21]. These studies have looked for either short term signalling outcomes such as release of the endocrine factor PGE_2 [16–18], mRNA expression of the growth factor BMP-2 [19], or matrix protein production [20,21]. In a 4-point bending model, Mauney et al. [21] indicated (qualitatively) that mineralisation may also be increased by short periods of cyclic strain *in vitro*.

MLO-A5 osteoblast-like cells are an ideal cell with which to examine modulation of mineralised matrix production as they have been shown to mineralise rapidly in culture [22] and are thought to represent a fully differentiated late-stage osteoblast or 'osteoid osteocyte'. The mineralisation process of MLO-A5s has been characterised using a variety of high resolution microscopy techniques, and energy dispersive spectrometry and shown to be more bone-like than that of other osteoblast cell lines such as MC3T3-E1 [23]. There is some evidence that these cells are sensitive to mechanical stimulation in the same way as other osteoblast cells lines, for example they release PTH after substrate stretch [24]. However prior to this study it was not known whether mineralisation by MLO-A5s could also be modulated by mechanical forces.

Our goal was to develop a model system with which matrix-formation responses can be systematically examined in long term culture in a 3D system analogous to the osteoid environment. To test our prediction that MLO-A5s would be a good model system, we first had to establish a method for 3D culture of MLO-A5 cells that could support repeated mechanical loading and long term culture. We chose an open cell highly porous industrial grade polyurethane foam (Caligen foams, UK) as a supporting scaffold because it has high elasticity and mechanical stability which allows it to retain a supporting role even at low material/pore ratios. In addition it is easily handled during *in vitro* culture and is produced in large blocks of consistent structure and mechanical properties, reducing experimental variability. Although this foam had not previously been used as a biomaterial other polyurethanes have been shown to be compatible with bone cells [25,26]. We wanted to be able to apply direct strain to the construct but not exclude the effect of strain induced fluid flow, so we chose to load the porous scaffold in unconfined compression using the commercially available 'Orthopaedic BioDynamic™ Chamber' from Bose Electroforce systems group, (MN, USA) in which samples can be subject to dynamic tension or compression, as with a standard mechanical testing machine, but the sample is retained in a sterile fluid-filled environment, as in bioreactor culture.

Our hypothesis was that mineralised ECM production by MLO-A5 cells would be sensitive to mechanical loading and that 3D MLO-A5 culture would provide a useful model with which to understand how mechanical forces influence matrix mineralisation *in vivo* and in tissue engineered bone.

Materials and methods

Materials and reagents

All cell culture and assay reagents were from Sigma Aldrich (Dorset, UK) unless otherwise stated. A polyether polyurethane foam was obtained as a large industrial grade block from Caligen Foam Ltd., (Lancashire, U). The foam was synthesised from the minimum number of components; a 3500 mw ether polyol and toluene diisocyanate (TDI) using water and methylene chloride as blowing agents with a siloxane silicone stabiliser and an amine catalyst (BDMAEE). MLO-A5 cells were originally derived from mouse long bone and immortalised as described by Kato et al. [22]. Basal culture medium for cell maintenance was alpha MEM (Invitrogen, Paisley, UK) supplemented with 5% fetal bovine serum, 5% bovine calf serum (Hyclone, Cramlington, UK), 0.25% fungizone (F) and 1% penicillin and streptomycin (PS). Medium used during loading was DMEM (Biosera, East Sussex, UK) with 2% FCS, 0.25% F and 1% PS.

Polyurethane (PU) scaffold preparation

To characterise the average strut and pore size of the scaffold, 45 struts and 45 pores were randomly selected from SEM images. Strut width was designated as width at the narrowest portion (e.g. Fig. 2) and average pore size was designated as the mean of the widest part of the pore and the width at 90° to this. All widths were measured using ImageJ (National Institutes of Health, USA) image analysis package. The pore width varied between 150–1000 μm with a mean ± SD of 384 ± 151 μm, the strut thickness has a mean ± SD of 67 ± 11 μm. To prepare sterile scaffolds, PU foam was cut into cylindrical scaffolds with a diameter of 10 mm and height of 10 mm, scaffolds were sterilised in 70% ethanol overnight at room temperature. Prior to cell seeding, the scaffolds were washed with Phosphate Buffered Saline (PBS) 5 times by shaking and were immersed in basal cell culture media for 10 min. The scaffolds were removed from the media, squeezed to remove the liquid and placed in 1 cm internal diameter stainless steel rings to act as a holder during initial cell attachment.

Cell culture

MLO-A5 osteoblastic cells, passage 31–33, were passaged under standard culture conditions in basal medium. At 80% confluence they were released from the tissue culture flask using trypsin/EDTA and resuspended in basal medium. 2.5×10^5 cells in 100 μL were added onto the top of each sterile scaffold contained in the stainless steel rings, in a 6 well plate (Fig. 1). After incubating for 1 h sufficient basal medium was added to cover the scaffold and rings and scaffolds were maintained in the rings overnight. On day 1 of culture the rings were removed and medical grade stainless steel wire holders were placed over the scaffold to keep it fully immersed in the media. At this time fresh media was added to cover the scaffolds, supplemented with 50 μg/ml of ascorbic acid and 2 mM of β-glycerophosphate. The cell-seeded scaffolds were cultured in the incubator for up to 20 days, media was changed every 3 days.

Cell localisation by MTT and DAPI

To test whether cells maintained viability and grew throughout the novel scaffold live cells were identified by MTT, in which the yellow MTT solution is reduced by active mitochondria in live cells to a dark blue or purple formazan insoluble salt [27]. Cell-seeded scaffolds were washed with PBS and incubated with 1 mg/ml MTT in PBS for 40 min at 37 °C. DNA staining by DAPI was used to observe the distribution of the cell nuclei along the scaffold struts. Cell-seeded scaffolds were fixed in 10% formalin solution for 10 min at room temperature, and then washed with PBS 3 times. DAPI solution (1:1000 DAPI in PBS) was added to cover scaffolds and incubated for 1 h. The DAPI was removed and replaced by PBS and cells were imaged on an Axon Instruments ImageExpress inverted stage microscope using a 10× objective and standard DAPI filter set.

Scanning electron microscopy (SEM)

To examine matrix production by cells after a 20 day culture period selected scaffolds were cultured without mechanical loading and processed for SEM. Cells seeded scaffolds were fixed with 2.5%

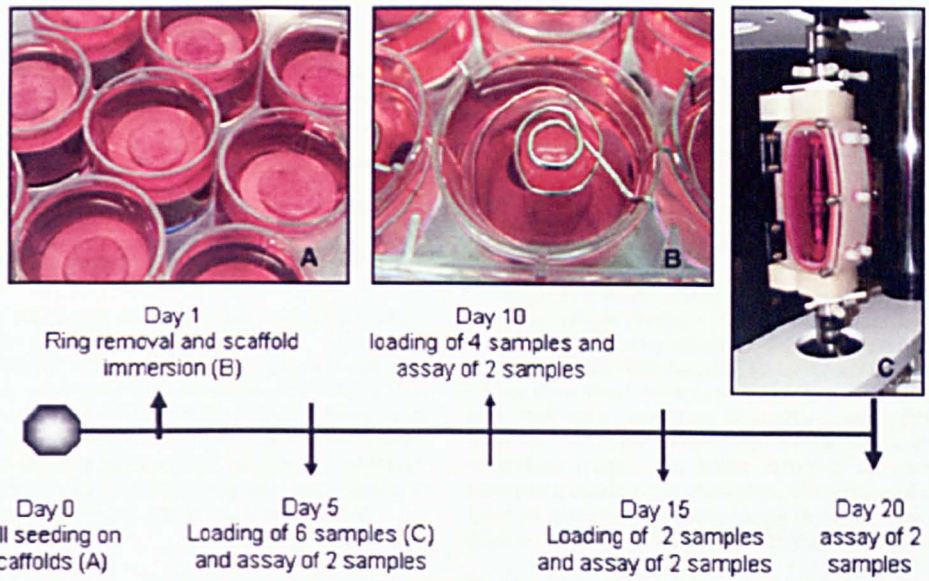

Fig. 1. Cell seeding method and experimental time line. Cells were seeded in polyurethane foam scaffolds retained in a steel ring (A). On day 1 of culture the ring was removed and foams allowed to float in media held down by a spiral stainless steel holder (B). Samples were subjected to loading (C) in the Bose ElectroForce BioDynamic™ chamber or control treatment (non-loaded) and collected at the timepoints shown (D).

glutaraldehyde in 0.1 M sodium cacodylate buffer for 30 min at room temperature, and post fixed with 2% osmium tetraoxide for 1 h. The samples were dehydrated in a graded series of ethanol up to 100% and freeze dried. Samples were mounted onto the 12.5 mm stubs and sputter coated with gold, and then observed with a scanning electron microscope (Phillips/FEI XL-20 SEM) at an accelerating voltage of 10–15 kV.

Application of mechanical loading

Dynamic cyclic compression was performed in a BioDynamic™ chamber mounted on a ELF3200 mechanical testing machine (ElectroForce Systems Group, Bose, MN, USA) (Fig. 1). All circuit components were sterilised by autoclave. The sample to be loaded was removed from the well plate and placed into the chamber, between two platens. The chamber was filled with 200 ml of loading media and mounted onto the mechanical testing machine. The cell-seeded scaffolds were dynamically loaded in compression using a sine wave at 1 Hz, 5% strain (displacement of −0.5 mm) in the media-filled chamber for 2 h on days 5, 10 and 15 of culture at room temperature (Fig. 1). Force and displacement data was recorded by WinTest software (Bose). During loading a paired non-loaded control was kept in a sterile media-filled T75 flask in the same volume of loading media under the same environmental conditions as the loaded sample. Between loading cycles, both loaded and non-loaded samples were cultured in an incubator under standard conditions. The mechanical properties of the scaffold were tested by a single cycle of loading to 50% strain in air at 0.2 mm/s immediately prior to the following assays.

Cell viability

The relative number of viable cells in the scaffolds was quantified using CellTiter 96® AQueous One Solution Reagent (Promega, Southampton, UK.). Similarly to the MTT assay the MTS salt changes colour due to cell metabolic activity but the product is soluble [28]. Cell-seeded scaffolds were washed with PBS until there was no more phenol red from the culture medium in the solution and placed in 10 mm internal diameter stainless steel rings. 0.5 ml of a 1:10 solution of MTS in PBS was added to the scaffolds and to an empty scaffold for the blank control. MTS was incubated for 3 h at 37 °C, 200 µl samples of the solution were pipetted out from the scaffolds read at 490 nm with a 96-well plate reader.

Collagen and mineral staining

After MTS assay, scaffolds were washed three times with PBS then fixed with 10% formalin for 10 min at room temperature. The formalin was removed and scaffolds were washed with PBS 3 times, cut into 5–6 pieces and all pieces from a single scaffold stained with alizarin red [29], (1 mg/ml, pH5.5) for 30 min at room temperature with shaking. The dye was then removed and the samples washed with distilled water, air-dried in a fume hood and observed qualitatively under light microscopy. For quantitative analysis, alizarin red was eluted with 5% perchloric acid, under mild shaking for 15 min and optical density measured at 490 nm. After alizarin red destaining, all samples were washed with distilled water and air-dried. Collagen was quantified by adding 5 ml of Sirius red (1 mg/ml in saturated picric acid), a strong anionic dye that binds strongly to collagen molecules [30] to each well and shaking for 18 h. The dye solution was removed and each well was washed four times with distilled water to remove unbound dye until no more red colouring was eluted, then air-dried. The bound dye was observed qualitatively under light microscopy. For quantitative analysis, the scaffolds in each well were destained with 0.2 M NaOH/Methanol, in a 1:1 ratio, under mild shaking for 15 min. Optical density was then measured at 490 nm using 96-well plate reader.

Messenger RNA (mRNA) isolation and reverse transcriptase (RT)-PCR

Cell-seeded scaffolds were grown until day 10 and loaded or subjected to control treatment as described above. Preliminary experiments in which RNA was collected at 4, 12 and 24 h after loading determined that the optimum time-point to detect effects of loading on matrix protein mRNA was 12 h (data not shown). mRNA was extracted using the Dynabeads® mRNA DIRECT™ Kit (Invitrogen, Paisley, UK) and reverse-transcribed and amplified using the

Table 1
Mouse primer sequences for RT-PCR

mRNA	Primer sequences	
GAPDH	Forward	5′-cca tgg aga agg ccg ggg-3′
	Reverse	5′-caa agt tgt cat gga tga cc-3′
Type I collagen	Forward	5′-aat ggt gag acg tgg aaa ccc gag-3′
	Reverse	5′-cga ctc cta cat ctt ctg agt ttg g-3′
Osteopontin	Forward	5′-gac cat gag att gac agt gat ttg-3′
	Reverse	5′-t ga tgt tcc agg ctg gct ttg-3′
Osteocalcin	Forward	5′-gac aaa gcc ttc atg tcc aag c-3′
	Reverse	5′-aaa gcc gag ctg cca gag ttt g-3′

JumpStartTM RED HT RT-PCR kit using primer sequences (MWG biotech, London, UK) as in Table 1.

The conditions were RT – 50 °C for 30 min, RT inactivation – 94 °C for 3 min, denaturation – 94 °C for 15 s, Annealing – 58.5 °C for 30 s, extension – 72 °C for 1 min, and final extension – 72 °C for 10 min for 28 amplification cycles, for all primer sets. RT-PCR products were visualised on a FlashGel™ system (Lonza, Berkshire, UK). The relative band density of the RT-PCR products was quantified using Bio image intelligent quantifier version 3.2.1 (Bio image Systems Inc., Michigan, USA).

Statistical analyses

All 20 day experiments were repeated three times with a minimum of $n = 2$ per condition, per repeat ($N = 6$). RNA experiments were repeated three times. Cell viability, calcium and collagen per cell, and mechanical properties were tested by two sample t-test. Differences were considered statistically significant if the p-value was less than 0.05 ($p<0.05$). Normalised loaded samples were compared to non-loaded controls using Mann–Whitney test with 95% confidence level. All statistical tests were performed using Minitab Inc. software (State College, PA, USA).

Results

Cell viability and matrix production in static culture

MTT staining showed that cells penetrated the scaffold and remained viable over 20 days of culture. Viable cells were present throughout the scaffold (Fig. 2). Nuclear staining by DAPI and fluorescence microscopy indicated that cells were contained within the scaffold pores by day 5 but did not show visual evidence of adhesion to the sides of the scaffold pores. However, by days 10 and 15 of culture, clusters of cells were found lining the walls of the scaffold pores and appeared to be embedded in extracellular matrix. SEM further confirmed the presence of thick extracellular matrix by day 20 of culture. The matrix contained fibres and spherical modules, the nodules having the appearance of calcospherulites as described by Kato et al. and Barragan-Adjemian et al. (Fig. 2).

The effect of mechanical loading on matrix deposition

All scaffolds showed evidence of matrix production as indicated by Sirius red staining from day 10 of culture. By day 20 loaded scaffolds

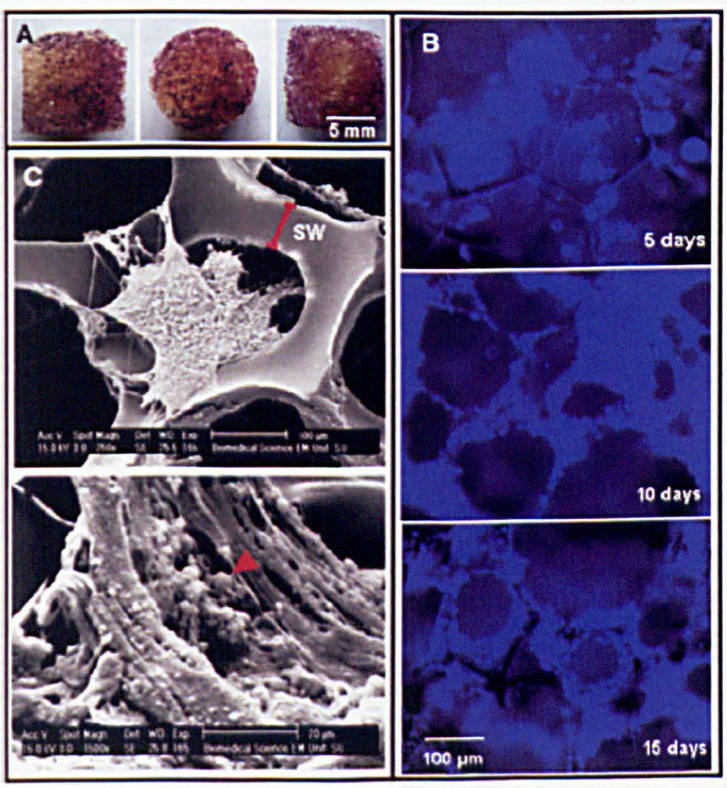

Fig. 2. Cell and matrix growth in static culture. (A) At selected timepoints a scaffold was stained with MTT assay for metabolic activity, metabolically active cells were found throughout the scaffold up to day 20 of culture (left: intact scaffold side view, centre: intact scaffold top view, right: transverse section of scaffold). (B) Samples were fixed and stained with DAPI nuclear stain, which confirmed that cells grow around the pores of the scaffold. (C) SEM images also indicated that cells were embedded in thick matrix which contained both fibrous and spherical (white arrow head) structures indicative of collagen and calcospherulites respectively. The line marked sw indicates where a typical scaffold strut width measurement was made, this strut has a minimum width of 63 μm.

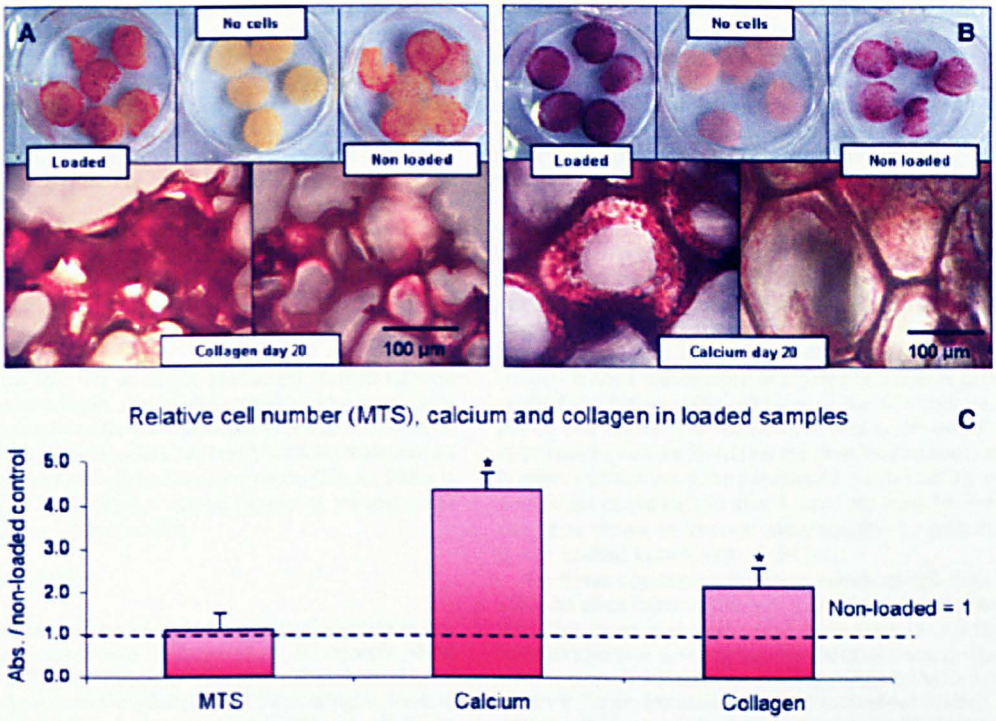

Fig. 3. Cell viability (MTS), calcium and collagen in the scaffolds. (A) Appearance of representative loaded, empty and non-loaded scaffolds, one scaffold per well, cut into cross sections and stained with Sirius red (collagen) a light micrograph of a random area of the scaffold is shown below. (B) As for A after alizarin red (calcium) staining. (C) Mean ± SD of MTS (cell viability), Alizarin red (calcium) and Sirius red (collagen) absorbance per loaded scaffold at day 20 normalised to its paired non-loaded scaffold ($n = 6$, * = $p < 0.05$ for Mann–Whitney test).

contained significantly more total calcium and collagen compared to non-loaded controls as indicated by the intensity of red staining. Also the stain was more evenly distributed throughout the scaffold (Figs. 3A and B). Colourimetry showed that alizarin red staining was significantly higher in loaded samples at days 20 (Fig. 3C). Total collagen content as determined by Sirius red staining was consistently significantly ($p < 0.05$) 2 times higher in loaded than non-loaded samples at all timepoints. When data were normalised to MTS levels to allow for cell number effects, calcium content per viable cell was low in non-loaded samples and barely increased over time. In contrast, in loaded samples calcium content was slightly higher by day 15 and increased rapidly between days 15 and 20. Collagen

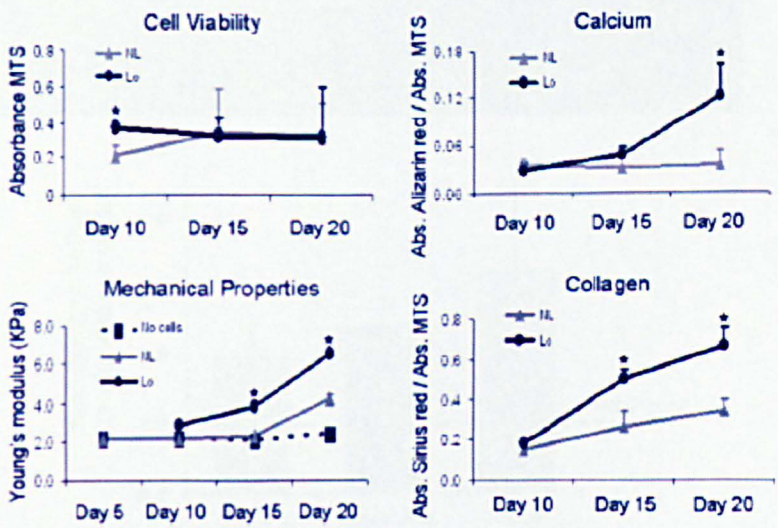

Fig. 4. Changes over time in cell viability, calcium per viable cells, collagen per viable cells and mechanical properties of the scaffolds. Mean ± S.D. (A) Colourimetric absorbance of MTS ($N = 6$). (B) Colourimetric absorbance of alizarin red/respective MTS value ($N = 6$). (C) Colourimetric absorbance of Sirius red/respective MTS value ($N = 6$). (D) Young's modulus of elasticity under a single compressive load to 50% strain ($N = 4$) *$p < 0.05$ Student's t-test (NL = Non-load, L = Load).

content per cell increased steadily over the time in culture under both treatments being more rapid in loaded samples throughout the culture period (Fig. 4).

The effect of mechanical loading on cell viability

In samples analysed on day 10, after just 1 bout of 2 h loading on day 5, there were significantly more metabolically active cells as indicated by MTS (Fig. 4), however this difference was not present in samples collected on days 15 or 20. Loading appears to accelerate cell proliferation in the short term but in both groups cell number ceases to increase after day 15.

Scaffold stiffness (Young's modulus of elasticity)

Similarly to the increase in matrix production scaffold stiffness increased in both loaded and non-loaded samples with a more rapid change in loaded samples. This was shown not to be due to changes in the properties of the scaffold material as empty scaffolds maintained a constant modulus over 20 days immersion in media (Fig. 4). Stiffness was significantly (2 fold) higher in loaded samples by the end of the experiments (~ 3.9 vs 6.2 kPa, $p < 0.01$).

mRNA expression (RT-PCR)

In order to examine a more immediate response to loading matrix protein gene expression of type I collagen (Col1) osteopontin (OPN) and osteocalcin (OCN) were measured 12 h after a single bout of 2 h of loading or control treatment. Loaded samples showed higher levels of Col1 mRNA (about 3 fold) as measured by band density relative to GAPDH, consistent with increased collagen protein by Sirius red staining. OPN mRNA was 2 times and OCN was 2.5 times non-loaded controls, though the semi-quantitative density differences were not statistically significant (Fig. 5).

Discussion

We have demonstrated for the first time that MLO-A5 rapidly mineralising cells are sensitive to mechanical load and their matrix production in 3D can be strongly modulated by just short periods of mechanical loading inserted into a static culture period. The secondary outcomes of this study were a demonstration of the potential for an inert industrially produced polyurethane foam to be a supporting scaffold for *in vitro* bone tissue engineering and the first published use of the commercially available orthopaedic BioDynamic™ chamber from Bose Electroforce systems group for bone tissue engineering and mechanobiology studies.

A few studies have shown that short periods of strain applied to scaffolds seeded with osteoblast precursors (MSCs) induce upregulation of differentiation markers at the mRNA level [17,19,21]. In our study mRNA levels of bone matrix protein are also modulated by mechanical loading in fully mature cells (Fig 5) and are followed by long term effects on matrix production, even with 4 days rest between loading bouts (Figs. 3 and 4). The higher matrix content of loaded samples is not a consequence of higher cell numbers as loading only resulted in a higher viable cell count at day 10 of culture, by days 15 and 20, cell number was the same. As well as the overall increase in matrix production we found that the short loading bouts also resulted in better distribution of the mineralised matrix (Fig. 3). Interestingly, short bouts of loading (30 min, 3 times per week for 2 weeks) have also been shown to increase mineralisation by primary cells in a porous scaffold in an *in vivo* model [31].

For tissue engineering purposes osteoblast cell lines or primary MSCs are often cultured in dynamic conditions using either perfusion [13,14,26] or rotating wall vessel bioreactors [11,32] these studies consistently show upregulation of mineralised matrix deposition and a more even distribution of mineral compared with static culture. However, those bioreactors applied continuous loading over many days in culture and it is difficult to separate the indirect effects of improved nutrient flow, waste removal and oxygen circulation with direct mechanotransduction effects. A study which superimposed daily bouts of 6 h of dynamic compression loading on perfusion culture of MSCs [20] indicated that compression increased bone matrix protein production compared with perfusion alone. Our results indicate that it may prove to be unnecessary to apply continuous mechanical stimulation in growing tissue engineered matrices which has implications in the design of economical scaled-up processes for tissue engineering [33].

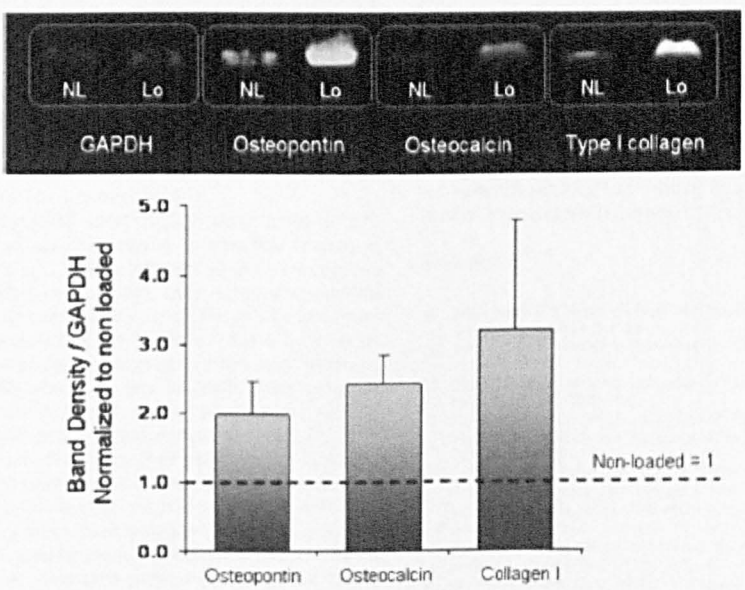

Fig. 5. mRNA expression of Col1 OPN and OCN 12 h after a single bout of 2 h of loading or control treatment. An example gel of 3 independent experiments is shown. Loaded samples showed increased levels of Col1, OPN and OCN gene expression as measured by band density relative to GAPDH ($N = 3$, NL = Non-load, L = Load).

One of the reasons for reduced matrix production in the centre of tissue engineered scaffolds is thought to be the reduced oxygen caused by limited media diffusion. Interestingly Zahm et al. [34] have shown that MLO-A5 mineralisation is lower when grown in 2% O_2 compared to 20% O_2. However, since in our system nutrient flow would only be improved during a short period of the total culture time, it is unlikely that our results are due to higher oxygen tension in the loaded scaffolds, unless a short period of higher oxygen results in long term changes in matrix production. We suggest that the cells are responding to the mechanical compression stimulus by directly sensing either the substrate strain or the fluid shear stress caused by media movement through the porous scaffold which initiates a cascade of events that result in an upregulation of survival and matrix producing genes, in the majority of cells including those in the centre of the scaffold. It is possible that improved nutrient transport, albeit for a short period, also contributes to the mechanosensitive response as has been demonstrated in 2D cultures. [35,36].

All osteoblastic bone cell lines we have grown on this scaffold have survived and produced matrix including MG63, SAOS-2 and MC3T3-E1, indicating that this system can be used for a variety of cells types and mechanobiological investigations. However, none of these cell types produced as much mineralised matrix as MLO-A5 cells within the same time frame (data not shown). We have tested whether this system will be suitable for mechanical modulation of primary human MSCs and have found that MSCs also respond to a similar loading regimen with an increase in collagen production. However, longer culture times were needed to obtain quantifiable levels of mineral and the amount produced was highly variable. Kato et al. [22] showed that MLO-A5 cells will mineralise even in the absence of β-glycerophosphate, therefore a low concentration of β-glycerophosphate was used in our cultures (2 mM) to minimise the chance of non-cell specific calcium phosphate deposits [37]. Culturing the cell/scaffold constructs in the standard concentration of 5 mM β-glycerophosphate may accelerate mineralisation further.

The initial rationale for the use of MLO-A5 cells in this study was to examine mechanical modulation of only the matrix forming stage of bone tissue engineering (as opposed to including mechanical effects on differentiation) and to produce enough matrix in a short time frame such that mechanically modulated changes could be readily detected. However, the ease with which a 3D bone-like matrix is formed by these cells indicates they may be useful in forming an *in vitro* decellularised pre-matrix to encourage human cell growth as described by Dutta et al. [38]. In addition, such a rapidly formed 3D matrix could be useful in *in vitro* studies of the mechanical and biochemical modulators of bone formation prior to animal studies. Studies such as this also help to inform the debate about how far along the differentiation pathway cells should be, prior to implantation for regenerative medicine [39], supporting the idea that bone matrix for implantation could be created *in vitro* using pre-differentiated, mature cells.

We utilised a non-degradable industrially produced polyurethane foam, not previously used as a biomaterial, as a scaffold to support MLO-A5 culture in 3D (Fig. 2). The advantage of using this type of foam is that it is highly reproducible, thus eliminating scaffold variability as a confounding variable in our experiments. Other porous materials have been investigated for bioreactor based bone tissue engineering from naturally derived materials to synthetic polymers and ceramics [14,16,18]. However, few scaffolds have adequate mechanical properties for repetitive direct strain on the scaffold material (extensively reviewed in Karageorgiou and Kaplan [40]).

Other laboratories have custom designed polyurethane foams for tissue engineering with positive results for example Fassina et al. [26], demonstrated that the osteosarcoma cell line SAOS-2 can grow and mineralise on laboratory synthesised polyurethane foams. Here we aimed to test whether a generic cheaply-produced material with no bioactive properties could adequately support 3D cell culture. It was interesting to note that although the cells did not show strong attachment to the scaffold (Fig 2), they remained contained within it and rapidly synthesised their own matrix in which they were embedded. Cell–ECM interactions have been shown to be crucial in encouraging mineralised matrix formation in tissue engineering scaffolds [38]. Similarly to Fassina et al. [26], we chose to use a non-degradable polyurethane that would maintain its properties over time (Fig. 4) and not leach degradation products into the culture. It is possible to produce biodegradable, implantable polyurethanes for bone tissue engineering scaffolds [25,41], which we are developing for further refinement of our system [42].

We applied a maximum of 5% global strain to our scaffolds at a frequency of 1 Hz. In 2D monolayer studies similar strains and rates have been shown to induce mineralisation in human MSCs, [43,44]. However, the global strain we applied cannot be easily compared with monolayer systems, as the deformation of foam structures is highly complex [45] and results in local variations in both substrate strain and strain induced fluid flow. Cells residing in bone [3] and osteoid [4,46] also inhabit a complex strain and fluid environment *in vivo*. Interestingly a global strain of 5% has been suggested to be optimal for intramembranous bone formation in a healing fracture [47]. Computer models similar to those used to model tissue differentiation during fracture healing [48] will be able to model the conditions in a tissue engineered system and help correlate ECM production to local mechanical parameters. Wood et al. [49] developed such a model for a simple cylindrical pore and found that calcium deposition by osteoblasts was maximal in the 'reduced strain' regions of their model.

The frequency of loading cycles applied in our model was 1 Hz, this is the frequency most commonly used in bone cell mechanotransduction studies as it replicates walking pace. However, observations that high frequency, low magnitude loading induces bone formation *in vivo* [50] and matrix production by MSCs *in vitro* [51] indicate that this mode of stimulation may also be useful in bioreactor culture. Research in the fields of mechanical stimulation for tissue engineering and fracture healing/osseointegration have produced little consensus on what the optimal mechanical parameters are or what the temporal sequence of applied loading should be to optimise matrix production. Our model system in which a large range of strains, strain rates, frequencies and loading durations can be applied to a highly reproducible industrially produced scaffold and a mature mineralizing cell line will be well placed to systematically address these issues.

Acknowledgments

We gratefully acknowledge Professor Sheila Mac Neil who provided access to cell culture facilities and reagents. Thanks to Keith Blackwood for technical assistance with SEM. Bose ElectroForce systems group supported this research by providing the ELF 3200 for an evaluation period. AS is supported by a Royal Thai Government Scholarship and the research was partially funded by a Royal Society of London Research Grant and the University of Sheffield Devolved Funds scheme.

References

[1] Klein-Nulend J, Bacabac RG, Mullender MG. Mechanobiology of bone tissue. Pathol Biol (Paris) 2005;53:576–80.
[2] Bonewald LF. Mechanosensation and transduction in osteocytes. BoneKEy Osteovision 2006;3:7–15.
[3] Rubin J, Rubin C, Jacobs CR. Molecular pathways mediating mechanical signaling in bone. Gene 2006;367:1–16.
[4] Smith-Adaline EA, Volkman SK, Ignelzi Jr MA, Slade J, Platte S, et al. Mechanical environment alters tissue formation patterns during fracture repair. J Orthop Res 2004;22:1079–85.
[5] Cullinane DM, Salisbury KT, Alkhiary Y, Eisenberg S, Gerstenfeld L, et al. Effects of the local mechanical environment on vertebrate tissue differentiation during repair: does repair recapitulate development? J Exp Biol 2003;206:2459–71.
[6] Clark PA, Rodriguez A, Sumner DR, Hussain MA, Mao JJ. Modulation of bone ingrowth of rabbit femur titanium implants by in vivo axial micromechanical loading. J Appl Physiol 2005;98:1922–9.
[7] Bacabac RG, Mizuno D, Schmidt CF, Mackintosh FC, Van Loon JJ, et al. Round versus flat: bone cell morphology, elasticity, and mechanosensing. J Biomech 2008;41:1590–8.

[8] Cukierman E, Pankov R, Stevens DR, Yamada KM. Taking cell-matrix adhesions to the third dimension. Science 2001;294:1708–12.
[9] Jarrahy R, Huang W, Rudkin GH, Lee JM, Ishida K, et al. Osteogenic differentiation is inhibited and angiogenic expression is enhanced in MC3T3-e1 cells cultured on three-dimensional scaffolds. Am J Physiol, Cell Physiol 2005;289:C408–14.
[10] Cancedda R, Giannoni P, Mastrogiacomo M. A tissue engineering approach to bone repair in large animal models and in clinical practice. Biomaterials 2007;28:4240–50.
[11] Botchwey EA, Pollack SR, Levine EM, Laurencin CT. Bone tissue engineering in a rotating bioreactor using a microcarrier matrix system. J Biomed Mater Res 2001;55:242–53.
[12] Meinel L, Karageorgiou V, Fajardo R, Snyder B, Shinde-Patil V, et al. Bone tissue engineering using human mesenchymal stem cells: effects of scaffold material and medium flow. Ann Biomed Eng 2004;32:112–22.
[13] Porter BD, Lin AS, Peister A, Hutmacher D, Guldberg RE. Noninvasive image analysis of 3D construct mineralization in a perfusion bioreactor. Biomaterials 2007;28:2525–33.
[14] Sikavitsas VI, Bancroft GN, Lemoine JJ, Liebschner MA, Dauner M, et al. Flow perfusion enhances the calcified matrix deposition of marrow stromal cells in biodegradable nonwoven fiber mesh scaffolds. Ann Biomed Eng 2005;33:63–70.
[15] Freed LE, Guilak F, Guo XE, Gray ML, Tranquillo R, et al. Advanced tools for tissue engineering: scaffolds, bioreactors, and signaling. Tissue Eng 2006;12:3285–305.
[16] Jaasma MJ, O'Brien FJ. Mechanical stimulation of osteoblasts using steady and dynamic fluid flow. Tissue Eng Part A 2008;23:23.
[17] Tanaka SM, Sun HB, Roeder RK, Burr DB, Turner CH, et al. Osteoblast responses one hour after load-induced fluid flow in a three-dimensional porous matrix. Calcif Tissue Int 2005;76:261–71.
[18] Vance J, Galley S, Liu DF, Donahue SW. Mechanical stimulation of MC3T3 osteoblastic cells in a bone tissue-engineering bioreactor enhances prostaglandin e2 release. Tissue Eng 2005;11:1832–9.
[19] Sumanasinghe RD, Bernacki SH, Loboa EG. Osteogenic differentiation of human mesenchymal stem cells in collagen matrices: effect of uniaxial cyclic tensile strain on bone morphogenetic protein (BMP-2) mRNA expression. Tissue Eng 2006;12:3459–65.
[20] Jagodzinski M, Breitbart A, Wehmeier M, Hesse E, Haasper C, et al. Influence of perfusion and cyclic compression on proliferation and differentiation of bone marrow stromal cells in 3-dimensional culture. J Biomech 2008;41:1885–91.
[21] Mauney JR, Sjostorm S, Blumberg J, Horan R, O'Leary JP, et al. Mechanical stimulation promotes osteogenic differentiation of human bone marrow stromal cells on 3-D partially demineralized bone scaffolds in vitro. Calcif Tissue Int 2004;74:458–68.
[22] Kato Y, Boskey A, Spevak L, Dallas M, Hori M, et al. Establishment of an osteoid preosteocyte-like cell MLO-A5 that spontaneously mineralizes in culture. J Bone Miner Res 2001;16:1622–33.
[23] Barragan-Adjemian C, Nicolella D, Dusevich V, Dallas MR, Eick JD, et al. Mechanism by which MLO-A5 late osteoblasts/early osteocytes mineralize in culture: similarities with mineralization of lamellar bone. Calcif Tissue Int 2006;79:340–53.
[24] Chen X, Macica CM, Ng KW, Broadus AE. Stretch-induced PTH-related protein gene expression in osteoblasts. J Bone Miner Res 2005;20:1454–61.
[25] Bonzani IC, Adhikari R, Houshyar S, Mayadunne R, Gunatillake P, et al. Synthesis of two-component injectable polyurethanes for bone tissue engineering. Biomaterials 2007;28:423–33.
[26] Fassina L, Visai L, Asti L, Benazzo F, Speziale P, et al. Calcified matrix production by SAOS-2 cells inside a polyurethane porous scaffold, using a perfusion bioreactor. Tissue Eng 2005;11:685–700.
[27] Mosmann T. Rapid colorimetric assay for cellular growth and survival: application to proliferation and cytotoxicity assays. J Immunol Methods 1983;65:55–63.
[28] Ng KW, Leong DT, Hutmacher DW. The challenge to measure cell proliferation in two and three dimensions. Tissue Eng 2005;11:182–91.
[29] Gregory CA, Gunn WG, Peister A, Prockop DJ. An alizarin red-based assay of mineralization by adherent cells in culture: comparison with cetylpyridinium chloride extraction. Anal Biochem 2004;329:77–84.
[30] Tullberg-Reinert H, Jundt G. In situ measurement of collagen synthesis by human bone cells with a sirius red-based colorimetric microassay: effects of transforming growth factor beta2 and ascorbic acid 2-phosphate. Histochem Cell Biol 1999;112:271–6.
[31] Duty AO, Oest ME, Guldberg RE. Cyclic mechanical compression increases mineralization of cell-seeded polymer scaffolds in vivo. J Biomech Eng 2007;129:531–9.
[32] Sikavitsas VI, Bancroft GN, Mikos AG. Formation of three-dimensional cell/polymer constructs for bone tissue engineering in a spinner flask and a rotating wall vessel bioreactor. J Biomed Mater Res 2002;62:136–48.
[33] Archer R, Williams DJ. Why tissue engineering needs process engineering. Nat Biotechnol 2005;23:1353–5.
[34] Zahm AM, Bucaro MA, Srinivas V, Shapiro IM, Adams CS. Oxygen tension regulates preosteocyte maturation and mineralization. Bone 2008;43:25–31.
[35] Donahue TL, Haut TR, Yellowley CE, Donahue HJ, Jacobs CR. Mechanosensitivity of bone cells to oscillating fluid flow induced shear stress may be modulated by chemotransport. J Biomech 2003;36:1363–71.
[36] Riddle RC, Hippe KR, Donahue HJ. Chemotransport contributes to the effect of oscillatory fluid flow on human bone marrow stromal cell proliferation. J Orthop Res 2008;26:918–24.
[37] Chung CH, Golub EE, Forbes E, Tokuoka T, Shapiro IM. Mechanism of action of beta-glycerophosphate on bone cell mineralization. Calcif Tissue Int 1992;51:305–11.
[38] Datta N, Pham QP, Sharma U, Sikavitsas VI, Jansen JA, et al. In vitro generated extracellular matrix and fluid shear stress synergistically enhance 3D osteoblastic differentiation. Proc Natl Acad Sci U S A 2006;103:2488–93.
[39] Mauney JR, Volloch V, Kaplan DL. Role of adult mesenchymal stem cells in bone tissue engineering applications: current status and future prospects. Tissue Eng 2005;11:787–802.
[40] Karageorgiou V, Kaplan D. Porosity of 3D biomaterial scaffolds and osteogenesis. Biomaterials 2005;26:5474–91.
[41] Guelcher SA, Patel V, Gallagher KM, Connolly S, Didier JE, et al. Synthesis and in vitro biocompatibility of injectable polyurethane foam scaffolds. Tissue Eng 2006;12:1247–59.
[42] Clarke DA, Coll C, Drury P, Crawford A, Ryan AJ, et al. Polyurethane scaffolds for long term mechanical loading in musculoskeletal tissue engineering. Tissue Eng 2007;13:1743.
[43] Diederichs S, Freiberger F, van Griensven M. Effects of repetitive and short time strain in human bone marrow stromal cells. J Biomed Mater Res A 2008;2:2.
[44] Simmons CA, Matlis S, Thornton AJ, Chen S, Wang CY, et al. Cyclic strain enhances matrix mineralization by adult human mesenchymal stem cells via the extracellular signal-regulated kinase (ERK1/2) signaling pathway. J Biomech 2003;36:1087–96.
[45] Kraynik AM. Foam structure: from soap froth to solid foams. MRS Bull 2003;28:275–8.
[46] Baksson H, Comas O, van Donkelaar CC, Mediavilla J, Wilson W, et al. Bone regeneration during distraction osteogenesis: mechano-regulation by shear strain and fluid velocity. J Biomech 2007;40:2002–11.
[47] Claes LE, Heigele CA. Magnitudes of local stress and strain along bony surfaces predict the course and type of fracture healing. J Biomech 1999;32:255–66.
[48] Lacroix D, Prendergast PJ. A mechano-regulation model for tissue differentiation during fracture healing: analysis of gap size and loading. J Biomech 2002;35:1163–71.
[49] Wood MA, Yang Y, Baas E, Meredith DO, Richards RG, et al. Correlating cell morphology and osteoid mineralization relative to strain profile for bone tissue engineering applications. J R Soc Interface 2007;11:11.
[50] Judex S, Lei X, Han D, Rubin C. Low-magnitude mechanical signals that stimulate bone formation in the ovariectomized rat are dependent on the applied frequency but not on the strain magnitude. J Biomech 2007;40:1333–9.
[51] Cowie R, Walker RD, Scutt A. The use of high-frequency, low-intensity vibration to stimulate the proliferation and differentiation of primary rat bone marrow cells. Cytotherapy 2006;8:63.

References

1. Barragan-Adjemian, C., et al., *Mechanism by which MLO-A5 late osteoblasts/early osteocytes mineralize in culture: similarities with mineralization of lamellar bone.* Calcif Tissue Int, 2006. **79**(5): p. 340-53.
2. Buckwalter, J.A., *Bone Biology Part I and II.* J bone Jt Surg, 1995. **77A**(8): p. 1256-1289.
3. P. J. Nijwe. H. Burger, J.K.N., A. Van der Plas, *Principles of Bone Biology.* 1996.
4. Hollinger, J.O., et al., *Bone Tissue Engineering.* 2005.
5. Salgado, A.J., O.P. Coutinho, and R.L. Reis, *Bone tissue engineering: state of the art and future trends.* Macromol Biosci, 2004. **4**(8): p. 743-65.
6. Sikavitsas, V.I., J.S. Temenoff, and A.G. Mikos, *Biomaterials and bone mechanotransduction.* Biomaterials, 2001. **22**(19): p. 2581-93.
7. Dempster, D.W., *Anatomy and function of the adult skeleton*, in *Primer on the metabolic bone diseases and disorders of mineral metabolism.*, M.J. Favus, Editor. 2006, American society for bone and mineral research. p. 7-11.
8. Sommerfeldt, D.W. and C.T. Rubin, *Biology of bone and how it orchestrates the form and function of the skeleton.* Eur Spine J, 2001. **10**: p. S86-S95.
9. Kjaer, I. and A. Bagheri, *Prenatal development of the alveolar bone of human deciduous incisors and canines.* J Dent Res, 1999. **78**(2): p. 667-72.
10. Sodek, J. and M.D. McKee, *Molecular and cellular biology of alveolar bone.* Periodontology 2000, 2000. **24**: p. 99-126.
11. Pavlin, D. and J. Gluhak-Heinrich, *Effect of mechanical loading on periodontal cells.* Crit Rev Oral Biol Med, 2001. **12**(5): p. 414-24.
12. Weiner, S., W. Traub, and H.D. Wagner, *Lamellar bone: structure-function relations.* J Struct Biol, 1999. **126**(3): p. 241-55.
13. Ito, M., et al., *Contribution of trabecular and cortical components to the mechanical properties of bone and their regulating parameters.* Bone, 2002. **31**(3): p. 351-8.
14. Caplan, A.I., *Review: mesenchymal stem cells: cell-based reconstructive therapy in orthopedics.* Tissue Eng, 2005. **11**(7-8): p. 1198-211.

15. Mauney, J.R., V. Volloch, and D.L. Kaplan, *Role of adult mesenchymal stem cells in bone tissue engineering applications: current status and future prospects.* Tissue Eng, 2005. **11**(5-6): p. 787-802.

16. Donahue, H.J., et al., *Cell-to-cell communication in osteoblastic networks: cell line-dependent hormonal regulation of gap junction function.* J Bone Miner Res, 1995. **10**: p. 881-889.

17. Baylink, D.J. and J.E. Wergedal, *Bone formation by osteocytes.* Am J Physiol, 1971. **221**(3): p. 669-78.

18. Ahuja, S.S., et al., *CD40 ligand blocks apoptosis induced by tumor necrosis factor alpha, glucocorticoids, and etoposide in osteoblasts and the osteocyte-like cell line murine long bone osteocyte-Y4.* Endocrinology, 2003. **144**(5): p. 1761-9.

19. Palumbo, C., S. Palazzini, and G. Marotti, *Morphological study of intercellular junctions during osteocyte differentiation.* Bone, 1990. **11**(6): p. 401-6.

20. Buttery, L.D., et al., *Differentiation of osteoblasts and in vitro bone formation from murine embryonic stem cells.* Tissue Eng, 2001. **7**(1): p. 89-99.

21. Simmons, C.A., et al., *Cyclic strain enhances matrix mineralization by adult human mesenchymal stem cells via the extracellular signal-regulated kinase (ERK1/2) signaling pathway.* J Biomech, 2003. **36**(8): p. 1087-96.

22. Knippenberg, M., et al., *Adipose tissue-derived mesenchymal stem cells acquire bone cell-like responsiveness to fluid shear stress on osteogenic stimulation.* Tissue Eng, 2005. **11**(11-12): p. 1780-8.

23. Heath, C.A., *Cells for tissue engineering.* Trends Biotechnol, 2000. **18**(1): p. 17-9.

24. Hall, B.K. and T. Miyake, *The membranous skeleton: the role of cell condensations in vertebrate skeletogenesis.* Anat Embryol (Berl), 1992. **186**(2): p. 107-24.

25. Olsen, B.R., A.M. Reginato, and W. Wang, *Bone development.* Annu Rev Cell Dev Biol, 2000. **16**: p. 191-220.

26. Olsen, B.R., *Bone Embryology*, in *Primer on the Metabolic Bone Diseases and Disorders of Mineral Metabolism*, M.J. Favus, Editor. 2006, The American Society for Bone and Mineral Research: Washington, D.C. p. 2-6.

27. Aaron, J.E. and T.M. Skerry, *Intramembranous trabecular generation in normal bone.* Bone Miner., 1994. **25**: p. 211-230.

28. Scott, C.K., S.D. Bain, and J.A. Hightower, *Intramembranous bone matrix is osteoinductive.* Anat. Rec., 1994. **238**: p. 23-30.

29. Lee, Y.S.a.C., C. M., *Adhesion molecules in skeletogenesis: I. Transient expression of neural cell adhesion molecules (NCAM) in osteoblasts during endochondral and intramembranous ossification.* J. Bone Miner. Res., 1992. **7**: p. 1435-1446.

30. Hu H, H.M., Tu X, Yu K, Ornitz DM, Long F, *Sequential roles of Hedgehog and Wnt signaling in osteoblast development.* Development, 2005. **132**: p. 49-60.

31. Haapasalo, H., et al., *Exercise-induced bone gain is due to enlargement in bone size without a change in volumetric bone density: a peripheral quantitative computed tomography study of the upper arms of male tennis players.* Bone, 2000. **27**(3): p. 351-7.

32. Aubin, J.E. and E. Bonnelye, *Osteoprotegerin and its ligand: a new paradigm for regulation of osteoclastogenesis and bone resorption.* Osteoporos Int, 2000. **11**(11): p. 905-13.

33. Bonewald, L.F. and S.L. Dallas, *Role of active and latent transforming growth factor beta in bone formation.* J Cell Biochem, 1994. **55**(3): p. 350-7.

34. Prockop, D.J. and K.I. Kivirikko, *Collagens: molecular biology, diseases, and potentials for therapy.* Annu Rev Biochem, 1995. **64**: p. 403-34.

35. Eyre, D.R., I.R. Dickson, and K. Van Ness, *Collagen cross-linking in human bone and articular cartilage. Age-related changes in the content of mature hydroxypyridinium residues.* Biochem J, 1988. **252**(2): p. 495-500.

36. Lian, J.B., et al., *Osteocalcin gene promoter: unlocking the secrets for regulation of osteoblast growth and differentiation.* J Cell Biochem Suppl, 1998. **30-31**: p. 62-72.

37. You, J., et al., *Osteopontin gene regulation by oscillatory fluid flow via intracellular calcium mobilization and activation of mitogen-activated protein kinase in MC3T3-E1 osteoblasts.* J Biol Chem, 2001. **276**(16): p. 13365-71.

38. Millan, J.L., *Alkaline Phosphatases : Structure, substrate specificity and functional relatedness to other members of a large superfamily of enzymes.* Purinergic Signal, 2006. **2**(2): p. 335-41.

39. Shui, C. and A. Scutt, *Mild heat shock induces proliferation, alkaline phosphatase activity, and mineralization in human bone marrow stromal cells and Mg-63 cells in vitro.* J Bone Miner Res, 2001. **16**(4): p. 731-41.

40. Rawadi, G., et al., *BMP-2 controls alkaline phosphatase expression and osteoblast mineralization by a Wnt autocrine loop.* J Bone Miner Res, 2003. **18**(10): p. 1842-53.

41. Osyczka, A.M. and P.S. Leboy, *Bone morphogenetic protein regulation of early osteoblast genes in human marrow stromal cells is mediated by extracellular signal-regulated kinase and phosphatidylinositol 3-kinase signaling.* Endocrinology, 2005. **146**(8): p. 3428-37.

42. Diefenderfer, D.L., et al., *Regulation of BMP-induced transcription in cultured human bone marrow stromal cells.* J Bone Joint Surg Am, 2003. **85-A Suppl 3**: p. 19-28.

43. Schwartz, Z., et al., *Pulsed electromagnetic fields enhance BMP-2 dependent osteoblastic differentiation of human mesenchymal stem cells.* J Orthop Res, 2008. **26**(9): p. 1250-5.

44. Reijnders, C.M., et al., *In vivo mechanical loading modulates insulin-like growth factor binding protein-2 gene expression in rat osteocytes.* Calcif Tissue Int, 2007. **80**(2): p. 137-43.

45. Chen, X., et al., *Stretch-induced PTH-related protein gene expression in osteoblasts.* J Bone Miner Res, 2005. **20**(8): p. 1454-61.

46. Porter, R.M., W.R. Huckle, and A.S. Goldstein, *Effect of dexamethasone withdrawal on osteoblastic differentiation of bone marrow stromal cells.* J Cell Biochem, 2003. **90**(1): p. 13-22.

47. Rickard, D.J., et al., *Induction of rapid osteoblast differentiation in rat bone marrow stromal cell cultures by dexamethasone and BMP-2.* Dev Biol, 1994. **161**(1): p. 218-28.

48. Reilly, G.C., et al., *Fluid flow induced PGE2 release by bone cells is reduced by glycocalyx degradation whereas calcium signals are not.* Biorheology, 2003. **40**(6): p. 591-603.

49. Reich, K.M. and J.A. Frangos, *Protein kinase C mediates flow-induced prostaglandin E2 production in osteoblasts.* Calcif Tissue Int, 1993. **52**(1): p. 62-6.

50. Bacabac, R.G., et al., *Nitric oxide production by bone cells is fluid shear stress rate dependent.* Biochem Biophys Res Commun, 2004. **315**(4): p. 823-9.

51. Klein-Nulend, J., et al., *Pulsating fluid flow increases nitric oxide (NO) synthesis by osteocytes but not periosteal fibroblasts--correlation with prostaglandin upregulation.* Biochem Biophys Res Commun, 1995. **217**(2): p. 640-8.

52. Jessop, H.L., et al., *Mechanical strain and fluid movement both activate extracellular regulated kinase (ERK) in osteoblast-like cells but via different signaling pathways.* Bone, 2002. **31**(1): p. 186-94.

53. Klees, R.F., et al., *Laminin-5 induces osteogenic gene expression in human mesenchymal stem cells through an ERK-dependent pathway.* Mol Biol Cell, 2005. **16**(2): p. 881-90.

54. Janmey, P.A. and C.A. McCulloch, *Cell mechanics: integrating cell responses to mechanical stimuli.* Annu Rev Biomed Eng, 2007. **9**: p. 1-34.

55. Whitfield, J.F., *The solitary (primary) cilium-A mechanosensory toggle switch in bone and cartilage cells.* Cell Signal, 2007. **8**: p. 8.

56. Rubin, C. and J. Rubin, *Biomechanics and mechanobiology of bone*, in *Primer on the Metabolic Bone Diseases and disorders of Mineral Metabolism*, M.J. Favus, Editor. 2006, American Society of Bone and Mineral Research. p. 36-48.

57. Duncan, R.L. and C.H. Turner, *Mechanotransduction and the functional response of bone to mechanical strain.* Calcif Tissue Int, 1995. **57**(5): p. 344-58.

58. Bassey EJ, R.S., *Increase in femoral bone density in young woman following high-impact exercise.* Osteoporosis Int, 1994. **4**: p. 72-75.

59. Firth, E.C., *The response of bone, articular cartilage and tendon to exercise in the horse.* J Anat, 2006. **208**(4): p. 513-26.

60. Lorentzon, M., D. Mellstrom, and C. Ohlsson, *Association of amount of physical activity with cortical bone size and trabecular volumetric BMD in young adult men: the GOOD study.* J Bone Miner Res, 2005. **20**(11): p. 1936-43.

61. Lange, U., et al., *Exercises and physiotherapeutic strategies for preventing and treating osteoporosis.* Eura Medicophys, 2005. **41**(2): p. 173-81.

62. Iwamoto, J., et al., *Effect of whole-body vibration exercise on lumbar bone mineral density, bone turnover, and chronic back pain in post-menopausal osteoporotic women treated with alendronate.* Aging Clin Exp Res, 2005. **17**(2): p. 157-63.

63. You, J., et al., *Substrate deformation levels associated with routine physical activity are less stimulatory to bone cells relative to loading-induced oscillatory fluid flow.* J Biomech Eng, 2000. **122**(4): p. 387-93.

64. Klein-Nulend, J., R.G. Bacabac, and M.G. Mullender, *Mechanobiology of bone tissue.* Pathol Biol (Paris), 2005. **53**(10): p. 576-80.

65. Sandy, J.R., et al., *Dual elevation of cyclic AMP and inositol phosphates in response to mechanical deformation of murine osteoblasts.* Biochim Biophys Acta, 1989. **1010**(2): p. 265-9.

66. Owan, I., et al., *Mechanotransduction in bone: osteoblasts are more responsive to fluid forces than mechanical strain.* Am J Physiol, 1997. **273**(3 Pt 1): p. C810-5.

67. Burr, D.B., et al., *In vivo measurement of human tibial strains during vigorous activity.* Bone, 1996. **18**(5): p. 405-10.

68. Dartsch, P.C. and E. Betz, *Response of cultured endothelial cells to mechanical stimulation.* Basic Res Cardiol, 1989. **84**(3): p. 268-81.

69. Johnson, D.L., T.N. McAllister, and J.A. Frangos, *Fluid flow stimulates rapid and continuous release of nitric oxide in osteoblasts.* Am J Physiol, 1996. **271**(1 Pt 1): p. E205-8.

70. Nagai, M., *The effects of prostaglandin E2 on DNA and collagen synthesis in osteoblasts in vitro.* Calcif Tissue Int, 1989. **44**(6): p. 411-20.

71. Hakeda, Y., et al., *Inductive effects of prostaglandins on alkaline phosphatase in osteoblastic cells, clone MC3T3-E1.* J Biochem (Tokyo), 1985. **97**(1): p. 97-104.

72. Jee, W.S. and Y.F. Ma, *The in vivo anabolic actions of prostaglandins in bone.* Bone, 1997. **21**(4): p. 297-304.

73. Jones, D.B., et al., *Biochemical signal transduction of mechanical strain in osteoblast-like cells.* Biomaterials, 1991. **12**(2): p. 101-10.

74. Mosley, J.R. and L.E. Lanyon, *Strain rate as a controlling influence on adaptive modeling in response to dynamic loading of the ulna in growing male rats.* Bone, 1998. **23**(4): p. 313-8.

75. Huang, C.Y., et al., *Effects of cyclic compressive loading on chondrogenesis of rabbit bone-marrow derived mesenchymal stem cells.* Stem Cells, 2004. **22**(3): p. 313-23.

76. Reilly, G.C. and J.D. Currey, *The development of microcracking and failure in bone depends on the loading mode to which it is adapted.* J Exp Biol, 1999. **202**(Pt 5): p. 543-52.

77. Tanaka, S.M., et al., *Effects of broad frequency vibration on cultured osteoblasts.* J Biomech, 2003. **36**(1): p. 73-80.

78. S H Cartmell, e.a., *Use of magnetic particles to apply mechanical forces for bone tissue engineering purposes.* Journal of physic: Conference Series, 2005. **17**: p. 77-80.

79. Yuge, L., et al., *Physical stress by magnetic force accelerates differentiation of human osteoblasts.* Biochem Biophys Res Commun, 2003. **311**(1): p. 32-8.

80. McGarry, J.G., et al., *A comparison of strain and fluid shear stress in stimulating bone cell responses--a computational and experimental study.* Faseb J, 2005. **19**(3): p. 482-4.

81. Vance, J., et al., *Mechanical stimulation of MC3T3 osteoblastic cells in a bone tissue-engineering bioreactor enhances prostaglandin E2 release.* Tissue Eng, 2005. **11**(11-12): p. 1832-9.

82. Kreke, M.R. and A.S. Goldstein, *Hydrodynamic shear stimulates osteocalcin expression but not proliferation of bone marrow stromal cells.* Tissue Eng, 2004. **10**(5-6): p. 780-8.

83. Lu, L., et al., *Effects of dynamic fluid pressure on chondrocytes cultured in biodegradable poly(glycolic acid) fibrous scaffolds.* Tissue Eng, 2005. **11**(11-12): p. 1852-9.

84. Datta, N., et al., *In vitro generated extracellular matrix and fluid shear stress synergistically enhance 3D osteoblastic differentiation.* Proc Natl Acad Sci U S A, 2006. **103**(8): p. 2488-93.

85. Mitsui, N., et al., *Optimal compressive force induces bone formation via increasing bone sialoprotein and prostaglandin E(2) production appropriately.* Life Sci, 2005. **77**(25): p. 3168-82.

86. Ignatius, A., et al., *Tissue engineering of bone: effects of mechanical strain on osteoblastic cells in type I collagen matrices.* Biomaterials, 2005. **26**(3): p. 311-8.

87. Duty, A.O., M.E. Oest, and R.E. Guldberg, *Cyclic mechanical compression increases mineralization of cell-seeded polymer scaffolds in vivo.* J Biomech Eng, 2007. **129**(4): p. 531-9.

88. Ozawa, H., et al., *Effect of a continuously applied compressive pressure on mouse osteoblast-like cells (MC3T3-E1) in vitro.* J Cell Physiol, 1990. **142**(1): p. 177-85.

89. Torzilli, P.A., et al., *Characterization of cartilage metabolic response to static and dynamic stress using a mechanical explant test system.* J Biomech, 1997. **30**(1): p. 1-9.

90. el Haj, A.J., et al., *Cellular responses to mechanical loading in vitro.* J Bone Miner Res, 1990. **5**(9): p. 923-32.

91. Brown, T.D., *Techniques for mechanical stimulation of cells in vitro: a review.* J Biomech, 2000. **33**(1): p. 3-14.

92. Jaasma, M.J. and F.J. O'Brien, *Mechanical stimulation of osteoblasts using steady and dynamic fluid flow.* Tissue Eng Part A, 2008. **23**: p. 23.

93. Bonewald, L.F., *Mechanosensation and Transduction in Osteocytes.* Bonekey Osteovision, 2006. **3**(10): p. 7-15.

94. Jacobs, C.R., et al., *Differential effect of steady versus oscillating flow on bone cells.* J Biomech, 1998. **31**(11): p. 969-76.

95. Engelmayr, G.C., Jr., et al., *Cyclic flexure and laminar flow synergistically accelerate mesenchymal stem cell-mediated engineered tissue formation: Implications for engineered heart valve tissues.* Biomaterials, 2006. **27**(36): p. 6083-95.

96. Jones, D.B., et al., *Development of a mechanical testing and loading system for trabecular bone studies for long term culture.* Eur Cell Mater, 2003. **5**: p. 48-59; discussion 59-60.

97. Kaspar, D., et al., *Dynamic cell stretching increases human osteoblast proliferation and CICP synthesis but decreases osteocalcin synthesis and alkaline phosphatase activity.* J Biomech, 2000. **33**(1): p. 45-51.

98. Zimmermann, H.D., *[Cilia in the fetal kidney of man].* Beitr Pathol, 1971. **143**(3): p. 227-40.

99. Whitfield, J.F., *Primary cilium--is it an osteocyte's strain-sensing flowmeter?* J Cell Biochem, 2003. **89**(2): p. 233-7.

100. Xiao, Z., et al., *Cilia-like structures and polycystin-1 in osteoblasts/osteocytes and associated abnormalities in skeletogenesis and Runx2 expression.* J Biol Chem, 2006. **281**(41): p. 30884-95.

101. Robert, A., et al., *The intraflagellar transport component IFT88/polaris is a centrosomal protein regulating G1-S transition in non-ciliated cells.* J Cell Sci, 2007. **120**(Pt 4): p. 628-37.

102. Wheatley, D.N., A.M. Wang, and G.E. Strugnell, *Expression of primary cilia in mammalian cells.* Cell Biol Int, 1996. **20**(1): p. 73-81.

103. Alieva, I.B. and I.A. Vorobjev, *Vertebrate primary cilia: a sensory part of centrosomal complex in tissue cells, but a "sleeping beauty" in cultured cells?* Cell Bio. Int. , 2004. **28**: p. 139-150.

104. Praetorius, H.A. and K.R. Spring, *A physiological view of the primary cilium.* Annu Rev Physiol, 2005. **67**: p. 515-29.

105. Jensen, C.G., et al., *Ultrastructural, tomographic and confocal imaging of the chondrocyte primary cilium in situ.* Cell Biol Int, 2004. **28**: p. 101-10.

106. Zhang, Q., et al., *Loss of the Tg737 protein results in skeletal patterning defects.* Dev Dyn, 2003. **227**(1): p. 78-90.

107. Murcia, N.S., et al., *The Oak Ridge Polycystic Kidney (orpk) disease gene is required for left-right axis determination.* Development, 2000. **127**(11): p. 2347-55.

108. Taulman, P.D., et al., *Polaris, a protein involved in left-right axis patterning, localizes to basal bodies and cilia.* Mol Biol Cell, 2001. **12**(3): p. 589-99.

109. Pazour, G.J., et al., *Chlamydomonas IFT88 and its mouse homologue, polycystic kidney disease gene tg737, are required for assembly of cilia and flagella.* J Cell Biol, 2000. **151**(3): p. 709-18.

110. Cole, D.G., et al., *Chlamydomonas kinesin-II-dependent intraflagellar transport (IFT): IFT particles contain proteins required for ciliary assembly in Caenorhabditis elegans sensory neurons.* J Cell Biol, 1998. **141**(4): p. 993-1008.

111. Qin, H., J.L. Rosenbaum, and M.M. Barr, *An autosomal recessive polycystic kidney disease gene homolog is involved in intraflagellar transport in C. elegans ciliated sensory neurons.* Curr Biol, 2001. **11**(6): p. 457-61.

112. Yoder, B.K., X. Hou, and L.M. Guay-Woodford, *The polycystic kidney disease proteins, polycystin-1, polycystin-2, polaris, and cystin, are co-localized in renal cilia.* J Am Soc Nephrol, 2002. **13**(10): p. 2508-16.

113. Hildebrandt, F. and E. Otto, *Cilia and centrosomes: a unifying pathogenic concept for cystic kidney disease?* Nat Rev Genet, 2005. **6**(12): p. 928-40.

114. Torres, V.E. and P.C. Harris, *Mechanisms of Disease: autosomal dominant and recessive polycystic kidney diseases.* Nat Clin Pract Nephrol, 2006. **2**(1): p. 40-55; quiz 55.

115. Praetorius, H.A. and K.R. Spring, *The renal cell primary cilium functions as a flow sensor.* Curr Opin Nephrol Hypertens, 2003. **12**(5): p. 517-20.

116. Praetorius, H.A. and K.R. Spring, *Removal of the MDCK cell primary cilium abolishes flow sensing.* J Membr Biol, 2003. **191**(1): p. 69-76.

117. Nauli, S.M., et al., *Polycystins 1 and 2 mediate mechanosensation in the primary cilium of kidney cells.* Nat Genet, 2003. **33**(2): p. 129-37.

118. Malone, A.M., et al., *Primary cilia mediate mechanosensing in bone cells by a calcium-independent mechanism.* Proc Natl Acad Sci U S A, 2007. **104**(33): p. 13325-30.

119. Wang, Y., et al., *Application of perfusion culture system improves in vitro and in vivo osteogenesis of bone marrow-derived osteoblastic cells in porous ceramic materials.* Tissue Eng, 2003. **9**(6): p. 1205-14.

120. Carter, D.R., P.R. Blenman, and G.S. Beaupre, *Correlations between mechanical stress history and tissue differentiation in initial fracture healing.* J Orthop Res, 1988. **6**(5): p. 736-48.

121. Batra, N.N., et al., *Effects of short-term recovery periods on fluid-induced signaling in osteoblastic cells.* J Biomech, 2005. **38**(9): p. 1909-17.

122. Prendergast, P.J., R. Huiskes, and K. Soballe, *ESB Research Award 1996. Biophysical stimuli on cells during tissue differentiation at implant interfaces.* J Biomech, 1997. **30**(6): p. 539-48.

123. Hing, K.A., *Maximising Osseointegration; Unique Bone Grafting Solutions for Different Surgical Applications.* Orthopedic Product News, 2003: p. 58-60.

124. Ishaug, S.L., et al., *Bone formation by three-dimensional stromal osteoblast culture in biodegradable polymer scaffolds.* J Biomed Mater Res, 1997. **36**(1): p. 17-28.

125. Griffith, L.G. and G. Naughton, *Tissue engineering--current challenges and expanding opportunities.* Science, 2002. **295**(5557): p. 1009-14.

126. Fassina, L., et al., *Calcified matrix production by SAOS-2 cells inside a polyurethane porous scaffold, using a perfusion bioreactor.* Tissue Eng, 2005. **11**(5-6): p. 685-700.

127. Curry, J., *Concerns raised about quality of banked bone.* OR Manager, 1994. **10**(2): p. 1, 6-9.

128. Ryan, G., A. Pandit, and D.P. Apatsidis, *Fabrication methods of porous metals for use in orthopaedic applications.* Biomaterials, 2006. **27**(13): p. 2651-70.

129. Cehreli, M.C. and K. Akca, *Mechanobiology of bone and mechanocoupling of endosseous titanium oral implants.* J Long Term Eff Med Implants, 2005. **15**(2): p. 139-52.

130. Konttinen, Y.T., et al., *The microenvironment around total hip replacement prostheses.* Clin Orthop Relat Res, 2005(430): p. 28-38.

131. Riminucci, M. and P. Bianco, *Building bone tissue: matrices and scaffolds in physiology and biotechnology.* Braz J Med Biol Res, 2003. **36**(8): p. 1027-36.

132. Wiesmann, H.P., U. Joos, and U. Meyer, *Biological and biophysical principles in extracorporal bone tissue engineering. Part II.* Int J Oral Maxillofac Surg, 2004. **33**(6): p. 523-30.

133. Cartmell, S.H., et al., *Effects of medium perfusion rate on cell-seeded three-dimensional bone constructs in vitro.* Tissue Eng, 2003. **9**(6): p. 1197-203.

134. Paolo Bianco, P.G.R., *Stem cells in tissue engineering.* Nature, 2001. **414**: p. 118-121.

135. Blau, H.M., T.R. Brazelton, and J.M. Weimann, *The evolving concept of a stem cell: entity or function?* Cell, 2001. **105**(7): p. 829-41.

136. Alison, M.R., et al., *An introduction to stem cells.* J Pathol, 2002. **197**(4): p. 419-23.

137. Annie John, Y.I., Yasuhiko Tabata, *Tissue engineered bone and adipose tissue - An in vitro study.* Trends Biomater. Artif. Organs., 2002. **16**(1): p. 28-33.

138. Mauney, J.R., et al., *Mechanical stimulation promotes osteogenic differentiation of human bone marrow stromal cells on 3-D partially demineralized bone scaffolds in vitro.* Calcif Tissue Int, 2004. **74**(5): p. 458-68.

139. Long, M.W., et al., *Regulation of human bone marrow-derived osteoprogenitor cells by osteogenic growth factors.* J Clin Invest, 1995. **95**(2): p. 881-7.

140. Hwang, W.S., et al., *Evidence of a pluripotent human embryonic stem cell line derived from a cloned blastocyst.* Science, 2004. **303**(5664): p. 1669-74.

141. Trounson, A., *Human embryonic stem cells: mother of all cell and tissue types.* Reprod Biomed Online, 2002. **4 Suppl 1**: p. 58-63.

142. Heng, B.C., et al., *Strategies for directing the differentiation of stem cells into the osteogenic lineage in vitro.* J Bone Miner Res, 2004. **19**(9): p. 1379-94.

143. Hutmacher, D.W., *Scaffolds in tissue engineering bone and cartilage.* Biomaterials, 2000. **21**(24): p. 2529-43.

144. Gorna, K. and S. Gogolewski, *Biodegradable polyurethanes for implants. II. In vitro degradation and calcification of materials from poly(epsilon-caprolactone)-poly(ethylene oxide) diols and various chain extenders.* J Biomed Mater Res, 2002. **60**(4): p. 592-606.

145. Gorna, K. and S. Gogolewski, *Preparation, degradation, and calcification of biodegradable polyurethane foams for bone graft substitutes.* J Biomed Mater Res A, 2003. **67**(3): p. 813-27.

146. Zhang, J., et al., *A biodegradable polyurethane-ascorbic acid scaffold for bone tissue engineering.* J Biomed Mater Res A, 2003. **67**(2): p. 389-400.

147. Grad, S., et al., *The use of biodegradable polyurethane scaffolds for cartilage tissue engineering: potential and limitations.* Biomaterials, 2003. **24**(28): p. 5163-71.

148. Goldstein, A.S., et al., *Effect of convection on osteoblastic cell growth and function in biodegradable polymer foam scaffolds.* Biomaterials, 2001. **22**(11): p. 1279-88.

149. Sumanasinghe, R.D., S.H. Bernacki, and E.G. Loboa, *Osteogenic differentiation of human mesenchymal stem cells in collagen matrices: effect of uniaxial cyclic tensile strain on bone morphogenetic protein (BMP-2) mRNA expression.* Tissue Eng, 2006. **12**(12): p. 3459-65.

150. Shih, Y.R., et al., *Growth of mesenchymal stem cells on electrospun type I collagen nanofibers.* Stem Cells, 2006. **24**(11): p. 2391-7.

151. Farrell, E., et al., *A collagen-glycosaminoglycan scaffold supports adult rat mesenchymal stem cell differentiation along osteogenic and chondrogenic routes.* Tissue Eng, 2006. **12**(3): p. 459-68.

152. Jungreuthmayer, C., et al., *Deformation simulation of cells seeded on a collagen-GAG scaffold in a flow perfusion bioreactor using a sequential 3D CFD-elastostatics model.* Med Eng Phys, 2009. **31**(4): p. 420-427.

153. Jungreuthmayer, C., et al., *A Comparative Study of Shear Stresses in Collagen-Glycosaminoglycan and Calcium Phosphate Scaffolds in Bone Tissue-Engineering Bioreactors.* Tissue Eng Part A, 2008. **2**: p. 2.

154. Farrell, E., et al., *A comparison of the osteogenic potential of adult rat mesenchymal stem cells cultured in 2-D and on 3-D collagen glycosaminoglycan scaffolds.* Technol Health Care, 2007. **15**(1): p. 19-31.

155. Tayapongsak, P., et al., *Autologous fibrin adhesive in mandibular reconstruction with particulate cancellous bone and marrow.* J Oral Maxillofac Surg, 1994. **52**(2): p. 161-5; discussion 166.

156. Brekke, J.H. and J.M. Toth, *Principles of tissue engineering applied to programmable osteogenesis.* J Biomed Mater Res, 1998. **43**(4): p. 380-98.

157. Solchaga, L.A., et al., *Hyaluronic acid-based polymers as cell carriers for tissue-engineered repair of bone and cartilage.* J Orthop Res, 1999. **17**(2): p. 205-13.

158. Kumarasuriyar, A., et al., *Poly(beta-hydroxybutyrate-co-beta-hydroxyvalerate) supports in vitro osteogenesis.* Tissue Eng, 2005. **11**(7-8): p. 1281-95.

159. St-Pierre, J.P., et al., *Three-dimensional growth of differentiating MC3T3-E1 pre-osteoblasts on porous titanium scaffolds.* Biomaterials, 2005. **26**(35): p. 7319-28.

160. Saruwatari, L., et al., *Osteoblasts generate harder, stiffer, and more delamination-resistant mineralized tissue on titanium than on polystyrene, associated with distinct tissue micro- and ultrastructure.* J Bone Miner Res, 2005. **20**(11): p. 2002-16.

161. Sikavitsas, V.I., et al., *Flow perfusion enhances the calcified matrix deposition of marrow stromal cells in biodegradable nonwoven fiber mesh scaffolds.* Ann Biomed Eng, 2005. **33**(1): p. 63-70.

162. Ichinohe, N., T. Takamoto, and Y. Tabata, *Proliferation, osteogenic differentiation, and distribution of rat bone marrow stromal cells in nonwoven fabrics by different culture methods.* Tissue Eng Part A, 2008. **14**(1): p. 107-16.

163. Cordewener, F.W. and J.P. Schmitz, *The future of biodegradable osteosyntheses.* Tissue Eng, 2000. **6**(4): p. 413-24.

164. Yang, X.B., et al., *Human osteoprogenitor growth and differentiation on synthetic biodegradable structures after surface modification.* Bone, 2001. **29**(6): p. 523-31.

165. Sikavitsas, V.I., G.N. Bancroft, and A.G. Mikos, *Formation of three-dimensional cell/polymer constructs for bone tissue engineering in a spinner flask and a rotating wall vessel bioreactor.* J Biomed Mater Res, 2002. **62**(1): p. 136-48.

166. Eichenlaub-Ritter, U. and I. Betzendahl, *Chloral hydrate induced spindle aberrations, metaphase I arrest and aneuploidy in mouse oocytes.* Mutagenesis, 1995. **10**(6): p. 477-86.

167. Reilly, G.C., et al., *Differential alkaline phosphatase responses of rat and human bone marrow derived mesenchymal stem cells to 45S5 bioactive glass.* Biomaterials, 2007. **28**(28): p. 4091-7.

168. Ducheyne, P. and Q. Qiu, *Bioactive ceramics: the effect of surface reactivity on bone formation and bone cell function.* Biomaterials, 1999. **20**(23-24): p. 2287-303.

169. Hench, L.L. and H.A. Paschall, *Direct chemical bond of bioactive glass-ceramic materials to bone and muscle.* J Biomed Mater Res, 1973. **7**(3): p. 25-42.

170. Hench, L.L., *Biomaterials: a forecast for the future.* Biomaterials, 1998. **19**(16): p. 1419-23.

171. Yoshikawa, H., et al., *Interconnected porous hydroxyapatite ceramics for bone tissue engineering.* J R Soc Interface, 2008. **23**: p. 23.

172. Kamitakahara, M., C. Ohtsuki, and T. Miyazaki, *Review paper: behavior of ceramic biomaterials derived from tricalcium phosphate in physiological condition.* J Biomater Appl, 2008. **23**(3): p. 197-212.

173. Lee, C.R., et al., *Fibrin-polyurethane composites for articular cartilage tissue engineering: a preliminary analysis.* Tissue Eng, 2005. **11**(9-10): p. 1562-73.

174. Guelcher, S.A., et al., *Synthesis and in vitro biocompatibility of injectable polyurethane foam scaffolds.* Tissue Eng, 2006. **12**(5): p. 1247-59.

175. Liu, Y., et al., *Composite articular cartilage engineered on a chondrocyte-seeded aliphatic polyurethane sponge.* Tissue Eng, 2004. **10**(7-8): p. 1084-92.

176. Ramrattan, N.N., et al., *Assessment of tissue ingrowth rates in polyurethane scaffolds for tissue engineering.* Tissue Eng, 2005. **11**(7-8): p. 1212-23.

177. Zanetta, M., et al., *Ability of polyurethane foams to support cell proliferation and the differentiation of MSCs into osteoblasts.* Acta Biomater, 2008. **24**: p. 24.

178. Santerre, J.P., et al., *Understanding the biodegradation of polyurethanes: from classical implants to tissue engineering materials.* Biomaterials, 2005. **26**(35): p. 7457-70.

179. Stokes, K., R. McVenes, and J.M. Anderson, *Polyurethane elastomer biostability.* J Biomater Appl, 1995. **9**(4): p. 321-54.

180. Phillips, R.E., M.C. Smith, and R.J. Thoma, *Biomedical applications of polyurethanes: implications of failure mechanisms.* J Biomater Appl, 1988. **3**(2): p. 207-27.

181. Santerre, J.P., et al., *Biodegradation evaluation of polyether and polyester-urethanes with oxidative and hydrolytic enzymes.* J Biomed Mater Res, 1994. **28**(10): p. 1187-99.

182. Slade, C.L. and H.D. Peterson, *Disappearance of the polyurethane cover of the Ashley Natural Y prosthesis.* Plast Reconstr Surg, 1982. **70**(3): p. 379-83.

183. Labow, R.S., E. Meek, and J.P. Santerre, *The biodegradation of poly(urethane)s by the esterolytic activity of serine proteases and oxidative enzyme systems.* J Biomater Sci Polym Ed, 1999. **10**(7): p. 699-713.

184. Leong, K.F., C.M. Cheah, and C.K. Chua, *Solid freeform fabrication of three-dimensional scaffolds for engineering replacement tissues and organs.* Biomaterials, 2003. **24**(13): p. 2363-78.

185. Ratcliffe, A. and L.E. Niklason, *Bioreactors and bioprocessing for tissue engineering.* Ann N Y Acad Sci, 2002. **961**: p. 210-5.

186. Martin, Y. and P. Vermette, *Bioreactors for tissue mass culture: design, characterization, and recent advances.* Biomaterials, 2005. **26**(35): p. 7481-503.

187. Portner, R., et al., *Bioreactor design for tissue engineering.* J Biosci Bioeng, 2005. **100**(3): p. 235-45.

188. Lappa, M., *Organic tissues in rotating bioreactors: fluid-mechanical aspects, dynamic growth models, and morphological evolution.* Biotechnol Bioeng, 2003. **84**(5): p. 518-32.

189. Meyer, U., U. Joos, and H.P. Wiesmann, *Biological and biophysical principles in extracorporal bone tissue engineering. Part III.* Int J Oral Maxillofac Surg, 2004. **33**(7): p. 635-41.

190. Jaasma, M.J., N.A. Plunkett, and F.J. O'Brien, *Design and validation of a dynamic flow perfusion bioreactor for use with compliant tissue engineering scaffolds.* J Biotechnol, 2008. **133**(4): p. 490-6.

191. Yu, X., et al., *Bioreactor-based bone tissue engineering: the influence of dynamic flow on osteoblast phenotypic expression and matrix mineralization.* Proc Natl Acad Sci U S A, 2004. **101**(31): p. 11203-8.

192. Kato, Y., et al., *Establishment of an osteoid preosteocyte-like cell MLO-A5 that spontaneously mineralizes in culture.* J Bone Miner Res, 2001. **16**(9): p. 1622-33.

193. Wall, M.E., S.H. Bernacki, and E.G. Loboa, *Effects of serial passaging on the adipogenic and osteogenic differentiation potential of adipose-derived human mesenchymal stem cells.* Tissue Eng, 2007. **13**(6): p. 1291-8.

194. Mosmann, T., *Rapid colorimetric assay for cellular growth and survival: application to proliferation and cytotoxicity assays.* J Immunol Methods, 1983. **65**(1-2): p. 55-63.

195. Ng, K.W., D.T. Leong, and D.W. Hutmacher, *The challenge to measure cell proliferation in two and three dimensions.* Tissue Eng, 2005. **11**(1-2): p. 182-91.

196. Gregory, C.A., et al., *An Alizarin red-based assay of mineralization by adherent cells in culture: comparison with cetylpyridinium chloride extraction.* Anal Biochem, 2004. **329**(1): p. 77-84.

197. Tullberg-Reinert, H. and G. Jundt, *In situ measurement of collagen synthesis by human bone cells with a sirius red-based colorimetric microassay: effects of transforming growth factor beta2 and ascorbic acid 2-phosphate.* Histochem Cell Biol, 1999. **112**(4): p. 271-6.

198. Stirling, J.M.S.B.a.D., *Methods in Molecular Biology.* second ed. PCR Protocols. Vol. 226, Totowa, NJ: Humana Press Inc. 525.

199. Aki, T., S. Yanagisawa, and H. Akanuma, *Identification and characterization of positive regulatory elements in the human glyceraldehyde 3-phosphate dehydrogenase gene promoter.* J Biochem, 1997. **122**(2): p. 271-8.

200. Noth, U., et al., *In vitro engineered cartilage constructs produced by press-coating biodegradable polymer with human mesenchymal stem cells.* Tissue Eng, 2002. **8**(1): p. 131-44.

201. Wong, M.L. and J.F. Medrano, *Real-time PCR for mRNA quantitation.* Biotechniques, 2005. **39**(1): p. 75-85.

202. Coleman, A.W., *Use of the fluorochrome 4'6-diamidino-2-phenylindole in genetic and developmental studies of chloroplast DNA.* J Cell Biol, 1979. **82**(1): p. 299-305.

203. Kepner, R.L., Jr. and J.R. Pratt, *Use of fluorochromes for direct enumeration of total bacteria in environmental samples: past and present.* Microbiol Rev, 1994. **58**(4): p. 603-15.

204. Dunlap, K., *Localization of calcium channels in Paramecium caudatum.* J Physiol, 1977. **271**(1): p. 119-33.

205. Chakrabarti, A., et al., *Chloral hydrate alters the organization of the ciliary basal apparatus and cell organelles in sea urchin embryos.* Cell Tissue Res, 1998. **293**(3): p. 453-62.

206. Bantounas, I., L.A. Phylactou, and J.B. Uney, *RNA interference and the use of small interfering RNA to study gene function in mammalian systems.* J Mol Endocrinol, 2004. **33**(3): p. 545-57.

207. Robling, A.G., et al., *Mechanical stimulation of bone in vivo reduces osteocyte expression of Sost/sclerostin.* J Biol Chem, 2008. **283**(9): p. 5866-75.

208. Noble, B.S., et al., *Mechanical loading: biphasic osteocyte survival and targeting of osteoclasts for bone destruction in rat cortical bone.* Am J Physiol Cell Physiol, 2003. **284**(4): p. C934-43.

209. Lewinson, D., et al., *Stimulation of Fos- and Jun-related genes during distraction osteogenesis.* J Histochem Cytochem, 2003. **51**(9): p. 1161-8.

210. O'Brien, F.J., et al., *The effect of pore size on permeability and cell attachment in collagen scaffolds for tissue engineering.* Technol Health Care, 2007. **15**(1): p. 3-17.

211. Heijkants, R.G., et al., *Design, synthesis and properties of a degradable polyurethane scaffold for meniscus regeneration.* J Mater Sci Mater Med, 2004. **15**(4): p. 423-7.

212. Karageorgiou, V. and D. Kaplan, *Porosity of 3D biomaterial scaffolds and osteogenesis.* Biomaterials, 2005. **26**(27): p. 5474-91.

213. Chung, C.H., et al., *Mechanism of action of beta-glycerophosphate on bone cell mineralization.* Calcif Tissue Int, 1992. **51**(4): p. 305-11.

214. Sun, T., et al., *Culture of skin cells in 3D rather than 2D improves their ability to survive exposure to cytotoxic agents.* J Biotechnol, 2006. **122**(3): p. 372-81.

215. Tanaka, S.M., et al., *Osteoblast responses one hour after load-induced fluid flow in a three-dimensional porous matrix.* Calcif Tissue Int, 2005. **76**(4): p. 261-71.

216. Grayson, W.L., et al., *Effects of initial seeding density and fluid perfusion rate on formation of tissue-engineered bone.* Tissue Eng Part A, 2008. **14**(11): p. 1809-20.

217. Barralet, J.E., et al., *Comparison of bone marrow cell growth on 2D and 3D alginate hydrogels.* J Mater Sci Mater Med, 2005. **16**(6): p. 515-9.

218. Strehl, R., et al., *Proliferating cells versus differentiated cells in tissue engineering.* Tissue Eng, 2002. **8**(1): p. 37-42.

219. Huminiecki, L., et al., *Magic roundabout is a new member of the roundabout receptor family that is endothelial specific and expressed at sites of active angiogenesis.* Genomics, 2002. **79**(4): p. 547-52.

220. Suchting, S., et al., *Soluble Robo4 receptor inhibits in vivo angiogenesis and endothelial cell migration.* Faseb J, 2005. **19**(1): p. 121-3.

221. Clarke DA, et al., *Polyurethane scaffolds for long term mechanical loading in musculoskeletal tissue engineering.* Tissue engineering 2007. **13**(7): p. 1743.

222. Bonzani, I.C., et al., *Synthesis of two-component injectable polyurethanes for bone tissue engineering.* Biomaterials, 2007. **28**(3): p. 423-33.

223. Verdejo, R., et al., *Reactive polyurethane carbon nanotube foams and their interactions with osteoblasts.* J Biomed Mater Res A, 2009. **88**(1): p. 65-73.

224. Meyer, U., et al., *Design and performance of a bioreactor system for mechanically promoted three-dimensional tissue engineering.* Br J Oral Maxillofac Surg, 2006. **44**(2): p. 134-40.

225. Vunjak-Novakovic, G.e.a., *Dynamic cell seeding of polymer scaffolds for cartilage tissue engineering.* Biotechnol. prog., 1998. **14**: p. 193-202.

226. Shearn, J., L. Hellmann, and G. Boivin, *Effect of initial cell-seeding density on postoperative cell number and dispersion.* Tissue Eng, 2005. **11**(11-12): p. 1898-904.

227. Botchwey, E.A., et al., *Tissue engineered bone: measurement of nutrient transport in three-dimensional matrices.* J Biomed Mater Res A, 2003. **67**(1): p. 357-67.

228. Rubin, J., C. Rubin, and C.R. Jacobs, *Molecular pathways mediating mechanical signaling in bone.* Gene, 2006. **367**: p. 1-16.

229. Cullinane, D.M., et al., *Effects of the local mechanical environment on vertebrate tissue differentiation during repair: does repair recapitulate development?* J Exp Biol, 2003. **206**(Pt 14): p. 2459-71.

230. Smith-Adaline, E.A., et al., *Mechanical environment alters tissue formation patterns during fracture repair.* J Orthop Res, 2004. **22**(5): p. 1079-85.

231. Clark, P.A., et al., *Modulation of bone ingrowth of rabbit femur titanium implants by in vivo axial micromechanical loading.* J Appl Physiol, 2005. **98**(5): p. 1922-9.

232. Rubin, C.T. and L.E. Lanyon, *Regulation of bone mass by mechanical strain magnitude.* Calcif Tissue Int, 1985. **37**(4): p. 411-7.

233. Pedersen, E.A., et al., *Bone response to in vivo mechanical loading in C3H/HeJ mice.* Calcif Tissue Int, 1999. **65**(1): p. 41-6.

234. Knothe Tate, M.L., et al., *In vivo demonstration of load-induced fluid flow in the rat tibia and its potential implications for processes associated with functional adaptation.* J Exp Biol, 2000. **203**(Pt 18): p. 2737-45.

235. Bacabac, R.G., et al., *Round versus flat: Bone cell morphology, elasticity, and mechanosensing.* J Biomech, 2008. **41**(7): p. 1590-8.

236. Cukierman, E., et al., *Taking cell-matrix adhesions to the third dimension.* Science, 2001. **294**(5547): p. 1708-12.

237. Jarrahy, R., et al., *Osteogenic differentiation is inhibited and angiogenic expression is enhanced in MC3T3-E1 cells cultured on three-dimensional scaffolds.* Am J Physiol Cell Physiol, 2005. **289**(2): p. C408-14.

238. Freed, L.E., et al., *Advanced tools for tissue engineering: scaffolds, bioreactors, and signaling.* Tissue Eng, 2006. **12**(12): p. 3285-305.

239. Jagodzinski, M., et al., *Influence of perfusion and cyclic compression on proliferation and differentiation of bone marrow stromal cells in 3-dimensional culture.* J Biomech, 2008. **41**(9): p. 1885-91.

240. Diederichs, S., F. Freiberger, and M. van Griensven, *Effects of repetitive and short time strain in human bone marrow stromal cells.* J Biomed Mater Res A, 2008. **2**: p. 2.

241. Burr, D.B., et al., *In vivo measurement of human tibial strains during vigorous activity.* Bone, 1996. **15**(5): p. 405-10.

242. Donahue, T.L., et al., *Mechanosensitivity of bone cells to oscillating fluid flow induced shear stress may be modulated by chemotransport.* J Biomech, 2003. **36**(9): p. 1363-71.

243. Pedersen, J.A. and M.A. Swartz, *Mechanobiology in the third dimension.* Ann Biomed Eng, 2005. **33**(11): p. 1469-90.

244. King, G.J., S.D. Keeling, and T.J. Wronski, *Histomorphometric study of alveolar bone turnover in orthodontic tooth movement.* Bone, 1991. **12**(6): p. 401-9.

245. Sittichokechaiwut A., C.D., Ryan A.J., Reilly G. C., *Mechanical Stimulation of Osteoblastic Cells in 3-Dimensional Polyurethane foam Scaffolds.* Journal of Bone and Mineral Research 2006. **21. suppl.**: p. s373.

246. Rath Bonivtch, A., L.F. Bonewald, and D.P. Nicolella, *Tissue strain amplification at the osteocyte lacuna: A microstructural finite element analysis.* J Biomech, 2006. **29**: p. 29.

247. Nicolella, D.P., et al., *Measurement of microstructural strain in cortical bone.* Eur J Morphol, 2005. **42**(1-2): p. 23-9.

248. Claes, L.E. and C.A. Heigele, *Magnitudes of local stress and strain along bony surfaces predict the course and type of fracture healing.* J Biomech, 1999. **32**(3): p. 255-66.

249. Kraynik, A.M., *Foam structure: From soap froth to solid foams.* MRS Bulletin, 2003. **28**(4): p. 275-278.

250. Hori, R.Y. and J.L. Lewis, *Mechanical properties of the fibrous tissue found at the bone-cement interface following total joint replacement.* J Biomed Mater Res, 1982. **16**(6): p. 911-27.

251. Lacroix, D. and P.J. Prendergast, *A mechano-regulation model for tissue differentiation during fracture healing: analysis of gap size and loading.* J Biomech, 2002. **35**(9): p. 1163-71.

252. Judex, S., et al., *Low-magnitude mechanical signals that stimulate bone formation in the ovariectomized rat are dependent on the applied frequency but not on the strain magnitude.* J Biomech, 2007. **40**(6): p. 1333-9.

253. Cowie, R., R.D. Walker, and A. Scutt, *The use of high-frequency, low-intensity vibration to stimulate the proliferation and differentiation of primary rat bone marrow cells.* Cytotherapy, 2006. **8**: p. 63-63.

254. Robling, A.G., D.B. Burr, and C.H. Turner, *Partitioning a daily mechanical stimulus into discrete loading bouts improves the osteogenic response to loading.* J Bone Miner Res, 2000. **15**(8): p. 1596-602.

255. Robling, A.G., et al., *Improved bone structure and strength after long-term mechanical loading is greatest if loading is separated into short bouts.* J Bone Miner Res, 2002. **17**(8): p. 1545-54.

256. Riddle, R.C., K.R. Hippe, and H.J. Donahue, *Chemotransport contributes to the effect of oscillatory fluid flow on human bone marrow stromal cell proliferation.* J Orthop Res, 2008. **26**(7): p. 918-24.

257. Zahm, A.M., et al., *Oxygen tension regulates preosteocyte maturation and mineralization.* Bone, 2008. **43**(1): p. 25-31.

258. Stevens, M.M. and J.H. George, *Exploring and engineering the cell surface interface.* Science, 2005. **310**(5751): p. 1135-8.

259. Ghosh-Choudhury, N., et al., *Immortalized murine osteoblasts derived from BMP 2-T-antigen expressing transgenic mice.* Endocrinology, 1996. **137**(1): p. 331-9.

260. Harris, S.E., et al., *Effects of transforming growth factor beta on bone nodule formation and expression of bone morphogenetic protein 2, osteocalcin, osteopontin, alkaline phosphatase, and type I collagen mRNA in long-term cultures of fetal rat calvarial osteoblasts.* J Bone Miner Res, 1994. **9**(6): p. 855-63.

261. Kinoshita, S., et al., *Three-dimensional collagen gel culture promotes osteoblastic phenotype in bone marrow derived cells.* Kobe J Med Sci, 1999. **45**(5): p. 201-11.

262. Pavlin, D., R. Zadro, and J. Gluhak-Heinrich, *Temporal pattern of stimulation of osteoblast-associated genes during mechanically-induced osteogenesis in vivo: early responses of osteocalcin and type I collagen.* Connect Tissue Res, 2001. **42**(2): p. 135-48.

263. Harter, L.V., K.A. Hruska, and R.L. Duncan, *Human osteoblast-like cells respond to mechanical strain with increased bone matrix protein production independent of hormonal regulation.* Endocrinology, 1995. **136**(2): p. 528-35.

264. Gerstenfeld, L.C., *Osteopontin in skeletal tissue homeostasis: An emerging picture of the autocrine/paracrine functions of the extracellular matrix.* J Bone Miner Res, 1999. **14**(6): p. 850-5.

265. Toma, C.D., et al., *Signal transduction of mechanical stimuli is dependent on microfilament integrity: identification of osteopontin as a mechanically induced gene in osteoblasts.* J Bone Miner Res, 1997. **12**(10): p. 1626-36.

266. Denhardt, D.T., et al., *Osteopontin as a means to cope with environmental insults: regulation of inflammation, tissue remodeling, and cell survival.* J Clin Invest, 2001. **107**(9): p. 1055-61.

267. Aubin, J.E., et al., *Osteoblast and chondroblast differentiation.* Bone, 1995. **17**(2 Suppl): p. 77S-83S.

268. Weinbaum, S., S.C. Cowin, and Y. Zeng, *A model for the excitation of osteocytes by mechanical loading-induced bone fluid shear stresses.* J Biomech, 1994. **27**(3): p. 339-60.

269. You, L.D., et al., *Ultrastructure of the osteocyte process and its pericellular matrix.* Anat Rec A Discov Mol Cell Evol Biol, 2004. **278**(2): p. 505-13.

270. Praetorius, H.A. and K.R. Spring, *Bending the MDCK cell primary cilium increases intracellular calcium.* J Membr Biol, 2001. **184**(1): p. 71-9.

271. Jackson, A.L., et al., *Expression profiling reveals off-target gene regulation by RNAi.* Nat Biotechnol, 2003. **21**(6): p. 635-7.

272. Scacheri, P.C., et al., *Short interfering RNAs can induce unexpected and divergent changes in the levels of untargeted proteins in mammalian cells.* Proc Natl Acad Sci U S A, 2004. **101**(7): p. 1892-7.

273. Giannoudis, P.V., H. Dinopoulos, and E. Tsiridis, *Bone substitutes: an update.* Injury, 2005. **36 Suppl 3**(3): p. S20-7.

274. Vaccaro, A.R., et al., *Bone grafting alternatives in spinal surgery.* Spine J, 2002. **2**(3): p. 206-15.

275. Mankin, H.J., et al., *Long-term results of allograft replacement in the management of bone tumors.* Clin Orthop Relat Res, 1996. **324**(324): p. 86-97.

276. Roth, C.C. and B.P. Kropp, *Recent advances in urologic tissue engineering.* Curr Urol Rep, 2009. **10**(2): p. 119-25.

277. Omori, K., et al., *Clinical application of in situ tissue engineering using a scaffolding technique for reconstruction of the larynx and trachea.* Ann Otol Rhinol Laryngol, 2008. **117**(9): p. 673-8.

278. Meinel, L., et al., *Bone tissue engineering using human mesenchymal stem cells: effects of scaffold material and medium flow.* Ann Biomed Eng, 2004. **32**(1): p. 112-22.

279. Kreke, M.R., et al., *Effect of intermittent shear stress on mechanotransductive signaling and osteoblastic differentiation of bone marrow stromal cells.* Tissue Eng Part A, 2008. **14**(4): p. 529-37.

280. Weissman, I.L., *Translating stem and progenitor cell biology to the clinic: barriers and opportunities.* Science, 2000. **287**(5457): p. 1442-6.

281. Bianco, P., et al., *Postnatal skeletal stem cells.* Methods Enzymol, 2006. **419**: p. 117-48.

282. Robey, P.G. and P. Bianco, *The use of adult stem cells in rebuilding the human face.* J Am Dent Assoc, 2006. **137**(7): p. 961-72.

283. Lecoeur, L. and J.P. Ouhayoun, *In vitro induction of osteogenic differentiation from non-osteogenic mesenchymal cells.* Biomaterials, 1997. **18**(14): p. 989-93.

284. Yoshikawa, T., H. Ohgushi, and S. Tamai, *Immediate bone forming capability of prefabricated osteogenic hydroxyapatite.* J Biomed Mater Res, 1996. **32**(3): p. 481-92.

285. Aubin, J.E., *Osteoprogenitor cell frequency in rat bone marrow stromal populations: role for heterotypic cell-cell interactions in osteoblast differentiation.* J Cell Biochem, 1999. **72**(3): p. 396-410.

286. Peter, S.J., et al., *Osteoblastic phenotype of rat marrow stromal cells cultured in the presence of dexamethasone, beta-glycerolphosphate, and L-ascorbic acid.* J Cell Biochem, 1998. **71**(1): p. 55-62.

287. Dieudonne, S.C., et al., *Differential display of human marrow stromal cells reveals unique mRNA expression patterns in response to dexamethasone.* J Cell Biochem, 1999. **76**(2): p. 231-43.

288. Maniatopoulos, C., J. Sodek, and A.H. Melcher, *Bone formation in vitro by stromal cells obtained from bone marrow of young adult rats.* Cell Tissue Res, 1988. **254**(2): p. 317-30.

289. Beresford, J.N., et al., *Evidence for an inverse relationship between the differentiation of adipocytic and osteogenic cells in rat marrow stromal cell cultures.* J Cell Sci, 1992. **102 (Pt 2)**(Pt 2): p. 341-51.

290. Turner, C.H., et al., *Recruitment and proliferative responses of osteoblasts after mechanical loading in vivo determined using sustained-release bromodeoxyuridine.* Bone, 1998. **22**(5): p. 463-9.

291. Sittichockechaiwut, A., et al., *Use of rapidly mineralizing osteoblasts and short periods of mechanical loading to accelerate matrix maturation in 3D scaffolds.* Bone, 2009. **44**(5): p. 822-829.

292. Sekiya, I., et al., *Expansion of human adult stem cells from bone marrow stroma: conditions that maximize the yields of early progenitors and evaluate their quality.* Stem Cells, 2002. **20**(6): p. 530-41.

293. Canalis, E., A.N. Economides, and E. Gazzerro, *Bone morphogenetic proteins, their antagonists, and the skeleton.* Endocr Rev, 2003. **24**(2): p. 218-35.

294. Taguchi, Y., et al., *Interleukin-6-type cytokines stimulate mesenchymal progenitor differentiation toward the osteoblastic lineage.* Proc Assoc Am Physicians, 1998. **110**(6): p. 559-74.

295. van Leeuwen, J.P., et al., *Vitamin D control of osteoblast function and bone extracellular matrix mineralization.* Crit Rev Eukaryot Gene Expr, 2001. **11**(1-3): p. 199-226.

296. Sugiyama, M., et al., *Compactin and simvastatin, but not pravastatin, induce bone morphogenetic protein-2 in human osteosarcoma cells.* Biochem Biophys Res Commun, 2000. **271**(3): p. 688-92.

297. Friedl, G., et al., *Undifferentiated human mesenchymal stem cells (hMSCs) are highly sensitive to mechanical strain: transcriptionally controlled early osteo-chondrogenic response in vitro.* Osteoarthritis Cartilage, 2007. **15**(11): p. 1293-300.

298. Shayesteh, Y.S., et al., *The effect of a constant electrical field on osseointegration after immediate implantation in dog mandibles: a preliminary study.* J Prosthodont, 2007. **16**(5): p. 337-42.

299. Moinnes, J.J., et al., *Ultrasound accelerated bone tissue engineering monitored with magnetic resonance microscopy.* Conf Proc IEEE Eng Med Biol Soc, 2006. **1**: p. 484-8.

300. Wozniak, M., et al., *Mechanically strained cells of the osteoblast lineage organize their extracellular matrix through unique sites of alphavbeta3-integrin expression.* J Bone Miner Res, 2000. **15**(9): p. 1731-45.

301. Forwood, M.R., et al., *Modification of the in vivo four-point loading model for studying mechanically induced bone adaptation.* Bone, 1998. **23**(3): p. 307-10.

302. Mauney, J.R., et al., *Osteogenic differentiation of human bone marrow stromal cells on partially demineralized bone scaffolds in vitro.* Tissue Eng, 2004. **10**(1-2): p. 81-92.

303. Lian, J.B., et al., *Transcriptional control of osteoblast differentiation.* Biochem Soc Trans, 1998. **26**(1): p. 14-21.

304. Sittichokechaiwut, A., et al., *Use of rapidly mineralizing osteoblasts and short periods of mechanical loading to accelerate matrix maturation in 3D scaffolds.* BONE, 2009. **44**(5): p. 822-829.

305. Byrne, E.M., et al., *Gene expression by marrow stromal cells in a porous collagen-glycosaminoglycan scaffold is affected by pore size and mechanical stimulation.* J Mater Sci Mater Med, 2008. **19**(11): p. 3455-63.

306. Karsenty, G., *Minireview: transcriptional control of osteoblast differentiation.* Endocrinology, 2001. **142**(7): p. 2731-3.

307. Bruder, S.P., et al., *The effect of implants loaded with autologous mesenchymal stem cells on the healing of canine segmental bone defects.* J Bone Joint Surg Am, 1998. **80**(7): p. 985-96.

308. Schliephake, H., et al., *Use of cultivated osteoprogenitor cells to increase bone formation in segmental mandibular defects: an experimental pilot study in sheep.* Int J Oral Maxillofac Surg, 2001. **30**(6): p. 531-7.

309. Jaiswal, R.K., et al., *Adult human mesenchymal stem cell differentiation to the osteogenic or adipogenic lineage is regulated by mitogen-activated protein kinase.* J Biol Chem, 2000. **275**(13): p. 9645-52.

310. Cancedda, R., P. Giannoni, and M. Mastrogiacomo, *A tissue engineering approach to bone repair in large animal models and in clinical practice.* Biomaterials, 2007. **28**(29): p. 4240-50.

311. Porter, B.D., et al., *Noninvasive image analysis of 3D construct mineralization in a perfusion bioreactor.* Biomaterials, 2007. **28**(15): p. 2525-33.

312. Botchwey, E.A., et al., *Bone tissue engineering in a rotating bioreactor using a microcarrier matrix system.* J Biomed Mater Res, 2001. **55**(2): p. 242-53.

313. Guharay, F. and F. Sachs, *Stretch-activated single ion channel currents in tissue-cultured embryonic chick skeletal muscle.* J Physiol, 1984. **352**: p. 685-701.

314. Duncan, R.L., K.A. Hruska, and S. Misler, *Parathyroid hormone activation of stretch-activated cation channels in osteosarcoma cells (UMR-106.01).* FEBS Lett, 1992. **307**(2): p. 219-23.

315. Walker, L.M., et al., *Calcium-channel activation and matrix protein upregulation in bone cells in response to mechanical strain.* J Cell Biochem, 2000. **79**(4): p. 648-61.

316. Lammens, J., et al., *Distraction bone healing versus osteotomy healing: a comparative biochemical analysis.* J Bone Miner Res, 1998. **13**(2): p. 279-86.

317. Hynes, R.O., *Integrins: bidirectional, allosteric signaling machines.* Cell, 2002. **110**(6): p. 673-87.

318. van den Dolder, J., et al., *Bone tissue reconstruction using titanium fiber mesh combined with rat bone marrow stromal cells.* Biomaterials, 2003. **24**(10): p. 1745-50.

319. Cinotti, G., et al., *Experimental posterolateral spinal fusion with porous ceramics and mesenchymal stem cells.* J Bone Joint Surg Br, 2004. **86**(1): p. 135-42.

320. Wiles, M.V. and B.M. Johansson, *Embryonic stem cell development in a chemically defined medium.* Exp Cell Res, 1999. **247**(1): p. 241-8.